

Technische Universität Darmstadt (D 17)  
Fachbereich Humanwissenschaften

# Computational Motor Control of Human Movements

Dissertation zur Erlangung des  
akademischen Grades  
Doctor rerum naturalium (Dr. rer. nat.)

vorgelegt von  
Diplom-Sportwiss. Thorsten Stein  
geboren in Langen

Eingereicht am 01. Dezember 2009  
Disputation am 11. Februar 2010

Erstgutachter: Prof. Dr. Josef Wiemeyer  
Zweitgutachter: Prof. Dr. Hermann Schwameder  
(Karlsruher Institut für Technologie)

Darmstadt 2010

This thesis was composed with KOMA-Script and L<sup>A</sup>T<sub>E</sub>X.

For my parents,  
Anita M. Stein and Walter Stein



# Acknowledgments

First of all, I would like to express my gratitude to my parents and my grandma for reasons too numerous to mention here! Moreover, I am profoundly grateful to Ilka for her love, active support and for her patience with someone who was glued to his desk and lost in his own thoughts during the last weeks of writing. Finally, I would like to thank “the boys” for keeping their fingers crossed for me.

During my studies, Prof. Dr. J. Wiemeyer aroused my interest in the topic “human motor control”. For this and for reviewing my thesis, I am deeply thankful. Moreover, I am profoundly grateful to Prof. Dr. H. Schwameder, who was always encouraging and supportive of my work. Our discussions were very helpful in shaping my ideas. At the same time, he gave me the freedom and the resources to pursue my own research goals. I also like to thank Prof. Dr. K. Bös for believing in my abilities.

Thanks to my colleagues at the Department of Sport and Sport Science - especially to Dr. M. Wagner, A. Schnur, B. Hermann and A. Fischer - for the close collaboration. In particular, I would like to thank Andreas for the great cooperation during the last five years, the many interesting discussions in our shared offices and for introducing me to biomechanical data acquisition.

Additionally, I sincerely appreciated the interdisciplinary cooperation with the colleagues from the Collaborative Research Center 588 “Humanoid Robots” during the last five years, especially D. Gehrig, I. Boesnach, Dr. J. Moldenhauer, H. Kühne, Dr. A. Wörner and Prof. Dr. T. Schultz from the Department of Computer Sciences as well as Dr. C. Simonidis, Dr. G. Stelzner, F. Bauer and Prof. Dr. W. Seemann from the Department of Mechanical Engineering. In particular, I would like to thank Christian for the great cooperation and many hours of stimulating discussions on the topics biomechanical modeling and optimal control in the context of human motor control.

This work was supported by the German Research Foundation within Collaborative Research Center (CRC) 588 “Humanoid Robots - Learning and Cooperating Multimodal Robots”.



# Contents

<b>Acknowledgments</b>	<b>vi</b>
<b>Zusammenfassung</b>	<b>ix</b>
<b>Summary</b>	<b>xv</b>
<b>1 Introduction</b>	<b>1</b>
1.1 Motivation . . . . .	1
1.2 Structure of the thesis . . . . .	5
<b>2 Human motor control</b>	<b>9</b>
2.1 Introduction . . . . .	9
2.2 The degrees of freedom problem . . . . .	12
2.3 Scientific approaches in the study of human motor control . . . . .	19
2.3.1 Motor approach . . . . .	20
2.3.2 Dynamical systems approach . . . . .	31
2.3.3 Computational neuroscience approach . . . . .	40
2.4 A computational approach for studying human movements . . . . .	83
2.4.1 Fundamental considerations about the study of human motor control . . . . .	84
2.4.2 Implementation of the considerations in the context of the degrees of freedom problem . . . . .	91
<b>3 Methods</b>	<b>95</b>
3.1 Subjects . . . . .	95
3.2 Procedures . . . . .	95
3.3 Motion capturing . . . . .	97
3.3.1 Data acquisition . . . . .	97
3.3.2 Data processing . . . . .	98
3.4 Biomechanical modeling . . . . .	99
3.4.1 Dynamic equations . . . . .	100
3.4.2 Motion mapping and inverse calculations . . . . .	101
3.5 Data analysis . . . . .	104

<b>4</b>	<b>Study I: The analysis of multi-joint pointing movements in 3D space</b>	<b>105</b>
4.1	Introduction . . . . .	105
4.2	Methods . . . . .	110
4.3	Results . . . . .	110
4.3.1	Hand kinematics . . . . .	111
4.3.2	Joint kinematics . . . . .	112
4.3.3	Joint torques . . . . .	123
4.4	Discussion . . . . .	123
4.4.1	Biological motor control . . . . .	123
4.4.2	Robotics . . . . .	126
4.4.3	Applied methods . . . . .	127
<b>5</b>	<b>Study II: The synthesis of multi-joint pointing movements in 3D space</b>	<b>129</b>
5.1	Introduction . . . . .	129
5.2	Methods . . . . .	134
5.2.1	Subjects . . . . .	134
5.2.2	Procedures . . . . .	134
5.2.3	Data acquisition and processing . . . . .	134
5.2.4	Biomechanical modeling . . . . .	134
5.2.5	Optimal control models . . . . .	134
5.2.6	Optimization method . . . . .	135
5.2.7	Simulation protocol . . . . .	137
5.2.8	Data analysis . . . . .	139
5.3	Results . . . . .	144
5.3.1	Validation of the optimization method . . . . .	144
5.3.2	Target 1: Comparison of the measured and predicted trajectories	147
5.3.3	Target 3: Comparison of the measured and predicted trajectories	181
5.4	Discussion . . . . .	220
5.4.1	Biological motor control . . . . .	220
5.4.2	Robotics . . . . .	231
5.4.3	Applied methods . . . . .	233
<b>6</b>	<b>Summary</b>	<b>241</b>
6.1	Results . . . . .	243
6.2	Further research . . . . .	246
	<b>References</b>	<b>249</b>
	<b>Eidesstattliche Erklärung</b>	<b>285</b>
	<b>Curriculum Vitae</b>	<b>287</b>

# Zusammenfassung

Die vorliegende Arbeit entstand im Rahmen des DFG-Sonderforschungsbereiches 588 “Humanoide Roboter - Lernende und kooperierende multimodale Roboter”. Eines der herausragenden Ziele der internationalen Robotik-Community ist die Konstruktion von Robotern, die in den Alltag des Menschen integriert werden können. Dabei wird der Standpunkt vertreten, dass diese Maschinen humanoid sein sollen, um die Interaktion zwischen Mensch und Maschine zu erleichtern. Humanoid bedeutet, dass Größe und Anatomie sowie die Anzahl der Bewegungsfreiheitsgrade und die Bewegungsamplituden in den einzelnen Gelenken dem menschlichen Vorbild nachempfunden sein sollen. Gleich dem biologischen Original verfügt eine solche Maschine über redundante Bewegungsfreiheitsgrade. Das redundante Design ermöglicht dem Roboter Hindernissen auszuweichen und während der Bewegungsausführung Gelenkansschläge zu umgehen. Allerdings wird diese Flexibilität mit einem Kontrollproblem erkauft. Welche Bewegungslösung soll der Roboter aus den vielen möglichen Lösungen in der jeweiligen Situation auswählen? Auf der Grundlage der bisherigen Ausführungen sollte die Maschine möglichst menschenähnliche Bewegungen ausführen. Demnach lautet die zu beantwortende Frage: Auf der Grundlage welcher Prinzipien wird im menschlichen ZNS für eine bestimmte Bewegungsaufgabe eine Bewegungslösung aus den vielen möglichen Bewegungslösungen ausgewählt? Wären diese Prinzipien bekannt, müssten sie in die formale Sprache der Mathematik übersetzt werden und wären somit zumindest prinzipiell einer computergesteuerten Maschine zugänglich. Bis heute haben Bewegungswissenschaftler keine zufriedenstellenden Antworten auf die Frage, auf der Grundlage welcher Prinzipien im ZNS die Selektion einer Bewegungslösung erfolgt. Dieses Forschungsdefizit ist der Ausgangspunkt der vorliegenden Arbeit.

Da eine Problemlösung eine detaillierte Problemkenntnis voraussetzt, beginnt der Theorieteil dieser Arbeit mit einer ausführlichen Aufarbeitung des Problems der redundanten Bewegungsfreiheitsgrade. Darauf aufbauend werden in den folgenden Abschnitten die aktuell einflussreichsten Lösungsansätze, jeweils eingebettet in den entsprechenden paradigmatischen Rahmen, dargestellt und diskutiert. Es sind dies Modelle, die dem Informationsverarbeitungsansatz, dem dynamischen Systemansatz sowie der komputationalen Neurowissenschaft zugeordnet werden können. Dieses Review bildet die Grundlage für den komputationalen Ansatz dieser Arbeit, der biomechanische Experimente mit mathematischen Modellierungen, Computersimulationen und Zeitreihenanalysen verbindet und eine Integration von neurophysiologischen, biomechanischen und verhaltenswissenschaftlichen Befunden ermöglicht.

Bei der Entwicklung von Modellen ist zu beachten, dass Modelle ihr jeweiliges Original nur in Teilen repräsentieren, d.h. sie erfassen nicht alle Attribute des Originalsystems. Dementsprechend können Modelle der motorischen Kontrolle auch nicht alle Arten menschlicher Bewegungen erklären. Im Kontext des Problems der redundanten Bewegungsfreiheitsgrade stellt die Analyse mehrgelenkiger Bewegungen im 3D-Raum ein aktuelles Forschungsfeld der internationalen Bewegungswissenschaften dar. Aus diesem Grund wird in der vorliegenden Arbeit ein Modell entwickelt, das die Untersuchung von Kontrollvorgängen im menschlichen ZNS bei der Ausführung mehrgelenkiger Bewegungen im 3D-Raum ermöglicht. Das Modell wird in der vorliegenden Arbeit zur Untersuchung mehrgelenkiger Zeigebewegungen im 3D-Raum in einem natürlichen Kontext eingesetzt. Diese Bewegungen sind weniger komplex als die meisten sportlichen Bewegungen. Im Gegensatz zu stark vereinfachten Bewegungsaufgaben unter Laborbedingungen sind diese Bewegungen aber trotzdem "ökologisch valide", da Menschen auf diese Bewegungen in ihrem Alltag häufig zurückgreifen.

Schnelle, hochgeübte Zeigebewegungen auf Ziele, die sich im unmittelbaren Sichtfeld der Person befinden, sind höchstwahrscheinlich feedforward kontrolliert. Dabei wird in der vorliegenden Arbeit davon ausgegangen, dass im ZNS eine Planungsinstanz einen Bewegungsentwurf bzw. einen Bewegungsplan erstellt und diesen an eine Kontrollinstanz weiterleitet, die die entsprechenden Muskelkommandos berechnet. Diese Kommandos werden schließlich an das Muskelskelettsystem gesendet, das die Kommandos in eine Bewegung umsetzt. Da das motorische System über eine sehr große Anzahl an Bewegungsfreiheitsgraden verfügt, existieren eine Vielzahl von möglichen zielführenden Bewegungsplänen. Um besser zu verstehen, auf Grund welcher Prinzipien im ZNS ein Bewegungsplan ausgewählt wird und auf welcher Ebene diese Prinzipien arbeiten, wurden zwei Studien durchgeführt. Beiden Studien liegt ein Experiment zugrunde, bei dem 20 Probanden in der Demonstratorküche des SFB 588 vier verschiedene Zeigebewegungen jeweils fünfmal ausführen mussten. Die Ziele, die Startposition sowie die Reihenfolge der Nummernansage waren standardisiert. Eine Berührung der Ziele war nicht vorgesehen. Darüber hinaus wurden die Probanden instruiert, die Bewegungen wie im täglichen Leben auszuführen. Es war den Probanden überlassen, mit welcher Hand sie auf welches Ziel zeigen. Alle Probanden wurden während der Bewegungsausführung mit einem markerbasierten Infrarot Tracking System (Abtastrate 120Hz) kinematisch vermessen. Für die Berechnung der inversen Kinematik und Dynamik sowie für die in Studie II durchgeführten Simulationen wurde auf ein im SFB 588 entwickeltes biomechanisches Mehrkörpermodell zurückgegriffen. Das in dieser Arbeit verwendete Standardmodell verfügt im Oberkörper über 32 Bewegungsfreiheitsgrade.

**Studie I: Bewegungsanalyse.** Eine zentrale Annahme bewegungswissenschaftlicher Forschung ist, dass Informationen über interne Planungs- und Kontrollprozesse aus Bewegungsmerkmalen abgeleitet werden können, die über verschiedene Aufgaben hinweg sowie über verschiedene Personen hinweg stabil auftreten.

---

Im Detail geht man davon aus, dass sich repräsentierte Bewegungsmerkmale von nicht-repräsentierten Merkmalen entweder nach dem Kriterium der Einfachheit und/oder dem Kriterium der Invarianz unterscheiden. Eine Analyse aller 400 Zeigegesten deutet daraufhin, dass man die 20 Probanden vier Gruppen zuordnen kann. Zehn Probanden haben die Startposition nicht verlassen und mit der linken Hand auf die Ziele 1 und 2 gezeigt und mit der rechten Hand auf die Ziele 3 und 4. Vier Probanden haben die Ausgangsposition ebenfalls beibehalten und mit der rechten Hand auf alle vier Ziele gezeigt. Zwei Probanden verließen die Startposition während der Zeigebewegung und zeigten mit der linken Hand auf die Ziele 1 und 2 sowie mit der rechten Hand auf die Ziele 3 und 4. Der vierten Gruppe können vier Probanden zugeordnet werden, die die Startposition nicht verlassen haben und unterschiedliche koordinative Muster zeigten. Ein Proband zeigte z.B. zweimal mit der linken Hand auf das Ziel 1 und dreimal mit der rechten Hand. Zusammenfassend kann konstatiert werden, dass sich 16 Probanden ähnlicher bzw. wiederkehrender Bewegungsmuster bedienten, während vier Probanden wechselnde Strategien wählten und damit die verfügbaren Freiheitsgrade in einem größeren Ausmaß nutzten. Da die beiden Probanden der dritten Gruppe vereinzelt den Aufnahmebereich des Infrarot Tracking Systems verlassen haben und die Probanden der vierten Gruppe die gleichen grundlegenden Bewegungsmuster wie die Probanden der ersten beiden Gruppen zeigten, konzentriert sich die Bewegungsanalyse auf die Probanden der ersten beiden Gruppen. Typische Resultate werden für die Ziele 1 und 3 präsentiert. Für die Analyse wurden die Zeitreihen der Handtrajektorien sowie die Zeitreihen der Gelenkwinkeltrajektorien mit Hilfe einer kubischen Spline-Interpolation zeitnormalisiert und Mittelwerte und Standardabweichungen berechnet. Die Analyse der verschiedenen Zeigegesten in extrinsischen und intrinsischen kinematischen Koordinaten zeigt, dass die Trajektorien der Hand in extrinsischen Koordinaten ein sehr viel einfacheres Verlaufsmuster aufweisen als in intrinsischen kinematischen Koordinaten. Darüber hinaus zeigt sich, dass die Trajektorien der Hand über die verschiedenen Bewegungsaufgaben und Probanden hinweg hochgradig invariant sind, ganz im Gegensatz zu den Gelenkwinkeltrajektorien. Sofern Informationen über den Prozess der Bewegungsplanung aus den beiden eingangs genannten Kriterien deduziert werden können, deuten die Resultate der ersten Studie darauf hin, dass im menschlichen ZNS Bewegungen eher in einem extrinsischen Koordinatensystem der Hand als in intrinsischen Gelenkkordinaten geplant werden. Darüber hinaus legen die Resultate die Vermutung nahe, dass der Mensch auf Gelenkwinelebene eine kompensatorische Strategie verfolgt, um die geplante Trajektorie der Hand umsetzen zu können. Eine Gegenüberstellung der einzelnen Winkelverläufe zeigt, dass die Probanden zum Teil Lösungen produzieren, bei denen sich annähernd lineare Beziehungen zwischen den einzelnen Bewegungsfreiheitsgraden der Schulter, des Ellbogens sowie der Thoraxrotation

zeigen. Diese Befunde deuten daraufhin, dass die Probanden in einigen Fällen die Tendenz erkennen lassen, einfache Kopplungen zwischen verschiedenen Bewegungsfreiheitsgraden zu generieren. Zusammenfassend kann konstatiert werden, dass trotz der immensen Anzahl an kortikalen Neuronen, Muskeln sowie Gelenkfreiheitsgraden konsistente und reproduzierbare Bewegungsmuster über die verschiedenen Bewegungsaufgaben und Probanden hinweg identifiziert werden können. Diese Beobachtung legt die Vermutung nahe, dass im ZNS das Redundanzproblem auf der Grundlage bestimmter Prinzipien aufgelöst wird. Die Identifikation dieser Prinzipien bzw. die Ebene, auf der diese Prinzipien wirksam werden, ist allerdings auf der Basis von Bewegungsanalysen nur sehr schwer zu bestimmen, da im ZNS unter Umständen Planungsprozesse auf der Grundlage anderer Variablen oder Prinzipien ablaufen und die gefundenen Regelmäßigkeiten in extrinsischen Koordinaten der Hand lediglich Beiprodukte dieser Prozesse sein könnten. Aus diesem Grund wurde in der zweiten Studie dieser Arbeit ein Modell entwickelt, das die Synthese menschlicher Bewegungen auf der Basis verschiedener Planungsprinzipien ermöglicht. Für die Konstruktion humanoider Roboter kann aus der ersten Studie abgeleitet werden, dass Roboter Zeigebewegungen mit leicht gekrümmten Bewegungsbahnen der Hand und seit langem bekannten eingipfeligen, glockenförmigen Geschwindigkeitsprofilen mit einer Höchstgeschwindigkeit von  $1.5 - 2.0 \text{ m/s}$  produzieren sollten. Die Analyse der Gelenkwinkeltrajektorien zeigt, dass die Probanden verschiedene Strategien wählen, um die soeben genannten Eigenschaften der Handtrajektorien sicherzustellen. Diese Variabilität bietet die Möglichkeit die Gelenkinematik zu selektieren, die sich am einfachsten auf den jeweiligen Roboter übertragen lässt. In Abhängigkeit von der gewählten Kinematik sollten die Motoren des Roboters Winkelgeschwindigkeiten von bis zu  $150 \text{ Grad/s}$  im Schulter- und Ellbogengelenk erzeugen können.

**Studie II: Bewegungssynthese.** In der zweiten Studie dieser Arbeit wird ein computationales Modell vorgestellt, das Planungsprozesse im ZNS nachbildet. Viele Studien haben gezeigt, dass Optimierungsmodelle invariante Merkmale menschlicher Bewegungen auf verschiedenen Ebenen reproduzieren können. Im Rahmen von Optimierungsmodellen wird die Anzahl der möglichen Bewegungsfreiheitsgrade durch die Definition zusätzlicher Randbedingungen eingeschränkt und auf diesem Weg eine einzelne Trajektorie selektiert. Diese zusätzlichen Randbedingungen werden durch ein Performanz-Kriterium abgebildet, das als Zielfunktion fungiert (z.B. minimaler Ruck). Obgleich diese Modelle seit einigen Jahren in der Fachliteratur diskutiert werden, fehlt ein quantitativer Vergleich der Modelle für mehrgelenkige Bewegungen im 3D-Raum fast völlig. Deshalb ist die Zielstellung der zweiten Studie zu untersuchen, ob Optimierungsmodelle in der Lage sind, mehrgelenkige Zeigebewegungen des Menschen im 3D-Raum zu rekonstruieren. Dabei werden insgesamt vier verschiedene Opti-

---

mierungsprinzipien getestet, die unterschiedlichen Planungsräumen zugeordnet werden können. Konkret wird eine Ruckminimierung auf Handebene (extrinsisch-kinematischer Planungsraum) und Gelenkwinklebene (intrinsisch-kinematischer Planungsraum) sowie eine Minimierung der Drehmomentänderung (intrinsisch-dynamischer Planungsraum) untersucht. Des Weiteren wird eine modifizierte Ruckminimierung der Hand implementiert, die auf einer extrinsischen und intrinsischen kinematischen Ebene operiert. Die Optimierungsprinzipien bilden in Kombination mit einem biomechanischen Mehrkörpermodell jeweils ein Optimierungsmodell, das eine Bewegungssynthese mittels Computersimulation ermöglicht. Die im Computer synthetisierten Bewegungen können dann mit experimentell bestimmten menschlichen Zeigebewegungen verglichen und so die Güte der einzelnen Optimierungsmodelle bestimmt werden. Hierzu werden die Bewegungen von acht Probanden der ersten Gruppe (siehe Studie I) herangezogen, so dass insgesamt 40 Datensätze für das erste Ziel und 40 Datensätze für das dritte Ziel zur Verfügung stehen. Eine Analyse der internationalen Fachliteratur zeigt, dass bei Anwendung von Optimierungsmodellen vereinzelt bis zu vier Bewegungsfreiheitsgraden optimiert wurden. In der vorliegenden Studie werden für das Ziel 1 die drei Bewegungsfreiheitsgrade der Schulter sowie der Bewegungsfreiheitsgrad im Ellbogengelenk optimiert. Die restlichen Bewegungsfreiheitsgrade des Mehrkörpermodells werden mit Motion-Capture-Daten bewegt. Für das Ziel 3 werden die drei Bewegungsfreiheitsgrade der Schulter, der Bewegungsfreiheitsgrad im Ellbogengelenk sowie der Bewegungsfreiheitsgrad der Thoraxrotation optimiert. Die restlichen Bewegungsfreiheitsgrade des Mehrkörpermodells werden wiederum mit Motion-Capture-Daten bewegt. Diese Forschungsmethodologie ermöglicht es Rückschlüsse zu ziehen, auf Grund welcher Prinzipien im menschlichen ZNS ein Bewegungsplan aus der großen Anzahl an möglichen Plänen ausgewählt wird und auf welcher Ebene der Selektionsprozess von statten geht. Die Resultate der zweiten Studie zeigen, dass keines der Optimierungsmodelle die gemessenen Zeigebewegungen vollständig reproduzieren kann. Dabei ist zu bedenken, dass aufgrund von Rauschen im sensomotorischen System und der komplexen intersegmentalen Dynamik geplante und tatsächliche Bewegungen höchstwahrscheinlich immer Differenzen aufweisen werden. Die gemessenen und berechneten Bewegungen wurden zunächst auf der Basis einer prozentualen mittleren quadratischen Abweichung ( $\%RMSD$ ) auf Unterschiede hin geprüft. Dabei zeigte sich, dass das Prinzip der Ruckminimierung auf Gelenkwinklebene in der Mehrzahl der Fälle signifikant kleinere Abweichungen von den gemessenen Bewegungen in extrinsischen und intrinsischen kinematischen Koordinaten produzierte, als die anderen Optimierungsmodelle. In einem zweiten Schritt wurde ein Ähnlichkeitskoeffizient zum Vergleich topologischer Verlaufscharakteristika zwischen gemessenen und berechneten Bewegungen bestimmt. Dabei zeigte sich, dass wiederum das Prinzip der Ruck-

minimierung auf Gelenkwinelebeue insgesamt die besten Resultate erbrachte, d.h. die höchsten Ähnlichkeitskoeffizienten aufwies. Demzufolge erscheint eine Planung in intrinsischen kinematischen Koordinaten auf der Grundlage einer Ruckminimierung am plausibelsten. Jedoch ist darauf hinzuweisen, dass das Prinzip der Ruckminimierung auf Gelenkebeue die menschlichen Bewegungen nicht vollständig reproduzieren konnte. Daher ist der Schluss, dass Bewegungsplanungsprozesse im menschlichen ZNS vollständig im Gelenkwinkelraum auf der Basis einer Ruckminimierung ablaufen, als zumindest unvollständig einzustufen. Es erscheint daher denkbar, dass im ZNS unter Umständen verschiedene Prinzipien an dem Prozess der Bewegungsplanung beteiligt sind, die unterschiedlichen Planungsräumen zugeordnet werden können und problem-spezifisch kombiniert und gewichtet werden. Das Prinzip der modifizierten Ruckminimierung der Hand war ein erster Versuch, eine Verknüpfung zwischen extrinsischem und intrinsischem kinematischen Planungsraum herzustellen. Ungeachtet dieser Einschränkungen deuten die Befunde darauf hin, dass man mit dem Prinzip der Ruckminimierung auf Gelenkwinelebeue menschliche Bewegungen nachbilden kann, so dass dieses Prinzip in der Robotik für eine Synthese menschenähnlicher Bewegungen auf Roboterplattformen eingesetzt werden kann. Eine Anwendung dieses Kriteriums hätte den Vorteil, dass man das invers-kinematische Problem umgehen könnte, da der Planungsvorgang in intrinsischen kinematischen Koordinaten ablaufen würde.

Zusammenfassend ist zu konstatieren, dass die Verknüpfung von Bewegungsanalyse und Bewegungssynthese zur Erforschung der menschlichen Bewegungskontrolle plausibel erscheint und in zukünftigen Untersuchungen weiterverfolgt werden sollte. In einem ersten Schritt ist ein Bewegungskatalog zu entwickeln, der verschiedene Alltagsbewegungen unter normalen und veränderten Umweltbedingungen (z.B. Zeit- oder Präzisionsdruck) abbildet. Dabei ist darauf zu achten, dass die Anzahl der Probanden reduziert und die Anzahl der individuellen Versuche erhöht wird. Auf der Ebene der Bewegungsanalyse sind die Kopplungen zwischen einzelnen Gelenkfreiheitsgraden sowie die Stabilität dieser Kopplungen bei modifizierten Aufgaben- oder Umweltbedingungen genauer zu untersuchen. Auf der Ebene der Bewegungssynthese erscheint die Beachtung physiologisch plausiblerer Prinzipien, die auf muskulärer oder neuronaler Ebene operieren, angebracht. Darüber hinaus sollten Feedback-Prozesse Berücksichtigung finden.

## Summary

This thesis is a result of the authors work in the Colobarative Research Center 588 "Humanoid Robots - Learning and Cooperating Multimodal Robots" over the past five years. One of the major goals of robotics research is the construction of robots that share their activity space with human partners. To promote man-machine interaction in a human environment, the size, geometry, arrangement of limbs, number of degrees of freedom (DOFs) and the range of motion of a humanoid robot should be comparable to those of humans. In addition to anthropometric resemblance, the robot should use human-like movements. The humanization of the robot has essentially two benefits. First, a robot with a human-like anthropometry would be able to easily access the human environment. Second, human-like movements by robots would allow the human user to better predict the robots movements, enhance user safety and acceptance and encourage the cooperation between man and machine. Humanoid robots of this kind dispose of a large number of DOFs. This redundancy is advantageous because it enables robots to avoid obstacles and joint limits similar to human action. However, this flexibility or movement abundance leads to a control problem. For instance, which particular movement among the large number of possible movements should be chosen in a given situation? Based on the above outlined considerations, a human like movement should be chosen. Consequently, the question that has to be answered is the following: Which principles does the human CNS use to choose one movement of the plethora of possible movements to solve the task at hand? Unfortunately, neuroscientists, psychologists, sports scientists, engineers, and computer scientists have not been able to provide adequate answers to this question. This lack of understanding about the CNS is the starting point of this thesis.

In a first step a thorough introduction to the problem of motor redundancy in the context of human motor control is given. Additionally, existing models from three different scientific paradigms that deal with the problem of motor redundancy are presented and discussed. These theoretical considerations form the basis of the computational approach developed and realized in this thesis. The approach links biomechanical experiments with theoretical modeling, computer simulations and time series analysis and thereby enables an integration of results from neurophysiological studies, studies on the physics of the musculoskeletal system and finally psychophysical studies.

However, since models reproduce their original only in parts, which means that they do not cover all available aspects of the original, motor control models can only account for specific classes or aspects of human movements. Since multi-joint

movements in 3D space are a current field of research in human motor control, the movements analyzed in this thesis will be multi-joint pointing movements in 3D space. These movements are less complex than most movements in sports, but are still “ecologically valid” compared to artificial labor tasks because humans use these movements in their daily life.

Highly practiced goal directed pointing movements towards targets in the field of vision are most likely feedforward controlled. Thereby, it is assumed that a planner computes a movement plan that is transmitted to a controller, which transforms the plan into adequate motor commands. Finally, the motor commands are sent to the musculoskeletal system which transforms the motor commands into limb movements according to the movement plan. Due to the numerous DOFs in the human motor system, there actually exist an infinite number of possible movement plans for any given task. To examine which principles the CNS uses to choose a movement plan and on which level these principles work (e.g. kinematic vs. dynamic coordinates or extrinsic vs. intrinsic coordinates) two studies were conducted. Both of them are based on an experiment in which several subjects had to point repeatedly to four different targets. The experiment was conducted in the test-kitchen of the CRC 588. All movements were tracked with an IR-tracking system. The calculation of inverse kinematics and inverse dynamics was done using a biomechanical model that was developed in CRC 588.

**Study I: Movement analysis** One of the main assumptions in human motor control is that information about the process of movement planning in the CNS can be deduced from behavioral regularities or invariant movement features. More precisely, represented movement features differ from non-represented features in the criterion of simplicity and/or the criterion of invariance. The coordination strategies used by the subjects can be assigned to one of four groups, as follows. Ten subjects, comprising group 1, did not leave the starting position and pointed with their left hand to targets 1 and 2 and with their right hand to targets 3 and 4. In group 2, four subjects again did not leave the starting position but pointed with their right hand to all four targets. Two subjects left the starting position and turned toward the targets, subsequently pointing with their left hand to targets 1 and 2 and with their right hand to targets 3 and 4. The fourth group, consisting of four subjects did not use consistent coordination strategies for each target. For example, in five separate tasks, one subject pointed to target 1 twice with the left hand and three times with the right hand. In other words, the subjects of the fourth group used the same strategies as the subjects of groups 1 and 2, but changed coordination strategies from trial to trial for each target. The results indicated that 16 subjects preferred recurring coordination strategies for each target, while four subjects preferred alternating coordination strategies for each target. The four subjects implementing alternating coordination strategies used the available DOFs to

---

a far greater extent. The two subjects from group 3 could not be analyzed because they left the capture volume during several of the trials. Therefore, typical results of groups 1 and 2 are presented. Moreover, the analysis focused on targets 1 and 3. To be able to compare the time series of the trajectories of the hand and joints of the different trials, the time series were normalized in time using a cubic spline interpolation. After the time normalization means and standard deviations were calculated. A comparison of the pointing movements in extrinsic and intrinsic coordinates revealed that the trajectories of the hand in extrinsic coordinates were much simpler than the joint angle trajectories in joint space. Furthermore, in contrast to the joint angle trajectories, the trajectories of the hand were highly invariant across different movement tasks. When information about the process of movement planning can be deduced from the criterion of simplicity and/or the criterion of invariance, the results of this study indicate that the CNS uses extrinsic instead of intrinsic coordinates in the process of movement planning. Furthermore, the CNS may use a compensatory control strategy on the joint level to assure the planned trajectory is achieved. Moreover, the inter-joint coordination analysis revealed highly linear relationships between different DOFs in some cases. This indicates that the CNS sometimes shows, even in joint space, a tendency to use rather simple couplings between different DOFs. Considering the large number of neurons, muscles and joints it is quite remarkable that in multi-joint pointing movements in 3D space consistent and reproducible patterns of motor behavior across different subjects and tasks were found. These observations suggest that the CNS solves the redundancy problem based on specific principles. However, it has to be admitted that it is difficult to determine on which level they arise since the brain may use other planning variables or principles and the simplicity and invariance of hand trajectories may be by-products of these. Therefore, in the second study of this thesis the planning principles themselves as well as the level on which these principles might work were focused. However, besides these biological aspects the results of this study indicate that humanoid robots should generate pointing gestures with slightly curved hand paths and single peaked, almost bell shaped velocity profiles with a peak velocity of 1.5 - 2.0 m/s. The analysis of the joint angle trajectories showed that humans use different coordination strategies. Different coordination strategies of different subjects provide the chance to select the kinematics that may best be mapped to a specific humanoid robot. Depending on the chosen kinematics, the motors of the robot should be able to produce angular velocities of up to 150 deg/s in the shoulder and elbow joint.

**Study II: Movement synthesis** In the second study a computational model of human movement planning was developed to unravel the principles the CNS might use to solve the redundancy problem. Many studies reveal that optimal con-

trol models can reproduce movement regularities on multiple levels. In optimal control models a unique trajectory is selected by adding additional constraints on the task and thereby reducing the effective DOFs. This is usually done by selecting a cost function, that has to be optimized (e.g. minimum jerk). Although, these models are established in technical literature for some years a quantitative comparison between the performance of those models for multi-joint movements in 3D space is rather new. Therefore, the purpose of the second study is to quantitatively examine the performance of different optimal control models in reproducing human multi-joint pointing movements in 3D space. Thereby different optimization principles are coupled with a multi-body model of the human musculoskeletal system to form different optimal control models that can be assigned to different planning spaces. We tested a minimum hand jerk model (extrinsic-kinematic planning space), a minimum angle jerk model (intrinsic-kinematic planning space), and a the minimum torque change model (intrinsic-dynamic planning space). Furthermore we developed a planning algorithm than works on an extrinsic and intrinsic kinematic level called a modified hand jerk model. With the help of this computational approach human pointing gestures are generated via computer simulations and are compared to experimentally determined pointing gestures. Thereby conclusions might be drawn, which principles the CNS uses to choose a movement plan and on which level or planning space these principles work. The results show that none of the optimal control models could completely reproduce the human trajectories. However, due to noise in the sensorimotor system and the complex intersegmental dynamics during movement production planned and executed movements will always differ to some extend. The variations between measured and predicted trajectories are quantified using percental root mean square differences (*%RMSDs*). The minimum angle jerk model exhibited in most of the cases significantly smaller deviations from the measured trajectories in extrinsic and intrinsic kinematic coordinates than all other optimal control models. However, our analysis indicated that an exclusive comparison of different optimal control models on the basis of a *%RMSD* is insufficient for the determination of the best model. Because of that, we calculated a similarity coefficient between measured and predicted trajectories. Once again, the minimum angle jerk model yielded the closest fit to the human data. Therefore, a planning in intrinsic kinematic coordinates based on a jerk minimization seems the most plausible based on our results. However, due to the fact that the minimum angle jerk model did not fully reproduce the measured trajectories an exclusive planning in intrinsic kinematic coordinates based on a minimum angle jerk principle seems at least debatable. It is therefore conceivable, that the CNS might combine different optimization strategies in motor planning depending on the movement task. The modified minimum hand jerk model is a first attempt to implement this idea. Despite these limitations, the findings of

---

this study exhibit that human movements can be emulated by a jerk minimization on joint level. The application of a minimum angle jerk model in robotics would have the advantage that the inverse kinematics problem would be solved, since the motor planning takes place in intrinsic kinematic coordinates.

In summary, it can be stated that the combination of movement analysis and movement synthesis for the study of human motor control seems plausible and should be continuously used in future studies. In these studies movement tasks of different complexity should be analyzed such as, for instance, movements that involve the use of different numbers and combinations of DOFs. In addition, subjects should carry out these movements under pressure of time or pressure of accuracy. In the context of movement analysis, couplings between different degrees of freedom should be analyzed. Furthermore, the stability of these couplings across different movement tasks and different environmental conditions have to be examined. Moreover, in the context of movement synthesis future studies should include the analysis of models that are physiologically more feasible than the models tested in this thesis. In addition, feedback processes should be taken into account.



# 1 Introduction

## 1.1 Motivation

“A remarkable machine, unlike any other I had seen before, was rushing towards me. It moved so quickly that it was difficult to see all its parts. It apparently did not have any wheels but nevertheless moved forward at an amazing speed. As I was able to see, its most important part was a pair of powerful, elastic rods, each one consisting of several segments. They changed their shape so quickly, stretched and retracted, extended and folded, flashing by each other and moving along peculiar arcs of such precision and beauty that it was impossible to penetrate into their essence and origin. How far is our technology from constructing such mechanisms!!!

I was given a tube called a “time magnifier”. Looking in it, I could see the movements of these objects slowed down and extended in time. Looking after the machine that rushed away, I could see it in more detail. Each rod moved along a complex curved arc suddenly made a soft contact with the ground. Then, it looked as if lightning ran along the rod from the top to the bottom, the rod straightened and lifted off the ground with a powerful, resilient push, and rushed upwards again. In the upper part of the machine, there were two more similar rods, but smaller in size. As I was able to understand, the upper rods were connected with the lower ones by some kind of transmission and moved at the same rhythm. However, their direct purpose remained unknown to me.

As I was told, the machine consisted of more than two hundred engines of different size and power, each one playing its own particular role. The controlling center was on the top of the machine, where electrical devices were located that automatically adjusted and harmonized the work of hundreds of motors. Due to these controlling structures, the rods and levels were able to move along the complex curves that allowed the machine to move without wheels faster than wind” (Bernstein, 1996, p. 121).

The term *robot* goes back to Karel Capeck’s play *Rossum’s Universal Robots (RUR)*. This play, which debuted in 1921, is largely credited as being the beginning of the robotics era. Capeck’s vision in regard to robots was twofold. First, he suggested that robots would be human-like and second, that they would interact with humans in a natural environment. Today, almost a century later, Capeck’s vision has yet to be realized. While many robots have been developed to date, the majority

of these are used primarily for highly repetitive and high-precision tasks in industrial applications (Craig, 2005). However, due to the technological progress within the last 20 years robotics research began to focus on the topic humanoid robots (Becher et al., 2004; Schaal, 2007b). It is generally accepted that humanoid robots will be an integral part of human life in the future, just as computers, the internet or email are today (Oztop et al., 2004). Possible future applications for humanoid robots are residential service, personal robots for the elderly, playmate robots in child education or robots for danger zones (e.g. space, nuclear power stations). Humanoid robots will undertake tasks where there are simply too few humans to cope with the social needs or where the environment is too dangerous for humans (Tanie, 2003; Fong et al., 2003; Brock et al., 2005; Schaal, 2007b). To promote man-machine interaction in a human environment, the size, geometry, arrangement of limbs, number of degrees of freedom (DOFs) and the range of motion of a humanoid robot should be comparable to those of humans. In addition to anthropometric resemblance, the robot should use human-like movements (Wank et al., 2004; Asfour et al., 2008). The humanization of the robot has essentially two benefits. First, a robot with a human-like anthropometry would be able to easily access the human environment. Second, human-like movements by robots would allow the human user to better predict the robot's movements, enhance user safety and acceptance and encourage the cooperation between man and machine (Khatib et al., 2004; Schaal, 2007b). One of the goals of robotics research is to create a team of humanoid robots that is able to defeat the current FIFA Football World Champion by 2050 (Ferrein, 2005). Hence, the question arises how far robotics research has come. Many advancements have been made in the development of humanoid robots. There already exist robots that can walk (Sakagami et al., 2002), that can manipulate objects (Asfour et al., 2008) or show emotions (Brooks, 2007). But humanoid robots who are able to walk, manipulate objects and show emotions in a changing human centered environment are still part of fundamental research (Asfour, 2003). Nevertheless, the field of robotic research has the ability to construct humanoid robots that dispose of a large number of DOFs (Fig. 1.1). This redundancy is advantageous because it enables robots to avoid obstacles and joint limits similar to human action (Atkeson et al., 2000). However, this flexibility or movement abundance leads to a control problem. For instance, which particular movement among the large number of possible movements should be chosen in a given situation? Robotics research is traditionally situated in mechanics and computer science, and based on control theory and optimization theory. To further the development of humanoid robots that work in human-centered environments, robotics research should begin to collaborate with additional fields of study including psychology, biology, and neuroscience (Schaal, 2007b). If a robot is developed for operating in a human environment, uses the same objects and tools that humans use in their daily life, and generates human-like movements, it is beneficial to understand how humans accomplish everyday motor tasks.

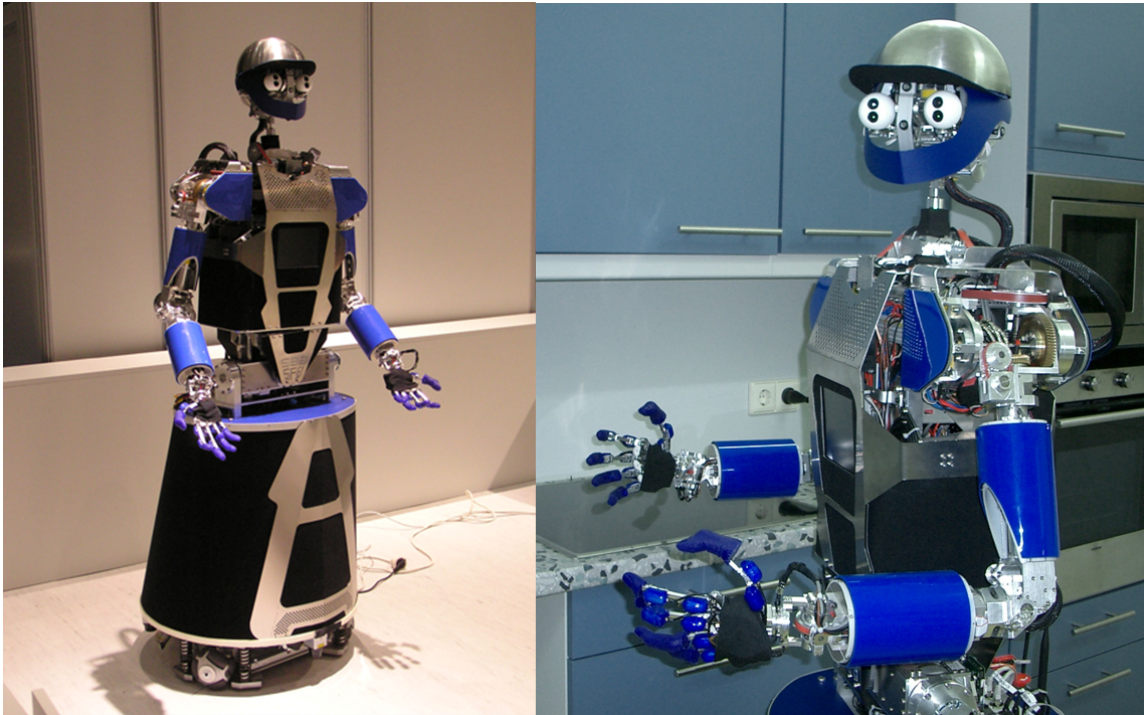


**Figure 1.1:** Partially anthropomorphic robot system *ARMAR IIIa* of the Collaborative Research Center (CRC) 588 “Humanoid Robots” consists of seven sub systems: sensor head with flexible neck, left and right arms, left and right five-finger hands, torso and mobile platform (43 DOFs) (Albers et al., 2006; Asfour et al., 2008).

Today, the fields of biological motor control and robotics have already started to interact (Schaal and Schweighofer, 2005; Ijspeert, 2006) and exchanged ideas (Hollerbach, 1982; Beer et al., 1998; Sternad and Schaal, 1999; Piazzini and Visioli, 2000; Atkeson et al., 2000; Sun and Scassellati, 2005; Konczak, 2005; Stein et al., 2006). The field of robotics has proved to be a useful environment for developing and testing hypotheses about biological motor control. In other words, models of biological motor control can be corroborated or discarded by testing them on robots. In addition, the capabilities of biological systems by far surpass those of artificial systems (Flash et al., 2004). Therefore, the body of knowledge gained in the field of biological motor control may help engineers to develop hardware and software components for humanoid robots that are able to generate human-like movements and operate in future human environments.

Although this thesis is inspired by robotics research, it is founded in biology. Studying the way humans coordinate their movements in daily life or more demanding activities such as sports is an important scientific topic in many fields of study including medicine, psychology, kinesiology, and certainly, cybernetics and robotics. With the technical enhancements for capturing motion sequences and the pioneering work of

Muybridge (1957) and Bernstein (1967) in this area <sup>1</sup>, the attempt to understand human movements by means of analysis and modeling has become an expanding field of study. The fact that human movements are part of everyday life hides their intrinsic complexity. The initial assumption that an understanding of human movements could be gained by simply improving measurement techniques and carrying out carefully designed experiments did not produce adequate results. Typically, the initial experiments brought about more questions than answers, and the attempt to understand the functionality of human movements is ever growing even after nearly 100 years of extensive multidisciplinary research (Morasso and Sanguineti, 2004).

Imagine sitting in front of a glass of water. To take a drink from the glass would require first grasping the glass and then directing it toward the mouth. However, when you feel thirsty, you simply grasp the glass and take a drink without much thought. In doing so, we are controlling perhaps the most complex system nature has ever produced. The human movement system consists of billions of interconnected neurons, approximately 800 muscles, and over 200 mechanical DOFs. This highly redundant system enables us to achieve movement tasks like the one just described in countless ways. In this context Bernstein (1996, p. 41) defines *coordination* as “overcoming the excessive degrees of freedom of our movement organs, that is, turning the movement organs into a controllable system.” Consequently, one of the central research questions in biological motor control is the following:

*How does the central nervous system (CNS) turn the movement organs into a controllable system and thereby choose one movement from the infinite number of possible movements?*

Unfortunately, neuroscientists, psychologists, sports scientists, engineers, and computer scientists have not been able to provide adequate answers to this question. This lack of understanding about the CNS is the starting point of this thesis. Although the topic of “coordination” is of great relevance for robotics, it should be mentioned that it may not be possible or even advantageous for a humanoid robot to use the same principles for movement generation as humans. Nonetheless, biological motor control is an important field for robotics research as it provides inspiration for hardware and software components for humanoid robots. Therefore, it is necessary to enhance our understanding of how humans move and which principles humans use for movement generation. If those principles are discovered, mathematical models need to be developed to describe the principles of human movement generation. In the future, those models may be used in robotics or for the control of prostheses (Flash et al., 2004).

---

<sup>1</sup>A comprehensive historical treatment of pioneering work in the field of the movement science can be found in the books of Latash and Zatsiorsky (2001) as well as Nigg and Herzog (2007).

## 1.2 Structure of the thesis

In July 2001, the CRC 588 “Humanoid Robots - Learning and Cooperating Multimodal Robots” was established by the German Research Foundation. This project is designed for 12 years. More than 50 scientists from the Universität Karlsruhe (TH), Forschungszentrum Karlsruhe, Forschungszentrum Informatik, and Fraunhofer Institute for Information and Data Processing are involved in this interdisciplinary research project. The goals of CRC 588 are to generate concepts, methods, and concrete mechatronical components for a humanoid robot that will be able to share its activity space with a human partner (Becher et al., 2004). This thesis is the result of the author’s work on this project over the past five years. During this period, the author worked with colleagues from the computer science department and the engineering science department on different research questions involving motion planning of humanoid robots or motion recognition with Hidden Markov Models. Working on these topics led finally to the research objective of this thesis and still has great impact on it. However, these studies are not covered in this thesis but already published or in print (Fischer et al., 2005; Stein et al., 2005, 2006; Moldenhauer et al., 2006; Boesnach et al., 2006a,b; Gehrig et al., 2008; Fischer et al., 2009a,b, 2010).

In addition to the topics of motion planning of humanoid robots and motion recognition that are classical topics of computer science or robotics, the author began to explore questions of biological motor control. This ultimately led to the establishment of the research objectives of this thesis (Chap. 1.1). The structure of this thesis is presented in the following paragraphs (Fig. 1.2).

*Chapter 2* begins with a preliminary discussion on the topic of human movements and narrows the focus of research for this thesis to the problem of motor redundancy. The next section presents a thorough introduction to the problem of motor redundancy. Additionally, existing models from three different scientific paradigms that deal with the problem of motor redundancy are presented and discussed. These theoretical considerations form the basis of the computational approach developed and realized in this thesis. This approach is presented at the end of Chapter 2.

*Chapter 3* describes the methods used in the two studies (Chap. 4 and 5) based on the theoretical considerations of chapter 2. A description of the biomechanical data acquisition and data processing is given. For the calculation of joint angles and joint torques, the Mkd-Tools framework is used. This framework was developed in the CRC 588 to establish a standardized biomechanical model of the human skeletal system. The model itself was developed by Stelzner (2008) and enhanced by Simonidis (2010). The author was involved in the development of the Mkd-Tools framework to aid in the establishment of an interface between biomechanical data acquisition and Mkd-Tools framework, and in an advisory function concerning aspects standardization and biological plausibility of the model. Portions of the methods described in chapter 3 have been published previously (Stein et al., 2008a; Simonidis et al., 2010).

In *chapter 4*, the first of two studies is presented. One of the key assumptions in biological motor control is that information about the process of movement planning and control can be deduced from behavioral regularities (Bernstein, 1967). A large number of such regularities have been reported in literature (Goodman and Gottlieb, 1995), however, the analysis of multi-joint daily life movements in 3D space is uncommon. Thus, the purpose of the first study is to analyze different multi-joint pointing movements in 3D space with respect to the selection of regularities. A definition of some regularities or principles of the system's behavior may be obtained through the observation of the behavior of the human movement system under different conditions. These regularities may provide an initial idea of how humans reduce the available DOFs and are also relevant for robotics research. If a humanoid robot is supposed to move in the same manner as a human, its movements should exhibit the same regularities as human movements. Some of the results presented in chapter 4 have been published previously (Stein et al., 2008b, 2009a).

The study presented in *chapter 5* is based on the work presented in chapters 2, 3 and 4. Different approaches to the problem of motor redundancy are discussed in the literature (Chap. 2). Many studies show that optimal control models can reproduce movement regularities on multiple levels (Todorov, 2004). In optimal control models, a unique trajectory is selected by adding additional constraints on the task and thus reducing the effective DOFs. This is usually accomplished by selecting a cost function to be optimized (Engelbrecht, 2001). Although these models have been established in technical literature for some years, a quantitative comparison between the performance of the models for multi-joint movements in 3D space is a fairly new concept (Flash et al., 2003; Admiraal et al., 2004; Hermens and Gielen, 2004; Kapfle and Eriksson, 2008; Gielen, 2009b). Therefore, the purpose of the second study is to quantitatively examine the performance of different optimal control models in reproducing human multi-joint pointing movements in 3D space. In addition, the study will examine the tested models to determine if they are able to reproduce the regularities found in the first study (Chap. 2). The developed optimization method for the movement generation based on different criteria has been published previously (Simonidis et al., 2009a,b). Some preliminary results of this study have also been published beforehand (Stein et al., 2009b,c; Simonidis et al., 2009a; Stein et al., 2010). Based on the previously published work, the author was awarded with the "Reinhard Dausgs Förderpreis" of the section "Sportmotorik" of the "Deutsche Vereinigung für Sportwissenschaft".

The results of this thesis are summarized in *chapter 6*. This chapter includes a discussion of the theoretical considerations (Chap. 2), the methods (Chap. 3) and finally the results of the two conducted studies (Chap. 4 and 5). Based on this summary an outlook on future research is given.

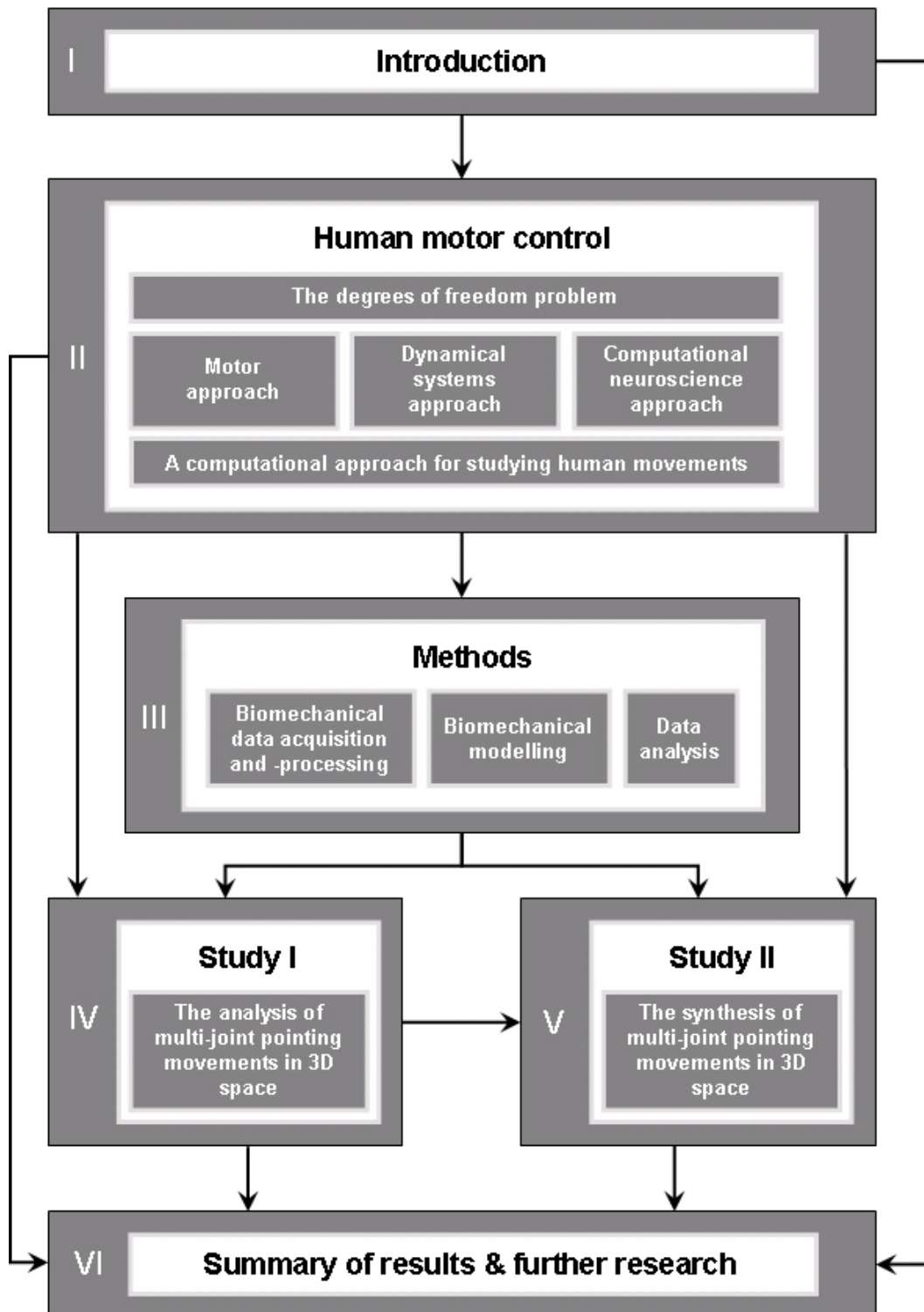


Figure 1.2: Structure of this thesis



## 2 Human motor control

### 2.1 Introduction

Moving our body and body segments in three dimensional space are a defining characteristic of human life. Without the ability to move, humans would not be able to speak, type, reach for a cup of coffee or ride a bicycle. Human movements can take on a variety of different forms that can be assigned to one of three categories: *reflexive*, *rhythmic*, and *voluntary* (Ghez and Krakauer, 2000; Konczak, 2008). Reflexive movements are rather involuntary, coordinated patterns of muscle contraction and relaxation elicited by peripheral stimuli. Among other things, rhythmic motor patterns include repetitive, alternating contractions of flexor and extensor muscles on both sides of the body during locomotion. Voluntary movements are often referred to as *skills* or *motor skills* (Ghez and Krakauer, 2000; Magill, 2001). A motor skill or *action* can be seen as a motor task that implies the achievement of a specific goal. Example motor skills may include grasping a glass of water or serving a tennis ball, with respective goals being the reduction of thirst and the avoidance of a double fault. In both cases however, different subjects will produce different movements to achieve the end goal. Furthermore, humans can accomplish the same goal using different effectors, or different goals using the same effectors. This phenomenon has been termed *motor equivalence* and indicates a remarkable flexibility of the human motor system. An example of motor equivalence is writing one's name with a pencil held between the fingers of the right or left hand, the toes of the right or left foot, or even between the teeth (Kelso et al., 1998). This dissertation addresses motor skills rather than reflexive or rhythmic motor patterns.

As in every scientific discipline, the object of research is classified according to a specific scheme. The field of human motor control is no exception. This is important for researchers to be able to communicate their research findings, which is a prerequisite for the development of a scientific field. Another important aspect is that the plethora of different movements humans can perform is an enormous challenge in the process of model building. Models typically do not include all features of the system to be simulated (Stachowiak, 1973). In the field of human motor control, this implies that motor control models can only account for specific classes or aspects of human movements. The issue is then to determine the distinguishing characteristics of specific motor skills or tasks. Two important schemes of classification are *discrete*, *serial* and *continuous* skills as well as *open* versus *closed* skills (Magill, 2001; Schmidt and Wrisberg, 2004; Schmidt and Lee, 2005). In the first scheme, discrete skills are

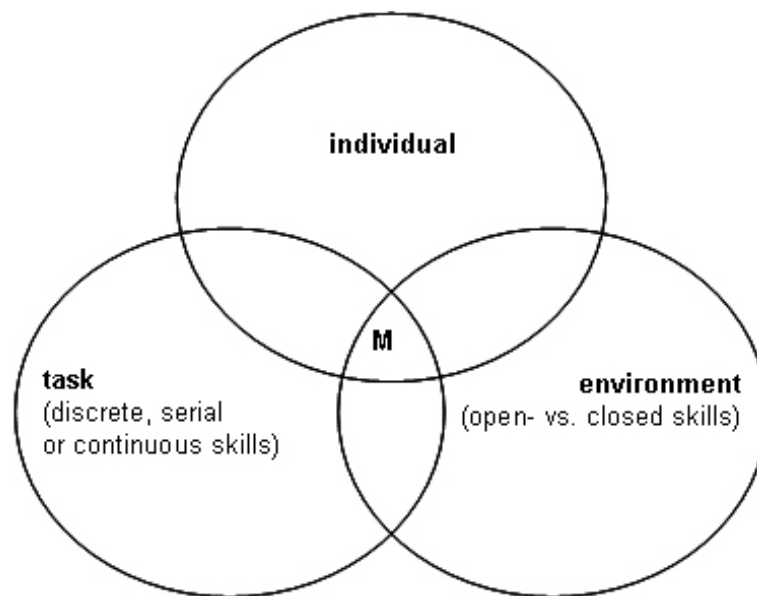


**Figure 2.1:** Human movements (M) emerge from the interaction of the individual, the task and the environment (adapted from Shumway-Cook and Woollacott, 2007)

organized in such a way that an action has a recognizable beginning and end (e.g., performing a serve in tennis). A serial skill is comprised of several discrete skills that are linked together in a sequence (e.g., the starting of a car). In such a case, the order of the actions is crucial for success. Finally, continuous skills, in contrast to discrete skills, have no recognizable beginning and end. Such actions are performed in an ongoing and repetitive way. Examples of continuous skills include steering a car, running and swimming. A second criterion for the classification of motor skills is the extent to which the environment is stable, or at least predictable, throughout the performance. In this context, open skills are performed in an environment that is constantly (and perhaps unpredictably) changing. Examples may include martial arts or games such as football or basketball. In these instances it is difficult for the performer to effectively predict the future moves of teammates and/or opponents. On the other hand, closed skills are performed in an environment that is stable and predictable. Examples include bowling, darts and a gymnastic routine. However, it should be noted that each of the two schemes represent end points of a continuum, and that there are many actions between those endpoints. Nevertheless, these designations are prevalent in the human motor control literature, and may even be combined to produce a more complex approach (e.g. Gentile, 2000). Together, the two schemes indicate that human movements emerge from the interaction of the *individual*, the *task* and the *environment* (Fig. 2.1). The individual produces a movement to achieve a task. This could be a task that requires a discrete, a serial or a continuous action. For instance, grasping a glass is a discrete task. Furthermore,

the skill may require rapid adaptations to a constantly changing environment (open skill) or the environment is stable and predictable (closed skill). Grasping a glass in a kitchen would be considered a closed skill. Finally, the movement organization is constrained by the functional capacity of the individual to achieve a specific goal. The actions analyzed in this thesis will be of a discrete nature, performed in a perfectly stable and predictable environment (closed skills).

The uniqueness of individuals, with the exception of identical twins, is a basic fact of life. Individual characteristics are obvious upon birth and continue to change with age. These differences are also reflected in human movement behavior. Why is one person a better gymnast or surgeon than another given the same amount of practice? Which aptitudes or abilities contribute to a skilled performance in gymnastics? The term *ability*, often used interchangeably with the terms *aptitude* or *capability*, usually refers to a hypothetical construct that supports performance in a number of tasks. The ability to react may underlie a number of specific skills such as those required in sprint starts in athletics or quick reactions in sports games. Abilities are relatively stable traits that have been genetically determined and/or developed during growth and maturation (Schmidt and Lee, 2005). The number of motor abilities humans possess is unknown and currently no common classification system exists (e.g. Roth, 1999; Bös, 2002; Schmidt and Lee, 2005). In this thesis, the author does not attempt to describe, explain, or predict performance differences among people based on abilities as is done in differential approaches. Instead, this thesis focuses on the fundamental movement principles of human motor control. The intent is to study mechanisms common to all healthy people.

To understand the functionality of human movements, analysis is carried out in the field of human motor control. This interdisciplinary field “is directed at studying the nature of movement and how humans control their movements” (Shumway-Cook and Woollacott, 2007, p. 4). In other words, motor control is “the study of postures and movements and the mechanisms that underlie them” (Rose, 1997, p. 4). Rosenbaum (1991, 2002) identifies four major problems or challenges in the field of motor control:

**Degrees of freedom problem.** When reaching for an object, individuals may adopt many postures at the beginning, end and on the way to the final posture. Much work has been conducted on the problem of the overabundance of degrees of freedom (DOFs) in the body relative to the description of the task at hand. The problem is how a particular solution emerges when an infinite number of solutions exist.

**Serial order problem.** Almost every skill, like speaking, typing, or running, consists of different elements that need to be ordered correctly. The challenge is to understand how humans control the serial order of their behavior.

**Perceptual-motor integration problem.** Movement without perception is impossible and sensory information is needed to plan and correct movements. How are

movements linked to perception? How are movements affected by perceptual processing and how is perceptual processing affected by movement?

**Skill-acquisition problem.** The field of motor learning concerns the study of the acquisition and modification of skills. The first challenge is in understanding how the relationship between movements and their effects evolve. The second challenge is distinguishing how the process of practice needs to be structured to support the development of those relationships.

It seems that these four problems cannot be solved independently. For example, if one tries to understand how the central nervous system (CNS) chooses one particular movement out of the plethora of possible movements (the degrees of freedom problem), it must also consider how afferent signals are transformed into efferent signals in the CNS and vice versa (the perceptual-motor integration problem), and how the strategies to overcome the redundancy of the human motor system are learned (skill acquisition problem). As described in the introduction (Chap. 1.1), the research objective of this thesis is to address the question of how the human CNS generates or produces coordinated movements, and in doing so, manages to overcome the excessive degrees of freedom of the human body. This problem will be outlined in more detail in the next chapter (Chap. 2.2) following the identification of the degrees of freedom problem as the object of research.

## 2.2 The degrees of freedom problem

“You probably do not know that God has a cousin who has never been very famous. So, the cousin asked God to help him achieve fame and glory in science. To please the cousin, God gave him an ability to get any information about physical systems in no time and to travel anywhere within a microsecond. First, the cousin decided to check whether there was life on other planets. No problems; he traveled to all the planets simultaneously and got an answer. Then he decided to find out what the foundation of matter was. Again, this was easy: He became extremely small, crawled inside the elementary particles, looked around, and got an answer. Then, he decided to learn how the human brain controls movements. He acquired information about all the neurons and their connections, sat at his desk and looked at the blueprint. If the story has its right, he is still sitting there and staring at the map of neural connections” (*Nikolai Alexandrovich Bernstein*) (Latash, 2008b, p. 33).

Movement generation in biological systems is ill-posed in the sense that the task requirements can generally be met by an infinite number of different movements. The notion of well-posed and ill-posed problems was developed in mathematics in the context of partial differential equations. A problem is well-posed when three criteria

are met: a solution exists, is unique, and continuously depends on the parameters that define the problem. In contrast, ill-posed problems do not fulfill at least one of the stated criteria (Kawato et al., 1990). Kawato (1996) distinguishes three kinds of ill-posed problems in human motor control, described as follows. In artistic gymnastics, experts can perform outstanding movements such as somersaults, back somersaults or handsprings. Novices however, may not be able to perform a simple handstand because of limitations of their motor skills and motor abilities. The nonexistence of a solution is the first kind of ill-posed problem. The second kind of ill-posed problem is when the solution to the problem is not uniquely determined. Bernstein (1967) was the first to draw attention to this kind of problem. In motor control literature, this problem is referred to as the *Bernstein problem*, the *degrees of freedom problem* or the *problem of motor redundancy* (Saltzman, 1979; Turvey, 1990; Latash, 1996). Most of the problems in motor control are ill-posed in the sense that the solution is not unique (Kawato et al., 1990). In connection with the third problem, consider a waiter delivering a glass and a bottle of water to a thirsty customer. Initially, the glass is inverted and the waiter grasps the glass in a thumb down position. By doing so, the waiter is able to easily rotate the glass hold it in a thumb up position while he pours water into the glass. The waiter tolerates an initial discomfort while picking up the glass for the sake of a later comfort while pouring water into the glass. This phenomenon is called *end-state comfort*. Rosenbaum et al. (2006) studied this phenomenon in a series of experiments in which they analyzed the choice of overhand grip versus underhand grip. Subjects were asked to grasp a handle and rotate it to a target orientation. In some cases, the choice of grip was consistent within a certain range of the initial and target handle orientation but abruptly changed at the boundary of these regions. If small changes in the parameters defining the motor task lead to discontinuous changes of solutions, then the third kind of ill-posed problem is encountered (Kawato, 1996). This thesis focuses on the second kind of ill-posed problem. Despite efforts made in human motor control, the problem remains unsolved (Latash et al., 2007). In this chapter, ill-posed problems with no unique solution in the context of movement generation are presented. These are problems that the CNS must solve when generating goal-directed movements. This thesis does not address how the CNS initially decides to perform a movement, as this seems to be an issue of philosophy or psychology. For this study, it is simply assumed that a goal has already been established. For example, the goal may be to reduce thirst, and thus the subject is required to reach for a glass of water. In generating or controlling a visually guided movement, the CNS needs to convert spatial information about the target location, initially defined in retinal coordinates, into patterns of arm muscle activity to be able to move the arm toward the target. It is generally assumed that there are intermediary coordinate frames used by the CNS for movement planning. Sensorimotor transformations between those frames are needed to translate retinal coordinates of the target into motor commands that lead to a goal-directed arm movement (Soechting and Flanders, 1992) (Fig. 2.2). A detailed description of

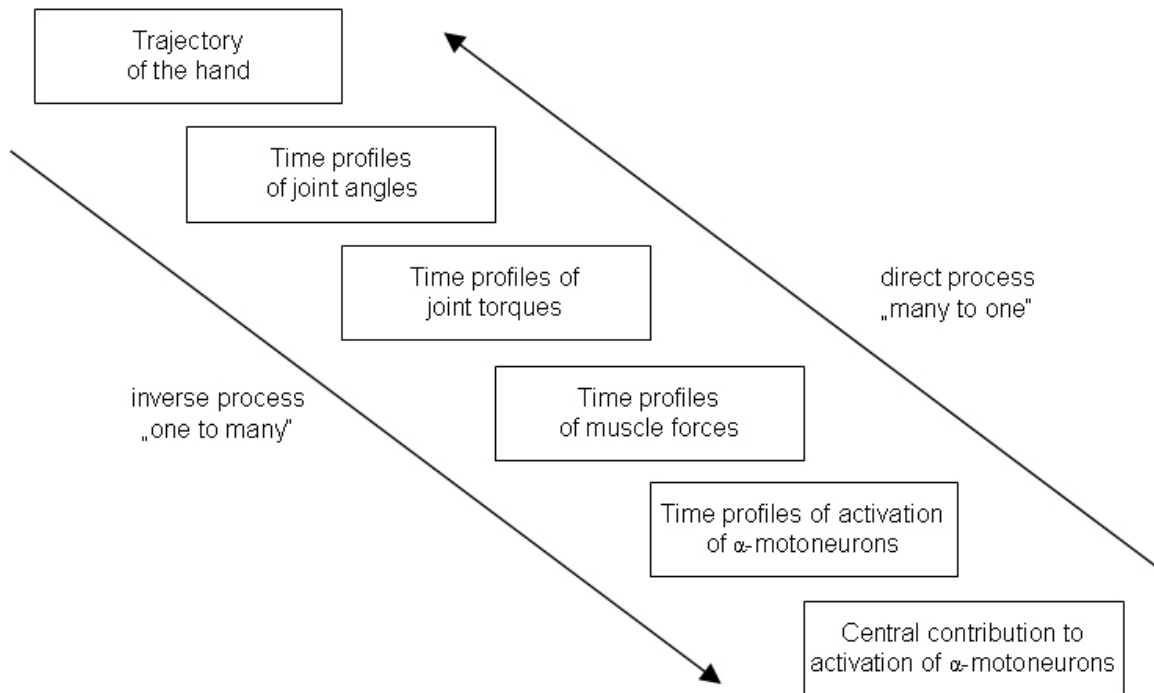


**Figure 2.2:** The problem of reaching toward a glass of water can be defined as a series of sensorimotor transformations between different coordinate frames. Information about spatial targets is converted into a number of intermediate frames from the trajectory of the hand to the required motor commands for the task. This is an inverse process that requires a one to many mapping, whereas the opposite direction is a direct process that requires a many to one mapping (adapted from Wolpert, 1997; Scott, 2000b, 2005; Latash, 2008a).

different frames of reference and sensorimotor transformations between them can be found in Lacquaniti (1997).

Reaching toward a glass of water requires that eye-centered visual information is transformed into a limb-centered goal of the intended movement. Andersen et al. (2004) distinguish between three options to perform this computation. The first option is a sequential transformation whereby the eye-centered location of the visual target is linked with the eye-orientation within the head. Thus, the coordinates of the target, or the glass of water, are transformed from an eye- or retina-centered frame of reference into a head-centered frame of reference. The position of the head with respect to the body is then taken into account to form a representation of the target in body-centered coordinates. In the last step, the body-centered position of the subject's hand is subtracted from the body-centered position of the target to generate a hand-centered representation of the target (Flanders et al., 1992). In the second option, all of the computations mentioned above are carried out in a single step and the location of the target is read out from this high-dimensional representation

(Battaglia-Mayer et al., 2000). The third option implies that the location of the target and the initial location of the hand are represented in eye-centered coordinates. Via a simple subtraction, a direct transformation of the target in hand coordinates is computed (Buneo et al., 2002). Regardless of which computational option is adopted by the CNS, both position and orientation can be characterized in each case by six Cartesian coordinates in external hand space (Zatsiorsky, 1998). The CNS now has to compute a trajectory of the hand toward the target in external hand space. The problem is that an infinite number of trajectories connect the position of the hand to the position of the target (Fig. 2.3). Thereby, the term trajectory refers to the spatial and temporal aspect of a movement. In other words, there are an infinite number of spatiotemporally routes connecting the starting position of the hand and the glass of water in 3D space. Consequently, there is no unique solution and the problem is ill-posed. This problem is usually referred to as the *trajectory formation problem* (Kawato et al., 1990; Kawato, 1996).

It should be noted that there is still a debate regarding on which level or in which space (e.g. extrinsic or intrinsic space) trajectories are planned (Soechting and Flanders, 1998). This problem is discussed in more detail in chapters 2.3.3.1, 4 and 5. Regardless of in which space trajectories are planned, so-called coordinate transformations from one space to another are an essential part of motor control. First of all, it is assumed that trajectories are planned in an extrinsic task space (Morasso, 1981; Georgopoulos et al., 1982, 1986). Because of the anatomical design of the human arm, joint rotations are needed to be able to translate the hand to the target location. Hence, the next step implies a coordinate transformation from external space into joint space. As a result, a joint angle configuration that can be used to attain the given position and orientation of the hand in 3D space is required. The human hand is part of a system consisting of segments (e.g. upper arm) connected by joints. The human arm and hand without fingers have at least seven DOFs: three at the shoulder (abduction/adduction, anteversion/retroversion and internal/external rotation), one at the elbow (flexion/extension), two at the wrist (flexion/extension and ulnar/radial deviation) and one between the wrist and elbow (pronation/supination). These seven DOFs are typically included in kinematic models of the human arm (Zatsiorsky, 1998). In reality, humans have 13 DOFs. Accordingly, the joint space in this case is seven-dimensional. To uniquely define seven angles about the seven axes of the described multi-link chain to place the hand at the starting point, a system of equations with seven unknowns has to be solved. Therefore, seven equations are needed but only three are available. This problem has no unique solution and is therefore ill-posed (Latash, 2008b). As the hand moves toward the glass, this problem has to be solved for each position of the hand along the desired trajectory. In other words, the CNS has to compute joint angle trajectories from the starting joint configuration to the final joint configuration in such a way that the hand reaches the glass of water (Fig. 2.3). This problem is called the *inverse kinematics problem* (Mussa Ivaldi et al., 1988; Zatsiorsky, 1998). Computations in the opposite direction,

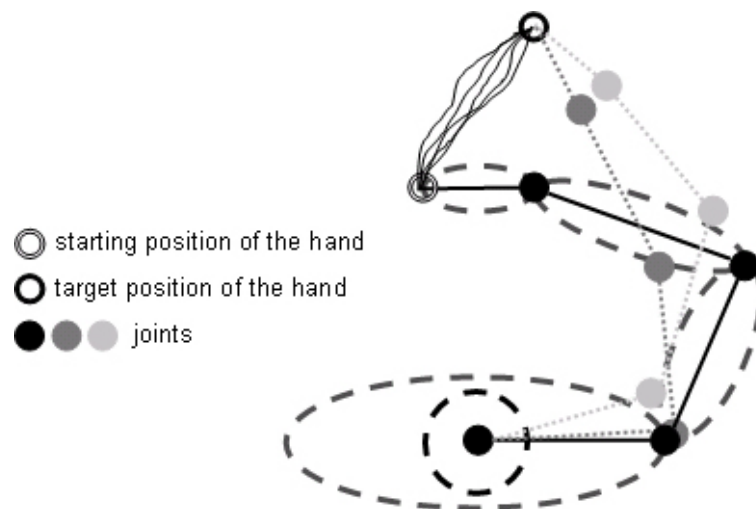


**Figure 2.3:** An infinite number of trajectories connect the initial and target position, five of which are shown. On the other hand, the kinematic redundancy of the human arm allows multiple task-equivalent effector configurations that lead to the same target position. Three possible configurations are depicted (adapted from Martin, 2005).

from intrinsic joint space to extrinsic space, are called *forward kinematics* (Wise and Shadmehr, 2002).

According to Newton's second law, one has to apply a force to accelerate a body. Therefore, to move the arm segments in the desired mode, one has to apply a force in the form of adequately timed joint torques. However, the equations of motion (Hollerbach, 1990b) reveal that the CNS not only has to generate appropriately timed joint torques, but also must take into account Reaction forces, Coriolis forces and Centripetal forces. Reaction forces are forces produced by the interactions between the joints, Coriolis forces are proportional to the cross products of the different joint angular velocities, and Centripetal forces are proportional to the square of a joint velocity. Thus, motor patterns at each joint must be carefully coordinated to smoothly move the segments through space, requiring the CNS to perform complex computation. This problem is known as the *problem of inverse dynamics* (Hollerbach, 1990a; Zatsiorsky, 2002). In contrast, computations that estimate the motion of the hand that will occur as a result of time profiles of joint torques are called *forward dynamics* (Wise and Shadmehr, 2002). Finally, the CNS not only has to take into account the physical characteristics of the musculoskeletal system, but also the weight of the external object that is to be manipulated. The required joint torques to lift a full versus an empty glass of water will differ significantly, although the trajectories of the hand may match perfectly.

Unlike robots, joint torques in biological systems are not produced via motors located in the joints, but by muscles that cross each joint. Because muscles can only

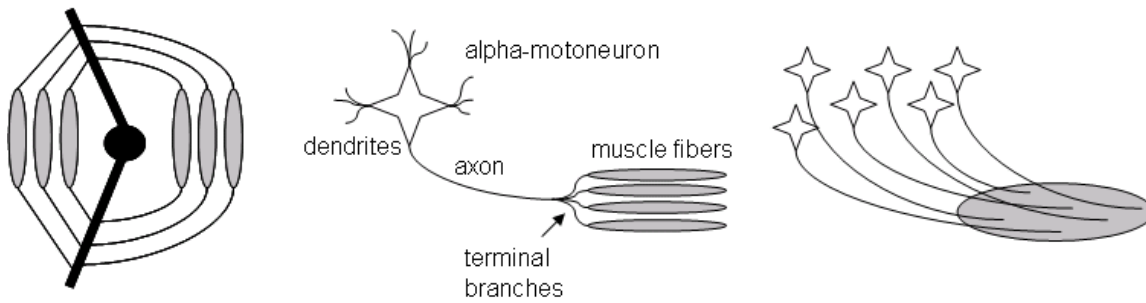


**Figure 2.4:** The elbow is crossed by three flexor and three extensor muscles. There exists an infinite number of possible muscle forces that can be combined to produce the required joint torque:  $M = \sum F_i R_i$ , where  $i = [1, \dots, 6]$  corresponds to muscles,  $F$  to the muscle force and  $R$  to the lever arm (left). Each of the six muscles is composed of motor units and each motor unit is composed of an alpha-motoneuron and a group of muscle fibers that receive action potentials from the terminal branches of the axon of this alpha-motoneuron (middle). A muscle is innervated by numerous alpha-motoneurons (right). The resultant muscle force  $F_M$  is caused by an activation of various motor units. The contribution of each unit to the overall muscle force may be modeled as a function  $f$  of its size, which could be represented by the peak force of its single contraction  $F_i$  and the frequency at which the motor unit under consideration is activated  $\phi_i$  (adapted from Latash, 2008b)

pull and not push, at least two antagonistic muscles are required to cross each joint. However, all joints of the human arm are crossed by more than two muscles. For example, the elbow joint is crossed by three flexors (biceps, brachialis and brachioradialis) and three extensors (three heads of the triceps). As a result, the same joint torque can be obtained by various muscle activation patterns. So the question arises as to what forces should be produced by each muscle to ensure the required time course of joint torques is met. In this case, we have one equation and six unknowns (Fig. 2.4). Again, the problem is ill-posed because no unique solution exists (Latash, 2008b).

Each of the six muscles around the elbow (e.g. biceps) consists of many fibers and is innervated by many *alpha-motoneurons* which are located in the spinal cord. However, there are fewer alpha-motoneurons than muscle fibers so that when a motoneuron sends an action potential to the muscle, the signal is received by a group of muscle fibers. Such a group is called a *motor unit* because all fibers within the group respond together when their alpha-motoneuron generates an action potential. Action potentials are the units of information transmission in the human body. Each muscle consists of motor units of different sizes; some of them are smaller and involve only a few muscle fibers, whereas others are considerably larger and include many muscle fibers. The CNS modifies the muscle force by changing the number of recruited alpha-motoneurons and/or by changing the frequency of the action potentials generated by

the individual motoneurons. If the frequency of the firing of an alpha-motoneuron is increased, its contribution to the total muscle force is increased. So the question is: How many motoneurons, and at what frequencies, should the CNS recruit to achieve a certain level of muscle activation to produce the required joint torques? At this point, there is one equation and many unknowns. However, according to the *size principle* (Henneman, 1965), motor units are recruited in an orderly fashion. During a slow increase in muscle force, smaller motor units are recruited first followed by larger motor units. But still the CNS has a vast amount of recruitment patterns to choose from, and therefore, no unique solution exists. Moreover, it should be noted that the force produced by a muscle fiber also depends on its length and rate of change. Therefore, the CNS has to take into account the expected changes of the muscle length when generating signals via its alpha-motoneurons (Latash, 2008b).

Alpha-motoneurons produce sequences of action potentials depending on their input. In general, there are two types of input: signals from the brain and signals from peripheral sensory endings. To ensure a proper input into the pool of motoneurons, the brain needs to estimate the peripheral contribution and generate a signal or signals such that the pool of motoneurons can produce the required activation patterns for the muscles (Latash, 2008b). Finally, we cannot assume that the firing patterns of the neurons in the different regions of the brain involved in motor control are uniquely defined because of the complexity of the human brain. These problems are known as the *problem of motor command generation* (Kawato, 1996; Nakano et al., 1999).

The computation of the different tasks on the different levels is an *inverse process* because it follows an order opposite to the natural order of events in human movement generation. After the inverse computational process is completed, the brain sends motor commands to the spinal neurons that activate the muscles so that the muscles produce the required joint torques, which in turn rotate the segments and translate the hand from starting position to the target. This transformation from the computed motor commands to the trajectory of the hand is a *direct process* and perfectly well-posed (Fig. 2.2). It seems that human motor control involves both ill-posed and well-posed problems, and therefore, motor control models should be able to address both types of problems. However, it has to be noted that the decomposition of motor control into a cascade of computational processes as described above, is an assumption that has been borrowed from robotics research conducted during the early 1980s (Soechting and Flanders, 1998) and should not be considered a perfect analogy. It is unknown whether the CNS solves the characterized problems step by step (Hollerbach, 1982), simultaneously (Uno et al., 1989), or if the strategy changes with learning (Kawato et al., 1990). The concept of coordinate transformation has at least heuristic value. It helps to get an idea about which problems biological movement systems face and how biological systems may solve these problems.

In summary, there are a vast number of DOFs associated with different levels in the human motor system (Turvey, 1990). Hence, the problem of motor redundancy

is a problem of choice: How does the CNS select one movement from the infinite number of possible movements to solve the task at hand or to achieve the intended goal (Latash, 1996)? In the context of a redundant motor system with specific physical and neurophysiological characteristics, motor control models need to explain how goals in extrinsic coordinates are transformed in trajectories of the hand and ultimately implemented in muscle commands. Sensorimotor transformations have to be carried out between different coordinate systems (extrinsic  $\rightarrow$  intrinsic) and between discrete and serial processes (targets  $\rightarrow$  trajectories of the hand  $\rightarrow$  time profiles of muscle forces). Considering the large number of neurons, muscles and joints, it is quite remarkable that in goal-directed movements like reaching, consistent and reproducible patterns of motor behavior across different subjects have been observed (e.g. Morasso, 1981; Abend et al., 1982; Flash and Hogan, 1985). These observations suggest that the CNS solves these ill-posed problems based on specific principles. In the next section (Chap. 2.3), answers to the problem of motor redundancy from three different scientific frameworks are presented and discussed.

## **2.3 Scientific approaches in the study of human motor control**

The question of which principles humans use in movement generation and how they overcome the problem of redundancy remains unsolved in human motor control research (Latash et al., 2007). This question has been addressed through different scientific approaches. The attempt to organize research in and between these fields has proven to be a difficult task because of the amount of research and the interdisciplinary nature of most of the research, making a selective assignment to a specific research field often impossible. For example, psychophysical or behavioral studies of human motor control now appear in journals that were strictly orientated toward neuroscience in the past (e.g. *Experimental Brain Research*, *Journal of Neuroscience*,...), and neuroscience-orientated studies are now published in journals that were formerly primarily behavioral publications (e.g. *Journal of Motor Behavior*, *Human Movement Science*,...). Studies of specific brain mechanisms involved during movement execution appear in special journals of the neuroscience community (e.g. *NeuroImage*) and continue to be published in journals devoted to specific professional topics (e.g. *Physical Therapy and Human Factors*). Based on these observations, Schmidt and Lee (2005) point out that more research is conducted and published in the field of human motor control than ever before. The research of human motor control involves people from diverse disciplines such as biology, psychology, kinesiology, computer science, physics and engineering science. In this chapter, the most important scientific approaches in the study of human motor control are briefly outlined. Within these scientific frameworks, the most influential models for solving the problem of mo-

tor redundancy (Chap. 2.2) are presented and discussed. It should be noted that the transitions between the different frameworks are not always well-defined and the following classifications are certainly idealized in some cases. Furthermore, it is impossible to take into account all models or studies conducted in the field of human motor control in this short summary. Therefore, this review remains inevitably incomplete.

### 2.3.1 Motor approach

Psychology is one of the classical fields that address the problems of motor control (Schmidt and Lee, 2005). In the middle of the 20th century, *behaviorism*, which was the dominant paradigm in psychology between the 1920s and the 1950s, was replaced by a new paradigm called *cognitive psychology*. A detailed description of the development from behaviorism to cognitive psychology can be found in Neumann (1993) or Moran (1996). Within cognitive psychology, the concept of *motor approach* evolved (Daugis, 1994). This chapter introduces the motor approach based on the topics of human information processing (Chap. 2.3.1.1), open-loop and closed-loop control (Chap. 2.3.1.2) and schema theory (Chap. 2.3.1.3). Finally, the schema theory is discussed in the context of the degrees of freedom problem (Chap. 2.3.1.4).

#### 2.3.1.1 Human information processing

Within motor approach, humans are seen as processors of information. Human information processing is based on a computer metaphor and according to this metaphor humans take in information from outside sources via their sensory systems. The information then undergoes transformations and is stored in different storage systems within the brain. The comparison of the brain to a computer led to the belief that movements are stored in the brain in the form of motor programs. In other words, the brain stores observable behavior in the form of a procedural code, like a computer program stored on a hard disc, which can be retrieved any time. Therefore, depending on the information received, the human information processing system selects a motor program and the required motor response is carried out. An important performance measure in studying human information processing is *reaction time* (RT).

“RT is the interval of time that elapses from the presentation of an unanticipated stimulus to the beginning of a subjects response” (Schmidt and Wrisberg, 2004, p. 58).

According to Schmidt and Lee (2005), central processing is carried out in three stages (Fig. 2.5, executive level). In the first stage, referred to as the *stimulus identification stage*, humans are required to distinguish between important and unimportant stimuli in the current context. The identification of a relevant stimulus requires time. It has

been shown that reaction time increases with an increasing complexity of the stimulus pattern or a decreasing stimulus intensity (Treisman, 1986). After the identification of a relevant stimulus, an individual has to choose an appropriate response. This stage, the second stage, is usually referred to as the *response-selection stage*. The selection of a response also requires time and the amount of time needed to select an appropriate response increases linearly with each doubling of the response alternatives. This relationship is known as *Hick's Law* (Hick, 1952) and is represented by the equation:

$$RT = a + b(\log_2(N)) \quad (2.1)$$

where  $N$  corresponds to the number of the response alternatives and  $a$  and  $b$  are empirical constants. In the third stage, the *response-programming stage*, the chosen reaction is programmed and carried out. Again, processing the response requires time and the RT increases with the complexity of movement to be programmed (Henry and Rogers, 1960). These findings led to the computer-analogous interpretation that a *motor program* is loaded from hard disk (human long-term memory), and the required loading time increases with the complexity of the motor program. In addition to movement complexity, speed and accuracy requirements should have an effect on the response programming. The trade-off between movement speed and accuracy is summarized by *Fitt's law* (Fitts, 1954) which states that in goal-directed movements, the movement time  $MT$  depends on the ratio of the movement amplitude  $A$  and the target width  $W$  at constant movement accuracy. Fitt's Law is given by the following equation:

$$MT = a + b(\log_2(2A/W)) \quad (2.2)$$

where  $a$  and  $b$  are empirical constants. There are three basic assumptions concerning the described information processing model. The first assumption is that human information processing requires time, although a decrease in the RT is possible via practice and anticipation (Rosenbaum, 1980). The second assumption is that error-free information processing requires attention, which is limited in source (Kahnemann, 1973; Wickens, 1984) and subject to the current level of arousal (Yerkes and Dodson, 1908; Landers and Arent, 2001). The third assumption is that there have to be mental representations of movements in the brain (Henry and Rogers, 1960).

### 2.3.1.2 Open-loop and closed-loop control

Motor control is modeled in two ways within motor approach: *open-loop models* and *closed-loop models*. In the case of open-loop models, a movement is programmed, the motor program is sent to the effector, and the movement is carried out with no possibility of modification if something goes wrong (Henry and Rogers, 1960; Keele, 1968). In contrast, closed-loop models contain the possibility of feedback processing against a reference of correctness (Adams, 1971). In figure 2.5, open-loop and closed-loop control are depicted. It should be noted that open-loop and closed-loop control are mutually exclusive. It appears that initially movements are under

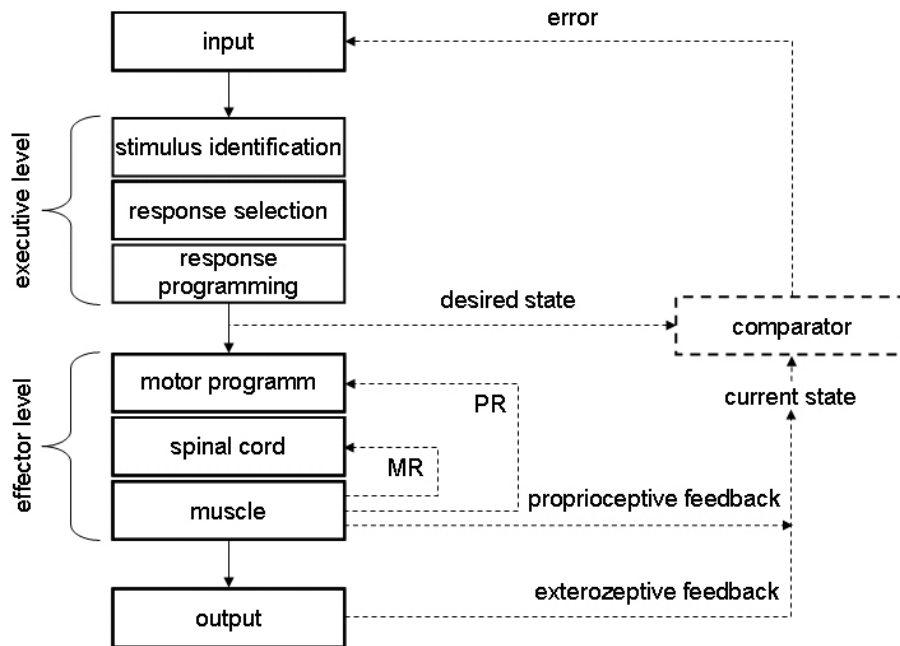


**Figure 2.5:** A human information processing model. The open-loop control portion is represented by solid lines and the closed-loop portion is represented by dashed lines. The abbreviations MR and PR stand for monosynaptic reflexes and polysynaptic reflexes, respectively (adapted from Schmidt and Wrisberg, 2004).

open-loop control. Then after approximately 150-200 ms, incoming feedback *can* be consciously processed, corresponding to closed-loop control (Slater-Hammel, 1960). The *Schema Theory* is a model developed to cover both open-loop and closed-loop control (Schmidt, 1975, 1982) and is intended to account for discrete actions. The schema theory will be outlined in the next chapter.

### 2.3.1.3 Schema theory

“Certainly the most important idea in schema theory, and what caused it to deviate from Adams (1971) theory from which schema theory takes much of its heritage, is the idea of the motor program. To me, it has always (at least since my days with Franklin Henry) been obvious that quick actions somehow have to be organized in advance and represented in memory. Sensory information, or response-produced feedback is too slow to account for events that occur in rapid tasks” (Schmidt, 2003, p. 367).

To address the problem of controlling fast movements, Keele and Posner (1968) suggested that the relevant commands for movement production are stored in a motor program. Based on this suggestion, if a movement is to be executed, the

corresponding motor program is retrieved. Keele (1968, p. 387) defines a motor program as:

“a set of muscle commands that are structured before a movement sequence begins, and that allows the sequence to be carried out uninfluenced by peripheral feedback.”

There are at least four lines of evidence that support the idea of motor programs: (1) RT increases with the complexity of the movement to be programmed (Henry and Rogers, 1960), (2) deafferentation studies show that movements are possible in the absence of proprioceptive feedback from the moved limbs (Lashley, 1917), (3) electromyography (EMG) patterns of rapid elbow extensions toward a target are similar under unblocked and blocked conditions (Wadman et al., 1979), and (4) learned movements can be executed with different muscle groups (Raibert, 1977). These lines of evidence indicate that movements are planned in advance via motor programs. However, if the CNS detects an error, for example the wrong motor program was selected, the CNS has to wait until the motor program has expired (Keele and Posner, 1968). In an experiment by Dewhurst (1967), a subject was asked to hold a light weight in the hand and maintain a right angle in the elbow joint. The EMG of the biceps and the kinematics of the arm were recorded. The subject was able to see the actual performance via a dot on a monitor that signaled the elbow angle. The weight was unexpectedly increased and naturally, the hand began to drop. According to the theory of Keele and Posner (1968), the subject has to process the visual and/or kinesthetic feedback from the arm through the information processing stages. Therefore, the first increase in the biceps EMG should appear after 150-200 ms, when a new motor program is chosen and sent to the effectors. However, the first small burst in the EMG appeared after only 30 ms and a larger, more irregular burst appeared another 20 ms later. These results indicate that at least two levels in the motor system have to be distinguished (Schmidt and Lee, 2005): (1) an *executive level* including the three stages of information processing for movement planning, and (2) an *effector level* for movement production (Fig. 2.5). Hence, two distinct types of errors can occur in the motor system, although each uses feedback in a distinctly different way. The first error is an error in *motor program selection* that has happened on the executive level. In other words, the wrong program was chosen for the task at hand, meaning the spatio-temporal goal cannot be achieved. In this case, a new motor program has to be selected in the response selection stage and must then be programmed in the response programming stage. Because this feedback-loop takes approximately 200 ms, in situations where rapid movements are required, the new program cannot be selected before the original movement has been completed and the error has already occurred. If the movement time is longer than the time required to select and implement a new program, there is a chance that the error is corrected while the movement is still being carried out. The second type of error occurs on the effector level. Such an error in *motor program execution* means that an

adequate motor program was selected but an unexpected event occurs that disrupts the movement. A correction of such an error in movement execution does not require the selection of a new motor program since the spatio-temporal goal can be achieved with the chosen program. The error may thus be compensated for with monosynaptic or polysynaptic reflexes. Monosynaptic reflexes carry feedback regarding the length of the muscle to the spinal cord which then passes modifications directly back to the muscle. This loop represents the lowest level of feedback corrections in motor control and is the most inflexible one. In contrast, polysynaptic reflexes return information about muscle force, muscle tension, and joint and body positions to higher centers of the brain that are concerned with movement programming. Based on this feedback information, minor modifications of the motor program are produced and sent back to the levels of the spinal cord and muscles. Compared to monosynaptic reflexes, polysynaptic reflexes are slower but more flexible because they involve higher brain centers. Nevertheless, the latencies of both loops are shorter than the required RT when the executive level is involved and they do not require attention because they are unconsciously performed. This means that depending on where the error has occurred, either on the executive level or the effector level, the human information processing system can utilize different feedback loops for corrections (Schmidt and Wrisberg, 2004). On the basis of these findings, Schmidt and Lee (2005) concluded that a centrally organized structure handles most of the movement details but is also very sensitive to movement-produced sensory information from a variety of sources. One way of viewing the combination of open-loop and closed-loop functioning is to consider a hierarchical control structure in which a higher level open-loop control structure contains a set of lower level closed-loop processes that ensure the movements produce the intended goal even when facing perturbations. These thoughts led to a modified and less restricted definition of a motor program (Schmidt and Lee, 2005, p. 190):

“The motor program is an abstract representation of action that, when activated, produces movement without regard to sensory information indicating errors in selection. Once the program has been initiated, the pattern of action is carried out for at least one RT even if the environmental information indicates that an error in selection has been made. Yet during the programs execution, countless corrections for minor errors in execution can be produced that serve to ensure that the movement is carried out faithfully.”

The advantage of this extended definition of a motor program is that previous studies on reaction time (Chap. 2.3.1.1) and the different control levels of the CNS are accounted for. Furthermore, the definition suggests that higher brain regions are freed from time consuming control tasks because sensory feedback can be processed on the spinal cord level. Schmidt and Lee (2005) compare this idea of a motor program to the concept of *coordinate structures* as discussed by Greene (1972), Turvey (1977), Fitch et al. (1982) and Berkinblit and Feldman (1988) (Chap. 2.3.2.2). According

to Schmidt and Lee (2005), both concepts reduce the numerous DOFs of the motor system via a structure that organizes the limbs into a single acting unit. Furthermore, the motor program concept and the coordinative structures involve a tuning of spinal centers, corrections for errors in execution and an independence of the executive level from details of movement execution on the effector level or lower levels of the motor system.

The traditional view of the motor program concept (Keele and Posner, 1968) implied that for each movement, a motor program is stored in the human brain. If one considers the countless number of movements humans are able to perform and that humans most likely cannot exactly reproduce a movement (Bernstein, 1967), then it seems that a vast majority of memory capacity would be needed to store all of the motor programs in long term memory. In literature, this dilemma is termed the *storage problem* (Schmidt and Lee, 2005). Related to the storage problem is the *novelty problem*. How are movements performed that have never been performed before? If no two movements are exactly the same and each movement is represented by a single motor program in long term memory, then where do these programs come from? It seems rather unlikely that, for example, different instances of a tennis stroke are genetically defined since these skills have no biological significance. It appears that a logical dilemma arises concerning the motor programming of novel movements (Schmidt and Lee, 2005). For the solution to these two problems, Schmidt (1982) suggests that the motor program is *generalized*, meaning that one program can run in a variety of different ways. In other words, the program covers an entire class of movements. Therefore, this *generalized motor program* (GMP) must dispose of components that separate the GMP “grasp” from the GMP “walk” and remain invariant when different grasps are performed. According to the *impulse-timing hypothesis*, the GMP “tells” the muscles when to contract, how much force to produce and when to turn off. In physics, impulse is the integral of force over time. The GMP controls the impulses produced across the muscles. The invariant features mentioned above include the order of muscular contractions (*order of elements*), the temporal structure of the contractions (*relative timing*) and the *relative force*, which means that the amount of force produced by the muscles remains in constant proportion (Schmidt and Lee, 2005). To produce an instance of a movement class (e.g. a particular grasp), certain *parameters* have to be entered into the GMP to define the particular instance. These parameters include *overall duration*, *overall forces* and *muscle selection*. This structure allows the GMP to be executed in countless ways simply by scaling the program linearly in time and amplitude by changing the parameters of overall time and overall force. There are numerous studies which provide a reference to the relative independence between the invariant and variable features. Detailed descriptions of the studies can be found in Schmidt (1985), Roth (1989) or Wulf (1994). It has to be noted that Gentner (1987), for example, has shown that the invariance of relative timing is not always completely constant. Nevertheless, it appears that the wide range of movements with a tendency toward a temporal

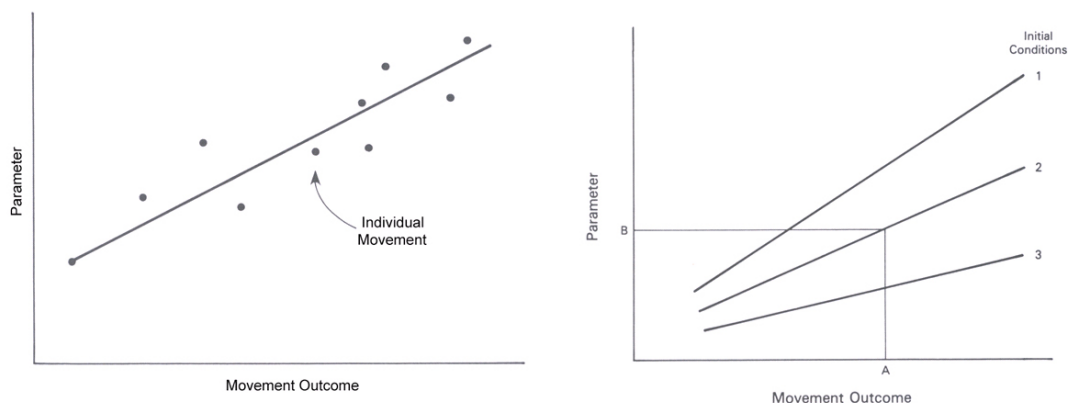


**Figure 2.6:** The hypothetical relationship between movement outcomes in the environment and the parameters used to produce them (left). The recall schema for different initial conditions (right) (adapted from Schmidt and Lee, 2005)

invariance is more impressive than some minor deviations (Heuer, 1991; Wulf, 1994). If one assumes, despite some contradictory results, that the bulk of the results support the GMP concept, then two questions remain unanswered: (1) How are the appropriate parameters selected? (2) How are errors recognized in sensory feedback? According to Schmidt (1975, 1982), within in the learning process the GMP is complimented via two schemas (or rules). After a GMP is selected in a given context and a movement is generated by adding the parameters, four types of information are stored in short-term memory: (1) the initial conditions before the movement, (2) the assigned parameters, (3) augmented feedback about the movement outcome, and (4) the sensory consequences of the movement. This information is stored until the performer can abstract two schemas about how the information is interrelated. The first schema is called the *recall schema* and is responsible for movement generation. This rule is a generalization of the relationship of the initial conditions, the assigned parameters and the movement outcome. The second schema is called the *recognition schema* and is responsible for movement evaluation. This rule is a generalization of the relationship of the initial conditions, the movement outcome and the sensory consequences. Thus, the recall schema is needed for open-loop control and the recognition schema is needed for closed-loop control. The development of both schemes is based on the same principle and is outlined below for the recall schema (Fig. 2.6). In figure 2.6, the movement outcomes, for example, the distance a ball traveled after being thrown, are presented on the X-axis. The Y-axis shows one of the parameters the individual has assigned to the GMP. The particular combination of the parameter and the resulting movement outcome can be thought of as a data point in a Cartesian coordinate frame. Correspondingly, each performance produces a new data point. During the learning process a pattern or a relationship that can be

represented by a regression line drawn through the data points emerges. Each time a new movement is produced, a new data point is created and the relationship is adjusted. After the adjustment, the various sources of information are deleted from working memory and only the rule, or schema, remains. Different initial conditions are represented by different regression lines (Schmidt and Lee, 2005). Because the GMP requires three parameters, the Cartesian frame in figure 2.6 has to be multi-dimensional. Theory predicts that practice under various circumstances should be most beneficial for the development of the two rules (*variability of practice hypothesis*). Much research on variability of practice has been conducted; however, the findings in this context are inhomogeneous (Van Rossum, 1990).

In the context of schema theory, the implication is that humans do not learn skills but learn *rules* about the functioning of their bodies. This concept is very important because storage of the rules requires less space than storage of a specific motor program for each movement. In addition, the schema concept suggests that an individual is able to perform new movements because he or she has learned how parameters, initial conditions, movement outcome and sensory consequences are interrelated.

#### 2.3.1.4 Discussion

The terms “information processing psychology” or “cognitive psychology” describe a research field in psychology which, in recent decades, was probably more successful than any other in experimental psychology (Neumann, 1993). In the field of human motor control and learning, the same might be said of the motor approach (in general) and the schema theory (in particular). Because of the large number of studies carried out in recent decades, it is not surprising that some findings contradict the motor approach and/or the schema-theory. Critical reviews of the motor approach as a scientific framework or paradigm in the field motor control and learning appear in Meijer and Roth (1988) or Roth and Hossner (1999). Also the strengths and weaknesses of the schema theory in particular appear frequently in literature (e.g. Wiemeyer, 1992a,b; Schmidt, 2003; Newell, 2003). In spite of this criticism, the concepts described above (Chap. 2.3.1) continue to appear in the latest editions of psychology textbooks (Hommel, 2008; Konczak, 2008), neuropsychology textbooks (Elsner, 2006), and in recent journal papers (Summers and Anson, 2009). In this thesis, the focus will be the potential for the numerous DOFs of the human motor system (Chap. 2.2) to be coordinated via GMPs to generate a movement. According to Schmidt and Wrisberg (2004, p. 143) a major role of a GMP is

”to organize the many degrees of freedom of the muscles and joints into a single unit to produce an effective and efficient action.”

Similarly, Schmidt and Lee (2005, p. 176) contend that GMPs

“have the capability to influence the activity of the many independent degrees of freedom so that they act as a single unit. If this temporary organization can

be imposed on the system, then the problem for the executive will have been simplified so that only a single degree of freedom will need to be controlled. In other words, the executive level is thought to control the selection of a motor program to ready it for action and to initiate it at proper time. Once underway, the program controls the individual degrees of freedom, and in this sense the executive is freed from the task.”

These are examples of typical cognitive views on motor control, in which all available DOFs are controlled by a motor program, corresponding to a fairly prescriptive top-down control approach. In other words, by selecting the appropriate GMP (e.g. grasp) and adding adequate parameters based on the recall schema, the CNS has solved all the problems discussed in chapter 2.2. During program execution, only minor corrections on the lower levels are possible to ensure that the movement is carried out faithfully. Schmidt and Lee (2005) do not explain how a GMP is formed or how an individual is able to perform a movement before any schema exists. Furthermore, there are two additional problems in the context of this thesis. The first problem concerns the neurophysiological plausibility of the introduced information processing model and the schema theory, and the second problem concerns the sensorimotor transformations needed to generate a movement.

The motor approach and the concept of motor programs are derived from cognitive psychology and have attracted attention in other disciplines such as robotics and neuroscience in recent decades. Therefore, the term or the idea of the motor program is used inconsistently and depends on the scientific discipline. It is often difficult to recognize whether the term is used as a metaphor for motor memory or according to the idea of a GMP as described above. As a metaphor, the concept of a motor program is not confutable and has only a limited explanatory value for the problem of how humans generate their movements and how they cope with excessive DOFs (Konczak, 1996, 2008). When used in the sense of a GMP, the neurophysiological correlation of the structures as presented in figure 2.5 need to be provided. The information processing model shows that there are two levels in motor control: an executive level including the three stages of information processing for movement planning and an effector level for movement production. Accordingly, the processing of information is carried out in form of a sequential process. In this context, Konczak (1996) refers to a scheme by Allen and Tsukahara (1974) that ascribes planning and programming activities to the association cortex, the basal ganglia and the lateral parts of the cerebellum. These structures correspond to the processes of response selection and response programming in the information processing model. In the primary motor cortex (M1), the output of the remainder motor areas are bunched and sent to the spinal motor neurons via the pyramidal tract. Certain areas of the cerebellum compare the intended movements with afferent sensory information from the periphery and if necessary, correct the intended movements. These structures correspond to the effector level of the information processing model (GMP level). Hence, neurons of the planning areas should encode other information (e.g. target

or goal of a limb movement) rather than neurons of the effector level (e.g. direction of limb movement). Alexander and Crutcher (1990) conducted a study in which monkeys executed pointing movements to defined targets. During the subject's performance, the activity of neural cells in the supplementary motor area, the primary motor cortex (M1) and the basal ganglia were recorded. The results indicate that both structures contain neurons that represent the goal of the limb movement and neurons that represent the direction of the limb movement itself. The observation that goal- and limb-dependent information are represented indicate that there is no clear distribution of tasks between areas of planning (e.g. basal ganglia) and areas of execution (e.g. M1) on a neurophysiological level. Furthermore, Konczak (1996) refers to a study by Dum and Strick (1991), in which it was shown that premotor areas in the frontal lobe not only project directly to M1, but also project directly to the spinal cord. It also seems that in most of the premotor areas, maps of the body comparable to M1 exist (He et al., 1993). Consequently, these premotor areas have the potential to influence the control of movements. The assumption of a one-to-one mapping of a cognitive function to a specific brain area does not appear to exist (Requin, 1992). Similarly, the sequential information processing postulated on a psychological level does not appear to exist on a neurophysiological level (Fig. 2.5). In summary, Konczak (2008) states that the control of human movements is not a strictly sequential process in which certain brain areas are activated one by one. The processing of sensorimotor information is instead parallel. However, parallel processing does not imply that there is no temporal order. It seems more likely that the sensorimotor system is hierarchically organized, but certain motor subsystem are simultaneously active during the different stages of planning and execution of human movements.

Furthermore, based on the assumptions of the schema theory, it appears that mental representations of the different movement classes exist in the brain. The Broadmann area 4 (M1) and Broadmann area 6 (premotor and supplementary motor cortex) seem to be plausible areas for the storage of motor programs because electrical stimulation of the areas leads to uncoordinated muscle contractions and to even more coordinated contractions, respectively. Furthermore, both structures contain motor maps of the human body, which appear as a distorted human figure drawn on the surface of the cortex, referred to as a *homunculus* (Latash, 2008a). Research in the area of neural population coding (Amirikian and Georgopoulos, 2003) suggests that there are no single neuron or group of neurons which could be assigned a specific innervation pattern of arm muscles or a specific joint configurations over time (e.g. a GMP "grasp"). More specifically, it seems that in cell populations in the motor cortex, the movement directions and the directions of the forces to be generated are coded. Moreover, it appears that a single cell participates in movements of various directions. In other words, a movement in a particular direction will engage an entire population of cells. Therefore, a unique signal for the direction of movement could reside in the activity of a neuronal ensemble. Georgopoulos (1996a)

proposed a vectorial code for the recovery of this signal from the neuronal ensemble (Chap. 2.3.3.1). Konczak (2008) suggests that the homunculus is not an intelligent agent that controls human movements. A certain topology does not imply a certain function for the control of human movements, but merely a certain way to save information. Additionally, the results of many neurophysiological studies revealed that somatotopic representations of the human body also exist in other parts of the CNS like the basal ganglia and the cerebellum (Latash, 2008a). Therefore, it is incorrect to assume that area 4 and area 6 are the exclusive neuroanatomical locations of motor memory or the place where GMPs are stored. A modular representation of human movements in the brain provides a number of evolutionary advantages. On the one hand, damage to brain during ontogenesis could be compensated for, and on the other hand, a relatively open and modular structure could enable a continuous adaptation and development of the brain during phylogenesis without complex reorganizations of large parts of the human brain (Roth, 2000).

In addition to the problem of the biological plausibility of the schema theory, it has to be discussed whether movement generation via the schema theory is possible. As an example, a relevant stimulus could be considered a glass of water in front of a thirsty individual. When the individual identifies the stimulus, an appropriate response needs to be selected. In the case of the glass of water, the response may be “reach for the glass” and “lead it to the mouth to drink”. The first response to be programmed is “reach for the glass”, which could be accomplished by the GMP “grasp”. When the GMP and the adequate parameters have been selected, the movement is specified and the GMP can be carried out. To be able to translate the external coordinates of the hand (starting position) and the glass (final position) to an adequate muscle activation leading to the desired hand trajectory, a series of complex and nonlinear motor transformations are necessary (Chap. 2.2). These transformations are not an issue in schema theory. Another problem is the postulated linear relationships in the recall and recognition schema. Schmidt (2003, p. 370) refers to this problem in the case of the recall schema as follows:

“But the more serious problem is that, with a GMP structured this way, it cannot account for actions involving gravity. One example is walking with a load, such as a backpack. Here, the extensor muscles, and those involved in the stance phase must operate differently as a function of the load; however, the flexor muscles and those involved with the swing phase can operate essentially independently of the load. Simply scaling all the muscles proportionately will not accomplish this. Another example is producing an action in different planes (e.g. horizontally vs. vertically); the effect of gravity in the flexors versus extensors will be different in horizontal versus vertical movements.”

There should only be a small number of movement classes in which the parameters of relative force and relative timing show a linear behavior. It is also unlikely that there are even two movements whose relative force and relative timing depend linearly on

each other. This leads again to a storage problem because the movement classes to be covered by a GMP are very small. Hence, a vast number of GMPs would be needed.

Within motor approach, however, there are conceptions of motor programs that are less prescriptive (e.g. Wulf, 1989; Rosenbaum et al., 1983). The problem with the less prescriptive and more emergent models is that additional constraints need to be added to cope with the released degrees of freedom. One possibility for dealing with the released degrees of freedom is to implement optimality principles such as the ones presented in chapter 2.3.3.1. Because these concepts did not become widely accepted like the schema theory, it is necessary to determine what the current trends concerning the field of human motor control are in cognitive psychology. Two developments or trends can be unmistakably observed. The first one is the increasing importance of neuroscience. Cognitive psychology seems to be developing toward a cognitive neuropsychology (Neumann, 1993; Rosenbaum, 2002; Prinz and Müsseler, 2008). The inclusion of neurophysiological methods and results in psychological research has led to doubts about the adequacy of the concept of sequential information processing as shown above. Although this process remains in use, it subsequently gave rise to new models about human information processing and action control. The second trend to be observed is that the *ideomotor principle* from James (1890) has been reestablished in the new models (Hommel, 2008). The idea is that voluntary action is gradually emerging from sensory motor experience. That is, novices are able to learn over time to form systematic relationships between movement patterns and sensory consequences. The representation of those consequences can thus be used in the future to anticipate wanted effects and at the same time, prime the action producing these effects (Hommel and Elsner, 2009). Models of this kind can be found in Hoffmann (1993), Hommel et al. (2001) and Hossner (2004). Although it has to be acknowledged that these models provide a powerful scientific framework for the integration of perception and action planning, it is necessary to mention that these models do not provide a strong explanation of how the human CNS, in detail, performs the complex computations needed to solve the problem of motor redundancy.

#### 2.3.2 Dynamical systems approach

In his seminal work on the philosophy of science, Kuhn (1962) demonstrated that knowledge and theory development in science are non-cumulative processes punctuated and disrupted by periods of paradigm crisis and competition. Over the years, some problems in the field of motor control have occurred to which the motor approach could not offer satisfactory results. In the late 1970s and early 1980s, a second paradigm evolved called the *dynamical systems approach*. The term *dynamic* does not refer to forces but to time changes. Compared to the previously introduced motor approach, the dynamical systems approach is a largely interdisciplinary approach. A very important school of thought in the dynamical systems approach is *synergetics*.

An overview on synergetics can be found in the textbook of Haken (2004), and the textbooks of Smith and Thelen (1993, 1994), Kelso (1995) and Birklbauer (2006) offer a general overview of the dynamical systems approach. Furthermore, several excellent confrontations of the two paradigms against the background of the Kuhnian view of science can be found in the technical literature (Summers, 1992; Piek, 1998). The goal of this chapter is to introduce the fundamental idea of the dynamical systems approach (Chap. 2.3.2.1). Based on these explanations, the concept of a *synergy* is introduced (Chap. 2.3.2.2) as a specific concept to address the degrees of freedom problem (Chap. 2.2) within the larger framework of the dynamical systems approach. In addition, the *uncontrolled manifold (UCM) hypothesis* is established as one possible mathematical basis for synergies (Chap. 2.3.2.3). Finally, the UCM is discussed in the context of the degrees of freedom problem (Chap. 2.3.2.4).

### 2.3.2.1 Key concepts of the dynamical systems approach

The center of the dynamical systems approach focuses on the question of how patterns are formed in complex systems. This chapter focuses on how movement patterns are formed in humans. The basic assumption is that patterns emerge in a self-organized fashion, without the need of entities telling the individual system parts what to do and when to do it. In other words, no executive agents or motor programs are required. Since movement patterns are continuously formed and changed, principles are needed that explain the evolution of movement patterns. Because of the complexity of the human motor system (Chap. 2.2), an explanation how a given pattern is constructed and how one pattern is selected from the myriad of possible patterns is needed (Kelso, 1995).

A complex system consists of a large number of parts and many different possible orderings of the parts. These different orderings are the *degrees of freedom* of the system. As outlined in chapter 2.2, the human body has many more DOFs than needed to perform a given task (Corbetta and Vereijken, 1999). However, the available DOFs are reduced because of constraints. Based on figure 2.1, constraints can be divided according to whether they originate in the individual, the task, or the environment (Newell, 1986).

In the dynamical systems approach it is assumed that movement patterns (e.g. walking) arise spontaneously as a result of the large number of interacting parts of the human body (e.g. neurons and muscles). The highly nonlinear interactions between various parts and between parts and the environment bring to mind the saying “the whole is greater than the sum of its parts.” Therefore, the complexity of the system and the nonlinearities make a predictive interpretation of the system’s behavior, based on the properties of the individual parts, impossible. The continuous interaction of the system parts on a microscopic level leads to a discrete change on a macroscopic level. Since biological systems, like humans, are *open, nonequilibrium systems* constantly interacting with the environment and thus exchanging energy and

information, a continuous process of information exchange and processing in the CNS on a microscopic level can lead to a change from one movement pattern to another on a macroscopic level. However, one has to keep in mind that the definition of a system level as micro- or macroscopic always depends on the research question.

The change from one system state to another is termed a *phase transition* or *state transition*, and the sum of all possible system states correspond to the *state space* of the system. Therefore, the term *stability* is usually used to describe existing states or identifiable forms of behavior. State transitions are preceded by *instabilities* called *critical fluctuations*. Unstable movement patterns can be considered predictors of change. These instabilities bring flexibility into the system and allow the evolution of new modes of functioning. The movement patterns before and after state transitions are comparatively stable and tend to be relatively resilient to change despite the nonequilibrium nature of the system. For example, if a person is walking and gradually increases the velocity, the walking pattern will become unstable with respect to time and fluctuations will begin to occur. If the velocity is increased further, the system will jump to a new stable state (i.e. running). The resulting running pattern is what physicists call a *collective* or *cooperative effect*, which arises without any external instructions. In this case, velocity is designated as a *control parameter*. The control parameter does not prescribe or contain any information about the new pattern, it simply leads the system through the state space. In other words, control parameters do not define the next state. If the velocity is decreased, the running pattern will become unstable. If the velocity is further reduced, another state transition will occur and the behavior of the system will revert to the walking pattern. The state transition from walking to running can occur at a different velocity than the state transition from running to walking. This phenomenon is called *hysteresis*.

Within a spectrum of possible system states, there are always a few dominant states that are comprised of *order parameters* or *collective variables*. Order parameters represent energetically favorable, attractive system states toward which a system progresses. Since order parameters represent attractive system states, they are also referred to as *attractors*. In human motor control, these attractors are the preferred modes of coordination. Collective variables or order parameters are created by the coordination of the parts of the system, but in turn influence the behavior of the parts. This is called *circular causality* and is a typical feature of self-organizing systems. Order parameters are usually found near phase transitions where the loss of stability gives rise to new system states and/or switching between system states (Kelso, 1995; Corbetta and Vereijken, 1999).

The dynamical systems framework has been used to analyze rhythmic movements (Haken et al., 1985) and discrete movements (Schöner, 1990). In this thesis, it is of special interest how the different components of the human motor system interact. This interaction forms a stable movement pattern and thus, the system is in the position to handle the excessive DOFs. To describe the interaction of the different parts of the human movement system (e.g. neurons and muscles), the concept of a

synergy is commonly used by proponents of the dynamical systems approach.

### 2.3.2.2 Synergies

In human motor control, the term *synergy* is usually associated with the work of Bernstein (1967, 1996). The concept is that a central command is sent from supraspinal structures that jointly and proportionally activate a group of muscles to form a synergy. Depending on the movement task, the central command sent to the synergy can change, leading to a corresponding change in all the muscles acting together to form the synergy (Latash et al., 2007). The notion of a muscle synergy can be extended to groups of muscles spanning multiple joints. In this context, the term *coordinative structures* is often used instead of synergy (Tuller et al., 1982; Fitch et al., 1982). However, not all authors use the terms synergy or coordinative structures in the same manner (e.g. Turvey, 1990; Turvey and Carello, 1996; Latash et al., 2007; Turvey, 2007; Latash, 2008b; Kelso, 2009). Some authors (Latash et al., 2004) argue that the term synergy is the most frequently used but least precisely defined term in the field of human motor control. Therefore, the notion of a synergy must initially be defined.

The author of this thesis prefers a definition of synergy that differs slightly from the classical definition presented above. In the classical view, the numerous DOFs are interpreted as a source of a computational problem for the CNS. This understanding of the DOFs problem is commonly accepted across the approaches discussed in this thesis. However, the view of Latash et al. (2007) on the redundant design of the human movement system differs. Latash et al. (2007) do not consider the numerous DOFs to be a computational problem for the CNS, but rather a luxury that enables the controller (CNS) to ensure the stability of important performance variables and the flexibility of patterns to deal with other task components and possible perturbations. Based on the idea that a reason exists for the design of the human body, the fundamental question concerning the problem of motor redundancy is (Latash et al., 2007, p. 279): “How does the solution to the DOFs problem leave the motor system more powerful than a system that starts with fewer DOFs from the outset?” To get an initial idea of how this question could be answered, Latash (2008b, p. 4) offers the following example:

“Imagine that you are conducting a choir. You want the choir to sing at a certain level of sound, but you have 50 singers to deal with. One strategy would be to tell each singer how loudly to sing. Potentially, this could solve the problem. If each singer performs exactly as instructed, this strategy will be very successful and lead to a perfectly correct level of sound. However, if one of the singers sings at a wrong volume, or gets sick and decides to quit altogether, the overall level of sound would be wrong. What would the alternative be? To make use of the fact that singers cannot only sing but also hear. Then, the

instruction could be 'Listen to the level of sound. If it is lower than necessary, sing louder; if it is louder than necessary, sing softer.' Now, even if one or more of the singers decide to quit, others will hear an 'error' in the overall level of sound and correct it without any additional instruction."

In both cases, the members of the choir sang together. In the first case, there was no synergy because everybody sang for themselves and did not pay attention to what the other members of the choir were doing. In the second case, a synergy existed because an individual's singing depended on how loudly the other members of the choir sang. If several members of a choir, or parts of a system, "work together" and adjust their actions based on the actions of the others or on how well the overall goal is being achieved, then they form a synergy. Latash et al. (2007) and Latash (2008b) distinguish three components of a synergy: (1) *sharing*, (2) *flexibility/stability* and (3) *task-dependence*. In technical literature, the second component is sometimes referred to as error compensation (Latash et al., 2004).

**Sharing** If a person grasps a glass of water with the thumb opposing the four fingers, the fingers need to produce a force that is equal to or slightly greater than the weight of the glass to be able to lift it and prevent it from slipping. Usually, all digits contribute to this task and thus share the task in some way.

**Flexibility/stability (error compensation)** If the person grasps a glass as described above and then lifts their index finger while leading the glass to their mouth, the finger has stopped contributing to the task of manipulating the glass. To prevent the glass from slipping, the remaining three fingers opposite the thumb have to redistribute their efforts so that the total force again equals the weight of the glass.

**Task dependence** The third component concerns the ability of a synergy to change its functioning in a task-specific way. In other words, the ability to form a different synergy in a different task with the same elements. The hand cannot only grasp a glass of water, but also write with a pen, open a bottle, or play a guitar. More precisely, synergies always do something and thereby the elements "work together". There exists no abstract synergy

To address the sharing component of synergies, *principal component analysis* (Mah et al., 1994) or more sophisticated *matrix factorization methods* (Tresch et al., 2006) are used. To quantify the flexibility/stability (error compensation) of a synergy, the concept of the UCM is used and is discussed in the next chapter. Overviews of the computational tools used to study synergies can be found in Schöner and Scholz (2007), Latash et al. (2007), Latash (2008b) and Müller and Sternad (2009).

### 2.3.2.3 Uncontrolled manifold hypothesis

Unlike robots, human beings are incapable of performing the same movement twice; there is always some variability (Bernstein, 1967). One of the features of a synergy is flexibility/stability (error compensation), which implies that effects of deviations in the contribution of one element of a synergy can be compensated for via adjustments in the contributions of the other elements. Therefore, the analysis of the variability of elements may help to understand whether a set of elements is united in a synergy and what the synergy tries to accomplish (Latash, 2008b). In this context, a promising computational approach for the quantification of synergies is based on the ideas of Schöner (1995). These ideas have been enhanced by Scholz and Schöner (1999) and are now known in technical literature as the *uncontrolled manifold (UCM) hypothesis*. In this chapter, a simple example is used to show the main concept of this approach. Latash et al. (2004) and Latash (2008b) provide a generalization of this approach to more complex tasks and offer a review of studies conducted in the context of the UCM hypothesis. A general scheme of analysis within the UCM approach can be found in Latash et al. (2007).

Biological systems control their movements using hierarchically organized multi-level structures and the CNS does not select a unique trajectory based on optimization (Chap. 2.3.3.1) but facilitates families of solutions that are equally capable of solving the movement task at hand. Furthermore, the proponents of this approach distinguish between *elemental variables* and *performance variables*. In the previous example of manipulating a glass of water, the forces and moments produced by the digits of the hand can be viewed as elemental variables, whereas the total grip force, the total resultant force, and the total moment of force produced on the object can be viewed as a performance variable. The distinction between elemental and performance variables always depends on the level of analysis as explained in the context of microscopic and macroscopic levels in chapter 2.3.2.1. For example, in the case of how individual muscles are coordinated to produce the force of a finger, the elementary variables and the performance variable refer to the level of muscle activation and the overall finger force, respectively. An important conclusion in this context is that in most cases, the individual elements of a synergy are themselves synergies on a different level of analysis (Latash, 2008b).

As an example, a subject is asked in a laboratory task to produce a total peak force of 40 N by quickly pressing on two force sensors with their two index fingers. An infinite number of finger force combinations can satisfy the task:  $F_{TOTAL} = F_1 + F_2$ . After a certain amount of practice, the subject is able to perform the task adequately. A series of trials is then collected and each of trial can be characterized by two force values called elementary variables. In figure 2.7, possible results of such an experiment are presented. In the left portion of the figure, the individual outcomes of each trial are distributed evenly around a center point corresponding to an average force-sharing pattern of approximately 50 : 50 between the two index fingers. This

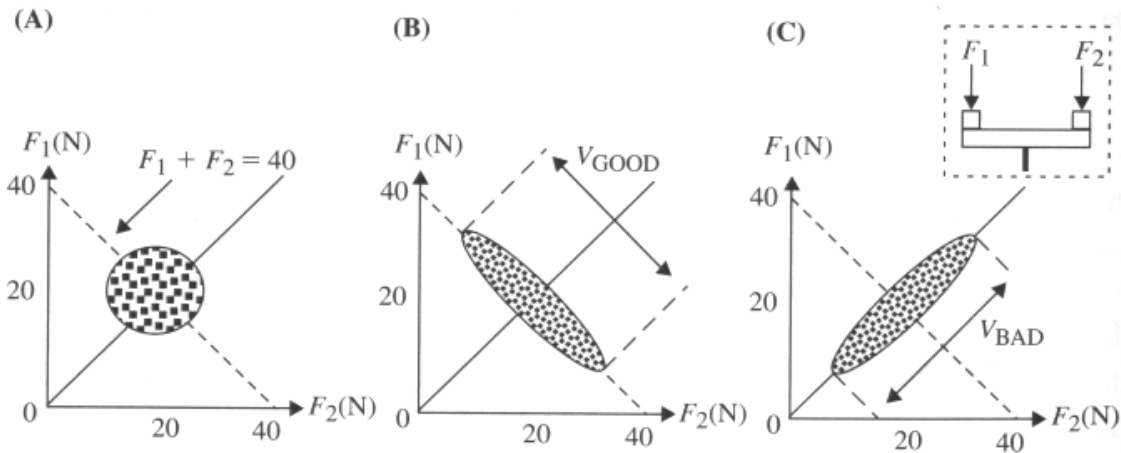


**Figure 2.7:** Three plots of data points representing possible outcomes of an experiment. (A) The data points form a circle about an average value representing sharing of the total force between two fingers. (B) The data points form an ellipse elongated along the line  $F_1 + F_2 = 40$  (dashed line). In the third plot (C), the ellipse is elongated perpendicular to the dashed line. The variance along the dashed line in (B) does not affect the total force (good variance,  $V_{GOOD}$ ) whereas the variance along the solid line does affect the total force (bad variance,  $V_{BAD}$ ) (adapted from Latash, 2008b).

circular distribution shows that if one of the two index fingers produces a higher peak force than its average contribution in a particular trial, the second index finger will reduce or amplify this error with an equal probability. Hence, there is no error compensation between the two fingers and therefore no synergy that stabilizes the total force output. The average forces of the two index fingers are the same in the middle plot (Fig. 2.7, (B)) as in the plot on the left (20 N). However, the data points from the individual trials form an ellipse elongated along a line with a negative slope ( $F_1 + F_2 = 40$ ) instead of a circle. In this case, there is a covariation between the two index fingers. This covariation reduces the error in total force if one of the two fingers produces more or less force than average. This behavior may be interpreted as a force-stabilizing synergy. A narrow ellipse would correspond to a strong synergy stabilizing the total force and a wider ellipse would correspond to a weaker synergy with a higher variance. In the right plot (Fig. 2.7, (C)) the elliptical cloud of data points is elongated along a line with a positive slope. In this third example, the covariation leads to a destabilization of the total force and thus, there is no force-stabilizing synergy (Latash, 2008b).

In the two-finger force production example, two one-dimensional subspaces can be identified. One subspace corresponds to the movement task (constant force value of 40 N), while the other subspace is orthogonal to the first. The distribution of

data points in the middle plot (Fig. 2.7 (B)) has most of the variance in the first subspace, while the distribution of data points in the right plot (Fig. 2.7 (C)) has most of the variance in the second subspace. The first subspace is called the UCM of the task and the second is referred to as its *orthogonal complement* (Latash et al., 2004; Latash, 2008b).

In regards to the DOFs problem, the CNS does not need to interfere as long as the movement system does not leave the UCM. This means that the controller allows the elements to show a high variability as long as this variability does not affect the performance variable in a negative way. If the movement system leaves the UCM, an error in the performance variable occurs and the CNS has to introduce a correction (Latash et al., 2004; Latash, 2008b).

Latash et al. (2007) also discusses possible neurophysiological foundations of synergies. For example, it has been shown in neural recording studies that task-specific and relatively high-level features of motor tasks are likely represented in the human brain (Chap. 2.3.3.1). These studies revealed that patterns of neural activity are related to performance variables such as the trajectory of the hand or the force vector applied to the hand (Georgopoulos et al., 1982; Schwartz, 1993; Cisek and Kalaska, 2005). In addition, several studies analyzed spinal mechanisms in multi-joint control in frogs (Giszter et al., 1993, 2000; Hart and Giszter, 2004). These experiments showed that the spinal cord cannot be viewed as a simple relay of central commands to the periphery. In fact, these studies support the computationally attractive idea that control is achieved by activating a few *motor primitives*. Motor primitives can be interpreted as patterns of muscle activations. Therefore, the control of the musculoskeletal system can be simplified because only a small number of motor primitives need to be controlled in task-specific configuration instead of individual muscles. The motor primitives could be interpreted as functional groupings or synergies. Berkinblit et al. (1986) showed that spinalized frogs (the spinal cord is cut at an upper region and consequently separated from the brain) are able to produce successful wiping responses on the first trial after a joint has been constrained. In summary, the results from the neurophysiological studies could be interpreted to mean that central commands from supraspinal structures activate motor primitives or synergies on the level of the spinal cord. These structures seem to possess a certain flexibility needed to stabilize task relevant performance without relying on supraspinal control structures.

### 2.3.2.4 Discussion

In chapter 2.3.2.1, a short overview on the dynamical systems approach was provided. As noted above, though, the dynamical systems approach is largely interdisciplinary and a comprehensive review was beyond the scope of this thesis. Although the concept of a synergy is commonly used to address the degrees of freedom problem in the dynamical systems approach, there exist different views on synergies (Chap. 2.3.2.2)

and different computational tools to analyze synergies (Chap. 2.3.2.2). However, the definition provided in this thesis and the concept of the UCM are, at present, the most promising approach to the DOFs problem as seen in the larger framework of the dynamical systems approach. Therefore, as presented in chapter 2.3.1.4, it should be asked whether it seems plausible that the many DOFs of the human body (Chap. 2.2) can be coordinated via the control structures introduced in this chapter to generate a movement. It bears mentioning that the first paper on the UCM hypothesis was published relatively recently (Scholz and Schönner, 1999), and this concept is in its infancy compared to those discussed in chapter 2.3.1.4. Nevertheless, additional research has been conducted since then, and some problems are beyond what might be considered “teething troubles”.

One of the major methodological challenges is that most studies used data that focused on a specific time during a motor act over several trials to quantify the two components of variance. In other words, data distributions with respect to certain UCMs at specific points in time of a trajectory were analyzed. However, it seems plausible that an UCM evolves during a movement. Even though the same performance variable is stabilized during the movement, it is possible that the variable is stabilized at different values corresponding to different subspaces inside the state space of the system. Therefore, proponents of this approach classify the reconstruction and quantification of the time evolution of the variance components with respect to an evolving UCM as a major challenge (Latash et al., 2004).

To be able to stabilize a performance variable, the elements of a synergy need to monitor the changes in the performance variable and/or changes in the outputs of all the elements comprising the synergy. However, monitoring the changes of the performance variable appears to be most important. If the movement system leaves the UCM, the controller has to interfere. Because of time delays in sensory information processing, such sensory information sent to the controller may be obsolete during fast movements. So the question arises as to what extent spinal feedback-loops have the ability to induce corrective changes in elements to bring the movement system back into the UCM (Latash et al., 2004).

Although the neurophysiological foundations of synergies seem to be much more plausible than in case of the GMPs, it has to be noted that it is still heavily debated in the neuroscience community what exactly is represented in supraspinal structures (Chap. 2.3.3.1). Some studies in the context of the UCM hypothesis considered joint rotations at individual joints as independent variables manipulated by the CNS. In addition to the problem that it is not currently known whether the CNS has direct access to variables such as joint angles, it is questionable if joint angles can be manipulated independently in a multi-body system that consists of coupled limbs. Thus, the design of the human body can lead to results that are an outcome of the system design rather than of control. So the main question yet to be answered is (Latash et al., 2004): What are the independently controlled variables that are used by the CNS to generate a movement?

### 2.3.3 Computational neuroscience approach

In the human brain, billions of neurons are interconnected forming one of the most complex structures nature has ever produced. In terms of complex patterns of activity occurring over populations of neurons, this network of neurons is able to process an enormous amount of information within a split second. Until now, no technical system has existed that works as reliably and quickly as the human brain. *Computational neuroscience* is an interdisciplinary field of research in which mathematicians, physicists, engineers, biologists, physicians, and psychologists jointly combine biomedical and biomechanical experiments with mathematical modeling to gain insight into the functioning of the human brain. Schaal (2007a) divides the field of computational neuroscience into two areas: the *low level* and the *systems level*. Low-level computational neuroscience focuses on models of the neurons, channel dynamics, computational abilities of individual neurons and smaller neural networks. The systems-level focuses on how the CNS accomplishes behaviors like object recognition, visual attention, decision making and reinforcement learning. Computational neuroscience on the systems-level can be divided into different research topics including perception, memory, learning and sensorimotor control. The problems treated in this thesis are on the systems-level and related to the topic of sensorimotor control.

From the perspective of computational neuroscience, the sensorimotor system allows humans to perform actions to achieve goals in an uncertain and constantly changing environment. The computational study of sensorimotor control is fundamentally about the transformation of sensory signals into motor commands and vice versa. The coupling of these two transformations forms a sensorimotor loop. The transformation from motor commands to sensory signals is governed by the physics of the outside world, the musculoskeletal system and the sensory receptors. Within this framework, it is assumed that this transformation is represented internally in CNS. Models that cover this motor-to-sensory transformation are known as *forward internal models* or simply, *forward models*. These models predict the future behavior of the human body and the outside world. Therefore, they are sometimes referred to as *predictors* in literature (Wolpert and Ghahramani, 2000). Models that represent the sensory-to-motor transformation are called *inverse internal models* or simply, *inverse models*. Because of the complexity of the human sensorimotor system (Chap. 2.2), a simple look-up table for the transformation of sensory signals to motor commands and vice versa does not seem probable. A less complex representation for the control of the human sensorimotor system can be defined as the *state* of the system. The state is a set of time-varying parameters that together with the fixed parameters of the system, the equations of motion of the body, the outside world and the motor output, allow for a prediction of the consequences of an action. For example, if a prediction is needed for how a pendulum will respond to an applied torque, knowledge of the pendulum's angle and angular velocity is required. Together, this information forms the state of the pendulum. The fixed parameters in this example would be the

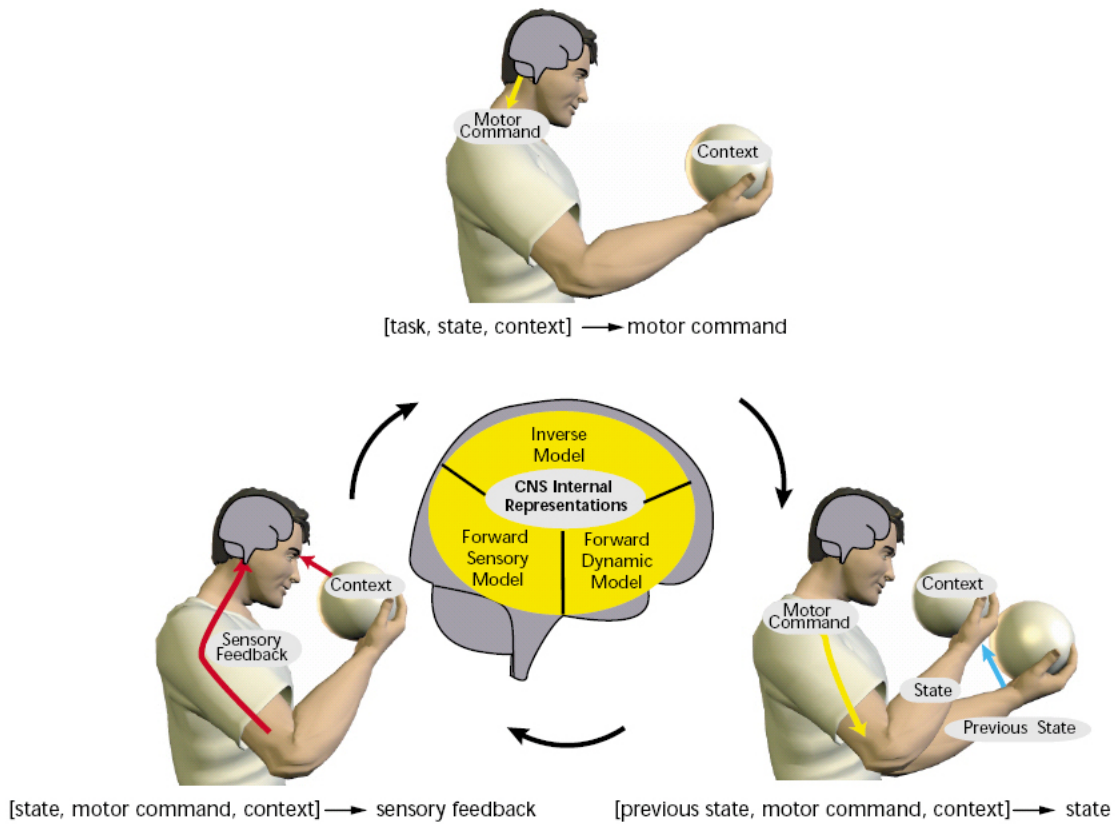


**Figure 2.8:** The sensorimotor loop consists of motor command generation (top), state transition (right) and sensory feedback generation (left). The internal representations of the three stages within the CNS are shown in the middle (Wolpert and Ghahramani, 2000)

length and the mass of the pendulum. With regards to the movement of the hand, the state can refer to muscle activations or the position and velocity of the hand in a goal-directed movement and change rapidly during the movement. Other key parameters such as the identity of the manipulated object or the mass of the limb change more discretely or on a slower time-scale. These slowly changing parameters are referred to as the *context* of the movement. The ability of individuals to show an accurate and appropriate behavior relies on the adaptation of motor commands to the current movement context (Wolpert and Ghahramani, 2004). Wolpert and Ghahramani (2000) divide the above mentioned sensorimotor loop into three stages (Fig. 2.8) that comprehend the overall behavior of the sensorimotor system. The first stage specifies the motor commands generated by the CNS based on a particular task and the current state. The motor commands will cause a movement, which in turn causes a change of the current state. The new state is determined during the

second stage. In the third stage, the sensory feedback is specified given the new state. It is assumed that these three stages are represented in the CNS in terms of internal models, being the inverse model, the forward dynamic model, and lastly, the forward sensory model. The three stages of the sensorimotor loop depicted in figure 2.8 represent a general framework of computational motor control which is outlined in more detail in the following chapters. As supported by Wolpert and Ghahramani (2004), the following sections discuss how movements are planned (Chap. 2.3.3.1), motor commands are generated (Chap. 2.3.3.2), and states (Chap. 2.3.3.3) and contexts (Chap. 2.3.3.4) are estimated. The following review does not address how internal models are learned. An introduction to sensorimotor learning in the context of internal models can be found in Wolpert et al. (2001); Wolpert and Flanagan (2003). Finally, the concepts that deal with the degrees of freedom problem are discussed (Chap. 2.3.3.5).

### 2.3.3.1 Task: Motor planning

The computational problem of motor planning arises from the redundancy of the human motor system. To solve the problem of motor planning two questions need to be answered:

1. What principles or rules does the CNS use to select one trajectory from the plethora of possible trajectories?
2. On which level do these principles or rules work and in which coordinate frame is the trajectory planned?

It is unsurprising that this approach, in the context of movement planning, led to the development of different and sometimes incompatible models (Hermens and Gielen, 2004). For example, some models assume that the CNS plans an entire trajectory in advance of the movement onset (Flash and Hogan, 1985; Uno et al., 1989). Other models do not depend on a precomputed desired trajectory (Hoff and Arbib, 1993; Ijspeert et al., 2002). In this chapter, results of three different experimental paradigms including psychophysical studies, neural recording studies, and optimization studies are reviewed.

#### Psychophysical studies

One of the main difficulties in assessing human motor control is that control strategies of the CNS cannot be directly accessed. In this context, a key assumption in motor control research is that information about these strategies can be deduced from behavioral regularities (Bernstein, 1967). Therefore, in order to understand fundamental control principles, one must begin by observing the system's behavior under various conditions. These observations will likely lead to a definition of general features or principles of the system's behavior. Given the redundancy of the human motor system, it is quite surprising that in unconstrained point-to-point reaching

movements, the human CNS does not appear to use the full repertoire of possible trajectories but produces movements with several invariant features. In a pioneering study, Morasso (1981) showed that in multi-joint arm movements, the hand paths between pairs of targets in the horizontal plane are roughly straight in external Cartesian space with single-peak, bell-shaped velocity profiles regardless of the initial and final location of the hand (Fig. 2.9). In contrast, when the trajectories of the hand were expressed in joint coordinates, the profiles were more complex and variable. These results were subsequently reproduced in a number of studies (Abend et al., 1982; Flash and Hogan, 1985; Gordon et al., 1994; Haggard et al., 1995). Because of the anatomical design of the human arm, joint rotations are needed to translate the hand from the starting position, along the planned trajectory, to the target location. Hence, the coordination process would imply a coordinate transformation from external hand space into joint space. This problem is called the inverse kinematics problem (Zatsiorsky, 1998) and it is known from robotics that this inverse computation has no unique solution (Craig, 2005). To resolve the joint redundancy, additional constraints need to be defined as it is done in the context of optimization models (Kawato, 1996). The constraints or combination of constraints used by the CNS is still under debate (Gielen et al., 1995). The results of the study conducted by Morasso (1981) do not seem to be uniformly valid (Atkeson and Hollerbach, 1985; Desmurget et al., 1996; Desmurget and Prablanc, 1997). For example, Atkeson and Hollerbach (1985) observed that hand paths in a vertical reaching movement were sometimes curved and that the amount of curvature varied as a function of the initial and final location of the hand, while the velocity profiles of the hand were the same for straight and curved movement paths. Despite such exceptions, the regularity of the roughly straight hand paths in external space with the single-peak, bell-shaped velocity profiles characterize a large class of movements and led, in combination with the more complex joint angular positions and velocity profiles, to the hypothesis that goal-directed movements like reaching toward an object are planned in external coordinates of the hand and not in internal coordinates (e.g. joint space) (Morasso, 1981; Hollerbach, 1982; Flash and Hogan, 1985; Ghez and Krakauer, 2000).

Flanagan and Rao (1995) compared two-joint planar reaching movements. During the movements, the subjects were not able see their hands but were provided visual feedback of the movement trajectory in either hand space or joint space on a computer monitor. In the hand space condition, the cursor on the monitor corresponded to the Cartesian coordinates of the hand. In the joint space condition, the cursor corresponded to the shoulder and elbow angles of the arm, where the shoulder angle was the ordinate and the elbow angle was the abscissa in terms of Cartesian coordinates. When the movement trajectory was displayed in hand space, the participants produced straight hand trajectories at the expense of curved joint trajectories after only several practice trials. In the joint space condition, considerably more trials were required before straight cursor paths on the monitor were produced. Straight movements of the cursor in the joint space condition corresponded to curved hand

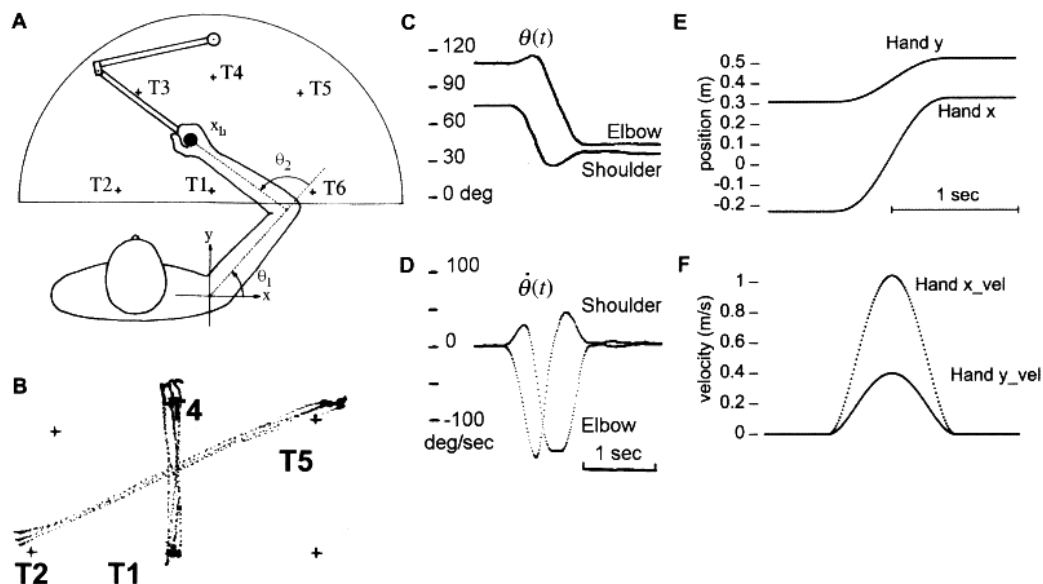


**Figure 2.9:** In the classical study by Morasso (1981), subjects performed point-to-point reaching movements in the horizontal plane using a mechanical linkage to track the movements (A). The trajectories of the hand between the targets (e.g. T1-T4, T2-T5) are approximately straight (B). Joint angles (C) and joint angular velocities (D) were more complex than hand paths (E) and hand velocities (F) (adapted from Shadmehr and Wise, 2005).

trajectories. Therefore, subjects moved the cursor almost directly to the target in visual coordinates regardless of the trajectories of the hand in Cartesian coordinates and the changes in joint coordinates.

Wolpert et al. (1995a) used kinematic transformations to investigate whether arm trajectories are planned in kinematic or dynamic coordinates. Subjects had to perform point-to-point arm movements, and during the movements, the visual feedback of the hand position was altered so that the subject perceived roughly straight hand paths instead of curved paths. The perturbation was at a maximum at the midpoint and was zero at the starting and end points of the movement. If trajectories are planned in kinematic hand coordinates, an adaptation to the perceived curvature of the hand trajectory in the opposite direction is expected to reduce the visually perceived curvature and produce a roughly straight hand path. If trajectories are planned in dynamic coordinates, no adaptation in the underlying planner should be found, provided that the desired movement end point can still be achieved. However, Wolpert et al. (1995a) observed corrective adaptations, meaning that after a few trials, subjects altered their hand trajectories such that the real trajectory moved in an arc to the right, when in fact the displayed hand location moved in an almost straight

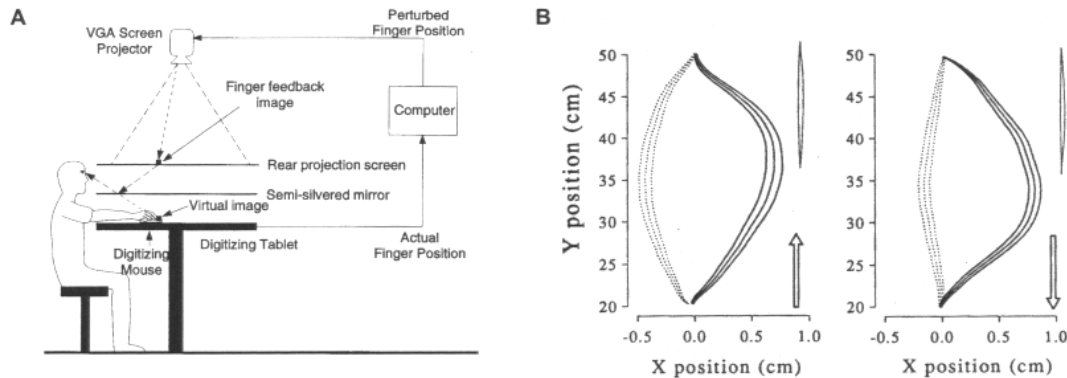


**Figure 2.10:** Experimental apparatus for the analysis of human arm trajectories under altered visual feedback (A). The movement of the hand was captured online by a computer, and perturbed and projected onto a screen as a white filled square. Looking down at a mirror, the subject could only see the perturbed cursor but not their hands. Among other activities, the subjects performed movements in the sagittal plane, toward and away from their body. (B) The dotted lines represent the mean hand trajectories with the standard deviation in the unperturbed condition. The solid lines represent the hand trajectories of the visually perturbed condition. The X-axis is enlarged to show the details. The vertical scale of the mean paths is shown on the right. The two arrows represent the movement direction (adapted from Wolpert et al., 1995a).

line (Fig. 2.10). These results suggest that trajectories are planned in visually-based kinematic coordinates and that spatial perception plays a fundamental role in trajectory planning. A trajectory planning in dynamic coordinates is incompatible with the results of the study.

In summary, the results of the studies by Wolpert et al. (1995a) and Flanagan and Rao (1995) suggest that given the choice between a trajectory that looks straight in visual coordinates and one that is straight in reality, the CNS appears to generate a visually straight trajectory (Shadmehr and Wise, 2005). In other words, there is strong evidence that the CNS plans visually guided reaching or pointing movements in a perceptual (i.e. visual) frame of reference.

Studies by Miall and Haggard (1995) and Sergio and Scott (1998) however, suggest that visual feedback itself is not sufficient to explain why subjects tend to produce visually straight hand paths. Both studies analyzed congenitally blind individuals who had never experienced visual feedback. Nevertheless, these subjects produced roughly straight reaching movements. Their hand paths sometimes showed less curvature than the hand paths of non-blind subjects. In almost all of the discussed studies, subjects did not produce perfectly straight hand paths, but hand paths that were nearly straight. It is possible that blind subjects are able to produce straighter move-

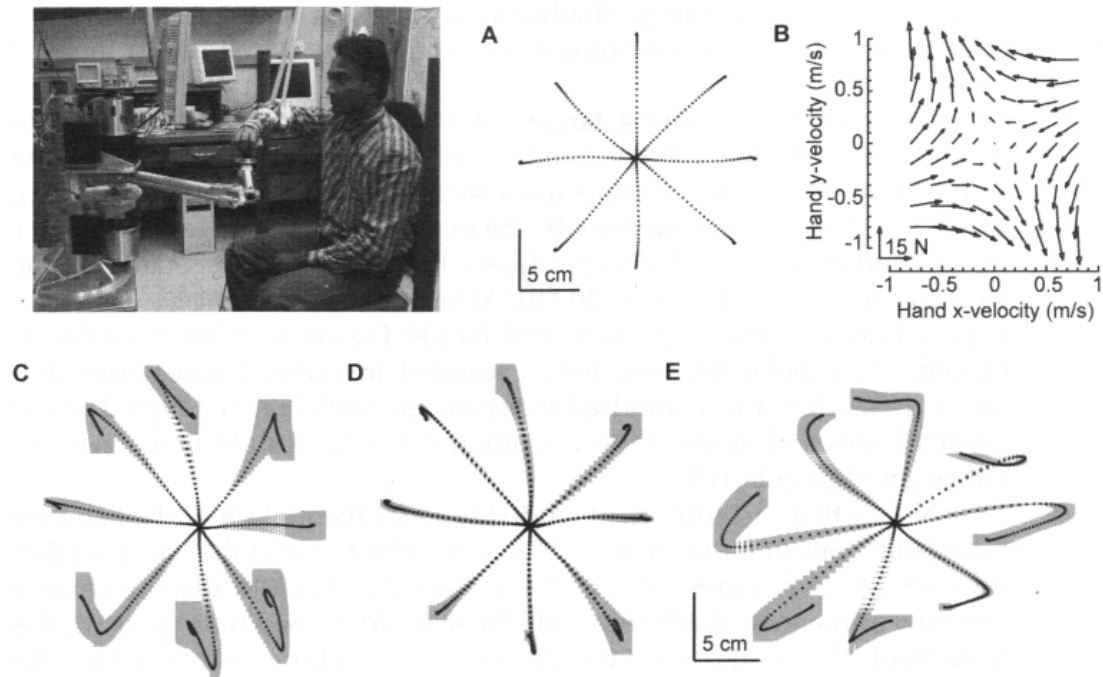


**Figure 2.11:** Subjects held the handle of the robot and reached toward a target (top left). Trajectories of the hand under null-field condition (A). Force fields are produced by the robot and the forces are plotted as a function hand velocity (B). Average hand trajectories of the first 200 trials under force field condition (C). Average hand trajectories of the trials 600-800 under force field condition (D). Average hand trajectories after the force field was occasionally turned off again (E) (adapted from Shadmehr and Wise, 2005).

ments because they do not experience any visual misperception of space. In other words, the visual system of humans distorts Cartesian space making slightly curved movements in Cartesian space appear straight in visual coordinates. The human CNS therefore may try to make straight-line movements in visual coordinates, but the actual movement produces a gentle curvature in Cartesian coordinates (Miall and Haggard, 1995; Shadmehr and Wise, 2005). In the case of the blind subjects, proprioception provides the only source of feedback to correct deviations from straight-line hand paths. Therefore, it could be argued that blind persons have a higher than normal ability in proprioceptive estimates of straight lines and that they use this ability to ensure that their movements are straight.

Shadmehr and Mussa-Ivaldi (1994) investigated how reaching movements are affected in the presence of externally imposed force fields produced by a robot manipulator. Subjects had to perform reaching movements while holding the end-effector

of the manipulandum. The targets were provided via a monitor. Under the null-field condition, subjects produced nearly straight hand trajectories (Fig. 2.11A). After recording initial trajectories, the force field was turned on and the strength of the force field was dependent on the velocity of the hand (Fig. 2.11B). Hand movements under the force field condition deviated significantly from the roughly straight-line hand paths (Fig. 2.11C). With practice, the trajectories of the hand in the force fields converged toward a path very similar to that produced before the perturbation (Fig. 2.11D). After the subjects were trained under force field condition, the force field was occasionally turned off. The resulting hand trajectories almost resembled mirror images of trials when the force field was turned on. It appears that when something disturbs the human arm during movement, like an unexpected external load, movements lose their smooth and regular characteristics. However, provided these disturbances are highly predictable, practice leads to straight hand trajectories. This convergence toward a straight and simple hand trajectory supports the idea that the human motor system plans movements in terms of extrinsic coordinates of the hand rather than in intrinsic coordinates (e.g. joint angles or muscle activations) (Wise and Shadmehr, 2002).

In summary, all of these studies showed roughly straight hand paths for both blind and sighted subjects, and even after adaptation when moving the arm against unusual loads. The results emphasize that the human motor system has a strong tendency to generate goal-directed reaching movements with relatively straight hand paths. Taken together, the results largely support the idea that arm trajectories follow a kinematic plan that is formulated in extrinsic kinematic space, independent of movement dynamics or external force conditions.

In contrast, Soechting and Lacquaniti showed in a series of psychophysical experiments (Soechting and Lacquaniti, 1981; Lacquaniti and Soechting, 1982; Soechting and Lacquaniti, 1983) in which subjects had to perform a goal-directed two-joint movement in the sagittal plane, that both joints reached their peak angular velocities at the same time and that the ratio of the peak velocity at the elbow to the peak velocity at the shoulder is equal to the ratio of the angular excursions of the two joints. The results were interpreted by the authors as evidence that movements are planned in intrinsic coordinates. Hollerbach and Atkeson (1984) challenged the conclusion by noting that at the same time the joint ratios were constant, the trajectories of the hand were almost straight in the above cited studies. This mutually contradictory result of straight lines in hand and joint space had been resolved by Hollerbach and Atkeson (1984) in favor of straight lines in hand space because of an experimental artifact in the case of two-joint kinematics near the workspace boundaries. In addition to these studies where the argument for a planning of movements in terms of joint angles seems to be attributed to the movement task, a few other researchers have suggested that reaching movements are planned on joint level because of internal control (Kaminski and Gentile, 1986; Hollerbach and Atkeson, 1987; Flanagan and Ostry, 1990; Desmurget and Prablanc, 1997).

In summary, it seems that both planning spaces are supported by a large number of experimental results. After a review of the experimental settings of several of the above mentioned studies, Desmurget et al. (1997) showed that there is an important methodological difference between the experiments describing straight and curved trajectories of the hand, namely the presence (constrained) or absence (unconstrained) of a tool that is used to track the movement (e.g. a pen or a manipulum). The results of the Desmurget et al. (1997) study indicate that in the absence of a tool, the trajectories of the hand do not appear to be programmed to follow a straight line in contrast to constrained movements. Therefore, Desmurget et al. (1997, 1998) suggest that constrained and unconstrained movements involve different planning strategies. However, it should be noted that kinematic regularities could also result from planning movements in an internal dynamical space (Uno et al., 1989; Nakano et al., 1999). Finally, some authors suggest that movement planning takes place on both levels, kinematic and dynamic (Soechting and Flanders, 1998).

Behavioral research has discovered various regularities in human goal-directed movements. These invariants have become central to understanding human sensorimotor control as they appear to suggest some fundamental organizational principles used by the CNS. The problem is that it is hard to determine on which level these invariants arise (Schaal et al., 2003). On the basis of the above discussed results, it is currently impossible to identify the level or space in which human movements are planned.

### **Neural recording studies**

In addition to the above presented studies, numerous neural recording studies have addressed the question about in which coordinate system movement planning takes place. In these studies, the neural activity of primates was recorded in an effort to link patterns of neural activity to one or more behavioral variables. Electrical stimulation was used to identify specific motor effects in the cerebral cortex in primates and humans. The results of these studies were correlated with clinical observations on the effects of local lesions. The area in which the lowest intensity stimulation initiated a movement is known as the *primary motor cortex (M1)*. M1 is organized *somatotopically*, denoting the existence of a *motor map* of the body laid out in the brain structure. The motor map is represented by the structure of a distorted human figure called a *homunculus*. The representation is characterized by disproportionately large areas for body parts such as fingers, hands and the face, which enables a fine control or coordination of movements in these parts of the body (Krakauer and Ghez, 2000). However, studies exist that challenge the homunculus representation (Schieber, 2001). The stimulation of adjacent areas in M1 does not necessarily induce motion of the same or adjacent body parts. Furthermore, the same body part can be moved by stimulating nonadjacent cortical areas. As a result, the representation of the human body in M1 seems to be rather mosaic and M1 does not appear to contain a one-to-one mapping of cortex areas to body parts or muscles. In addition, substan-

tial *convergence* and *divergence* of cortical projections exist. Substantial convergence means that the stimulation of different cortical cells activates the same group of motor units and leads to similar movements. Substantial divergence means that the stimulation of one cortical cell can activate different groups of motor units and move different parts of the body (Latash, 2008a). In addition, it should be noted that other regions of the brain, like the premotor areas or the cerebellum, also contain motor maps and that the somatotopic organization of M1 is plastic, indicating the possibility of an alteration following injury and/or motor learning (Krakauer and Ghez, 2000; Latash, 2008a). In neuroscience there is little disagreement that the M1 plays a fundamental role in the control of voluntary arm movements such as reaching for and grasping objects. M1 receives sensory input from the periphery and reciprocal input from other brain regions involved in motor control such as the basal ganglia and cerebellum. Furthermore, M1 provides the largest contribution to the descending corticospinal tract, sometimes even directly contributing to the alpha-motoneurons (Scott, 2003). Therefore, the following question arises: What information is encoded in a single neuron or a population of neurons in M1? Based on the idea that planning and executing arm movements requires a set of coordinate transformations (Chap. 2.2), it is of great interest where M1 is located in this set of transformations. After decades of research on this area of the brain, it seems plausible to assume that the role of M1 in the control of voluntary arm movements might have been uncovered. However, considerable debate still exists as will be discussed below.

Early studies of M1 used movements about a single joint to analyze the relationship between cell activity and parameters of limb activity (Evarts, 1968, 1969). Similar studies were undertaken for the cerebellum (Thach, 1970a,b), basal ganglia (DeLong, 1973) and spinal cord (Courtney and Fetz, 1973). The idea of these early studies was that the coding of motor output could be best understood by reducing movement to its elemental unit, rotation about a single joint. However, almost all voluntary movements require a precise activation of many muscles to rotate multiple joints in such a way that the hand reaches the object of interest. The generation of such a movement involves more than a simple linear combination of isolated single-joint rotations (Kalaska, 2009). This led to the question of whether neurons in M1 directly control the patterns of muscle activation or more global parameters like movement direction or movement extent in multi-joint movements. An influential study was conducted by Georgopoulos et al. (1982). In the study, monkeys were trained to move their right arm in eight different directions within a workspace to targets arrayed in a circle at  $45^\circ$  intervals around a central starting location. As shown in figure 2.12, the movements started from the same point and had the same amplitude. During the monkey's movements, the activity of 606 cells in M1 was recorded and 323 of the 606 cells were shown to be active during the task. The frequency of discharge of 241 of the 323 cells varied with movement direction in an orderly fashion. The cell discharge of each neuron was highest with movements in a particular direction, called the *preferred direction* of the cell, and was shown to decrease progressively with

movements made in directions away from the preferred direction, leading to a bell-shaped directional tuning curve (Fig. 2.12). It was found that for the directionally tuned cells, the frequency of discharge ( $D$ ) was a sinusoidal function of the movement direction ( $\theta$ ):

$$D = b_0 + b_1 \sin \theta + b_2 \cos \theta \quad (2.3)$$

or in terms of the preferred direction ( $\theta_0$ ):

$$D = b_0 + c_1 \cos(\theta - \theta_0) \quad (2.4)$$

where  $b_0$ ,  $b_1$ ,  $b_2$  and  $c_1$  are regression coefficients. Equations 2.3 and 2.4 can be applied to reaching movements in a plane and to reaching movements performed in 3D space (Georgopoulos, 1996a).

The previously presented results of single cell recording indicate that during reaching movements in a given direction, many neurons with a broad range of different preferred directions were active to varying degrees. In other words, a signal about a direction of movement seems to be embedded in a distributed activity pattern of a whole population of neurons (Kalaska, 2009). Georgopoulos et al. (1986) proposed a vectorial code for the reconstruction of the signal from a population of neurons. The population of cells is regarded as a population of vectors in which each vector represents the contribution of an individual cell. For example, the  $i$ th cell is represented by a vector that points in the cell's preferred direction  $C_i$  and has a length  $w_i(M)$ , which represents the change of the cell's activity associated with a particular movement direction  $M$ . The *population vector*  $P(M)$  is calculated as follows (Amirikian and Georgopoulos, 2003):

$$P(M) = \sum_{i=1}^N w_i(M) C_i \quad (2.5)$$

where  $N$  corresponds to the number of cells in the population. In the above described study (Fig. 2.12),  $N$  would be 241. The findings of the study conducted by Georgopoulos et al. (1983) indicate that the population vector closely matches the directions of movements in 2D and 3D space (Fig. 2.12). Furthermore, subsequent studies revealed correlations between neural activity and extrinsic parameters such as target location, movement distance, speed and tangential velocity during reaching movements (Kalaska, 2009). Based on these results, it appears that the motor cortex is involved in high-level processing in the form of a planner and that downstream systems like the spinal motor system are responsible for converting these high-level signals into patterns of muscle activity and ultimately, to a force (Georgopoulos, 1996b). Bizzi et al. (2000) showed that the spinal motor system is an active participant in the process of movement generation, and therefore in theory, it should be possible that this structure supports the mapping between high-level signals expressed in extrinsic spatial kinematics and low-level proximal-limb muscle activities. This interpretation is consistent with the findings from Chapter 2.3.2.3.

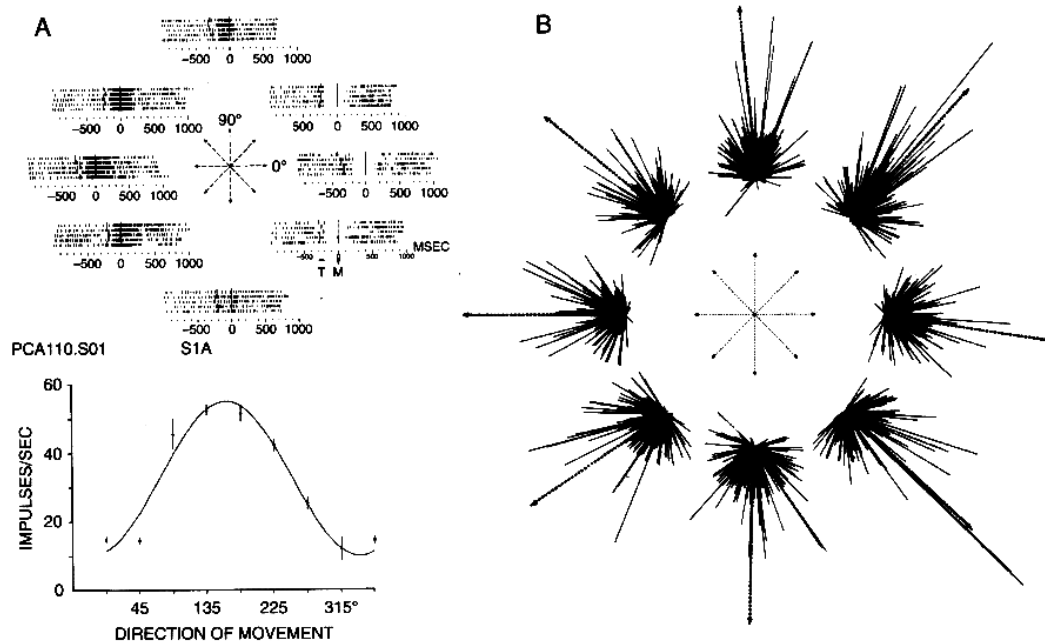


**Figure 2.12:** (A) The raster plots top left show the activity of a M1 neuron during five repeated movements in eight different directions in a 2D plane indicated by the center diagram. The signals are aligned to the onset of movement (M). Below the raster plots the directional tuning curve of the same neuron is displayed. The regression equation for the sinusoidal curve is  $D = 32.37 + 7.281 \sin \theta - 21.343 \cos \theta$  or equivalently  $D = 32.37 + 22.5 \cos(\theta - \theta_0)$ , where  $\theta_0 = 161^\circ$  (Georgopoulos et al., 1982). (B) Vector contributions of each of the 241 directionally tuned cells for each of the eight tested movements are shown. Notice the spatial congruence between the direction of movement indicated by the center diagram and the vectorial sum (dashed arrows). The vector sum or the population vector is calculated on the basis of equation 2.5 (Georgopoulos et al., 1983).

One problem in the studies cited above is that although the results seem to refer to a representation of extrinsic parameters in M1, they also produced equally broadly-tuned changes in other parameter spaces such as joint space or muscle space (Kalaska, 2009). Based on this observation, several studies were conducted that tried to decouple extrinsic spatial parameters of hand motions from intrinsic joint or muscle parameters. Studies by Caminiti et al. (1990, 1991) and Wu and Hatsopoulos (2006) revealed that the directional tuning functions of neurons in M1 changed when monkeys reached in the same spatial direction but in different areas of the arm's range of motion. Scott and Kalaska (1997) conducted studies in which monkeys had to perform reaching movements along the same hand path but use different arm postures. In other words, the hand paths of the reaching movements were the same

under the different experimental conditions, but the joint motions and the muscle activity changed. If the neurons in M1 only code extrinsic coordinates of the hand, their activity should not change under these different experimental conditions. However, Scott and Kalaska (1997) showed that a change in arm posture led to significant changes in the discharge of many single neurons in M1. Kakei et al. (1999) developed a protocol that dissociates between three different coordinate frames related to wrist movements: extrinsic (related to the direction of movement in space), muscle (related to the activity of individual or groups of muscles) and joint (related to the angle of the wrist joint). In a first study, neuronal activity in M1 of monkeys was analyzed. Based on the analysis, two types of M1 neurons were distinguished: one that appeared to represent the direction of movement in space (extrinsic parameter) and one that appeared to represent muscle activity (intrinsic parameter). In a second study, Kakei et al. (2001) recorded the activity of neurons in the ventral premotor area (PMv), which is a major source of input to M1 neurons, using the same protocol as before. PMv has strong interconnections with other regions of the brain including the posterior parietal cortex and area 46 of prefrontal cortex. Neurons in the PMv receive visual and somatosensory inputs and are active during the preparation for and execution of visually guided movements. Based on these observations, it is suggested that the PMv is an important member of a cortical network for directing limb movement in space. In contrast to results of their first study (Kakei et al., 1999), it was found that most directionally tuned PMv neurons encoded movement in an extrinsic coordinate frame and were not influenced by changes in forearm posture. These findings are consistent with a hierarchical relationship between PMv and M1. Therefore, the authors suggest that intracortical processing between PMv and M1 may contribute to a sensorimotor transformation between extrinsic and intrinsic coordinate frames.

Based on the reviewed studies, it is impossible to answer the question of whether extrinsic or intrinsic motor output parameters are represented in M1. As an intermediate result, it could be suggested that the representation of movements in M1 seem to reflect (to some degree) both intrinsic joint- or muscle-centered parameters and extrinsic parameters. Based on current knowledge, a definitive answer to the question of whether extrinsic and/or intrinsic motor output parameters are represented in M1 is not possible. However, the fact that M1 is the brain area where the lowest intensity stimulation initiates a movement, together with the results of Kakei et al. (1999), suggest that muscles are likely represented in the motor cortex. As force is generated by muscle activity (Ashe, 1997), force would be the most obvious parameter to study. Consequently, many neural recording studies have been conducted to resolve the degree to which M1 neurons encode kinematic or dynamic (kinetic) movement parameters.

Evarts (1968, 1969) was the first to study whether M1 activity was related to movement kinematics or dynamics in single-joint movements. The results from single cell recording indicated that the firing of M1 neurons correlate with the direction

and amplitude of muscle force. In most single-joint studies, the activity of a significant number of M1 neurons was highly correlated with the kinematics of the task, but not with the kinetics. Kalaska (2009) indicated that in single-joint studies, the response properties of M1 neurons were as heterogeneous in context of kinematics versus kinetics as they were for extrinsic versus intrinsic parameters. Few studies have addressed the question of whether M1 activity in multi-joint movement tasks is related to movement kinematics or dynamics. Kalaska et al. (1989) replicated and expanded on the study by Evarts (1968, 1969) to include whole-arm motor tasks. In this study, monkeys had to move a handle in 8 different directions starting from a central position. A force could be applied to the handle by the experimenter in any of the 8 movement directions. The magnitude of the force was constant. The results showed a broad range in the sensitivity of M1 neurons to the external loads ranging from neurons that were strongly modulated by both movement and load direction, to neurons that were strongly tuned for the direction of movement but were relatively insensitive to external loads. An important observation was that no neurons showed the opposite behavior (modulation with direction of the external load but not of the movement). Furthermore, neurons were only sensitive to external loads if they were also directionally tuned during movements without any external loads. This indicates a common functional contribution to both movement and compensation for external loads (Kalaska, 2009). In other words, the firing rate of the cells increased when the applied load pulled the arm in the opposite of the cell's preferred direction and the firing rate decreased when the load pulled the arm in the cell's preferred direction. These results indicate that the activity of the M1 neurons varies not only with movement direction but also with the direction of forces applied to the arm. These results are similar to the results presented above for single-joint movements (Krakauer and Ghez, 2000). Load-dependent responses were also found on the population level. The previously introduced population vector varied systematically in direction and length during reaching movements against external loads of different directions. When the loads pulled in the movement direction, the length of the population vector decreased, whereas the population vector length increased when the load pulled in the direction opposite to the movement, which means representing an increase in the activity of the M1 neurons (Fig. 2.13). It was also shown that loads pulling the arm perpendicular to the movement direction led to a deviation of the population vector in a direction that is opposite to the direction of the load (Kalaska, 2009). In this context, Kalaska et al. (1990) found an important difference between neurons in M1 (area 4) and the parietal area 5. Under the same experimental conditions, the neurons in the parietal area 5 did not show a significant change in the population activity when different loads were applied. The population vector always pointed in the direction of movement and no significant alteration of its length was observed. These results indicate that area 5 encodes primarily kinematic movement parameters whereas M1 (area 4) encodes both kinematic and dynamic movement parameters.

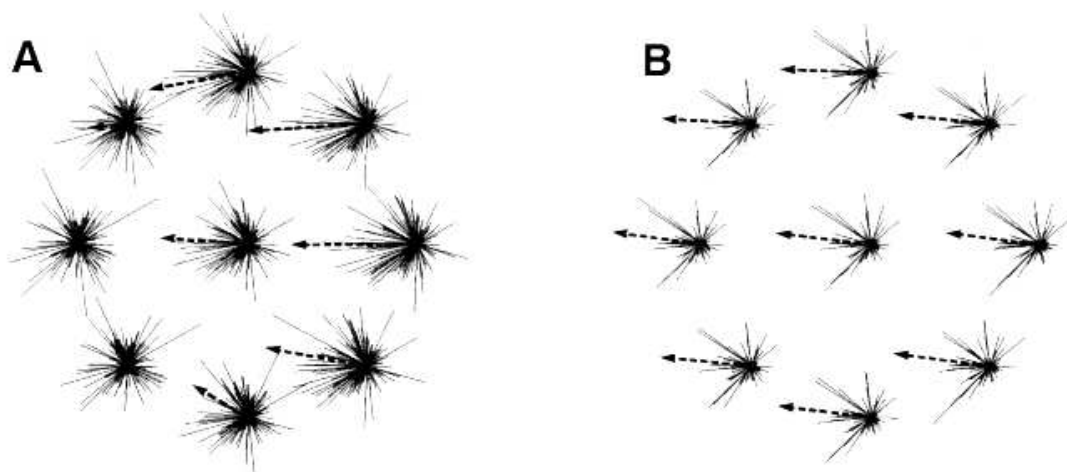


**Figure 2.13:** (A) Vector representation of the activity of a population of neurons in M1 during arm movements to the left. The central plot shows the neural activity of the neurons without load. All other plots around the central plot represent neural M1 activity under load condition. The position of the outer plots corresponds to the direction that the load pulled the arm. (B) Vector representation of the activity of a population of neurons in the posterior parietal area 5 during the same task under the same conditions (Kalaska, 2009).

Based on these results, it is difficult to make a coherent statement about the role of M1 in arm movement control. It seems that one interpretation is that M1 is involved in more global details of the motor task (e.g. specifying the direction of hand movement) and that the generation and coordination of the required motor patterns to produce the required forces is performed exclusively on the spinal level. Another interpretation is that M1 is involved in the generation and coordination of forces and that the descending motor commands from M1 include detailed information about the motor patterns at each joint (Scott, 2000c). In this context, the question arises as to whether there is one parameter of motor behavior that, if encoded in cell populations of M1, can explain most of the available results. Todorov (2000a, 2002, 2004) argued in a series of papers that muscle activation is probably the most plausible parameter. Although Todorov's approach seems to be controversial (Todorov, 2000a; Moran and Schwartz, 2000; Georgopoulos and Ashe, 2000; Todorov, 2000b; Scott, 2000a), its strength is that many of the above discussed observations can be accounted for by the complexity of the musculoskeletal system (Scott, 2000b). Whether or not M1 explicitly codes high-level task parameters such as the direction of the hand or intrinsic parameters such as joint angles or muscle forces is still a subject of active debate. Along with neural recording studies, many studies were conducted which used the *instructed delay period* method (Weinrich and Wise, 1982). In this method, a subject receives all relevant information about the goal of the movement but is not

allowed to begin the movement immediately. The idea is that neural correlations of a movement plan may be found during the instructed delay period. However, as reported by Cisek (2005), instructed delay period activity has been found in almost all movement-related brain regions. A methodological problem of many neural recording studies is the movement tasks used in the studies. The reaching movements in most experiments are heavily constrained so that these movements are often highly stereotypical and traverse a much lower-dimensional space than is theoretically possible. Consequently, movement parameters in different coordinate frames are often highly correlated. A neuron that appears to encode hand movement in one coordinate frame will likely appear to also be sensitive to joint movements (Reimer and Hatsopoulos, 2009). Besides the movement tasks, the correlation method itself is heavily debated in technical literature. Scott (2005) suggests that the population vector will point in the movement direction of the hand if the following three conditions are met: (1) The neural activity is symmetrically tuned to the movement direction of the hand, (2) The preferred directions of the neurons are uniformly distributed, and (3) There exists no coupling between a cell's preferred direction and the magnitude of modulation during movement. Despite these methodological problems, the presented results indicate that no single region of the brain represents extrinsic or intrinsic parameters exclusively. The reviewed literature indicates that the representation of these parameters is most likely distributed across multiple regions of the brain. In this context, it seems that neurophysiologists have only begun to understand the mechanism of the human motor system (Wise and Shadmehr, 2002).

### **Optimal control studies**

Because of the redundancy of the human motor system, humans can achieve everyday tasks like grasping a glass of water in an infinite number of ways (Chap. 2.2). Despite this redundancy, humans do not seem to use the full repertoire of possible movements to perform unconstrained movements, but instead produce highly stereotypical movement patterns. These patterns are observed under a variety of experimental conditions, over multiple repetitions of a task and between individuals performing the same task. This consistency indicates that some movement patterns are systematically preferred over others, likely based on perceived efficiency or comfort. This perspective leads to the field of optimal control, which is a promising way of dealing with such selection problems. In optimal control, a global measure (such as efficiency, smoothness, or accuracy) is used to describe a movement. This global measure is representative of the cost of the movement and can be seen as a kind of reward or punishment. The cost function, then, is usually defined as the integral of a cost over a certain time interval. In this context, the cost function is a mathematical means for specifying a movement plan based on a global measure. Movements are ranked according to cost, and the movement with the lowest cost is considered the optimal choice. Although optimal control is motivated by the problem of motor redundancy, these models are theoretically well justified a priori. The

human sensorimotor system is a product of evolution, development and learning. These three processes work on different time scales to improve actions. From an evolutionary point of view, the purpose of any action is to maximize the probability of passing on genetic material. In this view, some actions are more likely to lead to passing on genetic material, and the human brain may have learned to indirectly represent this probability through a cost function-based ranking of actions. Even if skilled performance is not always optimal, it has been made adequate by processes whose limit is optimality. However, the ultimate challenge in optimal control is to reverse engineer the cost function that is used to govern human behavior (Jordan and Wolpert, 1999; Todorov, 2004; Wolpert and Ghahramani, 2004). Current optimal control models can be grouped into two categories (Todorov, 2004): open-loop and closed-loop optimization models. Open-loop models typically assume a strict separation between trajectory planning and trajectory execution. These models are models of average behavior and differ mainly in the cost function used (Kawato, 1996). The second group of models attempt to construct the sensorimotor transformation that results in the best possible performance, taking into account motor noise, sensory uncertainty and delays (Todorov and Jordan, 2002; Todorov, 2004).

Most optimal control models are open-loop models. In open-loop models, a planner computes a desired trajectory that is transmitted to a controller, which in turn transforms the desired trajectory into adequate motor commands. Finally, the motor commands are sent to the plant. Depending on the open-loop model, the problem of motor redundancy is largely resolved during the planning stage via optimization. The only information needed by the planner to compute a desired trajectory is the current state (current position of the hand) and the desired final state (current position of the target in the workspace). Feed-forward control seems to be a plausible control scheme when movements are rapidly executed. These movements cannot be solely under feedback control because feedback loops in biological systems are slow. For example, the delay for visual feedback is approximately 150-200 ms (Slater-Hammel, 1960) and the delay for spinal feedback requires 30-50 ms, which is considered relatively fast (Kawato, 1999). It is likely the controller uses a servo mechanism to cancel instantaneous deviations between the desired and actual state of the body. In addition, the controller is provided with predicted sensory feedback, and in the case of long-lasting movements, sensory feedback. This information can be used by the controller to adapt the motor commands so that the desired trajectory can be executed. In addition, Bizzi et al. (1984) demonstrated that deafferented monkeys can reach toward a target without visual information. These results show that the entire trajectory, from the starting to the final position, is precomputed, meaning movements can be executed in a purely feed-forward manner. In addition to exploring which principles the CNS uses to solve the previously introduced ill-posed problems (Chap. 2.2), it is important to consider on which level in the sensorimotor system these principles work. In other words, determining in which coordinate frame or space human movements are planned. Besides psychophysical or neural recording studies optimal

control models can be used to examine the space in which trajectories are planned. Thereby, trajectories predicted by optimal control models defined in different planning spaces and experimentally determined trajectories are compared (Osu et al., 1997). According to Nakano et al. (1999), four planning spaces can be distinguished: an extrinsic-kinematic space (e.g. Cartesian coordinates of the hand), an intrinsic-kinematic space (e.g. joint angles or muscle length), an intrinsic-dynamic-mechanical space (e.g. joint torque or muscle tension), and lastly, an intrinsic-dynamical-neural space (e.g. motor commands controlling muscle tension or the firing rates of motor neurons). Figure 2.14 shows the different planning spaces and six of the most influential optimization models assigned to the different stages in movement planning. A comprehensive review of the existing open-loop optimization models is beyond the scope of this thesis, however a review of available models can be found in the paper by Kawato (1996). Below, a single optimization model for each planning space is discussed. Provided an initial state, a target state and the movement duration, the optimization models introduced below can be used to simulate the process of trajectory formation.

Based on the observation that in unconstrained point-to-point movements the trajectory of the hand shows a smooth, bell-shaped velocity profile, it was proposed that the square of the third derivate of the trajectory of the hand or *jerk* is minimized over the movement (Flash and Hogan, 1985). Letting  $X(t)$ ,  $Y(t)$  and  $Z(t)$  denote the position of the hand in a global or laboratory-fixed Cartesian coordinate system at time  $t$ , the *minimum hand jerk model* in 3D space is given by the following cost function:

$$J_{HJ} = \frac{1}{2} \int_{t_0}^{t_f} \left\{ \left( \frac{d^3 X}{dt^3} \right)^2 + \left( \frac{d^3 Y}{dt^3} \right)^2 + \left( \frac{d^3 Z}{dt^3} \right)^2 \right\} dt \quad (2.6)$$

where  $t_0$  and  $t_f$  define the duration of the movement. A review of the literature (Flash and Hogan, 1985; Hogan and Flash, 1987; Hogan et al., 1987) indicates that the trajectories predicted by the minimum jerk model are straight line paths. In addition, the model predicts smooth, single-peak, bell-shaped tangential velocity profiles. Finally, the shape of the hand trajectories are invariant in translation, rotation, amplitude and time scaling. It was also shown that the first derivative of a trajectory becomes progressively narrower and taller when using the fourth (snap), fifth (crackle), and even higher derivatives of the end effector location in the cost function (Richardson and Flash, 2002). Furthermore, the ratio of peak speed to average speed of the hand increases when the system minimizes jerk, snap, crackle and other higher derivatives. The minimum hand jerk model is a purely kinematic model; it cannot adapt planned trajectories to dynamic aspects of the motor task or the environment. Once the desired trajectory is determined in Cartesian space, a controller must be invoked to solve the problem of coordinate transformation and motor command generation.

According to the *minimum angle jerk model* trajectories are planned in joint space

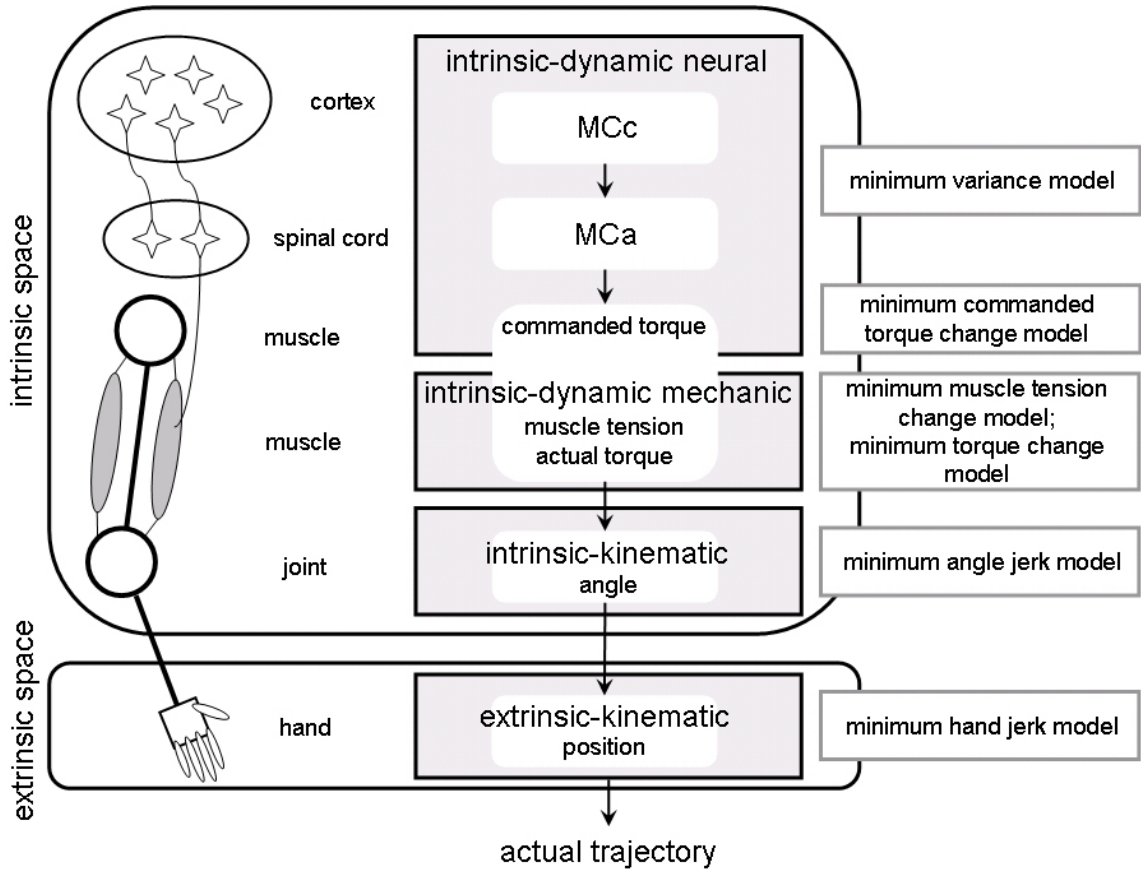


**Figure 2.14:** Conceptual schema of different trajectory planning spaces (adapted from Nakano et al., 1999) and corresponding optimal control models.

to minimize the change of the angular acceleration across the joints under consideration. The corresponding cost function is expressed by minimizing the integration of the jerk over the duration of the movement as follows:

$$J_{AJ} = \frac{1}{2} \int_{t_0}^{t_f} \sum_{i=1}^N \left( \frac{d^3 q_i}{dt^3} \right)^2 dt \quad (2.7)$$

where  $q_i$  is the joint angle  $q$  of the joint  $i$ . In the case of point-to-point movements, cost function 2.7 produces straight paths in joint space. When the planned trajectory is transformed into Cartesian coordinates via forward kinematics, the trajectory of the hand gradually curves depending on the position of the arm (Kawato, 1996; Wada et al., 2001). If movement planning takes places in joint space, the planner resolves the problem of trajectory formation and to some extent, the problem of coordinate transformation. The controller then has to transform the joint angles into torques and finally, compute the appropriate motor commands.

The solutions to movement tasks adopted by the human motor system should be flexible and adaptable to diverse environmental conditions. Otherwise, humans would not have the capacity for motor equivalence (Chap. 2.1). The minimum jerk models are based solely on kinematics. Therefore, these types of models are unable to adapt planned trajectories to changing dynamic aspects of the movement task or the environment, such as inertial characteristics of the manipulated objects or force fields (Kawato, 1996). Uno et al. (1989) proposed an optimal control model that depends on the dynamics of the musculoskeletal system, the *minimum torque change model*. According to the minimum torque change model, trajectories are planned as the sum of the changes of the torques  $\dot{\tau}$  across the joints  $i$  is minimized. The corresponding cost function is given by the following equation:

$$J_{TC} = \frac{1}{2} \int_{t_0}^{t_f} \sum_{i=1}^N \left( \frac{d\dot{\tau}_i}{dt} \right)^2 dt \quad (2.8)$$

If the plant is a point mass, then according to Newton's second law, the force is equal to the product of mass and acceleration. In other words, the rate of change of acceleration (minimum hand jerk) is identical to minimum force change (minimum torque change). If the plant is a multi-body system, these criteria are different (Kawato, 1996). If movement planning takes place in the intrinsic-dynamic-mechanical space by a minimization of the change rate of the torques in the joints of the body, then two ill-posed problems would be resolved: the problem of trajectory formation and the problem of coordinate transformation (inverse kinematics and inverse dynamics problem). Based on the computed torques for each instant of time, the controller needs to calculate the appropriate motor commands.

Although minimum jerk and minimum torque change models are able to reproduce many aspects of human trajectories, they do not provide an explanation as to why smoothness of movement is important. It is also debatable whether the CNS is able to estimate complex quantities, such as jerk and torque change, and integrate them over the entire duration of the movement (Jordan and Wolpert, 1999). Furthermore, all movements are subject to noise which causes deviations from the desired trajectory. Minimum jerk and torque change models do not account for these deviations. Harris and Wolpert (1998) proposed a *minimum variance model* that assumes that there is noise in the motor command proportional to the magnitude of the motor command. This model has several important ramifications. First, non-smooth movements require larger motor commands than smooth movements, and therefore generate an increase in noise. In the case of goal-directed movements, smoothness leads to accuracy but is not a specific goal. Secondly, consistent with Fitt's law, signal-dependent noise inherently imposes a trade-off between movement duration and final accuracy in the endpoint of the movement (Chap. 2.3.1.1). Thirdly, the minimum variance model provides a biologically plausible theoretical underpinning for goal-directed movements because such costs are directly available to the CNS, and

the optimal trajectory could be learned from the experience of repeated movements (Jordan and Wolpert, 1999).

One of the main limitations of open-loop optimization is that in large part these models fail to model trial-to-trial variability. The average behavior predicted by these models is much more common in constrained laboratory tasks than in real world movements (Todorov, 2004). Furthermore, one of the most remarkable properties of biological movement systems in comparison with technical systems is that they can accomplish complex movement tasks in the presence of noise, delays and unpredictable changes of the environment. Open-loop models are not ideal for models instances under these conditions. Instead, an elaborate feedback control scheme that is able to generate intelligent adjustments online is needed. Such a control scheme enables biological systems to repeatedly solve a control problem instead of repeating a specific solution (Bernstein, 1967). Todorov and Jordan (2002) developed an optimal feedback controller based on these needs. In the closed-loop optimization model, the controller is fully programmable, which means that it constructs the best possible transformation of information from states of the body and the environment into control signals. The idea is that the controller does not rely on preconceived notions of what control schemes the sensorimotor system may use, but does what is needed to accomplish the task. In other words, optimal feedback control allows the task and the plant to dictate the control scheme that best fits the task. In an isometric task, this may be a force-control scheme and in a postural task where a target limb position is specified, this may be a position control scheme. Because of the fact that the state of the plant is only observable through delayed and noisy sensors, the controller is only optimal when the state estimator is optimal. Such an estimator is modeled by an internal forward model (Chap. 2.3.3.3) that estimates the current state by integrating delayed noisy feedback with knowledge of plant dynamics and an efference copy of the control signals. One of the key features of internal forward models is their ability to anticipate state changes before the corresponding sensory data has arrived (Todorov, 2004). The distinction between open-loop and closed-loop control was traditionally seen as two complementary control schemes. A recent study by Desmurget and Grafton (2000) indicates that one scheme is simply a special case of the other. Based on optimal feedback control, Todorov and Jordan (2002) proposed a theory of motor coordination that a general strategy for movement generation may be formed in the presence of signal dependent noise. Since the model of Todorov and Jordan (2002) does not precompute a desired trajectory, the redundancy of the human movement system has to be resolved online by the feedback controller. This is accomplished by obeying a *minimum intervention principle*. This principle states that deviations away from the average behavior are not corrected unless those deviations interfere with task performance. The idea is that acting or making corrections is expensive because of control-dependent noise and energy. The basic concept is explained in figure 2.15. Configurations of the human body can be thought of as vectors in a multi-dimensional state space. In a redundant task,

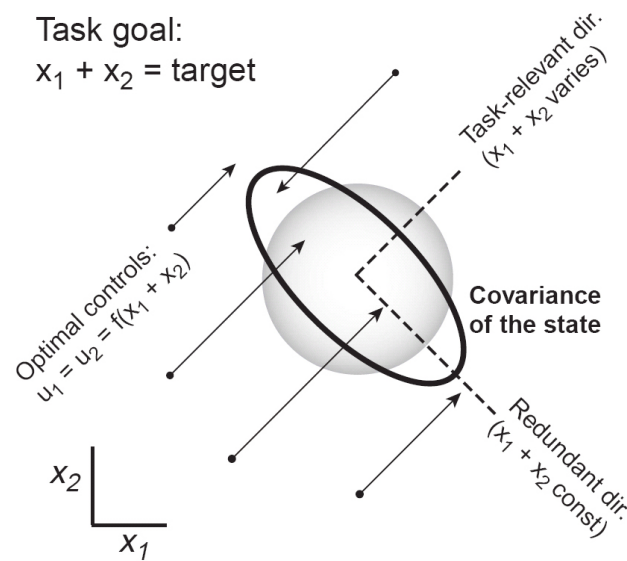


**Figure 2.15:** In this figure, the simplest redundant task is illustrated. There are two independent state variables  $x_1$  and  $x_2$ . Each variable is driven by a control signal ( $u_1$  and  $u_2$ ) in the presence of control dependent noise. The goal of the task is to use small controls to maintain  $x_1 + x_2 = 2$ . Nominally, each value could be 1.0 ( $x_1 = x_2 = 1.0$ ). Because of control dependent noise, when these commands are implemented, the output may be modified such that both values are 1.1. Consequently, the best strategy is to reduce both values toward 1. In another case, one value equals 1.1 and the second value equals 0.9. Since the optimal controller depends only on a result of 2.0 and not on the individual values  $x_1$  and  $x_2$ , it pushes the states along in the task-relevant direction and leaves the error in the redundant direction uncorrected (black covariance ellipse). Traditional open-loop methods force  $x_1 = x_2 = \text{target}/2$  and try to reduce the errors equally from all directions, resulting in the gray circle, by pushing the state toward the center (Todorov, 2004; Scott, 2004).

the state vector can vary in certain directions without interfering with the movement goal. The minimum intervention principle pushes the state vector orthogonally in the redundant directions. This leads to a probability distribution of observed states (Fig. 2.15, black covariance ellipse) that is elongated in the redundant directions (Todorov, 2004). Such effects can be quantified using an *uncontrolled manifold concept* for comparing task-relevant and redundant variances (Scholz and Schöner, 1999). Todorov (2004) showed that optimal feedback control creates an uncontrolled manifold because there are directions in which the control scheme does not act. In summary, the work of Todorov (2004) presented above combines a number of key ideas and concepts of motor control research. The optimal feedback control model is related to the dynamical systems view (Chap. 2.3.2.1) in the sense that the coupling of the optimal feedback controller, together with the controlled plant, generates a

specific dynamical systems model in the context of a given task. Furthermore, the minimum intervention principle is related to the uncontrolled manifold hypothesis (Chap. 2.3.2.3).

### **2.3.3.2 Motor command: Control**

In the previous chapter, three different approaches to the topic motor planning were introduced and discussed. However, questions regarding whether or not motor planning involves the computation of a desired trajectory, whether motor planning takes place in intrinsic or extrinsic coordinates and to which brain areas these processes can be assigned, still appear to be debatable. Independent of the concrete structure of the motor plan, the CNS has to compute a transformation of a motor plan into motor commands. In the literature, several models describing how motor commands are generated have been proposed. In this chapter a review of the two most prominent approaches, *inverse internal models* and *equilibrium point models*, will be provided.

#### **Inverse internal models**

Inverse internal models are neural mechanisms that represent a sensory-to-motor transformation. These models can calculate the necessary feedforward motor commands from a desired trajectory (Kawato, 1999). This implies that the control strategies implemented by the CNS reflect geometrical and inertial properties of the limbs and physiological properties of the muscles (Scott, 2005). Or in the words of Wolpert and Flanagan (2003, p. 1020):

”any good controller can be thought of as implicitly implementing an inverse model of the system being controlled. In other words, knowledge about the physical behavior of the system being controlled is employed by the controller.”

It is important to mention that inverse models (such as forward models) are not models of the CNS but models that approximate the properties of the musculoskeletal system. These models are used by the CNS to control the musculoskeletal system that ultimately transforms the motor commands into limb movements. Depending on the structure of the motor plan one has to distinguish between inverse kinematic and inverse dynamic models.

Several studies supporting the existence of inverse models as part of motor control are reviewed. These are studies in which subjects have to adapt to dynamic perturbations of limb movements. The perturbations are either caused by a robot manipulandum (Shadmehr and Mussa-Ivaldi, 1994) or by a rotating room (Lackner and Dizio, 1994, 1998). Both are typical experimental paradigms in the context of inverse internal models. The classical study by Shadmehr and Mussa-Ivaldi (1994) has been previously discussed in chapter 2.3.3.1. In the study, subjects had to move a handle of robot manipulandum to different targets. Under the null-field condition (robot’s motors off), subjects produced nearly straight hand trajectories. However,

when the force field was turned on, the dynamic characteristics of the arm changed, resulting in skewed trajectories. After a few hundred trials under the force field condition, subjects adapted to the new situation and the trajectories again became smooth and nearly straight. After the subjects were trained under force field conditions, the force field was occasionally turned off. The resulting hand trajectories resembled mirror images of trials when the force field was turned on. Lackner and Dizio (1994) conducted a study in which subjects had to perform reaching movements while they sat in the center of a room that slowly accelerated until it reached an angular velocity of  $60^\circ/sec$ . This rotation imposed a force on each body part not located at the precise center of the room. Every body part that moves in a rotating room will experience Coriolis forces. These forces are a function of the cross product of the angular rotation of the room, the linear velocity of the body part relative to the room and the effective mass of the body part. Because Coriolis forces are velocity-dependent, they increase as the body part moves faster and are absent prior to and after a movement. If the Coriolis forces are created by one's own body during a movement, the CNS accounts for these forces in the motor commands sent to the musculoskeletal system (Pigeon et al., 2003). In contrast, the CNS will not account for Coriolis forces if they are the result of an artificial external perturbation. This has a great impact on movement kinematics (e.g. Shadmehr and Mussa-Ivaldi, 1994). In the study mentioned above, when the room began to rotate, a Coriolis force acted on the moving arm leading to a deflection from the initially straight hand paths. After a few trials, the subjects were able to adapt to the Coriolis force and again produce nearly straight trajectories. The room was then slowly returned to zero angular velocity. The subject's post-rotation movements were observed to be mirror images of the initial reaching movements performed during rotation. Although there are some important differences between these two experimental setups (Lackner and DiZio, 2005), the results of both studies can be explained by the adaptation of the inverse dynamics model of the arm to the applied dynamic perturbation. Under normal conditions, the inverse dynamics model of the arm calculates motor commands that appropriately compensate for the dynamics of the arm. When the dynamic conditions are altered, the generated motor commands are insufficient, meaning they cannot compensate for the dynamic perturbation. In the case of goal-directed movements, this leads to deflections in the trajectories and large endpoint errors. In other words, the inverse internal model of arm dynamics is incorrect and cannot predict the forces that produce the planned trajectory. However, by allowing a period for training, the inverse dynamics model is able to adapt to the inverse of the combined arm dynamics and the dynamic perturbation. Consequently, almost straight hand trajectories are again observed and end-point errors are reduced. It is assumed that this adaptation involves plastic changes of the synaptic efficacy of neurons that constitute the inverse dynamics model. If the dynamic perturbation is removed, the adapted inverse dynamics model continues to generate motor commands that compensate for the dynamics of the arm and the dynamic perturbation that was removed. The re-

sults are distortions in the opposite direction (Kawato, 1999). Force field studies are increasingly accompanied by electromyography (Thoroughman and Shadmehr, 1999) and imaging techniques (Nezafat et al., 2001) for analysis of neuronal activity to detect the formation of inverse internal models on a neural level. This leads to the question of whether inverse internal models exist in the brain, and if so, where they are located. Based on the neurophysiological results presented in chapter 2.3.3.1, it seems reasonable to assume that inverse internal models are stored in brain regions where the skeletal muscles are represented, like the motor cortex, basal ganglia and cerebellum. Furthermore, it has to be assumed that inverse models cannot be assigned to a single brain structure, but are most likely broadly distributed across several brain structures. There are a few studies (Wolpert et al., 1998; Kawato, 1999; Grush, 2004; Bursztyn et al., 2006) supporting the idea that at least some inverse models, or parts of inverse models, are acquired and stored in the cerebellum.

If one assumes that the CNS uses inverse models to control the musculoskeletal system, then the next problem concerns the structure of internal models. Healthy children begin to reach toward objects of interest at the age of three months. At this age, the controller is not well developed and consequently, the reaching movements are jerky instead of smooth. Sometimes these movements even appear to be undirected. In contrast, "highly practiced" every day movements of older children, teenagers and adults are smooth. A sophisticated controller seems to be able to produce movements that are characterized by a minimal jerk (Chap. 2.3.3.1). With the help of the undirected movements, the child explores the dynamics of the musculoskeletal system and builds an inverse internal model of the plant. Over time, the inverse internal model is able to compute the appropriate forces so that the limbs move in the desired way. During motor development, bones grow and muscle mass increases changing the dynamics of the musculoskeletal system dramatically. In addition to these gradual changes, the dynamics of the arm change on a shorter time scale when external devices (e.g. a hammer) are used or objects (e.g. a cup of coffee) are grasped. To maintain performance, the controller needs to be robust to such changes in the dynamics of the arm (Shadmehr and Mussa-Ivaldi, 1994). Gandolfo et al. (1996) distinguishes between three possibilities for the motor control system to cope with these changing situations. First, the perturbing forces are internally represented as a look-up table that associates forces to states of the limbs (e.g. positions and velocities). During ontogenesis, this table evolves and each mapping between a specific state and force would correspond to an inverse internal model (hypothesis 1). There would be no generalization under this hypothesis. One alternative is that the adaptation is not limited to visited states of one's movement history, but to a small region around those explored states (hypothesis 2). In this case, there would be a local generalization around the visited states. A third hypothesis would be that the forces experienced locally generalize over the entire arm's workspace. To test these hypotheses, *generalization experiments* were conducted. Subjects are trained on a specific movement task with an altered kinematic or dynamic pertur-

bation as described above. After a learning phase, the subjects have to fulfill a new movement task. If the generalization of an inverse internal model is correct, new movement trajectories should be precisely controlled from the beginning of the movement (hypothesis 3). If generalization does not exist, new movement trajectories cannot be controlled from the beginning and the performance of the subject in the new movement task is as poor as those with no prior learning (hypothesis 1) (Kawato, 1999). The studies conducted in this context analyzed the generalization across different configurations of the same arm (Shadmehr and Mussa-Ivaldi, 1994; Malfait et al., 2002) and across different limbs (Criscimagna-Hemminger et al., 2003; Wang and Sainburg, 2004). Furthermore, generalization has been examined across different movement directions (Gandolfo et al., 1996; Thoroughman and Shadmehr, 2000), amplitudes and durations (Goodbody and Wolpert, 1998) and movement paths (Conditt and Mussa-Ivaldi, 1999). The results of these studies suggest that neither a perfect generalization (hypothesis 3) nor a local look-up table (hypothesis 1) exist. Instead, an intermediate generalization level was consistently observed. Kawato (1999) assumes that it may be plausible that internal models in the CNS are similar to artificial neural networks or connectionist models in their generalization ability.

The limitation of the generalization of inverse internal models to small regions around explored states implies the possible existence of several parallel-working models. If the CNS stores and uses more than one internal model, it is important to know whether the acquisition of an internal model is disrupted if a second internal model is learned during a critical time window. Furthermore, it is important to understand how several inverse models are associated. Do these models work in parallel, integratively, compensatory, or competitively? Shadmehr and Brashers-Krug (1997) investigated the ability of humans to learn two conflicting inverse models in different time lags. The tasks the subjects had to learn were movements in two distinct mechanical environments produced by a robot manipulandum. The results of this study indicate that there is a critical time interval for the learning and retention of two different inverse models. Results showed that the training sessions of the two tasks need to be separated by at least 5 hours. If the time lag between the two training sessions is shorter than 5 hours, the learning of the second inverse model starts on the basis of an inverse model appropriate for the first task. Based on the after-effects, the authors suggest that in the case of an insufficient time lag between training sessions, learning of the second inverse model leads to an unlearning of the inverse model acquired for the first task. Mah and Mussa-Ivaldi (2003) did not focus on the temporal interference of learning two inverse models in a row, but on the interference between variants of two tasks. To solve a movement task, the brain must transform a motor plan into adequate motor commands. The motor plan plays the role of an internal stimulus for the appropriate response (motor commands) (Chap. 2.3.1.4). Such a relationship between a stimulus (motor plan) and a response (motor commands) may involve a small number of appropriate responses, or even allow the responses to be graded according to the stimulus. In the context of retention,

Mah and Mussa-Ivaldi (2003) investigated two opposing hypotheses: the *conflict between mapping* and the *enhanced-response selection* hypotheses. The conflict between mapping hypothesis asserts that retention will be diminished when subjects learn two incompatible responses (inverse models) to the same stimulus because both responses will be recalled simultaneously and interfere with each other. In contrast, the enhanced-response selection hypothesis postulates that it will be easier to select and retrieve the most appropriate response from a group of responses that are contrasting, rather than from a group of responses that are similar. In other words, the correct response is selected from all recently learned responses, and the process of selection is simplified if incompatible responses have contrasting features. The results of the study support the enhanced-response selection hypothesis. Retention was not impaired when similar motions of objects required the retrieval of incompatible torque responses. In contrast, when similar motions of objects required the retrieval of similar torque patterns, retention was impaired (Mah and Mussa-Ivaldi, 2003). In addition to the studies just described, several studies exist that analyze the connection between inverse models of kinematic and dynamic sensorimotor transformations (Krakauer et al., 1999; Tong et al., 2002).

### **Equilibrium point models**

“This is a very arrogant hypothesis! Everybody is talking about how complex the system is, with all those DNAs, RNAs, numerous neurons and projections, and you suggest that the whole system is just a spring with regulated parameters!” *Michael Tsetlin* (Latash, 2008b, p. 87)

The CNS has to solve some difficult mechanical problems to control the musculoskeletal system. For instance, the CNS has to learn to control limbs that consist of segments connected via joints with different DOFs, which interact with each other and with external objects as they accelerate in the gravitational field of the earth (Shadmehr and Wise, 2005). In this context, the laws of mechanics are universal, relating kinetic (forces, torques) and kinematic variables (particularly acceleration). The laws are equally applied to non-living objects like stones and to living organisms like humans. Therefore, it seems plausible that a description and analysis of human movements has to rely on the laws of mechanics. As outlined above, in the context of internal models it is believed that the relationships inherent in these laws are imitated by neural structures in the CNS. The CNS uses these structures to directly calculate kinematics and muscular torques. According to Ostry and Feldman (2003), the internal model approach is flawed if one tries to incorporate physiologically realistic muscle and reflex mechanisms. This becomes particularly evident in connection with the posture-movement problem. The internal model approach does not account for the shift between postures without triggering resistance because of postural stabilizing mechanisms. Feldman and Levin (2009, p. 703) believe that

“although motor actions are described in terms of mechanics and EMG patterns, the question of how these actions are controlled cannot be answered in these terms.”

Consequently, an alternative approach for motor command generation has been created (Feldman, 2006; Feldman and Levin, 2009). The foundation of this approach is the distinction between *state variables* and *parameters*. State variables are variables that express relationships defined by the laws of physics (e.g. forces and kinematic variables). Any variable that can be deduced from state variables is also a state variable. However, the relationships between state variables include parameters that are not conditioned by the laws of physics, but define important characteristics of the system’s behavior under the action of the laws. Consider a simple pendulum (a mass on a rope), the equilibrium position and the period of oscillation in the gravitational field depend on parameters including the length of the rope, the coordinates of the suspension point and the local direction of gravity. A change in these parameters will lead to a new equilibrium position of the pendulum. Although all forces are balanced in an equilibrium state, the spatial coordinates of this state are not predetermined by forces, but by parameters (Latash, 2008b). Feldman (2006) is of the opinion that state variables cannot be specified or computed directly by the CNS. This view of biological motor control is diametrically opposed to the above presented arguments. Instead, it is assumed that parameters define essential characteristics of the behavior of the human motor system. In other words, biological motor control does not involve computation of state variables but uses changes in the parameters of the system. The CNS takes advantage of mechanical laws in producing the desired motor output without actually knowing the mechanical laws or imitating them in the form of internal models. If motor control implies changes in parameters, the question that needs to be answered is: Which parameters are used by the CNS?

One prominent form of parametric control is *equilibrium point (EP) models*, or simply *EP controllers*. Various EP controllers, defined differently throughout the literature, have been developed (Feldman, 1986; Bizzi et al., 1992). However, none of the controllers require an explicit computation of the torques required to move the limbs along a desired trajectory by solving the inverse dynamics problem (Chap. 2.2). Instead, EP control involves a specification of an arm configuration in which internal and external forces are at equilibrium. In the following, the main idea of one of the most influential EP controllers – the  $\lambda$ -*model* (Feldman, 1986; Feldman and Levin, 2009) – will be briefly outlined.

Various animal experiments (Matthews, 1959; Rack and Westbury, 1969) have shown that given a fixed level of descending commands, a slow increase in muscle length leads to a relatively small increase in muscle force. To ensure a fixed level of descending commands in these experiments, the pathways leading from the brain to the spinal cord were transected and a stimulator was placed at the spinal end of the severed fibers. It was found that if the lengthening of the muscle is continued past

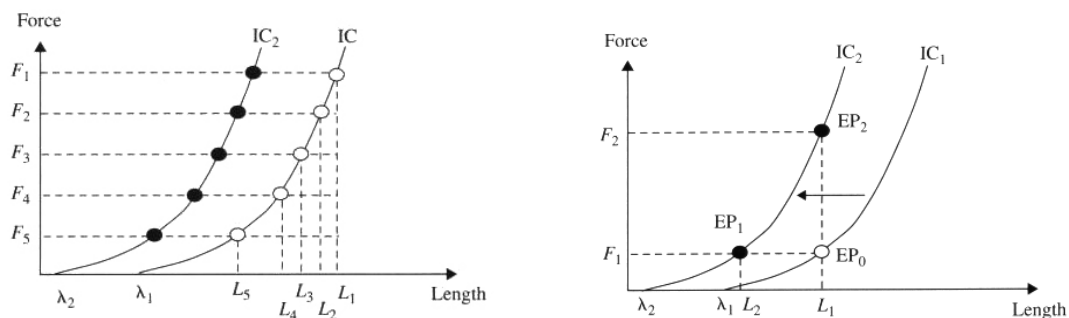


**Figure 2.16:** In the left figure two invariant characteristics (ICs) are shown. Subjects are asked to occupy a fixed joint position and act against an initially constant load. This corresponds to muscle length  $L_1$  and load  $F_1$ . A gradual unloading of the muscle leads to a sequence of EPs (open circles). An interpolation of the EPs yields the IC. If the subjects repeat the experiment starting from a different length-load combination, a new IC emerges ( $IC_2$ , filled circles). In the right figure a voluntary shift of  $\lambda$  is shown and consequently a shift of the IC from  $IC_1$  to  $IC_2$ . If the muscle acts against a constant external load, a movement will occur from the original length  $L_1$  to a new length  $L_2$ . If the muscle is forced to work under isometric conditions, the same shift of  $\lambda$  leads to a change in the muscle force from  $F_1$  to  $F_2$ . In other words, in the  $\lambda$ -model movement and force generation are different peripheral consequences of the same central control process (adapted from Latash, 2008b).

a specific length, the muscle begins to actively resist further lengthening because of an autogenic recruitment of the  $\alpha$ -motoneurons and the force-length ratio, or *stiffness*, increases substantially. In other words, the muscle will act like a stiff spring and oppose the stretch more vigorously. If the experimentally controlled descending signals are altered, the entire force-length curve is observed to perform a parallel shift (Fig. 2.16). The notion of the *tonic stretch reflex* is used to describe the results. Tonic reflexes are always polysynaptic and emerge in response to the level of a stimulus (e.g. muscle length). They lead to ongoing muscle contraction and therefore, to relatively smooth movements (Latash, 1993). A detailed description of different human reflexes can be found in Latash (2008a). It is interesting to note that despite nearly 100 years of research, a considerable debate on the term *reflex* still exists, especially in contrast of *voluntary movement* (Prochazka et al., 2000). In this thesis, the term reflex is used as introduced in chapter 2.1.

The force-length characteristic curves are termed *invariant characteristics*. The muscle length where the autogenic recruitment of the  $\alpha$ -motoneurons begins is termed the threshold of the tonic stretch reflex. The Greek letter  $\lambda$  is used to refer to this value. The examination of invariant characteristics in humans requires the analysis of joint torque-angle characteristics instead of muscle force-length characteristics. To guarantee fixed descending commands analogously to the animal experiments cited

above, Feldman (1966) developed the so-called *not to intervene voluntary* paradigm. Subjects are asked to occupy a joint position against a load and to not intervene voluntary when the load is suddenly modified. A change in the descending signals is accomplished by asking the subjects to adopt different starting positions against the same load. In figure 2.16 (left), typical results of such an experiment are illustrated. Given the external load  $F_1$ , the subject's elbow angle corresponds to the length  $L_1$  of the flexor muscles. This force-length combination defines the initial EP of the system. When the external load was decreased to  $F_2$ , the joint moved to a new angle corresponding to muscle length  $L_2$ . The combination of  $F_2$  and  $L_2$  defined a new EP. The assumption is that all EPs (Fig. 2.16, left, open circles) corresponded to the same unchanged voluntary command but different external loads. The EPs can be connected with a smooth line, resulting in the invariant characteristic introduced above. The experiment was conducted with different starting positions but with the same external load conditions. To stay at a different position against the same load requires a change in the central command. The procedure for the different starting positions is the same as above (Fig. 2.16, left, filled circles). One of the major experimental findings of these studies is that the invariant characteristics do not intersect, but rather shift almost parallel to each other for different starting positions. Because of the similarities of the results of the human experiments and the tonic stretch reflex characteristics recorded in animal experiments, Feldman (1966) used the same term (tonic stretch reflex) to describe his data. Based on the experimental data, it was concluded that the central command may be associated with the selection of a particular invariant characteristic, while muscle force, muscle length, and the level of muscle activation depend on the central command *and* the external load. When the external load is further decreased in these experiments, it was observed that the muscle activity disappears at a certain muscle length. This value is the above introduced threshold of the tonic stretch reflex, or  $\lambda$ . A value of  $\lambda$  defines a particular invariant characteristic and can be seen as a measure of the central command. The invariant characteristic consists of an infinite number of possible combinations of muscle force and muscle length. The chosen combination in a given situation is a result of the external force. One of the key points of the  $\lambda$ -model is that voluntary muscle control may be described by only one parameter (Latash, 1993, 2008b).

If a muscle is at an EP and a transient external force stretches the muscle to a new length, the muscle will return to the EP as soon as the force is removed. If the system wants to stay at the new position after the removal of the external force, a posture-stabilizing mechanism has to be considered. Movements within the  $\lambda$ -model can be a consequence of two processes. One possibility is that the central command stays the same but the external load is altered. The result of this change is a new combination of muscle force and muscle length along the same invariant characteristic. The second possibility is a voluntary shift in  $\lambda$  (Fig. 2.16, right). A shift from  $\lambda_1$  to  $\lambda_2$  leads to a movement from  $L_1$  to  $L_2$  at  $F_1$  if the external load is not changed. This leads to a shift of the EP of the system from  $EP_0$  to  $EP_1$ . If the movement is stopped because

of external resistance, the same change in  $\lambda$  will lead to a change in the muscle force without a movement. In this case, the new EP of the system would be  $EP_2$  (Latash, 2008b).

Until now, the description of the  $\lambda$ -model has been limited to the control of a single muscle. Because human muscles can only pull and not push, joint movement is controlled by a pair of antagonistic muscles that act at the joint and produce torques in opposite directions. In figure 2.17 (top row), two invariant characteristics for a flexor and an extensor muscle are illustrated. Thereby  $\lambda_{FL}$  corresponds to the control variable for the flexor muscle and  $\lambda_{EX}$  to the control variable for the extensor muscle. These variables define the position of the invariant characteristics of each muscle. The overall joint characteristic, as illustrated by the bold line in figure 2.17 (top row), is defined by the two invariant characteristics of the two muscles. If a constant external torque acts on the joint, the combination of the torque ( $T_0$ ) with an angle  $\alpha_0$  defines the EP of the system. Shifts of the two  $\lambda$ s lead to voluntary joint motion. If both  $\lambda$ s shift simultaneously and in the same direction along the angle axis, the activation level of one muscle increases whereas the activation level of the other muscle decreases. The mechanical characteristic of the entire joint, calculated by the algebraic sum of the two muscle characteristics, also shifts along the angle axis without changing shape (Fig. 2.17, bottom left). Simultaneous shifts of both  $\lambda$ s in opposite directions lead to a small change in the location of the joint characteristic but a large change in the slope (Fig. 2.17, bottom right) (Latash, 1993, 2008b). The availability of at least two muscles at a joint allows the behavior of the joint to change in two ways. One way the behavior can be changed is by activating one muscle and relaxing the opposing muscle. This corresponds to a unidirectional shift of the two  $\lambda$ s and will lead to a joint motion in the direction of the activated muscle. The behavior of a joint can also be changed by the simultaneous activation of both muscles, which will lead to a small movement and a large change in the stiffness of the joint. To reflect these two modes of joint control, Feldman (1986) introduced two variables equivalent to  $\lambda_{FL}$  and  $\lambda_{EX}$ . These variables are the reciprocal command  $r$  and the coactivation command  $c$ :  $r = (\lambda_{FL} + \lambda_{EX}) / 2$  and  $c = (\lambda_{FL} - \lambda_{EX}) / 2$ . The  $r$  command defines the angular range in which muscle can be activated and the  $c$  command defines the size of the angular range where both muscles are active (Latash, 2008b). Finally, the  $\lambda$ -model assumes that the tonic stretch reflex incorporates all the reflex loops that can be influenced at the levels of  $\gamma$ -motoneurons,  $\alpha$ -motoneurons and interneurons (Latash, 1993).

The  $\lambda$ -model provides an explanation for results where equifinality of movements was found despite transient external perturbations (Bizzi et al., 1978; Schmidt and McGown, 1980; Bizzi et al., 1982; Jaric et al., 1999). The term *equifinality* refers to the ability of the neuromuscular system to reach the same final position in the face of transient external perturbations (Feldman and Latash, 2005). However, there are several studies where equifinality of movements was not found, which are therefore incompatible with the  $\lambda$ -model. In these studies, the experimental conditions involved

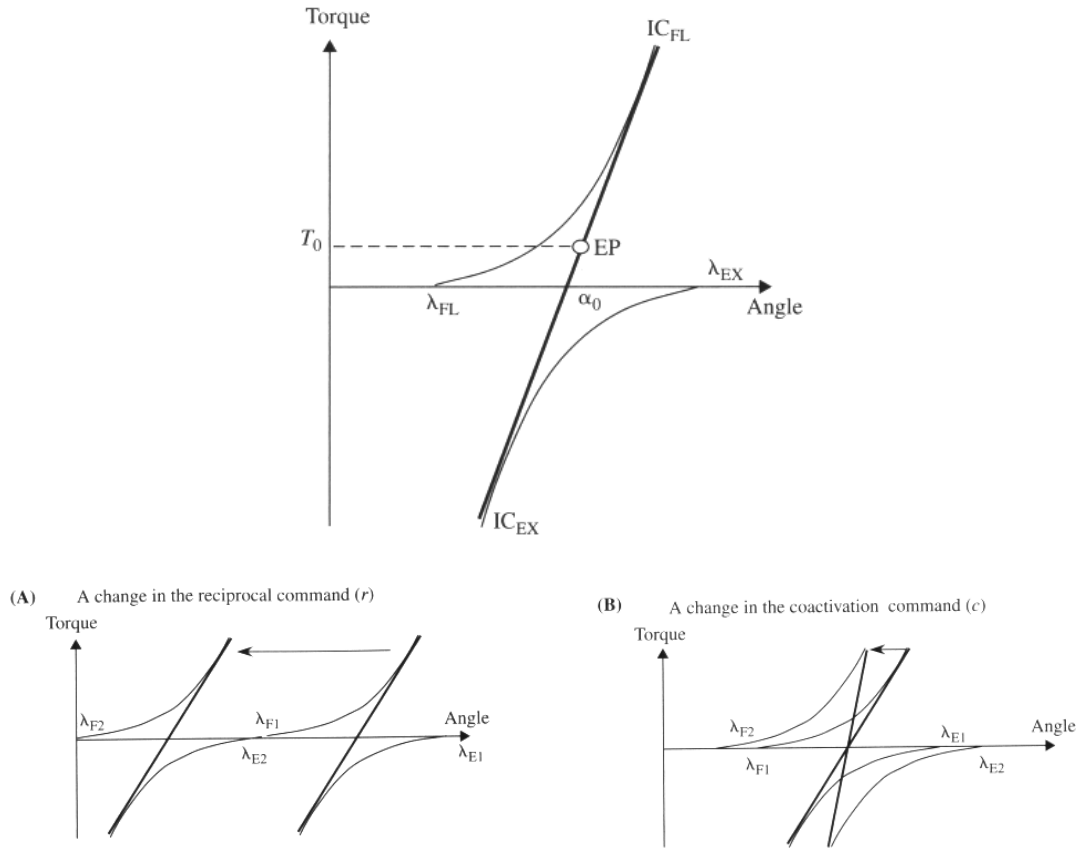


**Figure 2.17:** (Top row) Imagine a joint is spanned by a flexor and an extensor muscle. The ICs of those two muscles ( $\lambda_{FL}$  and  $\lambda_{EX}$ ) can be illustrated in a torque-angle plane, where the torques of the extensor are assumed to be negative. Joint behavior corresponds to the algebraic sum of the two ICs (thick, straight line). The EP of the joint is defined by the position of this line and the external torque ( $T_0$ ). Joint control can either be explained with the  $\lambda$  parameters of the two muscles or with the two variables  $r$  and  $c$ . (A) A unidirectional shift of the two  $\lambda$ s correspond to a change in the reciprocal command  $r$ . This leads to a major shift in the joint characteristic and to a small change in the slope. (B) A shift of the two  $\lambda$ s in opposite directions corresponds to a change in the coactivation command  $c$ . This leads in contrast to the  $r$ -command to a major change in the slope of the joint characteristic and to a small shift (adapted from Latash, 2008b).

the action of Coriolis forces (Lackner and Dizio, 1994) or other destabilizing forces (Hinder and Milner, 2003). Feldman and Levin (1995) point out that equifinality could be observed in some cases of transient external perturbations but it has never been suggested that this phenomenon must occur under all forms of perturbation. The  $\lambda$ -model predicts equifinality when two conditions are met: (1) The perturbation does not lead to a change in the central commands and (2) it does not modify the force-generating properties of the peripheral muscle. Proponents of the  $\lambda$ -model argue that violations of the equifinality, in the context of unexpected applications of motion-dependent forces acting during movement but not at a steady state, are because of changes in the central command signals even though the subjects were asked to not intervene (Feldman and Latash, 2005; Latash, 2008b).

If voluntary movements arise as a consequence of shifts of EPs, it is important to consider the shape of the EP trajectory. The EP trajectory is also called the *virtual trajectory*. Latash and Gottlieb (1991) developed an algorithm that enables the reconstruction of virtual trajectories that represent temporal changes in the control parameter  $\lambda$ . However, there is currently no consensus in technical literature on the shape of the virtual trajectory (Latash and Gottlieb, 1991; Feldman et al., 1995; Gomi and Kawato, 1996; Konczak et al., 1999). This seems partly a result of inadequate models of force generation that lead to deviations between virtual and actual trajectories (Gribble et al., 1998). The  $\lambda$ -model is founded on results showing that forces produced by the neuromuscular system are position-dependent. Springs were used as an example of a physical system with analogous properties. In other words, the joint appears to behave like a mass-spring system. The *spring-like behavior* refers to this special case and implies a similarity in behavior between two systems that have, apart from that, little in common (Feldman and Latash, 2005; Latash, 2008b). The spring analogy is probably one of the most crucial points in the discussion of the proponents and opponents about the validity of the  $\lambda$ -model. Feldman and Latash (2005) suggest that the spring analogy is taken too literally when muscles with or without reflexes are modeled as springs with parameters like stiffness and damping determined by the level of muscle activation. This leads to questionable estimates of EP trajectories like in the studies of Latash and Gottlieb (1991) and Gomi and Kawato (1996). The spring analogy also triggers discussions about violations of equifinality. A physical spring will be stretched if a load is applied and it will return to its resting length when the load is removed. In addition, if a metal spring is stretched beyond certain limits, it will not return to its previous resting length.

The previous explanations the  $\lambda$ -model may explain single-joint movements. However, almost all voluntary movements require a precise activation of many muscles to rotate multiple joints. It was shown in chapter 2.2 that movement generation in biological systems is ill-posed in the sense that the task requirements can generally be met by an infinite number of different movements because of the redundant DOFs on different levels. The  $\lambda$ -model implies that the redundancy problem is not solved on supraspinal levels and that these levels only constrain the coordination between

the different DOFs via central commands. The central commands specify the thresholds of the agonist and antagonist muscles and thus the invariant characteristic. The invariant characteristic of a joint contains a collection of potential EPs. Finally, a single EP is selected by the interaction of the joint segments with external loads. In the multi-joint case, it is suggested that all the muscles are controlled as a coherent unit by a global factor. The difference between the actual body configuration and its referent configuration is modulated by the CNS. This facilitates the control of the musculoskeletal system since a muscle is only activated if its current muscle length at the actual body configuration exceeds the threshold muscle length defined by the referent body configuration. Human walking (Günther and Ruder, 2003) and sit-to-stand movements (St-Onge and Feldman, 2004) are the first experimental confirmations of multi-muscle control in the context of  $\lambda$ -model.

By introducing the variable  $\lambda$  as a purely central control variable, the adopted  $\lambda$ -model can be greatly simplified. Based on a closer analysis of the neurophysiological pathways that lead to changes in the activity of  $\alpha$ -motoneurons, Feldman and Latash (2005) and Feldman and Levin (2009) are currently of the opinion that this assumption must be amended and that  $\lambda$  is a rather complex variable. As reviewed in Feldman and Levin (1995) and Feldman and Latash (2005), reactions of the muscle to changes of its length depend on a variety of factors including the velocity of change, the activation history of the motoneuronal pool, the effects of reflexes of other muscles and even muscles from other joints. The additive effects of these factors lead to the following definition of the threshold control of muscle activations in the  $\lambda$ -model:

$$\lambda^* = \lambda - \mu v + p + f(t) \quad (2.9)$$

where  $\lambda$  is a central command,  $\mu$  is a temporal parameter related to the dynamic sensitivity of muscle spindle afferents,  $v$  is the velocity of change in the length of the muscle ( $v = dx/dt$ ),  $p$  is the shift in the threshold resulting from reflex inputs like those responsible for inter-muscular interactions and  $f(t)$  represents history dependent changes of the threshold (Feldman and Latash, 2005; Feldman and Levin, 2009).

### 2.3.3.3 State: Estimation and prediction

To generate appropriate motor commands (Chap. 2.3.3.2), the CNS needs to have information about the current state of the body. Thus, the CNS has to cope with two problems. First, the transduction and transport of sensory signals to the CNS involves large delays in comparison to artificial systems like robots. For example, the delays for reactions in arm movements, based solely on visual feedback, range from 150-200 ms (Slater-Hammel, 1960). Even the fastest spinal feedback-loops still require 30-50 ms. Compared to very fast ( $\approx 150$  ms) or intermediate ( $\approx 500$  ms) human movements, these delays are still considered large (Kawato, 1999). The second problem concerns the fact that sensory signals are corrupted by noise. Noise

is defined as random fluctuations and disturbances that are not part of the actual sensory signal. Faisal et al. (2008) provides a recent review on sources of noise in the nervous system. Sensory signals that are contaminated with noise may only provide inaccurate information about the current state of the body (Wolpert and Ghahramani, 2000). Using these delayed and noise corrupted sensory signals to estimate the state of the body can result in large errors, especially in fast movements. As an example, if a tennis player performs a fast forehand stroke using only his visual system to estimate the position of the tennis ball, his estimate is delayed by approximately 100 ms. A predictive model could help to make a more precise estimate of the current position of the ball. The relationship between the generated motor commands and their consequences is governed by the physics of the musculoskeletal system and the outside environment. Consequently, a more precise prediction requires a model of this transformation. Computational neuroscience models that capture the forward or causal relationship between actions and their consequences are termed internal forward models, or forward models. The primary role of these models is to predict the future behavior of the body and the environment. Based on this primary role, these models are occasionally referred to as predictors. Because the physics of the musculoskeletal system change during motor development and humans are able to manipulate different tools with unequal intrinsic dynamics, humans need to acquire new forward models and constantly update existing models over the course of their lives (Wolpert and Flanagan, 2001). While evidence for forward models has been considerably strengthened by research conducted in psychophysical studies (see below), neurophysiological evidence is less widespread. Some authors believe that forward models are stored in the cerebellum (Wolpert et al., 1998; Kawato et al., 2003). Referring back to the tennis ball discussed above, components of the ball's state, like its spin, cannot easily be observed because of delays in the sensory system. However, since the spin of the ball has an impact on its trajectory, it could be estimated if sensory information is integrated over time. In other words, by observing the position of the tennis ball over time, an estimate of its spin can be obtained. This estimate is based on sensory feedback and can be improved by knowing how the ball was hit, or more specifically, the generated motor commands in combination with a forward model of the ball's dynamics (Wolpert and Ghahramani, 2004).

The combination of sensory feedback and a forward model for state estimation is called an *observer model*. In an observer model, the observer compensates for the delays in the sensorimotor system and reduces uncertainty in the state estimate, where uncertainty is a result of the inherent noise in sensory and motor signals (Wolpert and Ghahramani, 2000). An example of such a model is a Kalman filter (Fig. 2.18). A more detailed description of the Kalman filter model can be found in Wolpert et al. (1995b) or Wolpert (1997). Observer models for state estimation have been supported by empirical studies examining hand position (Wolpert et al., 1995b), posture (Kuo, 1995) and head orientation (Merfeld et al., 1999).

In the context of observer models, the forward model makes two types of predic-

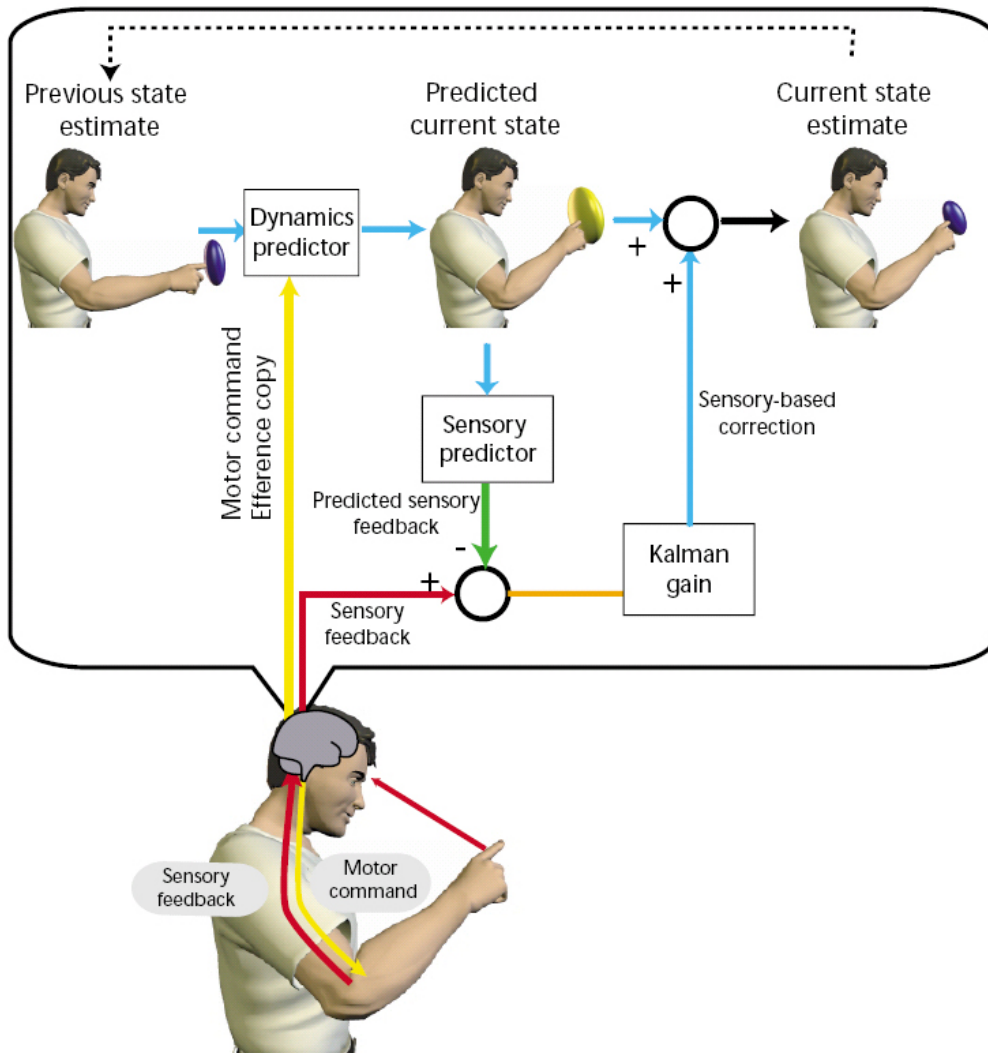


**Figure 2.18:** The figure shows one step of a Kalman filter model that recursively estimates the position of the finger during a movement. The current state is computed on the basis of the previous state estimate (top left). The previous state estimate represents the distribution of potential finger positions, illustrated as a blue cloud of uncertainty. In using an efference copy of the issued motor commands in combination with a model of the dynamics the current state can be predicted based on the previous state. Thus the uncertainty is increased as illustrated by the yellow cloud. The predicted current state estimate is refined by using it to predict the current sensory feedback. The discrepancy between the predicted sensory feedback and the actual sensory feedback is used to correct the current state estimate. The Kalman gain changes the sensory error into a state error and besides that determines the reliance placed on the efference copy and sensory feedback. The final or current state estimate now has a reduced uncertainty (top right). Delays in sensory feedback that have to be compensated for are left out of the figure for clarity (Wolpert and Ghahramani, 2000, 2004).

tions. First, the forward model predicts the actual outcome of the motor commands and compares these to the desired outcome. This comparison happens before the movement takes place and is used to estimate the state of the motor system that is not directly observable by the CNS. Based on this comparison, fine adjustments to ongoing motor commands can be made before reafferent feedback is available (Blakemore et al., 2002). For example, if a person holds a glass of water in a precision grip with the fingers and thumb on either side, the grip force is precisely controlled so that it is just slightly greater than the minimum grip force needed to prevent the glass from slipping. Based on the fact that an object's behavior is unpredictable, an estimation of the load is based solely on sensory feedback. For example, if someone suddenly strikes the glass from above, the grip force is modified reactively in response to the sensory feedback of the fingertips, and consequently, the grip force adjustment tends to lag behind. If the load is increased by a self generated action such as accelerating the hand, the fingers tighten their grip in anticipation to prevent the glass from slipping. Thus, the grip forces increase in parallel with the load force without delay. Sensory load detection is too slow to account for this increased grip force, which therefore relies on a predictive process (Wolpert and Flanagan, 2001). Anticipatory grip force adjustment with load during object manipulation has been found in a couple studies (Flanagan and Wing, 1997; Kawato, 1999) and is an important piece of evidence for predictive forward models (Davidson and Wolpert, 2005). The second type of prediction is a comparison between the predicted sensory consequences of the forward model and the actual sensory feedback. This comparison happens after movement execution and can be used to cancel out sensory effects of movement (reafference). The sensory changes induced by self-motion are predicted from an efference copy of the issued motor commands resulting in little or no discrepancy between the predicted and actual sensory feedback. Externally generated sensations cannot be predicted from a copy of the issued motor commands and will therefore lead to a higher discrepancy. In other words, if the discrepancy between the predicted and actual sensory feedback increases, the likelihood that the sensation is externally generated also increases. For example, Blakemore et al. (1999) examined why self-produced tactile stimulation is perceived as less intense than an externally produced stimulus. In the study, subjects tickled themselves using a robotic interface. Subjects used their left hand to move a robotic manipulator which in turn produced the same movement on a second robot manipulandum that introduced a tactile stimulus on the subject's right palm. In addition, an externally tactile stimulus condition was tested in which the second robot manipulandum was programmed to produce a stimulus. The results showed that the subjects rated the self-administered tactile stimulus as significantly less tickly than the externally administered tactile stimulus. In another experimental condition, the experiment was performed as before, however a time delay between the motion of the left hand and the resulting effect on the right palm was introduced. The delay between cause and effect led to temporal decoupling of the predicted and the actual feedback, resulting in a large sensory discrepancy. As

a result, this discrepancy is felt as a tickle. In summary, Blakemore et al. (1999) showed that the intensity of the self-applied stimulus depends critically on a precise temporal synchronization between the predicted and the actual sensory consequences of movement.

### 2.3.3.4 Context: Estimation

In daily life, humans interact with a plethora of different objects. Each object has its own physical characteristics such that the context of movement changes in a discrete manner. In other words, the CNS has to estimate the state of the body, as outlined above, and the changing movement context. The *Bayesian approach* can be used to estimate probabilities for possible contexts. The probability of each potential context is factored into two terms: *likelihood* and the *prior*. The prior corresponds to the belief in a particular context before sensory information is available. In the example in figure 2.19, a person wants to lift a milk carton. However, there are two possible contexts: (1) the carton is empty and (2) the carton is full. Based on visual information, the person believes the milk carton is full. When the motor commands are generated, an efference copy is sent to two forward models or predictors. These predictors simulate the sensory consequences of the two possible contexts. In the first context, where the milk carton is empty, the prediction suggests a large amount of movement compared to the second context. The predicted feedback is then compared to the actual sensory feedback. Since the milk carton is empty, the sensory feedback matches the predicted feedback of the first context, which leads to a high likelihood of an empty milk carton and a low likelihood of a full carton. The likelihood of a context corresponds to the probability of receiving the current sensory feedback given the hypothesized context.

The discrepancy between the predicted and actual sensory feedback is inversely related to the likelihood, which means that the smaller the prediction error, the more likely the context (Wolpert and Ghahramani, 2004). As suggested by Wolpert and Kawato (1998) and Haruno et al. (2001), a modular neural architecture in which multiple predictive models work in parallel may be implemented by the CNS to carry out the computations just described. Therefore, each predictive model is tuned to one context and estimates the relative likelihood of this context. The priors and the likelihoods can be combined using Bays theorem to calculate the posteriori contexts, which become the new prior beliefs for future context estimation. According to Bays theorem, the probabilities  $P(A)$  and  $P(B)$  and the conditional probabilities  $P(A|B)$  and  $P(B|A)$  are associated with each other as follows:

$$\underbrace{P(A|B)}^{\text{posterior}} = \frac{\overbrace{P(B|A)}^{\text{likelihood}} \overbrace{P(A)}^{\text{prior}}}{P(B)} \quad (2.10)$$

where  $P(B)$  is given by  $P(B) = P(B|A)P(A) + P(B|\bar{A})P(\bar{A})$ . If  $A$  is relabeled as

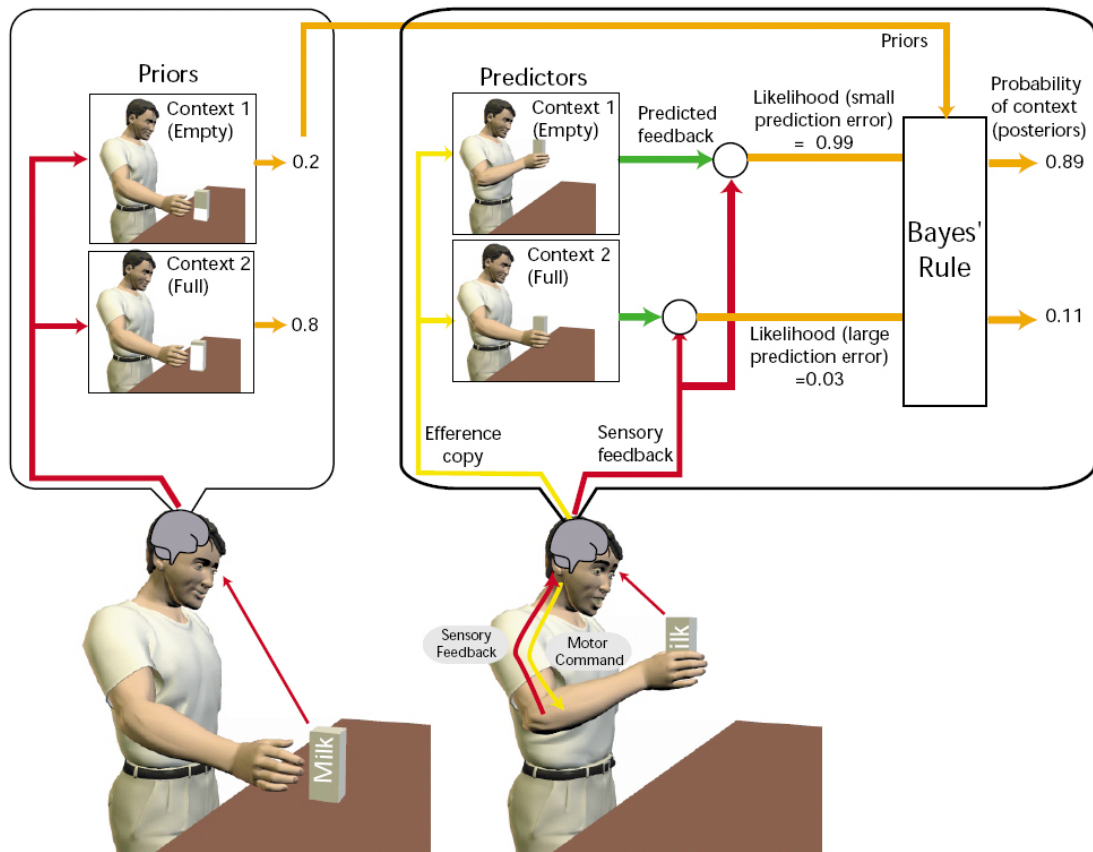


**Figure 2.19:** In this sketch a person wants to lift a milk carton. However, there are two possible contexts: (1) the carton is empty and (2) the carton is full. Based on visual information, the person believes that the milk carton is full. When the motor commands are generated, an efference copy is sent to two forward models or predictors. These predictors simulate the sensory consequences of the two possible contexts. The prediction in the first context suggests a large amount of movement compared to the second context because the milk carton is empty. The predicted feedback is then compared to the actual sensory feedback. Because the milk carton is empty, the sensory feedback matches the predicted feedback of the first context, which leads to a high likelihood of an empty milk carton and a low likelihood of a full carton. The priors and the likelihoods can be combined using Bays theorem to calculate the posteriori states, which become the new prior beliefs for future context estimation (Wolpert and Ghahramani, 2000, 2004).

“context” and  $B$  as “sensory input”, Bays theorem becomes applicable to the brain for the process of context estimation (Wolpert and Ghahramani, 2009):

$$\overbrace{P(\text{context}|\text{sensory input})}^{\text{posterior}} = \frac{\overbrace{P(\text{sensory input}|\text{context})}^{\text{likelihood}} \overbrace{P(\text{context})}^{\text{prior}}}{P(\text{sensory input})} \quad (2.11)$$

In accordance with Wolpert and Ghahramani (2000) and Wolpert and Ghahramani (2004), this review has introduced separate architectures for state and context estimation (Fig. 2.18 and 2.19). However, both architectures can be considered online ways of performing Bayesian inference in an uncertain environment. Studies involving Coriolis forces can be used as an example for context estimation. As outlined in chapter 2.3.3.2, Coriolis forces are velocity-dependent; they increase during a movement and are absent prior to and after a movement. In the study of Cohn et al. (2000), subjects performed goal-directed movements while rotating their torso. Under these circumstances, the CNS compensated for the Coriolis forces resulting from the rotation. Additionally, subjects had to perform goal-directed movements while experiencing compelling illusory self-rotation and displacement induced by rotation of a complex, natural, visual scene. In these cases, the subjects performed movements as if a Coriolis force was present. Based on visual priors, they expected the context of a Coriolis force. This led to errors in the performance of the goal-directed movement which were reduced over subsequent movements. The errors were reduced because the sensory feedback of the expected Coriolis force was not experienced and posteriori states were calculated, thus becoming new prior beliefs for future context estimation.

Currently much attention is given to the Bayesian approach in technical literature, particularly in combination with decision theory (Schaal and Schweighofer, 2005; Körding and Wolpert, 2006; Wolpert, 2007; Körding, 2007).

### 2.3.3.5 Discussion

In chapter 2.3.3, a short overview on the field of research of computational neuroscience in the context of sensorimotor control was provided. The most important research topics and studies were briefly outlined. As before, in the context of this thesis, the question to be discussed is whether it appears plausible that the many DOFs of the human body (Chap. 2.2) can be coordinated via the control structures introduced in this chapter to generate a movement. In principal, the field of computational neuroscience offers two approaches to the solution of the DOFs problem. The first approach is a combination of optimization models and internal models. The second approach uses equilibrium point models. Both solution approaches have been outlined above and a discussion on some of the weak points of both approaches follows.

### **Solution approach 1: Optimal control models and internal models**

Optimal control models can be grouped into open-loop and closed-loop models (Chap. 2.3.3.1), with most optimal control models being open-loop models. In open-loop models, a planner computes a desired trajectory that is transmitted to a controller, which in turn transforms the desired trajectory into adequate motor commands. Finally, the motor commands are sent to the plant. Depending on the open-loop model, the problem of motor redundancy is largely resolved on the planning stage via optimization. The only information needed by the planner to compute a desired trajectory is the current state and the desired final state. In chapter 2.3.3.1, some specific problems of individual models were discussed. Therefore, the following discussion concentrates on the general weaknesses of open-loop optimization. These problems can be interpreted as potential topics for future research.

Open-loop models cannot account for all types of human movements. As outlined in chapter 2.1, motor control models can only account for specific classes of movements. In the case of open-loop or feed-forward control, it seems plausible that the CNS uses such a control scheme for fast movements or highly practiced movements (Heuer and Konczak, 2003). It should be acknowledged that although the CNS may use many different control strategies to produce the same behavior, these strategies cannot be differentiated experimentally. As an example, a recent study by Desmurget and Grafton (2000) indicated that feed-forward control can be simulated by a fast feedback-loop on the basis of a well developed forward model.

The study by Desmurget and Grafton (2000) led to the discovery of a more serious problem in the context of open-loop optimization. The problem involves the assumption that there is a distinction between a *planner* that computes a desired trajectory and a *controller* that transforms the desired trajectory into motor commands. Concerns regarding this assumption, borrowed from engineering sciences, have been raised by various authors (Alexander and Crutcher, 1990; Kalaska et al., 1998; Cisek, 2005). Cisek (2005) suggests that actual neural data does not support the idea of a pre-generated plan or trajectory. In his opinion, the only plan constructed before movement begins is a rather crude representation of the movement in form of a “difference vector” (see also Shadmehr and Wise, 2005) between the current state of the musculoskeletal system and its desired end-state. Even for highly practiced movements, the only plan that is precomputed by the CNS would be a simple signal.

Despite his criticism of the separation of the two entities, Cisek (2005) admits that in the absence of an alternative, this scheme still serves as a major theoretical framework in motor control research. On the basis of the above discussed psychophysical and neurophysical studies, it is currently impossible to identify the level or space in which human movements are planned (extrinsic vs. intrinsic or kinematic vs. dynamic). However, as outlined in chapter 2.3.3.1, this research deficit can be approached in the context of open-loop optimization models. In other words, optimal control models can be used to examine the space in which trajectories are planned. Trajectories predicted by optimal control models defined in different planning spaces

and experimentally determined trajectories are compared (Osu et al., 1997) using optimal control models. According to Nakano et al. (1999), one can distinguish between four planning spaces: an extrinsic kinematic space, an intrinsic-kinematic space, an intrinsic-dynamic-mechanical space, and finally, an intrinsic-dynamical-neural space. Different optimal control models can be assigned to the four identified planning spaces (Fig. 2.14). It is unlikely that there is one general optimization model that can account for all the experimental data. As for motor control models in general, it is conceivable in the context of open-loop optimization, that there simply may not be a single optimal control model that can explain all aspects of human motor behavior. Instead, it is possible optimization criteria are chosen or weighed differently based on an individual's intentions or depending on the specific goal of the movement.

A lot of research has been conducted on simple 2D movements. The characteristics of these movements have been explained and are reasonably well understood (Gielen, 2009b). Compared to the success of open-loop optimization models for the assessment of 2D movements, the use of open-loop optimization models is still in an investigate phase for multi-joint movements in 3D space (Flash et al., 2003). Consequently, one of the major challenges in research is the application of optimization models to multi-joint movements in 3D space (Hermens and Gielen, 2004; Admiraal et al., 2004; Gielen, 2009b). A problem that arises when analyzing multi-joint movements in 3D space is the choice of metric for quantitative comparison of the different models (Gielen, 2009b).

In contrast to open-loop optimization, Todorov and Jordan (2002) developed an optimal feedback controller (Chap. 2.3.3.1). In such a closed-loop optimization model, the controller is fully programmable and does not rely on preconceived notions of what control schemes the sensorimotor system may use, but does what is needed to accomplish the task. In other words, optimal feedback control lets the task and the plant dictate the control scheme. In a postural task where a target limb position is specified, this may be a position control scheme. Because of the fact that the state of the plant is only observable through delayed and noisy sensors, the controller is only optimal when the state estimator is optimal. Todorov and Jordan (2002) proposed a theory of motor coordination based on optimal feedback control that may form a general strategy for movement generation in the presence of signal dependent noise. Since the model does not precompute a desired trajectory, the redundancy of the human movement system has to be resolved online by the feedback controller. Although the framework of stochastic optimal feedback control appears plausible, the mathematical modeling is very complex, even for simple linear control problems and is computationally expensive. The implementation of this approach becomes even more complex because it is believed that the CNS chooses the optimal control law depending on the task. Consequently, the implementation requires not only knowledge about motor planning and execution, but also about the intentions of the subject (Scott, 2002; Gielen, 2009a). Additionally, it should be mentioned that the computation of the control law requires knowledge about the initial and final

state, and the movement time. This implies that some kind of planning takes place prior to movement onset (Cisek, 2005). Since the optimal stochastic feedback control framework from Todorov and Jordan (2002) is in its infancy, it is difficult to assess how the approach will evolve in the coming years. Development of the framework depends on how many scientists utilize and enhance the approach.

Both types of optimal control models depend on internal models. Open-loop optimization requires a precise inverse model and closed-loop optimization requires a precise state estimate by a forward model. Although there is some criticism concerning internal models (Ostry and Feldman, 2003; Feldman and Latash, 2005), it seems relatively well established that the CNS makes use of internal models (Kawato, 1999; Sabes, 2000; Flash and Sejnowski, 2001; Schaal and Schweighofer, 2005; Shadmehr and Wise, 2005). However, one of the major scientific challenges in the context of internal models is the question of where in the human CNS these models are stored.

### **Solution approach 2: Equilibrium point models**

One alternative to optimal control and internal models are equilibrium point models. In this thesis, the  $\lambda$ -model was introduced because the author is of the opinion that this version of equilibrium control is the most plausible and most influential version in the field of motor control. The foundation of the  $\lambda$ -model is that the CNS controls posture and movement by relying on the spring-like properties of the muscles and reflex loops. Posture is defined by equilibrium positions and the movement by shifts of those positions. Therefore, motor control in biological systems does not rely on precomputed trajectories. Instead, trajectories are the result of the musculoskeletal system and the CNS interacting by the reflex pathways and external forces acting on the body. Compared to optimization and internal models in the field of motor control, the  $\lambda$ -model is dated but relevant. The hypothesis has survived the last 45 years because Anatol Feldman refined and extended the original  $\lambda$ -hypothesis (Feldman, 1966) in a long series of experiments, to encompass an entire threshold control theory (Feldman and Levin, 2009) even though some deficiencies in the  $\lambda$ -model still exist.

One of the deficiencies of the  $\lambda$ -model is the “not to intervene voluntarily” paradigm. Feldman (1966) developed this experimental paradigm to be able to guarantee fixed descending commands analogously to animal experiments. Subjects were asked to occupy a joint position against a load and “not to intervene voluntarily” when the load is suddenly modified. It seems unlikely that subjects are not able to voluntarily respond to an external stimulus. Even if different subjects are able or almost able to not intervene voluntarily, the performance of different subjects in that task will most likely differ.

To examine invariant characteristics in humans based on the “not to intervene voluntarily” paradigm, joint torque-angle characteristics are analyzed instead of muscle force-length characteristics as is done in animal experiments. Because of the similarities of the joint-angle curves in human subjects and the tonic stretch reflex

characteristics recorded in animal experiments, Feldman (1986) used the same term (tonic stretch reflex) to describe his data from human subjects. However, Latash (1993) refers to the problem that the internal mechanisms of the tonic stretch reflex are unknown and may differ significantly. Therefore, the human tonic stretch reflex is introduced as an abstraction without a clear neural counterpart.

In the context of the  $\lambda$ -model, voluntary movements arise as a consequence of shifts in equilibrium points. Presently, there exists no consensus on the manner in which the equilibrium shifts, that is, how the equilibrium trajectory or virtual trajectory appears. It was shown (Gribble et al., 1998) that the form of the virtual trajectory highly depends on the model used for force generation. Currently, no generally accepted algorithm exists for the reconstruction of the virtual trajectory.

Furthermore, the  $\lambda$ -model focuses on the peripheral neuromotor system rather than on supraspinal structures. How goals or intentions are transformed into central commands and how central commands are produced and thereby a virtual trajectory is constructed is not addressed. As Latash (1993, p. 3-4, 7) points out:

“So, we will hypothesize that there is a smart and experienced homunculus sitting at the upper level (supraspinal structures, T.S.) who gets proprioceptive information from the afferent sources, combines it with information from other sources (visual, auditory, and others), and generates relevant descending signals to the “intermediate” level (spinal cord, T.S.) based on the task (will) and memory. ... We shall restrict ourselves to analysis of the intermediate level of signal processing in the introduced scheme of voluntary motor control; we will pretend that, on the one hand, we give up the attempt to understand how the upper level generates correct descending commands, and, on the other hand, we know how the output signals are processed by the lower level leading to joint angle and torque changes.”

In this context, it is problematic to exclude the function of supraspinal structures in a motor control model. However, it has to be acknowledged that Feldman and Levin (2009) extended the approach during the last several years to include supraspinal structures.

## 2.4 A computational approach for studying human movements

Chapter 2.1 began with an introduction to the field of human motor control. At the end of the chapter, the four major challenges in motor control research were outlined. In the following chapter (Chap. 2.2), one of those four problems, the DOFs problem, was described in greater detail as it is central to this work. Subsequently, existing models from three different scientific paradigms that address the DOFs problem were

presented and discussed (Chap. 2.3). The selection of the approach that seems to be the most comprehensive (and should be used in this thesis) will be based on the review above. This chapter starts with some fundamental considerations about the study of human motor control (Chap. 2.4.1). In a second step, these considerations are transferred to the DOFs problem and the computational approach of this thesis is introduced and justified (Chap. 2.4.2).

### 2.4.1 Fundamental considerations about the study of human motor control

One way to assess the progress in the field of human motor control is to examine how well we can construct artificial limbs and machines that emulate human skills (Wolpert, 2007). For example, in the game of chess, humans can build machines that are able to beat the majority of players on the planet. There is likely only a very small group of chess experts that are able to win a single game against chess computers, like Deep Blue (Campbell et al., 2002). Although the computer most likely uses different strategies than the human brain to plan its moves, it seems that computers are able to solve the problem of which chess move should be implemented. If the chess computer is further enhanced, for example by constructing a body using the best humanoid robot, it is clear that every young child would be able to outperform this humanoid robot in the manipulation of a chess piece. So Wolpert (2007, p. 512) poses the question: “Why is choosing where to move a chess piece so much easier than actually moving it?” In the first task, choosing where to move a chess piece, the chess algorithm is obvious: look at all possible combinations of moves through to the end of the game and choose a move that ensures that you are winning. While the algorithm seems clear, the implementation is far from straight forward. A simple brute force method that calculates all possible solutions and chooses the best solution seems to be infeasible even for modern computers. However, given *Moore’s law* regarding the trend in the development of computer hardware, specific data structures, and algorithms that work on these structures (Knuth, 1999), it has been possible to approximate such a chess algorithm. In contrast, when it comes to the problem of skilled performance or motor control, the specific algorithm is simply not known. Compared to the game of chess where the state of the board and the consequences of each move are known, movement control requires an interaction with a variable and ever changing environment (Wolpert, 2007). Given the complexity of the human motor system, it is likely humans use different control algorithms. So, how should one proceed to understand these algorithms?

#### 2.4.1.1 Object of research: Control of goal-directed every day movements

In trying to understand the different motor control algorithms, one should not confound his or her analysis with the question of how the idea to perform a movement

first evolves. This issue is a topic of philosophy, or perhaps one of motivation psychology (Latash, 2008b) and is therefore beyond the scope of this thesis. The starting point for the following considerations is goal-directed daily life movements such as reaching for a glass of water. In this case it would be clear why the individual would execute the movement: because of thirst.

Because of the complexity of the human motor system, it seems reasonable to assess goal-directed daily life movements that are less complex than most movements in sports, but that are still ecologically valid. In other words, movements that are used by humans in their daily lives should be analyzed. This is an important point since artificial labor tasks often require movements that humans do not typically use in their daily routines. Understanding the functionality of daily life movements is important in rehabilitation, the development of artificial limbs, robotics, and may help form the basis for the understanding of more complex movements in sports.

### 2.4.1.2 Integration of different levels of research

One of the key assumptions in motor control is that information about the process of movement planning and control can be deduced from regularities in motor behavior (Bernstein, 1967). To understand basic coordination principles, one must begin by observing the system's behavior under various conditions. The results will likely lead to a definition of some general features or principles of the system's behavior. These features can then be used as a basis for the development of a motor control model. Observed motor behavior is the result of a complex interaction between the musculoskeletal system and the CNS as a highly distributed control system. Therefore, it needs to be confirmed that the chosen motor control model can be implemented in the human brain or that the human brain functions as predicted by the model against the background of current neurophysiological data. In addition, the developed model must be tested to ensure that it is able to control the musculoskeletal system as the CNS does. Based on these considerations, many different studies (Chap. 2.3) have been conducted to understand the functionality of human movements. These studies can be assigned to three different levels (Fig. 2.20) including neurophysiological studies, studies on the physics of the musculoskeletal system and behavioral studies.

#### Neural Control

In the context of neural control, there are two important features. First, the processing of sensory inputs and motor commands to spinal neurons and muscles are distributed in *hierarchically* interconnected areas of the cortex, the brain stem and the spinal cord. Each of the three areas possesses circuits that are able to organize or regulate complex motor responses. Second, movement related sensory information provided by afferents is processed in different systems that operate in *parallel* (Chap. 2.3.1.4). The hierarchical organization of the motor system is depicted in figure 2.20.

The spinal cord can be seen as the lowest level in this hierarchical organization.

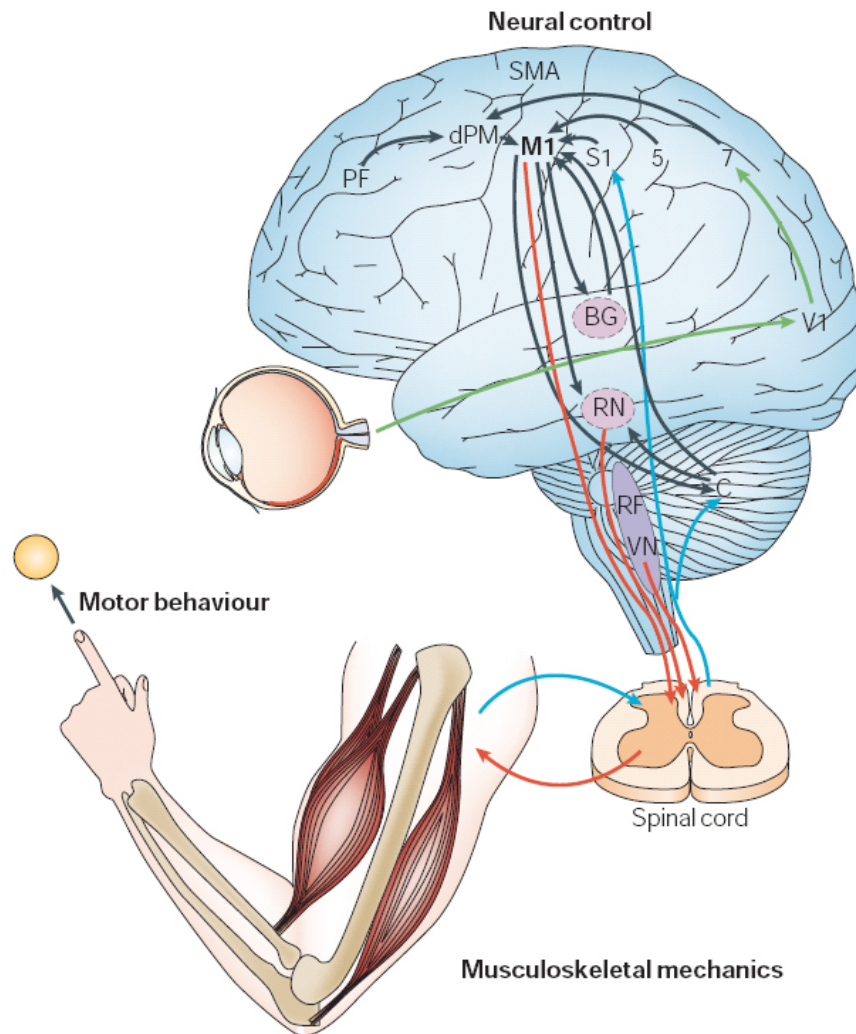


**Figure 2.20:** The *neural control* structures are typically divided into the cortex, brainstem and spinal cord. The structures innervate the motoneurons in the spinal cord which in turn activate muscles that act on a multi-articulated skeleton (*musculoskeletal mechanics*). Finally, the muscle activity leads to limb movement (*motor behavior*). The motor behavior describes how the limbs move during the motor task, reflecting the combined action of neural control and the musculoskeletal mechanics (Scott, 2004). More detailed descriptions can be found in the text.

It contains the neural circuits that mediate a variety of reflexes and rhythmic movements (Chap. 2.1). Reflexes can be monosynaptic, including only the primary sensory neuron and the motor neuron. Most of the reflexes are mediated by polysynaptic reflexes, where one or more interneurons are interposed between the primary sensory neuron and the motor neuron. Interneurons and motor neurons ( $\alpha$ - and  $\gamma$ -motoneurons) receive input from axons descending from supraspinal structures. These signals can modify reflex responses to peripheral stimuli by activating or inhibiting highly interconnected populations of interneurons. Moreover, voluntary movements are also coordinated by these interneurons. All motor commands eventually converge on spinal neurons or brain stem neurons to innervate skeletal muscles (Ghez and Krakauer, 2000).

The next level in the hierarchy is the brain stem. There are systems in this structure that receive input from the cerebral cortex and subcortical nuclei and project the information to the spinal level. The medial descending pathways are the phylogenetically oldest component of the descending motor systems and terminate predominantly on interneurons influencing motor neurons that innervate axial and proximal muscles. These pathways provide the basic postural control system upon which the cortical motor areas can organize more highly differentiated movements. The lateral descending pathways control distal limb muscles and are therefore important for goal-directed object manipulations such as grasping a glass of water. The main lateral pathway from the brain stem is the rubrospinal tract, originating in the red nucleus (RN) in the midbrain. This structure receives input from the primary motor cortex. In cats and monkeys, the rubrospinal tract is important in the control of distal limb muscles. However in humans, this function is largely adopted by the corticospinal tract (Ghez and Krakauer, 2000).

The highest level in the control hierarchy is the cortex. Systematic stimulation of the surface of the cortex in primates revealed somatotopic maps of the body, especially in the primary motor cortex (Brodmann's area 4) and the premotor cortex (Brodmann's area 6). The primary motor cortex (M1) and several premotor areas project directly to the spinal cord through the corticospinal tract and also regulate other motor tracts that originate in the brain stem. The premotor areas are important for planning and executing complex movements. The major input for these premotor areas is from prefrontal, parietal and temporal association areas, whereas these inputs are mainly focused on the premotor cortex and supplementary motor cortex. The primary motor cortex receives inputs from these two structures and from the primary sensory cortex (Ghez and Krakauer, 2000).

In addition to the above described hierarchical levels, two other parts of the brain are involved in the process of planning and executing movements. The *cerebellum* and the *basal ganglia* provide feedback circuits that regulate cortical and brain stem motor areas. They receive input from various areas of the cortex and project back to the motor areas via the thalamus, although both circuits pass through separate regions of the thalamus and terminate in different cortical areas. Likewise, the inputs

from the cortex are also separate. Moreover, the cerebellum and the basal ganglia do not send significant output to the spinal cord. Rather, they act directly on projection neurons in the brain stem. Although the precise contribution of these two structures to skilled movement behavior is still unknown, it is likely they are necessary for creating smooth movement and posture. Neurophysiological data shows that damage to the basal ganglia (e.g. Parkinson or Huntington) leads to the production of involuntary movements and abnormalities in posture. Likewise, damage to the cerebellum (cerebellar ataxia) leads to a loss of coordination and accuracy of movement (Ghez and Krakauer, 2000).

In summary, it seems that the vast amount of reflex circuits in the spinal cord and the brain stem simplify the instructions sent by the cortex. In facilitating some circuits and inhibiting others, supraspinal control levels appear to be in the position to let sensory inputs on lower levels govern temporal details of an evolving movement. The timing of the activation of the antagonistic muscles is intrinsic to the circuits of the spinal cord and therefore, descending signals themselves do not need to be precisely timed (Ghez and Krakauer, 2000).

### **Musculoskeletal mechanics**

In voluntary movements, commands from supraspinal structures are sent to interneurons and  $\alpha$ -motorneurons that activate the skeletal muscles. The skeletal muscle system is the largest organ in the human body. The entire muscle system consists of tightly packed substructures called muscle fibers, myofibrils, sarcomeres and actin and myosin strands. Furthermore, muscles consist of extrafusal and intrafusal fibers. Extrafusal fibers are connected to the bones by tendons and produce force and ultimately limb movements. This type of fiber is activated via  $\alpha$ -motoneurons. In contrast, intrafusal fibers contain muscle spindles that are arranged in parallel to the extrafusal fibers and have a sensory function. Intrafusal fibers are activated via  $\gamma$ -motoneurons. The term *motor unit* includes a motor neuron and the muscle fibers controlled by this motor neuron. The number of muscle fibers in a motor unit varies according to the function of the muscle. Motor units contributing to fine movements (e.g. finger movements) are usually comprised of a small number of muscle fibers, whereas other motor units, like those in the quadriceps, consist of up to a thousand muscle fibers per motor unit. Altogether, there are three types of motor units that can be categorized by the speed of muscle contraction because of an electrical stimulation and fatigability because of a repeated stimulation. These categories are: (1) fast, quickly fatiguing motor units, (2) fast, fatigue-resistant motor units and (3) slow, non fatiguing motor units. Independent of the type of motor unit, force generation occurs within the sarcomeres and is the result of an interaction of the actin and myosin filaments. This interaction process is energy demanding and is described by the *sliding filament theory*. The generation of force is the result of a cascade process of electrical and biochemical events, starting with the release of acetylcholine by the synapses of the motor neurons. This release leads to a depolarization of the postsy-

naptic membrane and finally to a release of calcium in the muscle. High intracellular calcium levels remove another protein, called tropomyosin, from active sites on the actin filaments. With removal of the tropomyosin, the myosin filaments are able to attach to the actin filaments, beginning the *cross-bridge cycle* described by the sliding filament theory. In this theory, the actin and myosin filaments slide against each other, causing a reduction of sarcomere length and a production of force resulting in limb movement. However, the length of the muscle, dependent on the length of the individual sarcomeres, affects the force generated by the muscle. This property is known as the *force-length relationship*. At a sarcomere length of approximately  $2.0 - 2.2 \mu\text{m}$ , an optimum overlapping of the actin and myosion filaments results in a maximum force generation. Furthermore, the generation of force depends highly on the velocity of muscle contraction (*force-velocity relationship*) (Wise and Shadmehr, 2002; Gollhofer, 2008). The amount of force produced by a muscle depends on the number of recruited motor units. According to the *size principle* (Chap. 2.2), small motor units are recruited first, whereas larger units are recruited later as force development progresses (Henneman, 1965). Additionally, the firing frequencies of motor neurons have an impact on the force production in muscles. All of these muscle characteristics, together with the large number of muscles (Chap. 2.2), increase the complexity of the mathematical modeling of muscle functions (Sandercock et al., 2003; Shadmehr and Wise, 2005).

In isolated single-joint movements, muscle force and joint motion are tightly coupled. The *muscular torque* ( $T$ ) is defined as  $T = I \times \ddot{\Theta}$ , where  $I$  corresponds to the moment of inertia and  $\ddot{\Theta}$  to the angular acceleration of the joint. This is an angular version of Newton's second law  $F = m \times a$ , where  $F$  is the force vector,  $m$  is the mass of the body and  $a$  is the acceleration vector. This simple relationship loses its validity when movement involves multiple joints. The equations of motion to describe a simple planar task involving flexion and extension at the shoulder  $T_S$  and the elbow joint  $T_E$  are as follows (Scott, 2004):

$$\begin{aligned} T_S = & (I_1 + I_2 + m_1c_1^2 + m_2(I_1^2 + c_2^2 + 2l_1c_2 \cos \theta_E)) \ddot{\theta}_S \\ & + (I_2 + m_2c_2^2 + m_2I_1c_2 \cos \theta_E) \ddot{\theta}_E - (m_2l_1c_2 \sin \theta_E) \dot{\theta}_E^2 \\ & - (2m_2l_1c_2 \sin \theta_E) \dot{\theta}_S \dot{\theta}_E \end{aligned} \quad (2.12)$$

$$\begin{aligned} T_E = & (I_2 + m_2c_2^2 + m_2I_1c_2 \cos \theta_E) \ddot{\theta}_S \\ & + (I_2 + m_2c_2^2) \ddot{\theta}_E + (m_2l_1c_2 \sin \theta_E) \dot{\theta}_S^2 \end{aligned} \quad (2.13)$$

where  $_1$  and  $_2$  correspond to the properties of the upper arm and forearm. The muscular torque at each joint depends on the moment of inertia ( $I$ ), the length ( $l$ ), the mass ( $m$ ) and the center of mass ( $c$ ) of each segment. These two equations show that there is no longer a direct relationship between joint motion and driving torque in each joint. Instead, torque at one joint can generate motion in the other

joint and vice versa. The mechanical coupling of motion and torque between joints is referred to as *intersegmental dynamics* or *interaction torques* (Zatsiorsky, 2002). The equations described above for a two-joint planar movement are quite simple compared to multi-joint movements in 3D space. Equations to describe the movement of the entire human body, with its over 200 DOFs, would fill multiple pages. The human CNS controls a system of approximately 800 motors, each of them with different “engine power” to move a complex coupled mechanical system.

### **Motor behavior**

Despite the complexity of neural control and musculoskeletal mechanics, it was shown in chapter 2.3.3.1 that psychophysical studies have revealed various regularities, or invariant features, in human motor behavior. These invariants have become central in understanding human sensorimotor control because they appear to indicate some fundamental organizational principles within the CNS.

#### **2.4.1.3 “What I cannot create, I do not understand”**

The title of this section was written by R. P. Feynman on his blackboard (Hawking, 2002, p. 91). This statement describes an approach that is fundamentally important in the context of the study of biological motor control. As research continues to grow in each of the three areas outlined in chapter 2.4.1.2, it becomes more and more challenging to establish links between research studies on the different levels of motor control. To be able to develop a cohesive framework incorporating all of the results, models of motor control need to be developed. Specific details of such a model can be tested through carefully designed experiments. However, whether or not the overall model works usually relies on the intuition of the modeler, which may be incorrect. Therefore, a promising way of integrating the three areas seems to be the construction of a computational model of human motor control. Given a movement task, the computational model can be used to generate movements via computer simulation. The results of the computer simulations can then be compared to the results of biomedical or biomechanical experiments and, thus, the functionality of the computational model can be tested. The next step would be the implementation of the computational model on a robot platform because simulations are more likely to oversimplify the problem. Furthermore, by testing computational models on robots, problems not foreseen during a simulation may emerge (Hoffmann, 2008). Although the fields of biological motor control and robotics have already started to interact (Chap. 1.1) and the outlined approach has already been implemented by some research groups (Kawato, 2008a,b), it remains arguable of how well a technical system can model a biological system (Webb, 2001). The construction of a computational model that is able to simulate human movement generation on a computer or a robot platform at least leads to an enhanced understanding of the difficulties that the CNS has to overcome. As Hildreth and Hollerbach (1987, p. 606) pointed out:

“It is often true that before we can understand how a biological systems solves an information processing problem, we must understand in sufficient detail at least one way that the problem can be solved, whether or not it is a solution for the biological system.”

In this dissertation, these considerations from the context of human motor control are applied to DOFs problem.

## 2.4.2 Implementation of the considerations in the context of the degrees of freedom problem

The first question to be answered is: Which of the discussed scientific approaches can incorporate the above outlined considerations when working on the DOFs problem? Based on the review of computational neuroscience studies (Chap. 2.3.3), computational neuroscience, in conjunction with the use of optimal control models and internal models, utilizes two concepts that best address the above presented considerations.. Furthermore, this approach has great potential of integration. For example, open-loop optimization criteria can be interpreted as attractors. In the dynamical system approach, these are favorable, attractive system states toward which a system progresses (Chap. 2.3.2.1). It is conceivable that the motor system is attracted in the perceptual-motor work space by system states represented by minimum jerk or minimum torque change principles. In addition, the concept of internal models is also used in current approaches of cognitive psychology (Hossner, 2004). Moreover, optimal feedback control is related to the dynamical systems view (Chap. 2.3.2.1) in the sense that the coupling of the optimal feedback controller, together with the controlled plant, generates a specific dynamical systems model in the context of a given task. Finally, the minimum intervention principle is related to the uncontrolled manifold concept (Chap. 2.3.2.3).

This thesis focuses on open-loop or feed-forward control. It seems plausible that the CNS uses such a control scheme in the context of fast and/or highly practiced movements (Heuer and Konczak, 2003). In figure 2.21, a conceptual control architecture that serves as a general theoretical framework for the thesis is presented. Based on the desired task, the state of the body, and the environmental context, a planner computes a movement plan ( $p(t)$ ) that is transmitted to a controller. The controller then transforms the movement plan into adequate motor commands ( $u(t)$ ). Finally, the motor commands are sent to the plant, thus transforming the motor commands into limb movements according to the movement plan ( $x(t)$ ). Depending on the type of open-loop model, the problem of motor redundancy is more largely resolved during the planning stage via optimization. Based on the reviewed psychophysical and neurophysiological data (Chap. 2.3.3.1), it is currently impossible to identify the level or space in which human movements are planned (extrinsic vs. intrinsic or kinematic vs. dynamic). However, as outlined in chapter 2.3.3.1, this area of research can be

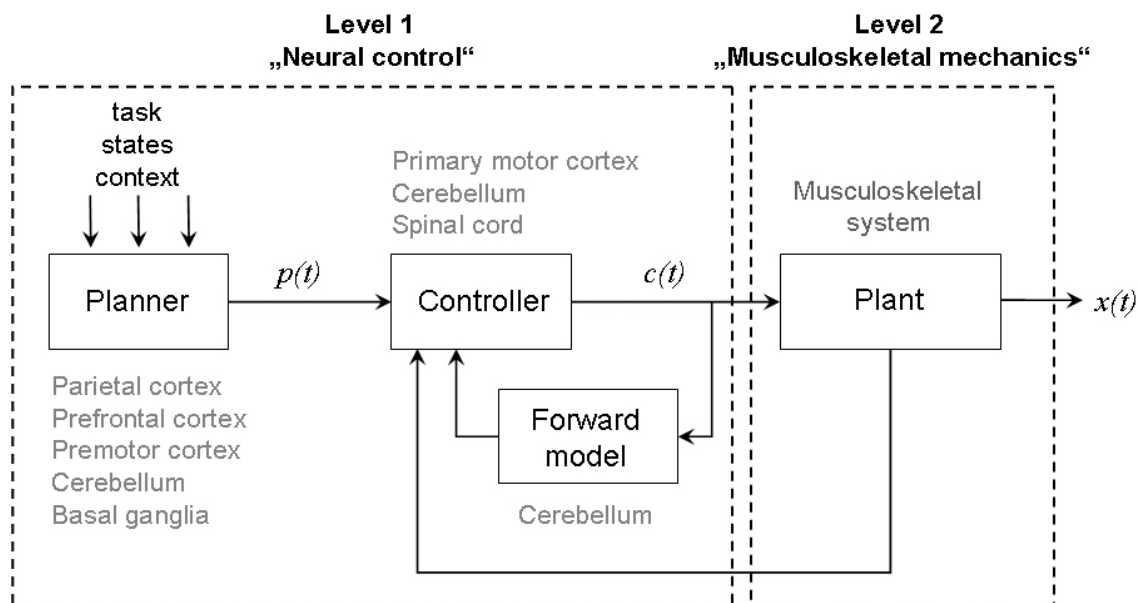


**Figure 2.21:** Based on the task, the current and final state of the body and the environmental context, a planner computes a movement plan  $p(t)$  that is transmitted to a controller, which in turn transforms the movement plan into adequate motor commands  $c(t)$ . Finally, the motor commands are sent to the plant which transforms the motor commands into a movement of the limbs according to the movement plan  $x(t)$ . The controller may use both sensory feedback and predicted feedback provided by a forward model that anticipates the consequences of the current motor command (adapted from Cisek, 2005). Based on the conducted review (Chap. 2.3), the brain structures where these functions possibly occur are described in the text. It is conceivable that the individual entities of this framework are highly distributed across these brain structures. Finally, the structures are attributive to the two levels “Neural control” and “Musculoskeletal mechanics” to establish a link to figure 2.20.

addressed in the context of open-loop optimization models. In other words, optimal control models are not only a solution approach to the DOFs problem, but can also be used to examine the space in which trajectories are planned. Thus, trajectories predicted by optimal control models defined in different planning spaces and experimentally determined trajectories can be compared (Osu et al., 1997). In this context, much research has been conducted on simple 2D movements. Compared to the success of open-loop optimization models for these movements, the use of open-loop optimization models is still in an investigate phase for multi-joint movements in 3D space (Flash et al., 2003). Consequently, one of the major challenges in motor control research is the application of optimization models to multi-joint movements in 3D space (Hermens and Gielen, 2004; Admiraal et al., 2004; Gielen, 2009b). Based on figure 2.14, we will focus on an extrinsic kinematic space, intrinsic kinematic space

and intrinsic dynamic mechanic space. The actions analyzed in this thesis will be discrete and each action will be performed in a perfectly stable and predictable environment (closed skills). Different multi-joint pointing movements in 3D space will be analyzed. Therefore, the context in which the subjects have to perform the different pointing movements should be as natural as possible.

The implementation of this research is carried out in two steps: Analysis and synthesis of human movements.

**Study I: Movement analysis** In this context one of the main assumptions is that the information about the process of movement coordination in the central nervous system can be deduced from behavioral regularities (Bernstein, 1967). A large number of such regularities have been reported in literature (Goodman and Gottlieb, 1995). Nevertheless, the analysis of multijoint daily life movements in 3D-space is uncommon. Thus, the purpose of the first study is to analyze multi-joint pointing movements in 3D-space with respect to the selection of regularities.

**Study II: Movement synthesis** In the second study, a computational model for human movement planning will be developed. In so doing, different optimal control models that can be assigned to different planning spaces are coupled with a multi-body system of the human musculoskeletal system. With the help of this computational model, human pointing gestures will be generated via computer simulation and compared to the experimentally determined pointing gestures. The computational data will be used to address which of the tested optimal control models can best reproduce the behavioral regularities found in the first study. Based on the results, conclusions regarding in which coordinate frame movements are planned by the CNS may be drawn.



## 3 Methods

The methods described here are the basis of the two studies conducted in this thesis. This section comprises a detailed description of the subjects (Chap. 3.1), the procedures (Chap. 3.2), the motion capturing (Chap. 3.3), the biomechanical modeling and the data analysis (Chap. 3.4).

### 3.1 Subjects

Twenty healthy students of the University of Karlsruhe (TH) (16 male; 4 female) between 20 and 25 years of age (mean age = 22.2 years; SD = 1.3 years) participated voluntarily in the study. Their height ranged from 160 to 189 *cm* (mean height = 177 *cm*; SD = 9 *cm*), and their mass ranged from 49 to 100 *kg* (mean mass = 70.6 *kg*; SD = 12.5 *kg*).

### 3.2 Procedures

Human pointing movements were captured in a kitchen at the Institute of Computer Science and Engineering at the University of Karlsruhe (TH). This kitchen serves as a test center for the development of hardware and software components for humanoid robots (Fig. 3.1). All subjects stood in a neutral upright posture at the same starting position (Fig. 3.1), looking at a robot's image projected onto the opposite wall representing the robot as a communication partner. Four plates with numbers were attached at different heights to the kitchen furniture, the wall, and the floor representing objects which the robot would have to bring to its human user (Fig. 3.1). Subjects were instructed to perform the gestures like they would in their daily life. Instructions concerning speed, accuracy or choice of hand were not provided. Besides the starting position, the order of number announcement was standardized. However, subjects were not informed about the order of number announcement before the trial. Each number was called five times resulting in 20 pointing movements. For instance, when the researcher called "Number 1", the subject pointed in the direction of the corresponding number without touching the target. Prior to data collection, one test trial was performed for each target.

**Table 3.1:** Subject data

Subjects	Sex	Age	Height (cm)	Mass (kg)
01	male	22	172	65
02	female	24	160	49
03	female	21	170	59
04	male	24	182	79
05	male	23	172	60
06	male	22	179	80
07	male	21	176	100
08	male	21	173	65
09	male	25	187	75
10	male	23	184	78
11	male	22	185	75
12	male	20	189	81
13	male	22	175	75
14	male	21	183	64
15	male	23	180	75
16	female	21	160	49
17	male	22	185	87
18	male	22	180	66
19	male	21	185	70
20	female	24	163	60
Mean		22.2	177	70.6
SD		1.3	9	12.5

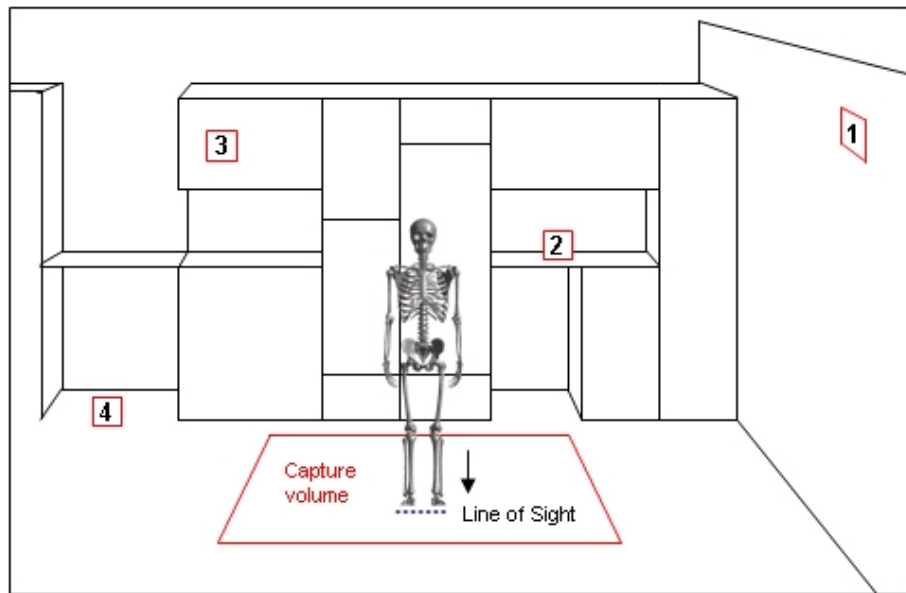


**Figure 3.1:** Starting position of all subjects in the kitchen. Numbers on the kitchen furniture, the wall and the floor indicate the pointing targets.

### 3.3 Motion capturing

A Vicon motion capture system was used for analysis. Motion Capturing means the recording of (human) movements by an array of cameras in order to reproduce the movement in a digital environment. The process of motion capturing can be divided in the steps data acquisition (Chap. 3.3.1) and data processing (Chap. 3.3.2).

#### 3.3.1 Data acquisition

All pointing movements were tracked at 120 *Hz*. To be able to capture human movements, reflective markers were attached to the subjects. For the reconstruction of joint angles (e. g. the elbow joint), at least three non-collinear markers are required on each body segment. Each body segment consists of a bone that is covered by soft tissues. The segments of the body to be modeled are considered “non-deformable”, representing rigid bodies according to classical mechanics (Wu, 1995). Markers are not rigidly associated with the bone. Soft tissues located between the markers and the underlying bone cause relative movements of the markers with respect to the bone. These movements represent artifacts that affect the estimation of the marker positions and joint kinematics and thus represent one of the most critical sources of error in motion capturing (Leardini et al., 2005). In addition, anatomical landmarks should be chosen, which can be identified relatively quickly and reliably (Croce et al., 2005). We developed a basic whole body marker set for studies in CRC 588. This

marker set consists of 78 markers and is based on the Vicon “PlugInGait” marker set and on recommendations found in technical literature (Cappozzo et al., 1995). The marker set is compatible to Vicon applications. 4 *mm* markers were used for the hands, and 9 *mm* markers were used for the rest of the body. For data analysis and synthesis performed in this thesis, 38 of the 78 markers were used (Fig. 3.3). Ten cameras were installed around the subject, making up the capture volume. It was ensured that each marker was recognized by at least two cameras, which was necessary to enable the transformation of coordinates of frame markers into 3D space. Each Vicon camera has a ring of LED strobe lights around the lens. As the subject performs a pointing movement within the capture volume, light from the strobes of each camera is reflected from the markers back into the camera lens and strikes a light sensitive plate creating a video signal. The camera software performs an estimation of the centroids of the marker images. This leads to an effective data reduction because the coordinates of only one point for each marker is being transferred to the computer for further processing rather than a complete video image. In technical literature different algorithms for estimation of the center of a marker can be found (Jobbagy and Furnee, 1994). The Vicon software uses a weighted center of mass fitter.

#### 3.3.2 Data processing

Within the Vicon Workstation software, the 2D data from each camera is linked with the calibration data for the system to reconstruct an equivalent digital motion in three dimensions using a built-in algorithm. Calibrations were performed prior to the first trial of a subject. There are two types of calibration: static and dynamic. With the help of the static calibration object (L-Frame) the global frame is constructed, in which Vicon provides the position data of the markers. In contrast to the recommendations of the International Society of Biomechanics for standardization in the reporting of kinematic data (Wu and Cavanagh, 1995), the Vicon global reference system is defined as a right-handed orthogonal triad fixed to the ground with the  $Z$  axis pointing upward and parallel to the field of gravity. The  $X$  and  $Y$  axes are in a plane perpendicular to the  $Z$  axis. The dynamic calibration involves the movement of a calibration wand throughout the entire capture volume. This process allows the system to calculate the relative positions and orientations of the cameras. In the ideal case, the reconstruction will result in smooth and continuous trajectories throughout the calibration trial. Unfortunately, broken trajectories, meaning that not all markers could be reconstructed in all frames, were unavoidable. In addition, phantom markers and ghost trajectories, because of reflections, were observed. The reflections were deleted and the gaps in the trajectories were filled using a copy pattern algorithm by Vicon, by which points from a similar continuous trajectory are copied to a given discontinuous trajectory to fill the gap. In some cases, the markers were unavoidably hidden for longer periods of time. Consequently, large gaps in

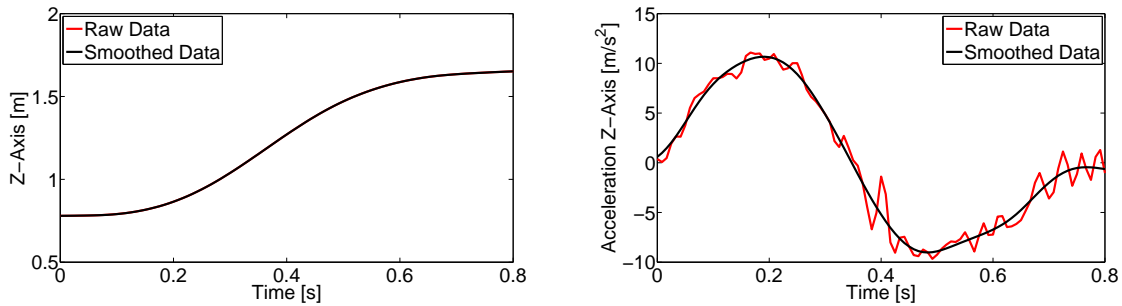


**Figure 3.2:** Vertical displacement and acceleration of a hand marker point (LH7). The times series of the raw data are red and the time series of the smoothed data are black.

some of the trajectories were produced which could not be fixed by copying patterns of continuous to discontinuous trajectories. In such cases, the course of the hidden markers over time was calculated using the Vicon Body Builder Software and the results from the neighboring markers placed on the same rigid body. However, it was not always possible to calculate the time courses of the occluded markers without falsifying the data. For this reason, some trajectories were deleted or left incomplete. When calculating the first and second derivation, it was observed that the two derivations were not continuous. The raw data obviously contains high-frequency signal portions not produced by the biological system. These signal portions, or *noise*, may be the result of skin movement, incorrect digitization or other factors. In the field of biomechanics, different procedures are used to eliminate noise (Wood, 1982; Winter and Patla, 1997), and each of these procedures has strengths and limitations. If the data sets are not too noisy, cubic or quintic spline algorithms often yield adequate results (Winter and Patla, 1997). Because the data sets in the case under consideration were of adequate quality, a quintic spline algorithm by Woltring (1986) was used. In figure 3.2, the time series of the  $Z$ -axis of a hand marker point (LH7) of a typical pointing movement towards target 1 is shown before and after smoothing. Lastly, the trajectories were transferred to the MKD-Tools framework described in the next section.

### 3.4 Biomechanical modeling

A biomechanical model is needed for calculating inverse kinematics and inverse dynamics (Zatsiorsky, 1998, 2002). In this thesis, the MKD-Tools framework, developed in CRC 588, was used. The framework was implemented in Matlab on the basis of a recursive multi-body algorithm, enabling the user to create multi-body models of musculoskeletal mechanics. Marker-based motion capture and anthropometric data was used as input to these models facilitating inverse kinematics and dynamics anal-

ysis. The calculated quantities were available in terms of model-based trajectories, e.g., joint angles, velocities, accelerations, driving joint torques and muscle forces. Large-scale analysis and synthesis required an automation of the different computations and efficient algorithms to accomplish the studies in an acceptable time. Therefore, an automatic scaling algorithm was introduced to adopt the models to the subject's dimensions and to the multi-body algorithm. All algorithms were considered to be of low computational complexity. To provide comparability with other groups, the whole-body models were developed taking modeling standards in robotics and biomechanics into account. In this chapter, a brief introduction of the MKD-Tools framework is provided. The MKD-Tools framework was developed by Stelzner (2008) and enhanced by Simonidis (2010). The reader is referred to these theses for a comprehensive introduction and further details regarding the framework.

### 3.4.1 Dynamic equations

The performance of recursive formulations establishing the dynamic equilibrium equations have proven to be very efficient in terms of computational complexity (Featherstone, 2008). The algorithm introduced below has a complexity of  $O(n)$  computing the kinematic and the inverse dynamic equations. The implementation of the algorithm does not rely on matrix inversion (Cloutier et al., 1995). However, performance relevant details (e.g. the position of body-related coordinate systems) have been taken into account during its development (Stelzle et al., 1995). The user can specify an arbitrary multi-body model, e.g. number and inertial properties of the rigid bodies, holonomic and nonholonomic joint constraints, driving constraints, generalized coordinates and rotation parameters like Euler or Cardan angles, to overcome singularities. The algorithm establishes a minimal set of the spatial dynamic equilibrium equations of the form

$$\mathbf{M}(\mathbf{q}) \ddot{\mathbf{q}} - \mathbf{Q}(\mathbf{q}, \dot{\mathbf{q}}, t) = \mathbf{T} \quad (3.1)$$

where  $\mathbf{q}$  corresponds to the vector of generalized coordinates,  $\mathbf{M}(\mathbf{q})$  to the mass matrix of the system,  $\mathbf{Q}(\mathbf{q}, \dot{\mathbf{q}}, t)$  to the vector of bias forces and torques, including coriolis, centrifugal terms, gravity and external forces.  $\mathbf{T}$  is the vector of generalized forces.

The recursive algorithm is described in detail in Stelzner (2008). An introduction to the theoretical foundations of recursive algorithms can be found in Bae and Haug (1987), Wood and Kennedy (2002) as well as Featherstone (2008).

### 3.4.2 Motion mapping and inverse calculations

Quantitative analysis of human motion requires models of the musculoskeletal mechanics. The topology and parameterization of those models may conveniently rely on surveys of populations and have scaling capabilities avoiding recurrent modeling for any subject. Motion capture data from different trials were mapped on the models using the recursive kinematics formulation together with an optimization-based approach to solve the inverse kinematics. Scaling was also based on inverse kinematics. Using the data from the inverse kinematics, the inverse dynamics calculations were performed. The model of human musculoskeletal mechanics used in this thesis relied on the inertial parameters of De Leva (1996). Furthermore, the recommendations of Wu and Cavanagh (1995), Cappozzo et al. (1995) as well as Cappozzo et al. (2005) for the model topology and the bone-fixed reference frames were used. The kinematic structure of the model, i.e. location and number of joints (Fig. 3.3), were in line with the software packages SIMM and OpenSIM (Delp and Loan, 1995, 2000; Delp et al., 2007). Joint constraints were introduced to improve the inverse kinematics mapping and enable not only the analysis (Chap. 4) but also the synthesis of human movements (Chap. 5). Moreover, the joint constraints ensured comparability between the analyzed and synthesized motion and allowed for specific generalized coordinates to be optimized, while others were driven by data from the analysis. Joint limits were defined both kinematically and dynamically (Simonidis, 2010).



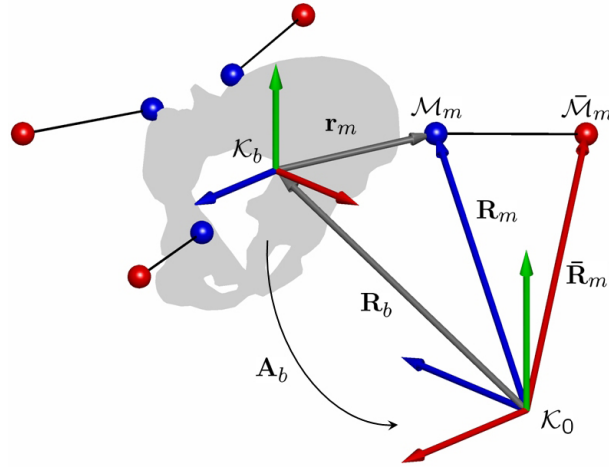


**Figure 3.4:** Absolute and relative marker positions (Stelzner, 2008).

Despite the automatic scaling of the model to subject specific dimensions, a difference between motion capture markers and model markers was observed. To reduce this error, the mapping was implemented as a nonlinear least-squares optimization problem with bounds solving for the values of generalized coordinates by minimizing the error between the position of motion capture markers and the model-defined counterparts with a *Levenberg-Marquardt algorithm*. The absolute position of a marker  $\mathcal{M}_m$  was given by its experimental position  $\bar{\mathbf{R}}_m$  and its model position  $\mathbf{R}_m(\mathbf{q})$  depending on the set of generalized coordinates (Fig. 3.4). The error of  $\mathcal{M}_m$  was defined as  $\mathbf{F}_m = |\bar{\mathbf{R}}_m - \mathbf{R}_m(\mathbf{q})|$ . Minimizing the error over all markers of the system  $m = 1, \dots, n_m$  leads to the nonlinear least-squares problem

$$\min \sum_m \mathbf{F}_m^T \mathbf{F}_m. \quad (3.2)$$

An automatic and subject specific scaling of the model was achieved using markers on specific anatomical landmarks (Cappozzo et al., 2005), the problem (3.2) was solved for  $\hat{\mathbf{q}}$  for a recorded initial pose of the subject. Then, the scales were fixed for the mapping of the time series of the captured motion. The proposed method also allowed for the use of dynamic markers which could be calibrated after the scaling process improving the quality of the mapping process. The resulting kinematic trajectories were Butterworth-filtered according to standards in biomechanics (Wood, 1982; Winter and Patla, 1997) because the procedure introduced sometimes none smooth transitions between the captured frames. Finally, the inverse dynamics was performed to obtain the net joint torque and the reaction force trajectories.

**Table 3.2:** Description of the DOFs analyzed in this study. All subjects stood in a neutral upright posture at the same starting position (Fig. 3.1). Movement amplitudes are the same for the left and right side of the body. All movement amplitudes are provided in degrees.

DOF	Segments	Amplitudes [deg]
Shoulder I	Clavicle - Humerus: Abduction / Adduction	[-120 90]
Shoulder II	Clavicle - Humerus: Rotation	[-90 90]
Shoulder III	Clavicle - Humerus: Anteversion / Retroversion	[90 -90]
Elbow	Humerus - Ulna: Flexion / Extension	[0 130]
Thorax	Thorax - Pelvis: Rotation	[-70 70]

### 3.5 Data analysis

Data analysis was carried out using Matlab (V. 7.7). For all recorded trials, the begin of the movement was defined as the point the origin of the local coordinate frame of the left or right hand segment ( $R$ ), depending on which arm was used for the pointing movement, surpassed 5% of its peak velocity. Time normalization was conducted using a cubic spline interpolation. In both studies, the hand path was determined based on the local coordinate frame of the hand ( $R$ ) and the tangential velocity profiles of the hand were calculated on the basis of the velocity of the local coordinate frame of the hand ( $Rp$ ). Moreover, the shoulder abduction/adduction, shoulder rotation, shoulder anteversion/retroversion, elbow flexion/extension and thorax rotation were of particular interest (Tab. 3.2). In the MKD-Tools output file, angles are abbreviated with the letter  $q$ , angular velocities with the letter  $qp$ , and driving torques with the letter  $T$ . In the first study (Chap. 4), the time courses of the joint angles, joint angular velocities, and driving torques of these DOFs were analyzed and in the second study (Chap. 5), the movement in these joints was synthesized using different optimal control models.

## 4 Study I: The analysis of multi-joint pointing movements in 3D space

### 4.1 Introduction

The technological progress during the last 20 years is reflected in the development of robotics research and its focus on humanoid robot development (Becher et al., 2004). Possible future applications of humanoid robots are residential service, personal robots for elderly, playmate robots in child education or robots for danger zones (e.g. aerospace, nuclear power stations). Humanoid robots are able to accomplish tasks that are difficult to be carried out by humans because of the social need or the dangerous nature of the environment (Tanie, 2003; Fong et al., 2003; Brock et al., 2005; Schaal, 2007b). To promote man-machine interaction in a human environment, the size, geometry, arrangement of limbs, number of DOFs and range of motion of a humanoid robot should be comparable to those of humans (Asfour et al., 2008). Besides anthropometric resemblance, a robot should use human-like movements (Wank et al., 2004; Khatib et al., 2004; Schaal, 2007b). Robotics research is traditionally situated in mechanics and computer science and based on control theory and optimization theory. For the development of humanoid robots that operate in human centered environments, robotic research needs to apply principles from other fields including psychology, biology, and neuroscience (Schaal, 2007b). For the development of a robot that is supposed to work in human environment and use objects and tools of human daily life, it is crucial to understand how humans coordinate their upper-body movements during daily motor tasks. These aspects are especially important if the robot should move in the same fashion as humans. Scientists in the fields of biological motor control and robotics have already started to interact (Schaal and Schweighofer, 2005; Ijspeert, 2006) and exchanged ideas (Hollerbach, 1982; Beer et al., 1998; Sternad and Schaal, 1999; Piazzi and Visioli, 2000; Atkeson et al., 2000; Sun and Scassellati, 2005; Konczak, 2005; Stein et al., 2006). The field of robotics has proved to be a useful environment for developing and testing hypotheses about biological motor control. In other words, models of biological motor control can be corroborated or discarded by testing them on robots. Moreover, the capabilities of biological systems by far surpass those of artificial systems (Flash et al., 2004). Hence, the body of knowledge gained in the field of biological motor control may help engineers to develop hardware and software components for humanoid robots that generate human-like movements and operate in future human environments. In

addition, the analysis of daily upper extremity movements is of great interest not only to researchers in biological motor control (see below) and clinicians (Buckley et al., 1996; Anglin and Wyss, 2000), but also for robotics research (Schaal, 2007b).

The use of the upper limbs during daily life is manifold: they allow us to reach toward objects, grasp objects, perform complex manipulations with different objects, throw objects, point toward objects, and gesticulate and so on, with either the right or the left arm or using both arms and in a variety of different environments and conditions. The diverse manipulations humans are able to perform are the result of the kinematic redundancy of the upper body. This redundancy is advantageous because it enables humans, for example, to avoid obstacles and joint limits. However, this flexibility or movement abundance leads to a control problem. Which particular movement of the large number of possible movements should be chosen? The process of coordinating upper-extremity movements like reaching or pointing toward an object is ill-posed in the sense that the task requirements can theoretically be met by an infinite number of different movements. Bernstein (1967) defined the coordination of a movement as the process of mastering redundant DOFs of the moving organ or its conversion to a controllable system. Given the complexity of the human motor system, the question arises as to which principles humans use for the coordination of their movements. In this context, one of the key assumptions in motor control is that information about the process of movement planning and control can be deduced from behavioral regularities (Bernstein, 1967). To understand basic coordination principles, the systems behavior must be observed under various conditions. This will presumably lead to a definition of some general features or principles of the system's behavior. The system's complexity and the enormous number of possible movement tasks make the analysis of all behaviors for all tasks impossible. Therefore, a model of human control should be developed on the basis of limited information about the system's behavior and probably also limited information about the system's structure (Latash, 1996).

The importance of computational models in biological motor control (Arbib, 2003; Shadmehr and Wise, 2005) is expanding. In computational frameworks it is often assumed that the coordination of goal-directed movements is carried out in a two-stage process. The first stage of the process is the planning stage and the second stage is the execution stage (Bizzi and Mussa-Ivaldi, 2004). During the planning stage a desired trajectory is computed and the corresponding movement is performed during the execution stage. Indeed, many experiments and models have been based on the two-stage framework.

In studies involving biological motor control, the process of trajectory planning has most often been analyzed separately from the execution and control of the movement. Studies concerning movement planning seek mainly to determine the frame of reference in which movements are planned. A pioneering study by Morasso (1981) showed that in multi-joint arm movements, the hand trajectories between pairs of targets in the horizontal plane are roughly straight-line paths in external Cartesian

coordinates with single-peak, bell-shaped velocity profiles regardless of the initial and final location of the hand. In contrast, when the trajectories of the hand were expressed in joint coordinates, the profiles were more complex and variable. These results were subsequently reproduced in a number of studies (e.g. Abend et al., 1982; Flash and Hogan, 1985; Gordon et al., 1994; Haggard et al., 1995) and led to the hypothesis that goal-directed movements, like pointing or reaching toward an object, are planned in external coordinates of the hand and not joint coordinates. The anatomical design of the human arm requires joint rotation to be able to translate the hand from the starting position along the planned trajectory to the target location. Hence, the coordination process would imply a reference frame transformation from external coordinates into joint coordinates. This transformation is referred to as the inverse kinematics problem (Zatsiorsky, 1998) and the study of robotics has shown that there is no unique solution to the computation (Craig, 2005). As described in the optimization models (Kawato, 1996), additional constraints need to be defined to resolve the joint redundancy issues. The specific constraints or combination of constraints used by the CNS in motor control has yet to be determined (Gielen et al., 1995). The results of the Morasso study (Morasso, 1981) do not appear to be uniformly true (e.g. Atkeson and Hollerbach, 1985; Desmurget et al., 1996; Desmurget and Prablanc, 1997). Atkeson and Hollerbach (1985) observed that hand paths in a vertical reaching movement were sometimes curved and that the amount of curvature varied as a function of the initial and final location of the hand. In addition, it was observed that the velocity profiles of the hand were the same for straight and curved movement paths. In contrast, Soechting and Lacquaniti showed in a series of psychophysical experiments (Soechting and Lacquaniti, 1981; Lacquaniti and Soechting, 1982; Soechting and Lacquaniti, 1983) in which subjects had to perform a goal-directed two-joint movement in the sagittal plane, that both joints reached their peak angular velocities at the same time and that the ratio of the peak velocity at the elbow to the peak velocity at the shoulder is equal to the ratio of the angular excursions of the two joints. The results were interpreted by the authors as evidence that movements are planned in intrinsic coordinates. Hollerbach and Atkeson (1985) challenged the conclusion by noting that at the same time, the joint ratios were constant and the trajectories of the hand were almost straight in the above cited studies. This mutually contradictory result of straight lines in hand and joint space had been resolved by Hollerbach and Atkeson (1985) in favor of straight lines in hand space because of an experimental artifact in the case of two joint kinematics near the workspace boundaries. Besides these studies, where the argument for a planning of movements in terms of joint angles appears to be attributed to the movement task, several other researchers have suggested that reaching movements are planned on joint level due to internal control (Kaminski and Gentile, 1986; Hollerbach and Atkeson, 1987; Flanagan and Ostry, 1990; Desmurget and Prablanc, 1997). The studies appear to suggest that both planning spaces are supported by a large number of experimental results. After a review of the experimental settings of

several of the above mentioned studies, Desmurget et al. (1997) showed that there is an important methodological difference between the experiments describing straight and curved trajectories of the hand, namely the presence (constraint) or absence (unconstrained) of a tool that is used to track the movement (e.g. a pen or a manipulandum). The results of the Desmurget et al. (1997) study indicate that in the absence of a tool, the trajectories of the hand do not appear to be programmed to follow a straight line in contrast to constraint movements. Therefore, Desmurget et al. (1997) suggests that constraint and unconstrained movements involve different planning strategies. However, it has to be mentioned that kinematic regularities may also result from planning movements in an internal dynamical space (Uno et al., 1989; Nakano et al., 1999). Currently, there is no consensus on this issue.

The primary question regarding the second stage of the process is how the planned trajectory is executed. On the basis of force field studies (Shadmehr and Mussa-Ivaldi, 1994; Lackner and Dizio, 1994, 1998), it has been suggested that a controller (inverse internal model) computes the necessary feed-forward motor commands for the execution of the desired trajectory and the plant (musculoskeletal system) transforms the motor commands into limb movement. This process contains two mappings: an inverse mapping from the desired trajectory to motor commands by the inverse model and a forward mapping from the current state and the motor commands to the desired state by the musculoskeletal system. Thus, an ideal feed-forward controller can be described as the inverse of the plant. Because feedback loops in biological systems tend to be slow in contrast to robotics, it seems plausible that rapid arm movements are, at least in part, under feed-forward control and not exclusively under feedback control. Since biological systems do not have the ability to generate perfect controllers and unexpected external disturbances cannot be excluded, error corrections are usually necessary. Depending on the duration of the movement, visual and proprioceptive feedback may be available and adjustments can be made if required. However, there has been growing recognition in computational motor control that biological systems may use predicted sensory feedback provided by a forward model of the plant aside from sensory feedback (Kawato, 1999; Desmurget and Grafton, 2000). Thereby a continuous stream of feedback would be provided by the forward model driven by efferent copies of the motor commands sent to the plant. Functionally, this fast internal loop is equivalent to an inverse dynamic model (Miall, 2003). Based on this information, it is conceivable that the brain does not plan an entire desired trajectory but rather monitors the current state of the arm and the target, and continuously formulates small desired changes in the end effector state. Hoff and Arbib (1993) developed a model in which a minimum jerk principle (Flash and Hogan, 1985) is embedded into a controller that is able to use feedback to resist target perturbations and look ahead modules (forward models) to compensate for the delays in sensory feedback. The Hoff-Arbib model can generate end effector trajectories with smooth, bell-shaped velocity profiles as reported in the experimental studies cited above. It still has to be considered why the CNS should

produce movements that minimize jerk. Harris and Wolpert (1998) provided a model answering this question. In their minimum variance model, sequences of muscle activations are planned such that the variance of the final hand position is minimized. The minimum variance model is based on the fact that the magnitude of motor noise is proportional to muscle activation. Accordingly, the choice of control signals affects the variability of movements. Fast or none-smooth movements require large muscle activations, which leads to increased endpoint errors due to increased signal depended noise. The model will therefore predict smooth movements and is compatible with the experimental results discussed above. In other words, smoothness leads to accuracy, but is not a goal in movement planning in its own right. Whereas the minimum variance model by Harris (1998) is a feed-forward model, Todorov and Jordan (2002) showed in a recent study that a feedback system optimized to reduce endpoint error produces many of the above discussed movement features (Chap. 2.3.3.1) without a precomputed desired trajectory. Optimal feedback control creates an uncontrolled manifold (Scholz and Schönner, 1999), which means that motor errors along the most relevant DOFs for the task are minimized and variations are allowed along the DOFs which are not relevant for the task. Optimal feedback controllers can be viewed as special forms of internal models that contain forward and inverse components.

Behavioral research has discovered various regularities in human goal-directed movements. These invariants have become central in understanding the coordination of human movements, as they appear to indicate some fundamental organizational principles within the CNS (“what is regular is controlled”). However, the problem is that it is hard to determine on which level regularities arise because of the complexity of the human motor system, the limited information about the motor system’s behavior, and methodological differences in the study of the motor system. Therefore, it is unsurprising that, as previously outlined, different motor control models have evolved. Although the previously mentioned studies address different research questions and thereby highlight key principles underlying the coordination of goal-directed movements, they overlook important features of natural movements due to somewhat artificial experimental protocols and partial restriction to certain movement planes. In comparison to planar movements, little research has been performed on unconstrained multi-joint movements in 3D space, even though these types of movements are more common in daily life. Accordingly, the purpose of the following study is the analysis of multi-joint goal-directed movements in 3D space in a natural environment. On the basis of different pointing movements, it will be investigated how humans coordinate their redundant movement system in 3D space and if the coordination strategies are robust across the different pointing tasks. Furthermore, it will be examined if the behavioral regularities found in less complex movement tasks are also present in more complex movement tasks. The results will be discussed against the background of the theoretical assumptions of biological motor control outlined above and the background of the development of humanoid robots that move in a human-like fashion. Finally, the applied methods are discussed.

## 4.2 Methods

A detailed description of the study regarding subjects, procedures, data acquisition and processing, and biomechanical modeling and data analysis is provided in chapter 3. In psychophysical studies it is common to analyze the trajectories of the hand as outlined in the preceding chapter. Therefore, the first step in this study was to analyze the hand paths. In addition, the tangential velocity profiles of the hand were examined. The analysis of the hand was conducted on the basis of the local coordinate frame of the left or right hand segment. Furthermore, the time profiles of the joint angle trajectories, the joint angular velocities, and the driving joint torques were examined. Shoulder abduction/adduction, shoulder anteversion/retroversion, elbow flexion/extension and torso rotation were of particular interest (Tab. 3.2). Apart from this, the inter-joint coordination was analyzed and identification of possible couplings between different DOFs was examined.

## 4.3 Results

The coordination strategies used by the subjects in this study could be assigned to one of four groups, as follows. Ten subjects (Tab. 3.1, subjects 1-10), comprising group 1, did not leave the starting position and pointed with their left hand to targets 1 and 2 and with their right hand to targets 3 and 4. In group 2, four subjects (Tab. 3.1) again did not leave the starting position but pointed with their right hand to all four targets. Two subjects (Tab. 3.1), group 3, left the starting position and turned toward the targets, subsequently pointing with their left hand to targets 1 and 2 and with their right hand to targets 3 and 4. The fourth group, consisting of four subjects (Tab. 3.1), did not use consistent coordination strategies for each target. For example, in five separate tasks, one subject pointed to target 1 twice with the left hand and three times with the right hand. In other words, the subjects of the fourth group used the same strategies as the subjects of groups 1 and 2, but changed coordination strategies from trial to trial for each target. The results indicated that 16 subjects preferred recurring coordination strategies for each target, while four subjects preferred alternating coordination strategies for each target. The four subjects implementing alternating coordination strategies used available DOFs to a far greater extent. In the following sections, typical results of groups 1 and 2 are presented. The fourth group used the same coordination strategies as the subjects of groups 1 and 2. The two subjects from group 3 could not be analyzed because they left the capture volume during several of the trials. Moreover, the analysis focused on targets 1 and 3 given that in the second study, the movement synthesis was conducted for these two targets.

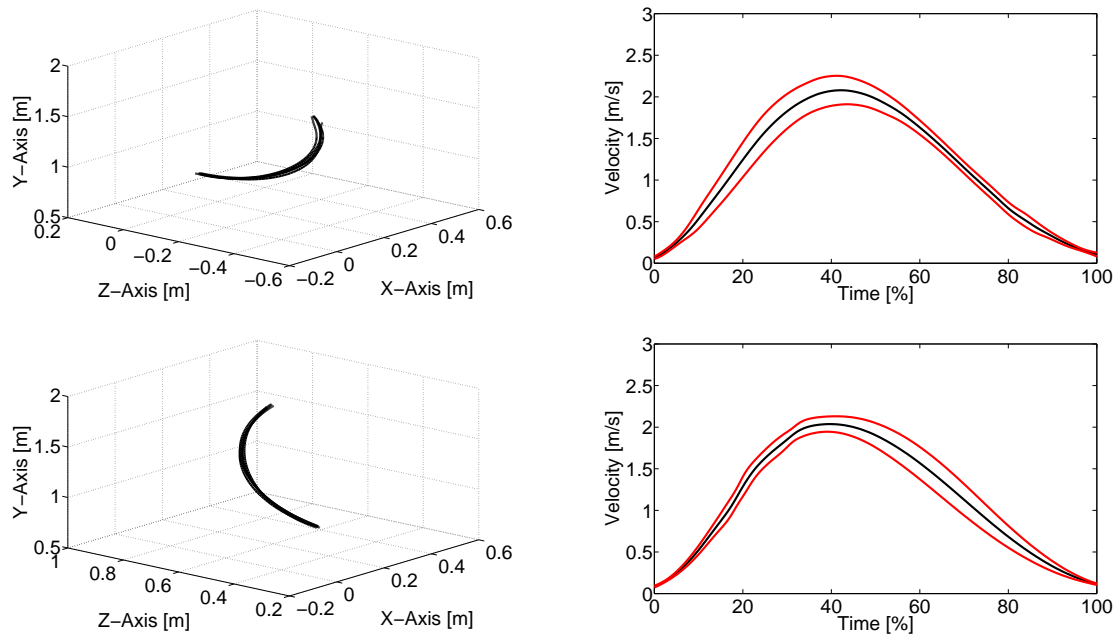


**Figure 4.1:** Five typical hand paths (left column) and corresponding tangential velocity profiles of the hand (mean=black, standard deviation=red; right column) for subject 5 (target 1 = top row, target 3 = bottom row).

### 4.3.1 Hand kinematics

The subjects of group 1 produced curved hand paths as illustrated in Figure 4.1 (left column) showing five typical hand paths produced by subject 5 to targets 1 and 3. Subjects in group 2 also showed curved hand paths as depicted in Figure 4.2 (left column) illustrating five typical hand paths of subject 13 to targets 1 and 3. A visual inspection of the subject trials in groups 1 and 2 revealed that the hand paths appear to always be curved, not straight. Although there were some unsystematic differences concerning the trial to trial variability between and within the subjects, these results indicate that movements of the hand in space show a topological invariance concerning the shape of the hand path despite the different pointing tasks and different coordination strategies (e.g. left hand or right hand).

Subjects of group 1 showed smooth and single-peak tangential velocity profiles. The velocity profiles do not appear to be precisely bell-shaped. In most cases, the peak velocity was reached slightly before 50 % of the movement time had passed indicating a slightly longer deceleration than acceleration phase. There are several cases where the tangential velocity profiles show some distortions at the end. In Figure 4.1 (right column), the velocity profiles of subject 5 for targets 1 and 3 are illustrated. The tangential velocity profiles for the subjects of group 2 revealed the same features as the profiles produced by group 1. In Figure 4.2 (right column), the

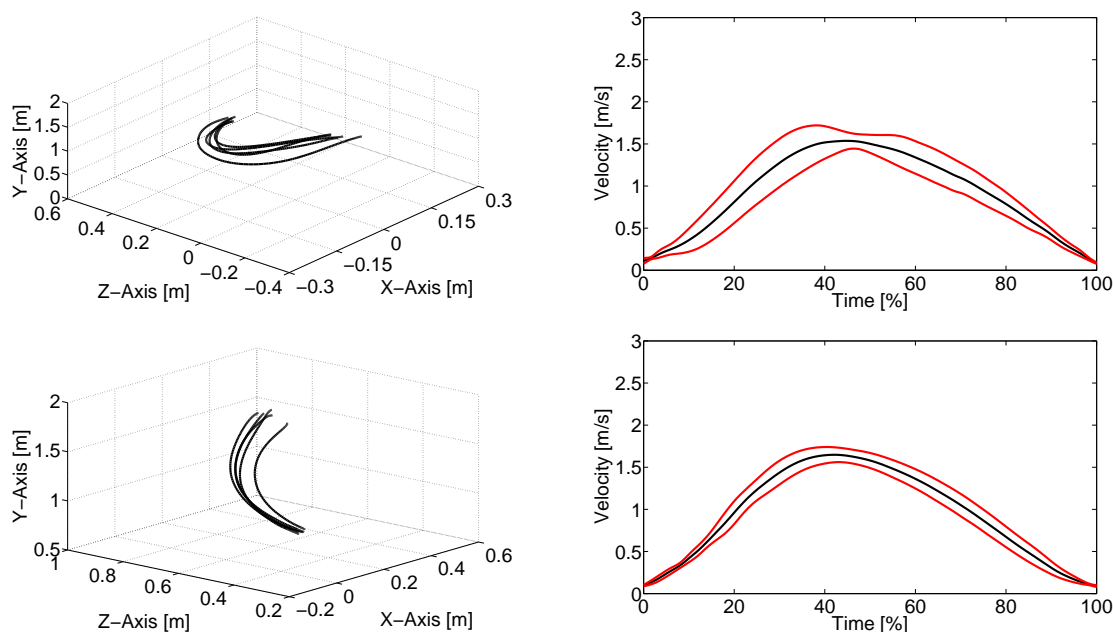


**Figure 4.2:** Five typical hand paths (left column) and corresponding tangential velocity profiles of the hand (mean=black, standard deviation=red; right column) of subject 13 (target 1 = top row, target 3 = bottom row).

corresponding velocity profiles of subject 13 for targets 1 and 3 are shown. Interestingly, the velocity profiles of these subjects were sometimes more variable when pointing with the right hand to the left side.

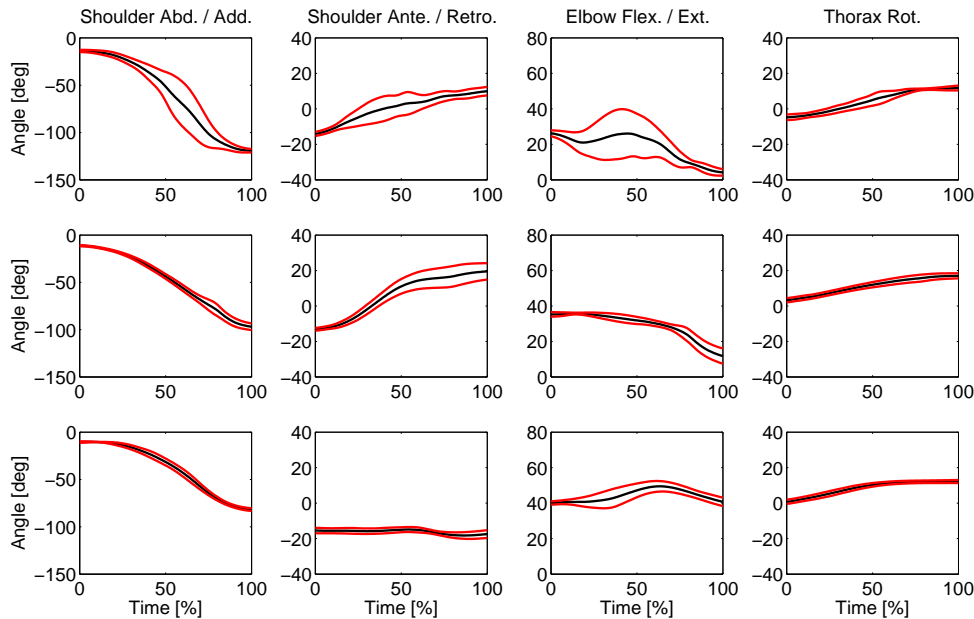
The analysis of the hand trajectories of the subjects across groups 1 and 2 showed that the hand path is curved with smooth, single-peak and approximately bell-shaped velocity profiles. In other words, different subjects exhibited highly stereotypical hand trajectories with common invariant characteristics across different movement tasks.

### 4.3.2 Joint kinematics

The examination of joint kinematics was accomplished in two steps. First, the joint angle trajectories of the shoulder joint, elbow joint, and thorax rotation were analyzed across the two pointing targets, and typical results are presented. In the second step, couplings between the individual DOFs across the pointing targets were analyzed. Again, typical results from the study are presented.

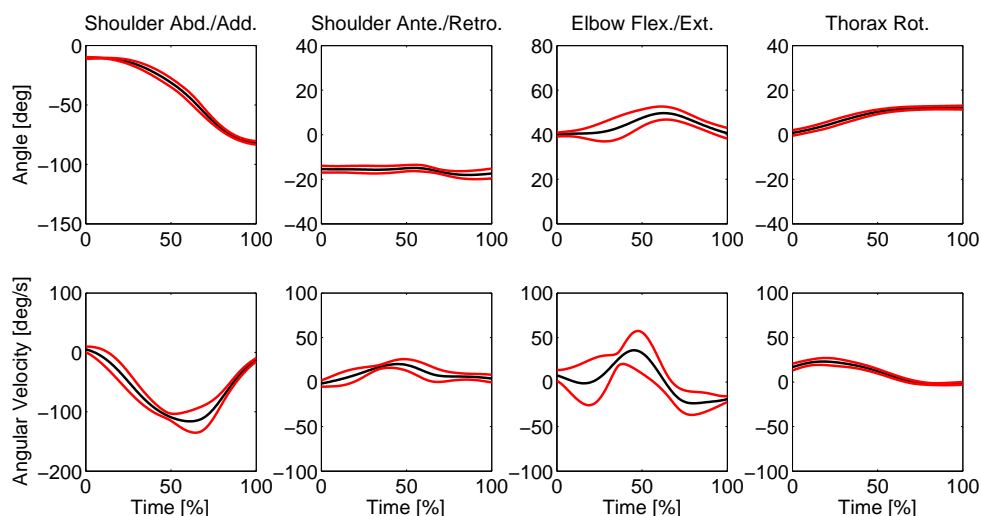
#### Joint kinematics: target 1 & group 1

Figure 4.3 illustrates typical joint angle trajectories of three different subjects from group 1. The three subjects did not leave the starting position and pointed with their



**Figure 4.3:** Mean (black) and standard deviation (red) of five joint angular courses of four different DOFs for three representative subjects (target 1). The joint angle trajectories of subject 2 are displayed in row 1, the joint angle trajectories of subject 5 are displayed in row 2 and the joint angle trajectories of subject 8 are displayed in row 3.

left hand to target 1. Subject 2 (first row) performed the pointing movements rather quickly. In contrast, subject 5 (second row) and subject 8 (third row) performed the pointing movements reasonably slower than subject 2. Subject 2 showed the largest amplitude and variability in the shoulder abduction followed by subject 5 and subject 8. The amplitudes of the shoulder anteversion and retroversion are much smaller than the amplitudes of the shoulder abduction. Subject 2 showed the largest movement variability. The joint angle trajectories of subjects 2 and 5 exhibited a transition from retroversion to anteversion in the shoulder joint. In contrast, subject 8 showed little movement in this DOF. In the elbow joint, subject 2 again showed the largest movement variability. Subjects 2 and 5 performed an extension in the elbow joint during the pointing movement, and the smallest elbow angle tended to occur at the end of the movement. Subject 8 performed a flexion-extension movement in the elbow joint during the pointing gesture, and the elbow angle at the end of the movement was nearly the same as the angle at the beginning of the movement. The torso rotation toward the left side during the pointing movement was similar in the three subjects. However, subject 2 showed slightly greater movement variability than subjects 5 and 8. These results are representative for all the subjects from group 1.



**Figure 4.4:** In the first row the joint angles of subject 8 are illustrated (target 1). In the bottom row the corresponding angular velocities are illustrated. As above, black time courses correspond to mean values and red time courses to standard deviations.

Figure 4.4 illustrates the joint angle trajectories of shoulder abduction, shoulder anteversion/retroversion, elbow flexion/extension and thorax rotation for subject 8. The corresponding angular velocities are also depicted in this figure. The largest angular velocities occurred in shoulder abduction, followed by elbow flexion/extension, then shoulder anteversion/retroversion, and finally thorax rotation. These results were typical for the subjects from group 1 because the highest peak angular velocities across these four DOFs occurred in shoulder abduction. No obvious trend was observed in the results for the three other DOFs. The largest movement amplitude was found for shoulder abduction. As before, no clear trend across the subjects of group 1 was observed for the other three DOFs. Compared to the velocity profiles of the hand (Fig. 4.1), the angular velocities tended to be more complex and irregular indicating an increase in the number of sub-movements in joint space. These are typical movement characteristics of the subjects of group 1.

### Joint kinematics: target 1 & group 2

Figure 4.5 (top row) illustrates typical joint angle trajectories and angular velocities of shoulder abduction/adduction, shoulder anteversion/retroversion, elbow flexion/extension and thorax rotation for subject 13 from group 2. The joint angle profiles for the two DOFs of the shoulder joints showed similar characteristics. In both cases, the peak amplitudes were reached at the end of the movement. The peak values of the shoulder anteversion were slightly larger than those of the shoulder adduction. Moreover, the movement of the shoulder anteversion started earlier than the shoulder adduction. This feature is also evident when comparing the correspond-

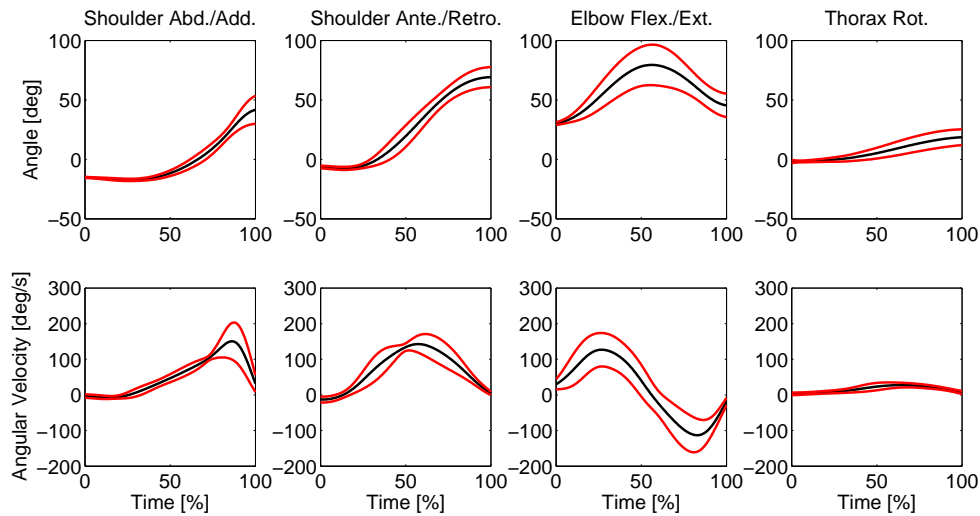


**Figure 4.5:** In the first row, the joint angles of subject 13 are illustrated (target 1). In the bottom row, the corresponding angular velocities are illustrated. Black time courses correspond to mean values and red time courses to standard deviations.

ing velocity profiles (Fig. 4.5, bottom row). Compared to the joint angle profiles of group 1, the subjects of group 2 showed a shoulder adduction instead of abduction and generate much larger movement amplitudes and peak velocities for shoulder anteversion. Compared to the subjects of the first group, subject 13 performed a rather large extension in the elbow joint during the pointing movement. Across the four DOFs, relatively large variations in the movements in the elbow joint were observed. In contrast, thorax rotation toward the left side during the pointing movement was similar across the five trials. In addition, the movement amplitudes in this DOF were comparable to those of group 1 (Fig. 4.3, right column). The angular velocity profiles for the joint angles were more complex and irregular compared to the velocity profiles of the hand (Fig. 4.1) indicating an increase in the number of sub-movements in joint space. These results were representative for the four subjects from group 2.

### Joint kinematics: target 3 & group 1 and 2

The subjects of groups 1 and 2 pointed with their right arm to target 3. Therefore, the joint angle trajectories of both groups were analyzed in one step. In Figure 4.6, joint angle trajectories of two subjects from the first group are displayed, as well as joint angle trajectories of one subject from the second group. Shoulder abduction was highly stereotypical for all subjects (Fig. 4.6, first column). Furthermore, the subjects produced large joint angular amplitudes in this DOF. In contrast, only small movement amplitudes were produced in the second DOF of the shoulder. Except for two subjects (Fig. 4.6, subject 14), all angle courses were negative in this DOF, which corresponded to retroversion. During the pointing toward target 3, no subject

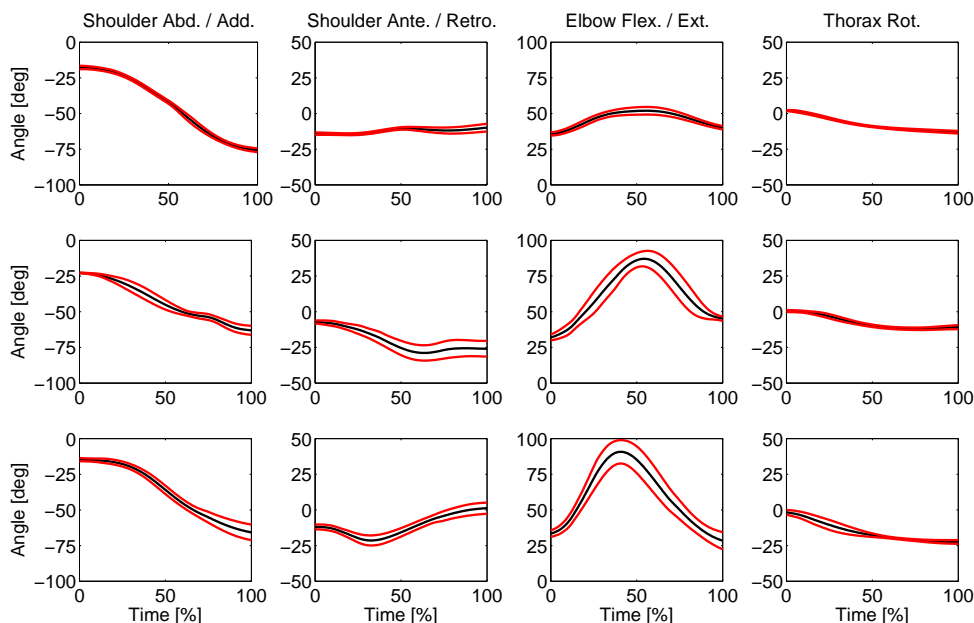


**Figure 4.6:** Mean (black) and standard deviation (red) of the joint angles of four different DOF of three representative subjects (target 3). The joint angle trajectories of subject 5 are shown in row 1, the joint angle trajectories of subject 7 are shown in row 2 and the joint angle trajectories of subject 14 are shown in row 3.

showed a complete extension of the arm. Almost all subjects performed a flexion-extension movement in the elbow joint during pointing toward target 3, and all subjects tended to show nearly the same elbow angle at the end of the movement as at the beginning of the movement. The movement amplitudes were considerably different from each other. Larger movement amplitudes appeared to be associated with larger movement variability across the trials (Fig. 4.6). Thorax rotation toward the right side during the pointing movement was similar across all subjects of groups 1 and 2. Furthermore, the rotation amplitude was comparable to the amplitudes of thorax rotation during pointing toward target 1. The joint angle values were negative because the subjects turned to the right side instead of to the left side.

In figure 4.7, the joint angle trajectories of shoulder abduction, shoulder anteversion/ retroversion, elbow flexion/extension and thorax rotation of subject 5 are illustrated. The corresponding angular velocity profiles are also shown in the figure. The largest movement amplitudes and angular velocities occurred in the shoulder abduction. Some subjects also produced both large movement amplitudes (Fig. 4.6, subject 14) and large angular velocities in the elbow joint. The results indicated similar angular velocity profiles in the shoulder abduction and thorax rotation for all subjects. In contrast, joint angular velocities in the shoulder retroversion and elbow

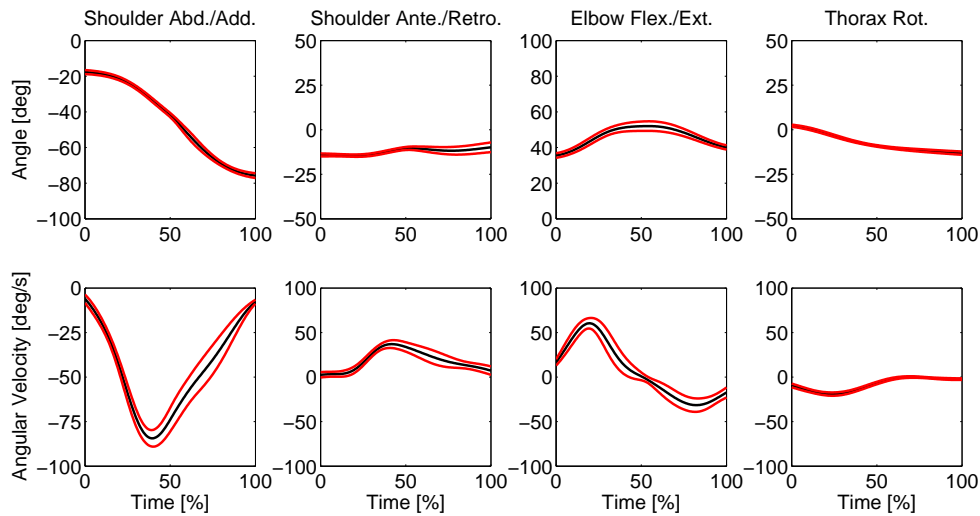


**Figure 4.7:** The joint angles of subject 5 are illustrated in the first row (target 3). In the bottom row, the corresponding angular velocities are illustrated. Black time courses correspond to mean values and red time courses to standard deviations.

flexion/extension varied to a larger degree across subjects. Compared to the velocity profiles of the hand (Fig. 4.1, 4.2), the angular velocities were more complex and irregular indicating an increase in the number of sub-movements in joint space.

In summary, it can be stated that the trajectories of the hand were highly stereotypical across different subjects and different movement tasks. In other words, all subjects produced movements across the two tasks sharing the same invariant movement features independent of whether the right arm or the left arm was used for pointing. Larger differences were identified on the joint level, including intra-individual comparison of the joint angular trajectories across different pointing tasks. In addition, the differences in the joint angular trajectories between groups 1 and 2 during pointing toward target 1 were largely due to the fact that the subjects used different arms. Additionally, analysis showed that within the groups, different coordination strategies were used during pointing to a target. For example, some subjects tended to extend their arm at the end of pointing toward target 1, whereas others showed flexion at the end of the pointing movement. The inter-individual differences in the joint angular trajectories of the individual DOFs in the shoulder and elbow joint indicate that the subjects may use different coordination strategies in the interaction of these DOFs. In contrast, the inter-individual differences in thorax rotation were small and unsystematic. Next, the interaction of the individual DOFs was analyzed more precisely.

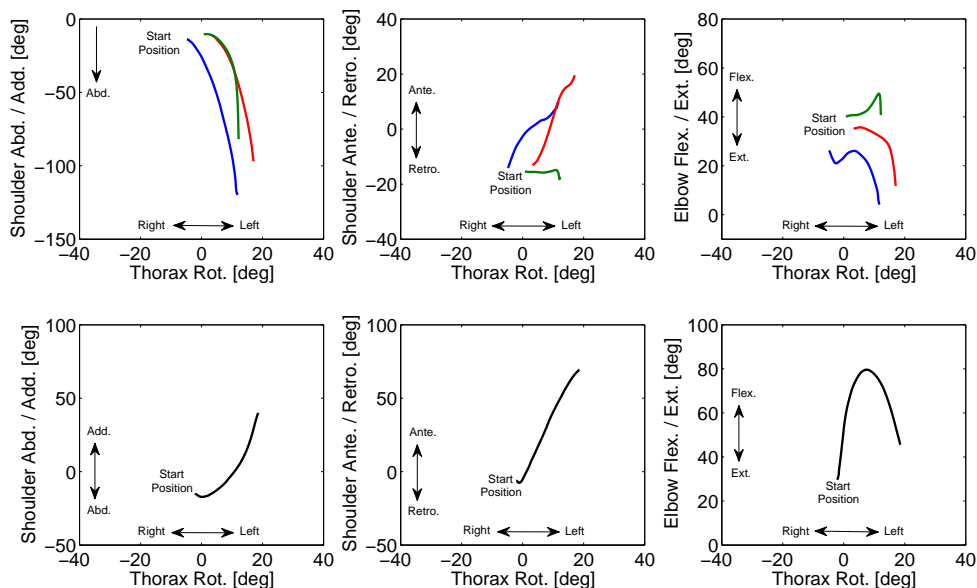


**Figure 4.8:** Inter-joint coordination for thorax rotation versus the movement in shoulder and elbow joint during pointing toward target 1. In the first row, the inter-joint coordination of three representative subjects from group 1 are illustrated (blue=subject 2, red=subject 5, green=subject 8). In the bottom row, the inter-joint coordination of one representative subject of group 2 is illustrated (subject 13). The scaling of the axes of the plots between the two rows is not uniform since the subjects of group 2 pointed with their right arm toward target 1. Accordingly, these movements took place in another region of the joint space. All time courses are mean values ( $N = 5$ ).

### Inter-joint coordination: target 1 & thorax movements vs. shoulder and elbow movements

The top row of figure 4.8 depicts the inter-joint coordination of thorax rotation versus shoulder and the elbow joint during pointing toward target 1 of three representative subjects from group 1. In the first plot, thorax rotation is plotted against shoulder abduction/adduction. All three subjects showed small thorax rotation and large shoulder abduction. Furthermore, during the pointing movement, an almost permanently increasing value in both joints was exhibited, indicating that the relationship is almost linear. In the middle plot, thorax rotation is plotted against shoulder anteversion/retroversion. Subject 8 did not use shoulder anteversion/retroversion. During thorax rotation the arm remained at approximately  $20^\circ$  retroversion. In contrast, subjects 2 and 5 showed permanently increasing values in both DOFs during the pointing movement. Moreover, the maximum amplitudes were reached at the end of the movement forming an almost linear relationship between the two excursions.

However, the gradient of the two time courses differed. In the third plot of the top row, thorax rotation is plotted against elbow flexion/extension. Subject 8 showed only small movement amplitudes in both joints. Thorax movement to the left and extension of the arm during the pointing toward target 1 were observed for subjects 2 and 5. Both subjects reached the peak amplitudes in both joints at the end of the movement.

In the bottom row of figure 4.8, the inter-joint coordination of one subject from group 2 during pointing toward target 1 is illustrated. As before, in the top row, thorax rotation is plotted against shoulder abduction/adduction, shoulder anteversion/retroversion and elbow flexion/extension. The left plot shows that angle/angle course was slightly curved because thorax rotation started before shoulder adduction. In the middle plot, thorax rotation is plotted against shoulder anteversion. The relationship between the movements in these two joints was highly linear. In the right plot, thorax rotation is plotted against elbow flexion/extension. The path was strongly curved because of the flexion and extension in the elbow joint. The peak amplitude in the elbow joint was reached almost in the middle of the movement, whereas the peak amplitude of thorax rotation was reached at the end of the movement. The result revealed a nonlinear relationship between these two DOFs.

#### **Inter-joint coordination: target 1 & shoulder movements vs. shoulder and elbow movements**

Figure 4.9 (top row) illustrates the inter-joint coordination of the shoulder and elbow joint during pointing toward target 1. In the top row, angle-angle figures of three representative subjects from group 1 are plotted. In the left figure, shoulder abduction is plotted against shoulder anteversion/retroversion. As shown in the graph, Subject 8 did not use shoulder anteversion/retroversion. During abduction, the arm remained at approximately  $20^\circ$  retroversion. In contrast, subjects 2 and 5 showed consistently greater values in both DOFs during the pointing movement. Furthermore, the maximum amplitudes were reached at the end of the movement, forming an almost linear relationship between the two excursions. In the middle plot, shoulder abduction is plotted against elbow flexion/extension. Subject 8 showed only a small flexion and extension in the elbow joint during shoulder abduction. Subjects 2 and 5 exhibited almost permanently increasing values in the shoulder joint and decreasing values in the elbow joint, and reached maximum amplitudes in both DOFs at the end of the movement. Again, the excursions over time in both joints showed an almost linear relationship. In the right plot, shoulder anteversion/retroversion is plotted against elbow flexion/extension. Because subject 8 only performed a small flexion and extension in the elbow joint and almost no anteversion or retroversion in the shoulder, the time course of the angle/angle plot forms a small bell-shaped curve. Subjects 2 and 5 showed a transition from retroversion to anteversion and simultaneously an extension of the arm in the elbow joint during the pointing toward target 1. Because both subjects accelerated their arm extension at the end of the

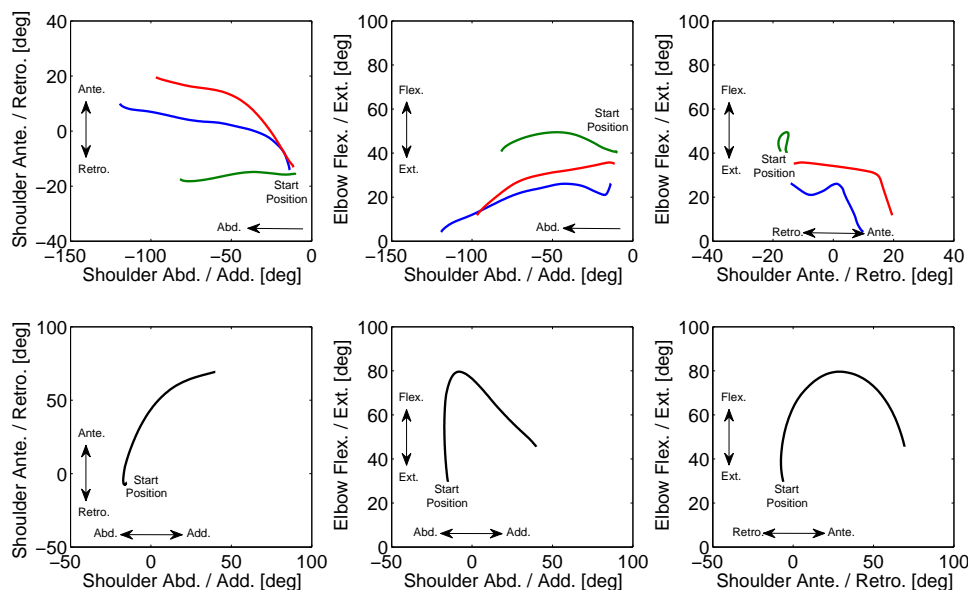


**Figure 4.9:** Inter-joint coordination for the shoulder and elbow joint during pointing toward target 1. In the top row, the inter-joint coordination of three representative subjects from group 1 are illustrated (blue=subject 2, red=subject 5, green=subject 8). In the bottom row, the inter-joint coordination of one representative subject from group 2 is illustrated. The scaling of the axes of the plots between the two rows is not uniform since the subjects of group 2 pointed with their right arm toward target 1. Accordingly, these movements took place in another region of the joint space. All time courses are mean values ( $N = 5$ ).

movement, the angle/angle course appears bent.

In the bottom row of figure 4.9, the inter-joint coordination of one subject from group 2 during pointing toward target 1 is illustrated. As before, in the top row, the two DOFs in the shoulder joint are plotted against one another. Subject 13, similar to all other subjects in group 2, showed almost constantly greater values in both DOFs, forming a nearly linear relationship between the two DOFs. However, because anteversion started before adduction, the angle/angle path is slightly curved. In the middle plot, shoulder adduction is plotted against elbow flexion/extension. The path is strongly curved because of the flexion and extension in the elbow joint. This, together with the sigmoid profile of shoulder anteversion, leads to a nonlinear relationship between these two DOFs. In the right plot, shoulder anteversion is plotted against elbow flexion/extension. As before, the angle/angle path is strongly curved because of the flexion and extension in the elbow joint. Because shoulder anteversion started earlier in time than shoulder adduction (bottom row, middle plot) and had a larger peak amplitude, the shape of the course was more elongated

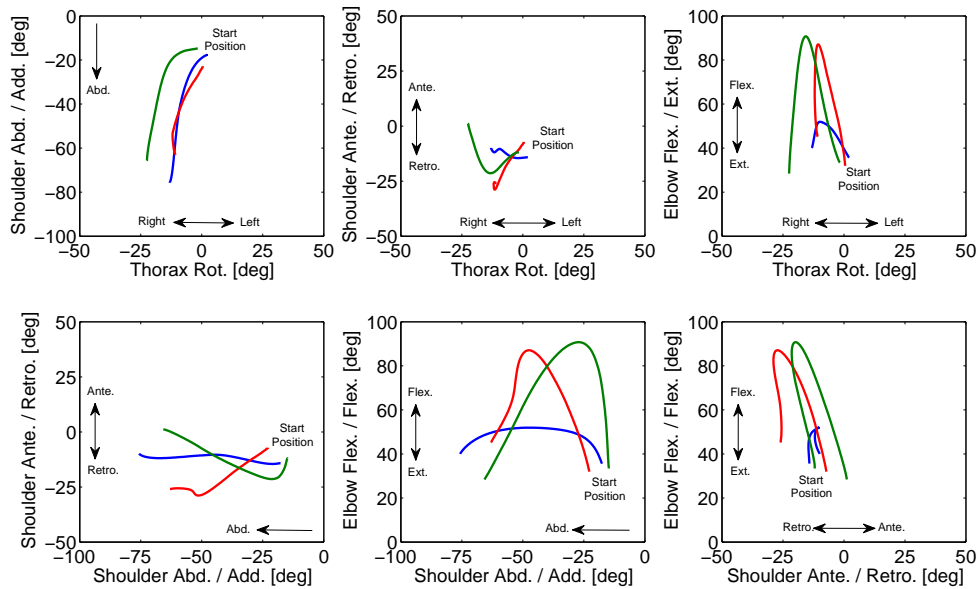


**Figure 4.10:** Inter-joint coordination for the thorax rotation, the shoulder and elbow joint of three representative subjects during pointing toward target 3 (blue=subject 5, red=subject 7, green=subject 14). Subjects 5 and 7 belong to group 1 and subject 14 belongs to group 2. All time courses are mean values ( $N = 5$ ).

along the shoulder axis. The interaction of these two DOFs cannot be approximated via a simple linear relationship, but requires a parabolic relationship.

### Inter-joint coordination: target 3

Because the subjects of groups 1 and 2 pointed with their right arm toward target 3, angle/angle trajectories of both groups were analyzed in one step. In the top row of Figure 4.10, the inter-joint coordination of thorax rotation, the shoulder and the elbow joint of three representative subjects during pointing toward target 3 are depicted. In the top row, thorax rotation is plotted against shoulder abduction/adduction. All three subjects showed only small thorax rotations and large shoulder abduction. The angle/angle profiles of subjects 5 and 14 exhibited a slightly curved profile at the beginning, followed by an almost straight line indicating a highly linear relationship. In contrast, the corresponding profile of subject 7 was straight at the beginning and slightly curved at the end. In the middle plot, thorax rotation is plotted against shoulder anteversion/retroversion. Subject 5 did not show large movement amplitude in this DOF of the shoulder. During thorax rotation to the right, the arm remained approximately between  $-15^\circ$  and  $-10^\circ$  retroversion and therefore the angle/angle profile is almost horizontally. Subject 7 showed a comparable thorax rotation but larger shoulder retroversion. The coupling of these two

DOFs formed an almost straight profile with some distortions at the end, producing a linear relationship. Subject 14 showed the largest thorax rotation and a shoulder retroversion that was followed by an anteversion. The combination of movements in these two DOFs lead to a rectangular angle/angle profile. In the right plot, thorax rotation is plotted against elbow flexion/extension. Because all three subjects showed a flexion/extension of the arm, the angle/angle profiles for the three cases were almost bell-shaped. Because the excursions in the elbow and the thorax joint differed across the three subjects, the shapes of these curves also differed.

In the bottom row of figure 4.10, typical examples of the inter-joint coordination of the shoulder and elbow joint during pointing toward target 3 are illustrated. In the left plot, shoulder abduction is plotted against shoulder anteversion/retroversion. The plot shows that subject 5 does not use shoulder anteversion/retroversion. During abduction of the shoulder, the arm remained between approximately between  $-15^\circ$  and  $-10^\circ$  retroversion. Therefore, the interaction of these two joints could be approximated by a simple linear relationship. Subjects 7 and 14 also did not exhibit a large excursion in shoulder anteversion/retroversion. Subject 7 performed retroversion during abduction, resulting in a highly linear coupling of these two DOFs until the last quarter of the movement. In the last portion of the movement, the retroversion remained at approximately  $-25^\circ$  and abduction was continuous. Subject 14 showed the opposite behavior in the interaction of these two DOFs. During shoulder abduction and at the beginning of the angle/angle course, a small retroversion in the shoulder followed by an anteversion was observed. Thus, a coupling between these two DOFs was observed leading to a highly linear relationship. In the middle plot, shoulder adduction is plotted against elbow flexion/extension. Subjects 7 and 14 exhibited flexion and extension of the arm during shoulder abduction, and the resulting angle/angle profiles were single-peak and nearly bell-shaped. Since subject 5 exhibited a larger amplitude in shoulder abduction and a smaller amplitude in flexion/extension movement in the elbow joint, the shape of the path was more elongated along the shoulder axis. However, compared to the interaction of the two DOFs of the shoulder, the coupling of shoulder abduction and elbow flexion/extension was more complex. In the third plot, shoulder anteversion is plotted against elbow flexion/extension. Given that subject 5 performed only a small flexion and extension in the elbow joint and almost no movement in the shoulder, the time course of the angle/angle plot formed a small distorted bell-shape. The angle/angle profiles of subjects 7 and 14 also showed a bell-like shape, but much more elongated along the elbow axis because of the fact that both subjects performed a large flexion and extension of the arm. Both courses started at almost the same point on the shoulder axis, but ran in different directions because subject 7 showed a retroversion and subject 14 showed an anteversion in the shoulder joint.

### 4.3.3 Joint torques

Figure 4.11 illustrates typical examples of the driving joint torques of three subjects. The highest variability in the torque profiles were found among the subjects from the second group, who pointed with their right arm to target 1 on the left side (Fig. 4.11). However, a comparison of the torque profiles between the subjects of groups 1 and 2 during pointing toward target 1 showed that the subjects of the first group produced, on average, higher torques in shoulder abduction/adduction and lower torques in shoulder anteversion and retroversion and in elbow flexion/extension. The same tendency was observed when comparing the movements of the subjects pointing with their right hand to target 1 with the subjects pointing with their right hand to target 3. When pointing toward target 3 with the right hand, the subjects produced, on average, higher torques in shoulder abduction/adduction and lower torques in shoulder anteversion and retroversion and in elbow flexion/extension than the subjects pointing with the right hand to target 1. Furthermore, the subjects of group 2 generated larger torque amplitudes during thorax rotation when pointing toward target 1 than the subjects of group 1, and compared to the subjects of groups 1 and 2 during pointing toward target 3.

## 4.4 Discussion

The implications of the results presented above are discussed in the context of the background of the introduced theoretical assumptions of biological motor control and the development of humanoid robots moving in a human-like fashion. Finally, the applied methods are discussed.

### 4.4.1 Biological motor control

The analysis of human movements can be assigned to two domains: gait analysis and upper extremity analysis. Comparing gait analysis to upper-extremity analysis reveals some problems since in gait analysis, a 2D lateral view of the human gait yields a good approximation of the most important movement components (Rau et al., 2000). Typical upper extremity movements cannot be described in 2D. These movements require a 3D analysis due to the kinematic redundancy of the upper body. Nevertheless, most upper extremity studies are restricted to planar movements or use rather simple biomechanical models of the upper body (Chap. 2.3.3.1, 4.1). Therefore, these studies probably neglected important features of natural multi-joint movements in 3D space. The purpose of this study was the examination of different multi-joint upper-extremity movements in 3D space, and this was accomplished by utilizing with different pointing gestures. Based on the pioneering work of Morasso (1981) and Shadmehr and Mussa-Ivaldi (1994), an important assumption of motor psychophysics is as follows: Represented movement features differ from non-represented

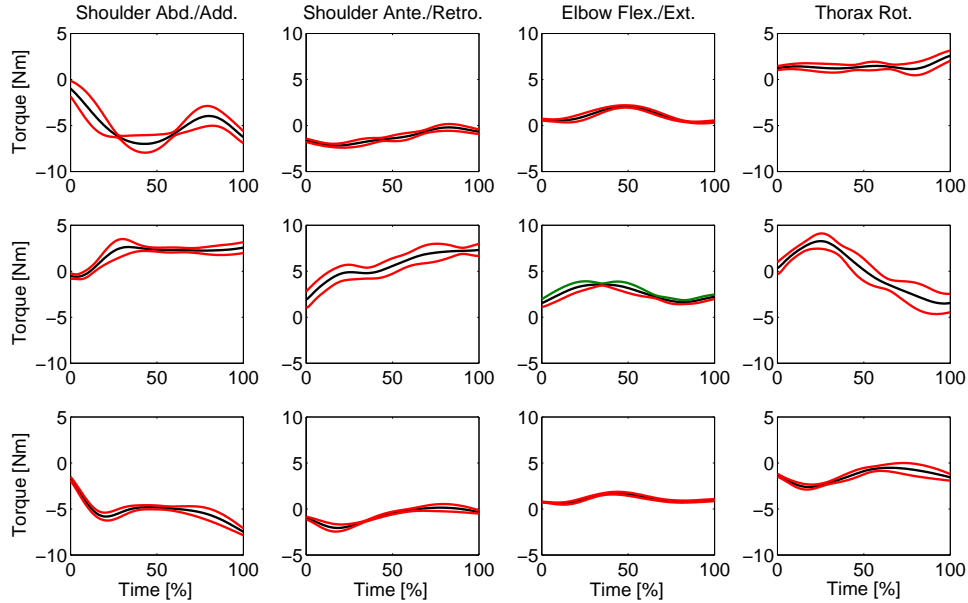


**Figure 4.11:** Mean (black) and standard deviation (red) of the joint torques of four different DOFs of three representative subjects ( $N = 5$ ). In first row, the joint torque profiles of subject 8 (group 1) during pointing toward target 1 are illustrated. In the second row, the joint torque profiles of subject 13 (group 2) during pointing toward target 1 are shown. In the third row the joint torque profiles of subject 5 (group 1) during pointing toward target 3 are shown.

features in the *criterion of simplicity* and *the criterion of invariance* (see also Heuer and Konczak, 2003). The results of this study are discussed in the context of the background of these assumptions.

The analysis of the trajectories of the hand of the subjects from groups 1 and 2 showed that the hand paths are curved with smooth, single-peak and almost bell-shaped velocity profiles. In other words, the subjects produced movements across the two tasks that shared the same invariant movement features no matter if the right or the left arm was used during the task (criterion of invariance). Furthermore, compared to joint angles and joint angular velocities, the hand paths and tangential hand velocities are rather simple (criterion of simplicity). It is known that unconstrained hand movements in 2D space (Desmurget et al., 1997) and 3D space (Flash et al., 2003) are more curved than constraint movements restricted to a plane, consistent with the results of this study. Based on the findings of the analysis, a motor planning in extrinsic coordinates of the hand appears to be plausible. Since these movement features were found across different unconstrained movement tasks, they are most likely not a result of the experimental protocol. Therefore, the question arises as to why the subjects produced movements with these features. If the ob-

served human behavior is seen in a larger evolutionary context, the human brain may have learned during evolution that some movements will lead to a reward and others to punishment. The idea that some movements will lead to reward (e.g. food) and some to punishment (e.g. hunger) establishes a link to the field of optimal control (Chap. 2.3.3.1). In other words, some movements are optimal since they assure a reward while others are not. Optimal control models incorporate a cost (e.g. minimum jerk), defined as some function of the movement, and the movement with the lowest cost is chosen and executed. However, the human CNS did not evolve to optimize movements to produce certain invariant features, but it evolved to promote the transmission of genes to future generations. It is possible that some movements with certain features are more likely to pass on genes and the human CNS may have learned to indirectly represent this through cost functions. The great challenge has been, and still is, to reverse engineer the cost functions that are used by the human CNS, especially in the case of natural multi-joint movements in 3D space (Wolpert and Ghahramani, 2004; Shadmehr and Wise, 2005). A possible explanation for the above described features is provided by the minimum variance model (Harris and Wolpert, 1998) described in chapter 4.1 and chapter 2.3.3.1.

Because of the anatomical design of the human arm, joint rotations are required to be able to translate the hand from one position to another. If movements are planned in extrinsic coordinates, a transformation from external space into joint space is needed. This computation is called inverse kinematics and is ill-posed (Chap. 2.2). It appears the CNS is capable of solving this problem since humans are able to translate their hand from one position to another. However, since the inverse kinematics problem is difficult to solve, the human CNS may have adopted a strategy during evolution that avoids the problem. One possibility is that motor planning takes place in joint space. Based on the above outlined assumptions of motor psychophysics, invariant movement features and/or simple couplings should be found in joint space. The analysis of the joint kinematics revealed that not all subjects used the same joint coordination strategy. Several subjects used different arms to accomplish the pointing tasks. Some even used different arms in the same movement task and therefore different combinations of joint angles. Even if subjects used the same arm for a pointing task, different coordination of arm joint kinematics were observed. For example, subject 14 used a much larger extension in the elbow joint than subject 5 during pointing toward target 3 (Fig. 4.6). Nevertheless, the qualitative analysis of the joint movements indicated that the different coordination strategies can be grouped. In the next step, a quantitative grouping or classification is required (e.g. Park et al., 2005). Despite some differences in the coordination of the analyzed DOFs, the inter-joint coordination analysis revealed highly linear relationships between different DOFs in some cases (Fig. 4.8, first plot in the upper row). This indicates that the CNS sometimes shows, even in joint space, a tendency to use rather simple couplings between different DOFs (criterion of simplicity). In future studies, a joint space with higher dimensions than 2D should to be examined. These analyses can

be conducted in the context of the theoretical background of the presented definition of synergies (Chap. 2.3.2.2).

Subjects were urged to execute the pointing movements as they would do in their daily life. This led to large differences in movement speed and therefore in movement duration. For example, subject 2 showed a rather fast execution when compared to subject 8. The large variability between the different trials of subject 2 could be a result of the movement speed (Fig. 4.3), which corresponds to the predictions of Fitt's law (Chap. 2.3.1.1). Compared to the velocity profiles of the hand (Fig. 4.1), the angular velocity profiles are more complex and irregular indicating an increase in the number of sub-movements in joint space. Given the highly stereotypical tangential velocity profiles of the hands, the CNS might use a compensational strategy. In other words, sub-movements or oscillations in one joint can lead to almost equal and opposite oscillations in other joints. In the literature, couplings of this kind are described as *coordinative structures* (Tuller et al., 1982).

According to Newton's second law one has to apply a force to accelerate a body. Therefore, to move the segments of the arm in the desired mode, adequately timed joint torques need to be applied. In producing the torques, the CNS has to solve some difficult mechanical problems (equation 2.12, 2.13). The results of this study indicated that the different coordination strategies on a kinematic level led to different torque profiles. For example, in contrast to the subjects of the first group, the subjects of the second group had to pass their arm in front of their body when pointing to target 1. This coordination strategy led to lower torques in shoulder abduction/adduction, and higher torques in the shoulder anteversion and retroversion and the elbow flexion/extension.

#### 4.4.2 Robotics

It seems to be only a question of time until robots will be integrated into families and serve as personal robots for elderly or playmate robots in child education. To promote man-machine interaction in a human environment, the size, geometry, arrangement of limbs, number of DOFs and range of movement of a humanoid robot should be comparable to those of humans. Modern humanoid robots dispose of a large number of mechanical DOFs. This redundancy is advantageous because it enables these robots to avoid obstacles and joint limits, just as a human being (Atkeson et al., 2000). However, this flexibility or movement abundance leads to a control problem. Which particular movement among the large number of possible ones should be chosen in a given situation? Besides the anthropometric resemblance, the robot should use human-like movements to promote man-machine interaction (Wank et al., 2004; Khatib et al., 2004; Schaal, 2007a). Therefore, it seems plausible to study human movements and transfer the kinematics of human movements to humanoid robots. The stereotypical features of human pointing gestures identified above denote a first step in this direction. A humanoid robot should generate pointing gestures with

curved hand paths and single-peaked, almost bell-shaped velocity profiles with a peak velocity of  $1.5 - 2.0 \text{ m/s}$ . The analysis of the joint angle trajectories showed that humans use different coordination strategies. The analysis of the inter-joint coordination revealed in some cases an almost linear relationship. The relationships, both linear and nonlinear, could be approximated via polynomials to quantify couplings between different joints. These functions may be used in movement generation. Different coordination strategies of different subjects provide the chance to select the kinematics that may best be mapped to a specific humanoid robot. Depending on the chosen kinematics, the motors of the robot should be able to produce angular velocities of up to  $150 \text{ deg/s}$  in the shoulder and elbow joint. Given the joint kinematics of a typical human subject, as well as the moment of inertia, the length, the mass, and the center of mass of each of the robot's segments, inverse dynamics can be calculated to determine the engine power needed in each of the joints. Calculations of this kind can be carried out with the biomechanical model used in this thesis (Chap. 3.4). Furthermore, such a model can be used to study the effects of a mass reduction on the required engine power in different joints.

#### 4.4.3 Applied methods

The analysis of complex multi-joint movements in 3D space requires the application of specific measurement and modeling techniques. In this study, a marker-based IR-tracking-system that can be classified as state of the art regarding sampling frequency and spatial resolution was utilized. Ten cameras were installed around the subject to ensure that each marker was recognized by at least two cameras. Most of the markers were recognized by more than two cameras during the movement which improves the quality of the 3D reconstruction of the markers. When calculating the first and second derivation of the marker data, the derivations are not continuous. The raw data obviously contain higher-frequency signal portions which are not caused by the biological system. These signal portions, or noise, may be the result of skin movement, incorrect digitization, or other factors. Cubic or quintic spline algorithms are commonly used in biomechanics to smooth raw data in data sets with noise (Winter and Patla, 1997). Since the data sets under consideration are of good quality, we used a quintic spline algorithm by Woltring (1986). In summary, the applied methods in the process of data acquisition and processing are state of the art, and the achieved data quality indicates a correct application of the described methods.

The biomechanical model used in this study has a large impact on the results. Modeling is required for the calculation of joint angles and driving joint torques, however, the analysis of multi-joint movements in 3D space requires a complex kinematic and dynamic multibody model. The biomechanical multibody model used in this thesis is based on the recommendations of the International Society of Biomechanics (Wu and Cavanagh, 1995; Wu et al., 2002, 2005; Cappozzo et al., 1995), as well as the inertial parameters of De Leva (1996) and Zatsiorsky (2002). The kine-

matic structure of the model, i.e. location and number of joints, are in line with the software packages SIMM and OpenSIM (Delp and Loan, 1995, 2000; Delp et al., 2007). Although the applied model reflects the state of the art in biomechanical modeling, it should be noted that the calculation of joint angles and joint torques are always a result of the applied method. If other methods were used to analyze the same data set, for example Euler's instead of Cardan's angles or other inertial parameters, the range of motion in the individual DOFs as well as the joint torques would differ. Another methodological problem is the calculation of the inverse dynamics. The torque profiles appear spiked in several cases due to the fact that the experimental data were not continuous. There are two options to address this problem: the experimental data should be smoothed to a larger extent, or approximated via polynomials or splines to get an analytic function to describe the data. In the first case, the original signal may become heavily distorted and in the second case, it is conceivable that no suitable polynomial or spline exists.

Within the scope of outlined objectives, the methodology of this study has to be considered adequate. The small number of trials per subject per movement task is one key limitation, and a greater number of trials should be recorded in future studies.

## 5 Study II: The synthesis of multi-joint pointing movements in 3D space

### 5.1 Introduction

The fact that pointing to distant visual targets is a part of everyday life hides the intrinsic complexity of these movements. Therefore, it is not surprising that despite decades of basic research attempting to understand human motor control, the fundamental neural and computational principles of simple goal-directed movements like pointing remain poorly understood (Thoroughman et al., 2007). Breakthroughs in understanding certain aspects of human motor control have often been produced by computational studies (Flash and Hogan, 1985; Bullock and Grossberg, 1988; Uno et al., 1989; Hoff and Arbib, 1993; Shadmehr and Mussa-Ivaldi, 1994; Harris and Wolpert, 1998; Todorov and Jordan, 2002). These studies are based on classical fields of engineering including cybernetics (Wiener, 1948), optimal control (Bellman, 1957) and, to a certain extent, control theory (Slotine and Li, 1991). In computational frameworks, the problem of motor control is modeled in terms of four entities: (1) a *planner* computes a desired trajectory or, more generally, a movement plan based on the task, (2) the current state of the body, (3) the final state of the body and (4) the environmental context. Once the desired trajectory has been established, it is transmitted to a *controller*. Inverse internal models are ideal controllers because they transform the desired trajectory into adequate motor commands. The motor commands are then sent to the *plant*, or the system, being controlled. In human motor control, the plant corresponds to the musculoskeletal system. The system then performs a forward mapping, meaning that it transforms motor commands into limb movement according to the intended trajectory and depending on factors such as limb geometry, limb inertia, muscle mechanics and environmental loads. The controller may use sensory feedback to correct the movement or predicted sensory feedback provided by a *forward model* that anticipates the consequences from efferent copies of the issued motor commands (Kawato, 1999; Scott and Norman, 2003). However, rapidly executed movements cannot be solely under feedback control because feedback loops in biological systems are slow; for example, the delay for visual feedback is approximately 200 ms (Slater-Hammel, 1960; Kawato, 1999). The context of the internal model hypotheses suggests that the central nervous system (CNS) must construct inverse dynamic models of the plant. These neural representations of the properties of the plant enable a feed-forward movement control. Theoretically, it is

also possible that a forward model of the musculoskeletal system embedded in a fast internal feedback loop mimics a feed-forward control via an inverse model (Kawato, 1999). Most computational models are based on the assumption that movements are planned before being executed. However, some models do not depend on a precomputed desired trajectory (Hoff and Arbib, 1993; Todorov and Jordan, 2002). Bizzi et al. (1984) demonstrated that deafferented monkeys can reach a target with their hands by feed-forward control alone. Seemingly, if the corresponding inverse model is sufficiently developed, an almost natural movement appears possible and the remaining movement error is more or less negligible. Under normal circumstances, this error may be corrected via feedback-control (Heuer and Konczak, 2003). These results indicate that the trajectory, from the starting position to the final position, can be precomputed. In other words, the trajectory can be planned and controlled in a pure feed-forward manner.

In the context of feed-forward control, Kawato (1996) distinguishes three *indeterminacy problems* involved in the process of planning and executing unconstrained visually guided movements like pointing. There are an infinite number of spatiotemporal routes, or trajectories, connecting the starting point with the target position. However, it is necessary to select one trajectory from the infinite number of possible trajectories (*problem of trajectory formation*). The spatial coordinates of the desired trajectory need to be transformed into intrinsic coordinates like joint angles or muscle lengths. This inverse transformation is not uniquely determined because of the redundant DOFs on the level of joint angles or on the level of muscles (*problem of coordinate transformation*). If a desired trajectory is determined in joint angle coordinates, the generalized actor forces can be calculated via inverse dynamics equations. Again, there are an infinite number of patterns of muscle activation generating the same driving torques moving the hand along the desired trajectory. Furthermore, it is impossible to uniquely determine the appropriate firing rates of the spinal cord neurons and the cortex neurons to produce the muscle activations and therefore, the required torques needed at each point in time (*problem of motor command generation*). A more detailed discussion of these problems can be found in chapter 2.2. The main difficulty in solving these problems is that the planning and control strategies of the CNS cannot be directly assessed. One of the key assumptions in motor control research is that information about these strategies can be deduced from behavioral regularities (Bernstein, 1967). Therefore, to be able to understand basic control strategies, the system's behavior must be observed under various conditions. The results will likely lead to a definition of general features or principles of the system's behavior, as was done in the first study of this thesis. Due to the system's complexity and the vast amount of movement tasks, it is impossible to analyze all likely behaviors for all potential tasks. Therefore, it is necessary to develop a model of human motor control based on limited information about the system's behavior and structure (Latash, 1996). It is unsurprising that this approach has led to many different and sometimes incompatible models (Brown and Rosenbaum, 2002; Her-

mens and Gielen, 2004). Latash (2008a) distinguishes two major approaches to the indeterminacy problems presented above. In *optimal control models*, a unique trajectory is selected by adding additional constraints to the task and thereby reducing the effective DOFs. This is most often done by selecting a cost function that serves as a goal function (Kawato, 1996; Engelbrecht, 2001; Todorov, 2004). A detailed discussion of the most influential optimal control models can be found in chapter 2.3.3.1. The second approach assumes that the CNS does not eliminate the DOFs and does not select a unique trajectory but rather uses all available DOFs to facilitate families of solutions that are equally successful in solving the movement task at hand. This idea has recently been formalized in the *uncontrolled manifold hypothesis* (Scholz and Schöner, 1999; Latash et al., 2004, 2007). A detailed discussion of the uncontrolled manifold hypothesis can be found in chapter 2.3.2.3.

If human movements are viewed in a larger evolutionary context, the human brain may have learned through evolution that some movements will lead to a reward and others to punishment. The idea that some movements will lead to reward (e.g. food) and some to punishment (e.g. hunger) establishes a link to the field of optimal control (Chap. 2.3.3.1). In other words, some movements are optimal because they assure a reward and others are not. Optimal control models can reproduce behavioral regularities on multiple levels (Todorov, 2004). In the literature, different optimal control models are discussed. Determining the optimal control model requires a “reverse engineering” approach, with the objective of replicating observed human movement features. In the case that there is no single model being superior to all other models, testing different optimization models can be useful in the development of a categorization of motor behavior. Furthermore, these models can help to enhance the understanding of the neural processes underlying human motor behavior (Flash et al., 2003), and have the benefit of being objectively and experimentally examinable because of their quantitative predictions.

In addition to determining which principles the CNS uses to solve the above introduced ill-posed problems, on which levels in the sensorimotor system these principles work must be ascertained. In other words, which coordinate frame or space human movements are planned must be considered. This question was addressed using two types of studies. In the first type of study, the neural activities of primates during movements were recorded to observe if patterns of neural activity could be linked to one or several behavioral variables (Chap. 2.3.3.1). However, as shown by Nakano et al. (1999), the data from these studies are consistent with different planning spaces. It appears that the interpretation of the results of these studies continues to be debated (Todorov, 2000a; Moran and Schwartz, 2000; Georgopoulos and Ashe, 2000; Todorov, 2000b; Scott, 2000a). In the second type of study, adaptation processes in artificially altered environments or performance changes are investigated to objectively examine the planning space (Chap. 2.3.3.1). If the trajectory of the hand is planned in kinematic space, it will be altered under kinematic transformations in visual space and it will be unaffected when the dynamics are altered (e.g. force

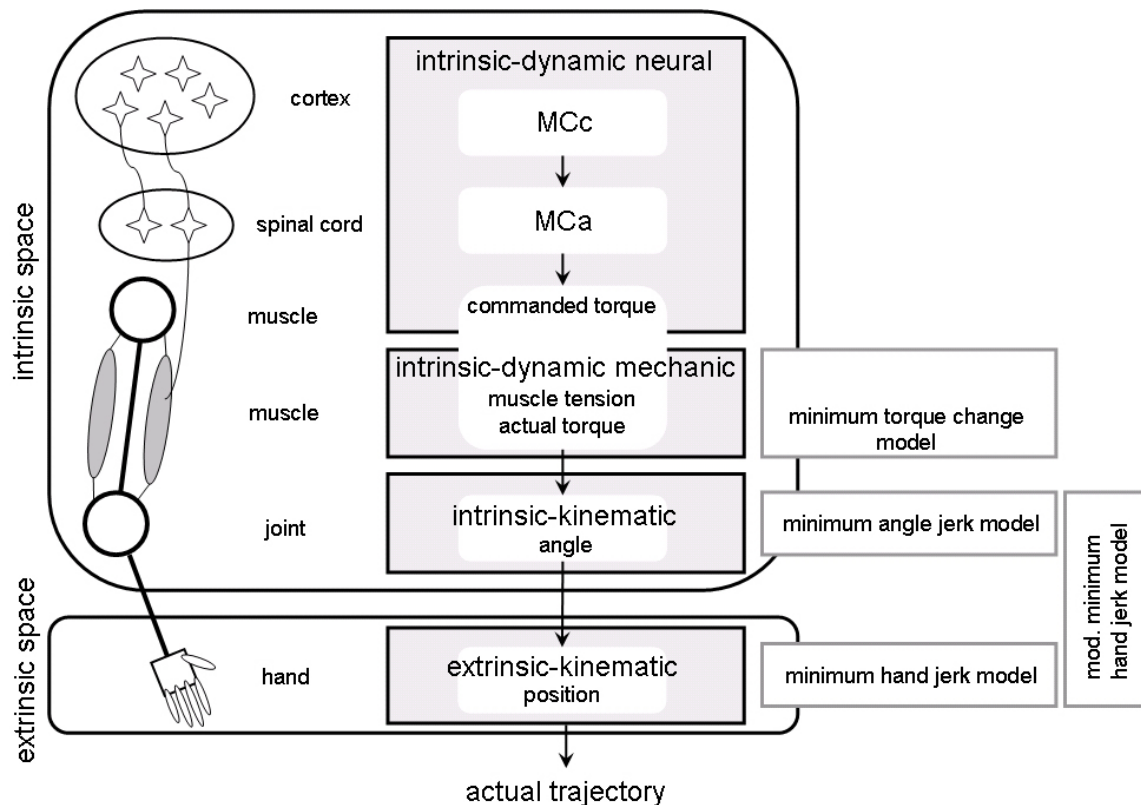


**Figure 5.1:** Conceptual schema of different trajectory planning spaces and the corresponding optimal control models examined in this thesis (Nakano et al., 1999)

fields). If the trajectory of the hand is planned in dynamic space, the opposite will occur. Results supporting a kinematic planning space were reported by Wolpert et al. (1995a) using kinematic transformations and by Shadmehr and Mussa-Ivaldi (1994) using dynamic transformations. In contrast, the results of Uno et al. (1989), Osu et al. (1997) and Nakano et al. (1999) support the notion of a dynamic planning space. The question concerning what planning space is utilized is important in the context of the computational framework presented above. If planning takes place in an intrinsic-dynamic space, then this would place a heavy computational burden on the planner. On the other hand, if the planner produces a kinematic plan that defines the trajectory of the hand, then the controller would have to deal with coordinate transformation and motor command generation. In conclusion, it can be said that on the basis of the above discussed results, it is currently impossible to identify the space in which human movements are planned. Another possibility to examine the space in which trajectories are planned is to compare trajectories predicted by optimal control models defined in each space with experimentally determined trajectories (Nakano et al., 1999). According to Osu et al. (1997) and Nakano et al.

(1999), one can distinguish four planning spaces: an extrinsic-kinematic space (e.g. Cartesian coordinates of the hand), an intrinsic-kinematic space (e.g. joint angles or muscle length), an intrinsic-dynamic-mechanical space (e.g. joint torque or muscle tension) and an intrinsic-dynamical-neural space (e.g. motor commands controlling muscle tension or the firing rate of motor neurons) (Fig. 2.14). The following work is based on the assumption that actual trajectories are similar to planned trajectories (Osu et al., 1997; Nakano et al., 1999). The first focus of the study is on extrinsic-kinematic space, intrinsic-kinematic space and intrinsic-dynamic-mechanical space. We tested a minimum hand jerk model (Flash and Hogan, 1985), a minimum angle jerk model (Wada et al., 2001) and a minimum torque change model (Uno et al., 1989). Furthermore, we developed a planning algorithm working on an extrinsic- and intrinsic-kinematic level. In figure 5.1, the different planning spaces and the corresponding optimization models analyzed in this study are illustrated. Although these models have been established in technical literature, a quantitative comparison between the performance of these models for multi-joint movements in 3D space is a new concept (e.g. Admiraal et al., 2004; Kaphle and Eriksson, 2008; Gielen, 2009b). The purpose of the following study is to quantitatively examine which of the four optimal control models can best reproduce multi-joint pointing movements in 3D space.

## 5.2 Methods

### 5.2.1 Subjects

The motion capture data from subjects 1 through 8 was used in this study (Tab. 3.2). The age of the eight subjects (6 men and 2 women) from the University of Karlsruhe (TH) was between 21 and 25 years (mean age = 22.9 years; SD = 1.5 years). Heights of the subjects ranged from 160 to 187 *cm* (mean height = 175.9 *cm*; SD = 8.8 *cm*) and weights ranged from 49 to 80 *kg* (mean mass = 68.1 *kg*; SD = 11.5 *kg*).

### 5.2.2 Procedures

For the comparison of the trajectories predicted by the different optimal control models, the experimentally determined pointing gestures to target 1 and 3 (Fig. 3.1) of the eight subjects were used. All subjects pointed with their left hand to target 1 and with their right hand to target 3. Furthermore, none of the subjects left the starting position during the pointing movement. In total, 40 experimentally determined pointing gestures for each of the two targets were obtained and

### 5.2.3 Data acquisition and processing

All pointing movements were tracked using a Vicon IR-Motion Capturing System. A detailed description of the data acquisition and processing is provided in chapter 3.

### 5.2.4 Biomechanical modeling

The kinematic and dynamic multibody approach used for the calculation of joint angles and joint torques is described in chapter 3. A more comprehensive introduction to the model can be found in the theses of Stelzner (2008) and Simonidis (2010).

### 5.2.5 Optimal control models

To apply the above described biomechanical model to the generation of trajectories, an optimal control model has to be linked to the multibody system. The optimal control model consists of two factors: first, an optimization criterion (cost or goal function) must be defined (Fig. 5.1) and, second, an optimization method must be implemented to calculate optimal trajectories based on the previously defined criterion. As outlined in chapter 5.1, a minimum hand jerk model (MHJM), a minimum angle jerk model (MAJM) and a minimum torque change model (MTCM) will be examined. A detailed description of these models is given in chapter 2.3.3.1. We also developed a modified minimum hand jerk model (mMHJM) by which the optimization is conducted on hand level (extrinsic coordinates of the hand). An additional

boundary condition used during the optimization included setting the limits of the individual joints. During optimization, the joint movements are driven by experimental data and some joints are released, meaning that the optimization method can use this DOF within the joint limits to find a minimum hand jerk trajectory. A detailed description of the mathematical basis for the method can be found in Simonidis (2010).

### 5.2.6 Optimization method

The optimization method is needed for the computation of optimal trajectories with respect to the above introduced criteria. Mathematically, the problem involves the optimization of a general nonlinear cost function with nonlinear constraints, bounds of the optimized variables and boundary conditions at start and target times (Gill et al., 1981). The problem is stated as to find a set of trajectories  $\mathbf{q}(t)$ ,  $\dot{\mathbf{q}}(t)$ ,  $\ddot{\mathbf{q}}(t)$  and  $\mathbf{T}(t)$  for a time domain  $t = [t_0, t_f] \in \mathbb{R}$ , which minimizes a nonlinear cost function

$$J = \int_0^{t_f} C(\mathbf{x}(t))dt, \quad (5.1)$$

where  $\mathbf{x}(t)$  may depend on  $\mathbf{q}(t)$ ,  $\dot{\mathbf{q}}(t)$ ,  $\ddot{\mathbf{q}}(t)$  and  $\mathbf{T}(t)$  or even on higher derivatives, with respect to nonlinear constraints, the dynamic equilibrium equations

$$\mathbf{M}(\mathbf{q}(t))\ddot{\mathbf{q}}(t) - \mathbf{Q}(\mathbf{q}, \dot{\mathbf{q}}, t) - \mathbf{T}(t) \equiv 0, \quad (5.2)$$

bounds in the form of  $\mathbf{x}_{min} \leq \mathbf{x}(t) \leq \mathbf{x}_{max}$  and boundary conditions  $\mathbf{x}_0(t_0)$ ,  $\mathbf{x}_f(t_f)$ .

The problem can be efficiently solved with collocation methods, which are known to provide a quick insight into the optimal solution (Gill et al., 1981). Direct collocation is a numerical method for solving optimal control problems (Betts, 1998). It is based on discretization of the state and control variables of the mechanical system transforming the optimal control problem into a constrained nonlinear optimization problem that can be solved with well-known and efficient standard solvers. Piecewise polynomial approximations of state variables based on quintic Hermite splines utilizing the structure of the dynamic equations of motion were used in this study. The dynamic equations of motion can be explicitly solved for the control (Stryk, 1998) and thus, the discretized control variables are obtained automatically by only discretizing the state variables on a defined number of nodes. The nodes are equidistantly spaced and the unknowns of the optimization problem are the parameters of the discretization, which are the function values and the first and second derivatives at each node. At equidistant time instances  $k$ , for example  $\mathbf{k} = [0 \ 0.25 \ 0.5 \ 0.75 \ 1]$  on a time interval  $t = [0 \dots 1]$  including the start and end values of  $t$ , the free parameters of a single trajectory  $q_i(t)$  were chosen to be  $q_i(k)$ ,  $\dot{q}_i(k)$  and  $\ddot{q}_i(k)$ .

Values between the supporting points were then interpolated by piecewise quintic splines  $q_i(t) = S_i^5(q_i(\mathbf{k}), \dot{q}_i(\mathbf{k}), \ddot{q}_i(\mathbf{k}), t)$ , where  $S_i^5$  denotes a coefficient function assembling the piecewise quintic splines together to the trajectory  $q_i(t)$ . Therefore,  $q_i(t)$

is parameter dependent and  $C^2$ -continuous. The parameterized trajectories can be summarized in matrix form (5.3) and the derivatives are obtained by differentiating  $\mathbf{S}^5$ , the coefficient functions of the quintic splines.

$$\begin{aligned}\mathbf{q}(t) &= \mathbf{S}^5(\mathbf{q}(\mathbf{k}), \dot{\mathbf{q}}(\mathbf{k}), \ddot{\mathbf{q}}(\mathbf{k}), t) \equiv \mathbf{S}_k^5(t) \\ \dot{\mathbf{q}}(t) &= \dot{\mathbf{S}}^5(\mathbf{q}(\mathbf{k}), \dot{\mathbf{q}}(\mathbf{k}), \ddot{\mathbf{q}}(\mathbf{k}), t) \equiv \dot{\mathbf{S}}_k^5(t) \\ \ddot{\mathbf{q}}(t) &= \ddot{\mathbf{S}}^5(\mathbf{q}(\mathbf{k}), \dot{\mathbf{q}}(\mathbf{k}), \ddot{\mathbf{q}}(\mathbf{k}), t) \equiv \ddot{\mathbf{S}}_k^5(t) \\ \dddot{\mathbf{q}}(t) &= \dddot{\mathbf{S}}^5(\mathbf{q}(\mathbf{k}), \dot{\mathbf{q}}(\mathbf{k}), \ddot{\mathbf{q}}(\mathbf{k}), t) \equiv \dddot{\mathbf{S}}_k^5(t)\end{aligned}\quad (5.3)$$

Now the equations of motion can be formulated dependent on time and the set of trajectories (5.3) to

$$\mathbf{T}(t) = \mathbf{M}(\mathbf{S}_k^5(t))\ddot{\mathbf{S}}_k^5(t) - \mathbf{Q}(\mathbf{S}_k^5(t), \dot{\mathbf{S}}_k^5(t), t). \quad (5.4)$$

Equation 5.4 was solved on a collocation grid at  $4(nk - 1) + 1$  Gaussian points (de Boor and Swartz, 1973) and thus, four points per node were determined to solve the resulting system of equations. Therefore, the structures of the appearing matrices are large and sparse.

The four optimal control models used in this thesis are MHJM, mMHJM, MAJM and MTCM (Chap. 5.2.5). The corresponding cost function of MHJM is defined as:

$$J_{HJ} = \frac{1}{2} \int_{t_0}^{t_f} \ddot{\mathbf{R}}^T \ddot{\mathbf{R}} dt \quad (5.5)$$

where  $\mathbf{R} = [x, y, z]^T$  are the coordinates of the origin of the local coordinate frame of the hand and  $\ddot{\mathbf{R}}$  is the corresponding translational jerk. Furthermore, the optimization on hand level does not depend on equation 5.4. The cost function of mMHJM is defined as follows:

$$J_{mHJ}(\bar{\mathbf{q}}, t) = \frac{1}{2} \int_{t_0}^{t_f} \ddot{\mathbf{R}}^T(\bar{\mathbf{q}}) \ddot{\mathbf{R}}(\bar{\mathbf{q}}) dt \quad (5.6)$$

where  $\bar{\mathbf{q}}^T = [\mathbf{q}^T, \dot{\mathbf{q}}^T, \ddot{\mathbf{q}}^T, \dddot{\mathbf{q}}^T]^T$  are the variables of the individual joints. In the case of MAJM the cost function is given by the following equation:

$$J_{AJ}(\mathbf{q}, t) = \frac{1}{2} \int_{t_0}^{t_f} \sum_{k=1}^{n_q} \ddot{\mathbf{q}}_k^2(t) dt \quad (5.7)$$

where  $\mathbf{q}$  represents the number of the  $n_q$  DOFs to be optimized. Finally, the cost function of the MTCM is

$$J_{TC} = \frac{1}{2} \int_{t_0}^{t_f} \dot{\mathbf{T}}^T(t) \dot{\mathbf{T}}(t) dt. \quad (5.8)$$

The optimization problems were solved using efficient solvers for nonlinear and sparse optimization problems. A more comprehensive introduction to the optimization method used in this thesis can be found in (Simonidis et al., 2010).

### 5.2.7 Simulation protocol

The trajectories generated by computer simulations are compared to the experimental data of eight subjects for targets 1 and 3. In total, there are 40 experimentally determined human trajectories for each of the two targets that can be used for the validation of the different optimal control models.

Because the minimum hand jerk model (MHJM) is defined in extrinsic coordinates of the hand and not in joint or torque space, 40 simulations for each target must be conducted. In the case of the optimal control models defined in intrinsic coordinates, the DOFs to be optimized need to be specified. The three models utilizing intrinsic coordinates include MAJM, MTCM and mMHJM. Analysis of the pointing gestures (Chap. 4) showed that the most relevant DOFs are those of the shoulder, the elbow and thorax rotation. To determine how the developed computational framework operates under different conditions, simulations began by utilizing one DOF for each target. In the experiments, 31 of the 32 available DOFs of the biomechanical model were driven by experimentally determined movement data from motion capture studies (Tab. 5.1). In a second step, the number of DOFs driven by experimental data was reduced to 28 for target 1 and 27 for target 3. In other words, four DOFs for target 1 and five DOFs for target 3 will be optimized.

**Table 5.1:** Simulation protocol for target 1 and target 3 for MAJM, MTCM and mMHJM. A total of 11 different conditions were tested.

Target	Number of optimized DOFs	Description of DOFs
1	1	shoulder abduction/adduction
1	1	shoulder rotation
1	1	shoulder anteversion/retroversion
1	1	elbow flexion/extension
1	4	shoulder abduction/adduction + shoulder rotation + shoulder anteversion/retroversion + elbow flexion/extension
3	1	shoulder abduction/adduction
3	1	shoulder rotation
3	1	shoulder anteversion/retroversion
3	1	elbow flexion/extension
3	1	thorax rotation
1	5	shoulder abduction/adduction + shoulder rotation + shoulder anteversion/retroversion + elbow flexion/extension + thorax rotation

### 5.2.8 Data analysis

Measured trajectories were compared with those predicted by the four models for spatio-temporal properties. Based on the experimental data, the starting pose, the final pose, and the movement duration were determined (Chap. 3.5). The analysis of the performance of the different optimal control models was accomplished in four steps. Matlab (V. 7.7) and SPSS (V. 17) were used for data analysis.

#### Step 1: Validation of the optimization method

Before the above described optimization method can be used to test the performance of the different optimal control models, a procedure validation must be carried out. The validation of the optimization method for the minimum hand jerk model is straightforward. MHJM trajectories are straight with single-peak bell-shaped velocity profiles. The test results indicate that the optimization method produces hand trajectories with the previously described features (e.g. Fig. 5.5). The validation of the optimization method for mMHJM, MAJM and MTCM requires the use of a less complex task than the one for which it has been developed. The idea is to use tasks where the solution is well known and therefore, the behavior of the optimization method can be judged by comparing the results of the tasks with the known solution. In the case under consideration, the optimization procedure is validated with a two joint pendulum (Fig. 5.2). The pendulum has to swing from the starting position ( $q_1 = 0^\circ$  and  $q_2 = 0^\circ$ ) to the final position ( $q_1 = 90^\circ$  and  $q_2 = 0^\circ$ ) in one second with 100 supporting points. Anthropometric parameters of the upper arm and lower arm from De Leva (1996) were used for the two segments of the pendulum. The third segment, the hand segment in figure 5.2, was not included in the calculations. This validation procedure was conducted for mMHJM, MAJM and MTCM. In addition, a minimum torque criterion (MTM) was tested. This additional criterion helped to assess the results of MTCM. Besides a qualitative analysis of the movement of the pendulum's segments, the sums of the HJ vectors were calculated using equation (5.9):

$$sRppp = \frac{\sum_{i=1}^{100} |Rppp_i^X| + \sum_{i=1}^{100} |Rppp_i^Y|}{2 \times 100} \quad (5.9)$$

where  $i$  are the number of the supporting points,  $Rppp_i^X$  are the X-coordinates of the HJ vector and  $Rppp_i^Y$  are the Y-coordinates of the HJ vector. The sums of the AJ vectors of the two joints were quantified using equation (5.10) is used:

$$sqppp = \frac{\sum_{i=1}^{100} |qppp_i^1| + \sum_{i=1}^{100} |qppp_i^2|}{2 \times 100} \quad (5.10)$$

where  $i$  is the number of the supporting points,  $qppp_i^1$  are the angles of the AJ vector for the first joint and  $qppp_i^2$  are the angles of the AJ vector for the second joint. Equation 5.10 is also used to calculate the sums of the torque vectors ( $sT$ ) and TC vectors  $sTp$ . If the optimization method works correctly, mMHJM should

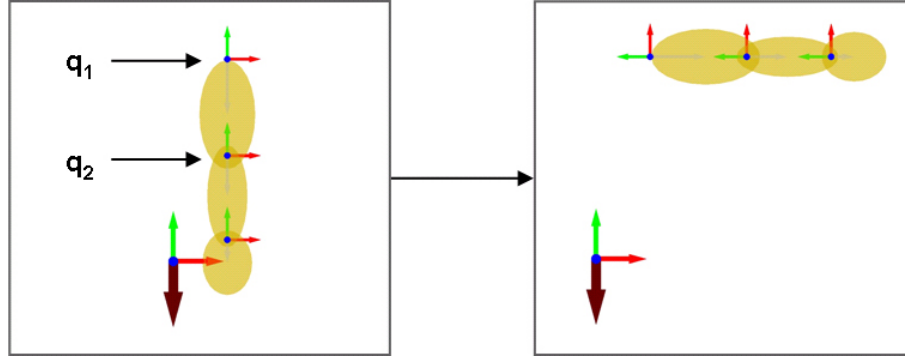


**Figure 5.2:** Validation task: The pendulum has to swing from the position  $q_1 = 0^\circ$  and  $q_2 = 0^\circ$  to the position  $q_1 = 90^\circ$  and  $q_2 = 0^\circ$ .

produce the smallest  $sRppp$  value, MAJM should produce the smallest  $sqpp$  value, the MTM should produce the smallest  $sT$  and MTCM should produce the smallest  $sTp$  value. Several simulations were conducted with each criterion to determine if the optimization method produced repeatable results.

### Step 2: Qualitative analysis of measured and predicted trajectories

After the validation of the optimization method, the results of all simulation runs were examined to observe the behavior of the models. Variations and similarities between human and predicted movement data were of special interest. In this context, some representative trajectories are presented and qualitatively analyzed.

### Step 3: Variations between measured and predicted trajectories

The third step involves quantification of the variations between the trajectories predicted by the different optimal control models and the experimentally determined trajectories. Therefore, the percent root-mean-square differences ( $\%RMSDs$ ) (Corradini et al., 1993) were obtained for the hand path, tangential velocity of the hand, joint angles, joint angular velocities and joint torques between the measured and predicted data. For the quantification of the differences between the human and predicted hand paths in three dimensional space (3D space), the  $\%RMSD$  for each dimension of the hand ( $h_x, h_y, h_z$ ) was calculated using equations (5.11):

$$\%RMSD_{h_x} = \sqrt{\frac{\frac{1}{N} \sum_{i=1}^N (X_i^{me} - X_i^{pr})^2}{\frac{1}{N} \sum_{i=1}^N (X_i^{me})^2}} \times 100 \quad (5.11)$$

where  $i$  is the number of 8.3 ms sampling points,  $X_i^{me}$  are the measured X-coordinates of the hand in the global reference frame,  $X_i^{pr}$  the predicted X-coordinates of the hand in the global reference frame and  $N$  is the total number of sampling points. For the Y- and Z-dimensions and for the hand velocities along these dimensions, the calculations were carried out analogously. To quantify the deviation across all three

dimensions, equation (5.12) was used:

$$\%RMSD_{h_{3D}} = \sqrt{(\%RMSD_{h_x})^2 + (\%RMSD_{h_y})^2 + (\%RMSD_{h_z})^2} \quad (5.12)$$

Equation (5.12) was also used to calculate the deviation of the velocities for all three dimensions.

In addition to the spatio-temporal features of the hand, an interest lies in the deviations introduced by the optimal control models on joint level. It is necessary to distinguish between the optimization of a single DOF and multiple DOFs. In the former case, the differences between the measured and predicted joint angles are quantified according to equation (5.13):

$$\%RMSD_{angle} = \sqrt{\frac{\frac{1}{N} \sum_{i=1}^N (q_i^{me} - q_i^{pr})^2}{\frac{1}{N} \sum_{i=1}^N (q_i^{me})^2}} \times 100 \quad (5.13)$$

where  $i$ ,  $q_i^{me}$ ,  $q_i^{pr}$  and  $N$  denote the number of 8.3 *ms* sampling points, the measured joint angles, the predicted joint angles and the total number of sampling points, respectively. Equation (5.13) was also used in the calculation of differences on the level of angular velocities and joint torques. If optimization of multiple DOFs is required, a single quantity is needed to account for all the deviations between the measured and predicted time series of angles across the optimized DOFs. To achieve this, equation 5.13 was used to calculate the  $\%RMSD_{angle}$  for each DOF. In a second step, the deviations for all DOFs were calculated using the following equation:

$$\%RMSD_{angles} = \sqrt{\sum_{j=1}^M (\%RMSD_{angle_j})^2} \quad (5.14)$$

where  $j$  corresponds to an optimized DOF and  $M$  to the total number of optimized DOFs. Equation 5.14 was also used to calculate the differences on the level of angular velocities and joint torques.

The calculated parameters were used to analyze the performance of the different optimal control models. For each model, the mean values and 99 % confidence intervals of the  $\%RMSDs$  were calculated from the 40 test trials. Using these parameters, each model was tested to determine which model exhibited the best results under each of the different simulation conditions (Tab. 5.1). The optimal control models were then examined separately to determine if there were performance differences across the optimized DOFs. This was carried out for the different conditions “1 DOF optimized” and “4 DOFs optimized” / “5 DOFs optimized” for MAJM and MTCM. In both cases, repeated ANOVAs measurements were conducted. The  $P$ -value for statistical significance was set at .01 and the Greenhouse-Geisser adjustment was used because the preconditions of homogeneity of variance and sphericity were not always

fulfilled. Post-hoc pairwise comparisons were performed using Bonferroni tests to further analyze significant results of ANOVAs. Finally, the different optimal control models were tested to determine if an increase of the DOFs to be optimized had an effect on the behavior of model. Therefore, we tested the differences between the two conditions "1-DOF optimized" and "4-DOFs optimized" / "5-DOF optimized" with paired two-sample t-tests. The  $P$ -value for significance was set at .01.

#### Step 4: Similarities between measured and predicted trajectories

Finally, the similarities between the measured and predicted movements were calculated using an approach enabling the comparison of topological course characteristics of movement patterns (Schöllhorn, 1998). A brief outline of the approach is provided below. A more comprehensive introduction can be found in Birklbauer (2006).

The first step involves correlating the time courses of the measured and predicted hand trajectories, tangential velocity profiles, joint angles, joint angular velocities and joint torques of the optimized joints with reference functions. Thereby, nine Taylor polynomials served as a reference system. The reference functions satisfied the following condition of orthogonality:

$$\int_0^t f(x)g(x)dx = \begin{cases} 1 \forall f(x) = g(x) \\ 0 \forall f(x) \neq g(x) \end{cases} \quad (5.15)$$

By correlating a single course (e.g. time series of elbow angles) with the nine Taylor polynomials the course characteristic is represented as a topological quantity to a  $1 \times 9$  vector. Accordingly,  $n$  courses (e.g. times series of shoulder and elbow angles) of a measured and predicted movement are represented as a topological quantity to a  $n \times 9$  matrix. The similarity coefficient  $sim$  of two single courses of a measured and a predicted movement (e.g. time series of elbow angles) is defined with the help of the reference specific correlation coefficients  $r^{me}$  and  $r^{pr}$ :

$$sim = \frac{\sum_{j=1}^9 r_j^{me} r_j^{pr}}{\sqrt{\sum_{j=1}^9 (r_j^{me})^2} \sqrt{\sum_{j=1}^9 (r_j^{pr})^2}} \quad (5.16)$$

Accordingly, the similarity coefficient  $SIM$  of  $n$  courses of a measured and a predicted movement (e.g. times series of shoulder and elbow angles) is defined with the help of the reference specific correlation coefficients  $R^{me}$  and  $R^{pr}$ :

$$SIM = \frac{tr(R^{me'} R^{pr})}{\sqrt{tr(R^{me'} R^{me})} \sqrt{tr(R^{pr'} R^{pr})}} \quad (5.17)$$

Therefore,  $R^{me'}$  and  $R^{pr'}$  are the transpose of the matrices of the reference specific correlation coefficients and  $tr$  corresponds to the trace of a matrix. The similarity coefficients  $sim$  and  $SIM$  can be interpreted as correlation coefficients as shown by Birklbauer (2006).

To calculate a mean similarity coefficient across a number of trials, the similarity coefficients need to be transformed to  $Z$ -values (Bortz, 1999). The transformation, called Fisher's  $Z$ -transformation, was computed using the following equation (5.18):

$$Z = \frac{1}{2} \ln \left( \frac{1 + sim}{1 - sim} \right) \quad (5.18)$$

where  $\ln$  is the logarithm to the base  $e$ . After the transformation, the mean values were calculated and the means of the  $Z$ -values were transformed back to similarity coefficients using equation (5.19):

$$sim = \frac{e^{2Z} - 1}{e^{2Z} + 1} \quad (5.19)$$

Equations (5.18) and (5.19) were also used to calculate the mean  $SIM$  values.

## 5.3 Results

### 5.3.1 Validation of the optimization method

The optimization algorithm was tested on the basis of mMHJM, MAJM, MTM and MTCM. Figures 5.3 and 5.4 depict the results of a typical run in the pendulum task for these optimization models.

As can be seen in the case of mMHJM, the trajectory of the hand is nearly straight. For MAJM, the optimization process produced a solution where movement only occurred in joint  $q_1$ . Because the initial and final position of one of the joints was prescribed to be  $0^\circ$  and MAJM optimization sought to minimize jerk across the two joints, a result that involves motion in only one joint seems logical. The solution found by the optimization method for MAJM requires a large torque in joint  $q_1$ . However, this is irrelevant because the minimum angle jerk is a kinematic criterion. In the case of MTM, this result would not be plausible. The optimization method for the minimum torque criterion produced a solution where joint  $q_2$  was flexed more than  $90^\circ$  to reduce the torque in joint  $q_1$  during the movement. Again, this result appears appropriate and the sum of the torques should be less compared to the solution of MAJM. Similarly in the case of MTCM, the results indicate that joint  $q_2$  is flexed. This is logical because the model works on the torque level. However, the maximal flexion is lower than for MTM and thus the changes in torques are smaller. Once again, this seems plausible because the strategy leads to a minimization of changes in joint torques. Moreover, the experiments showed that the optimization method produced the same results in repeated trials under identical conditions.

The results displayed in table 5.2 indicate that the optimization procedure works correctly. mMHJM produced the smallest  $sRppp$  value, MAJM produced the smallest  $sqppp$  value, MTM produced the smallest  $sT$  value and MTCM produced the smallest  $sTp$  value.

**Table 5.2:** Results of the validation procedure for the different optimal control models based on the equations (5.9) and (5.10).

Optimal control model	$sRppp$	$sqppp$	$sT$	$sTp$
mMHJM	0.002 $m/s^3$	134205.45 $deg/s^3$	4.50 $Nm$	0.46 $Nm/s$
MAJM	83.62 $m/s^3$	3564.09 $deg/s^3$	4.96 $Nm$	0.12 $Nm/s$
MTM	323.40 $m/s^3$	114031.42 $deg/s^3$	3.06 $Nm$	0.18 $Nm/s$
MTCM	127.60 $m/s^3$	46383.67 $deg/s^3$	3.88 $Nm$	0.08 $Nm/s$

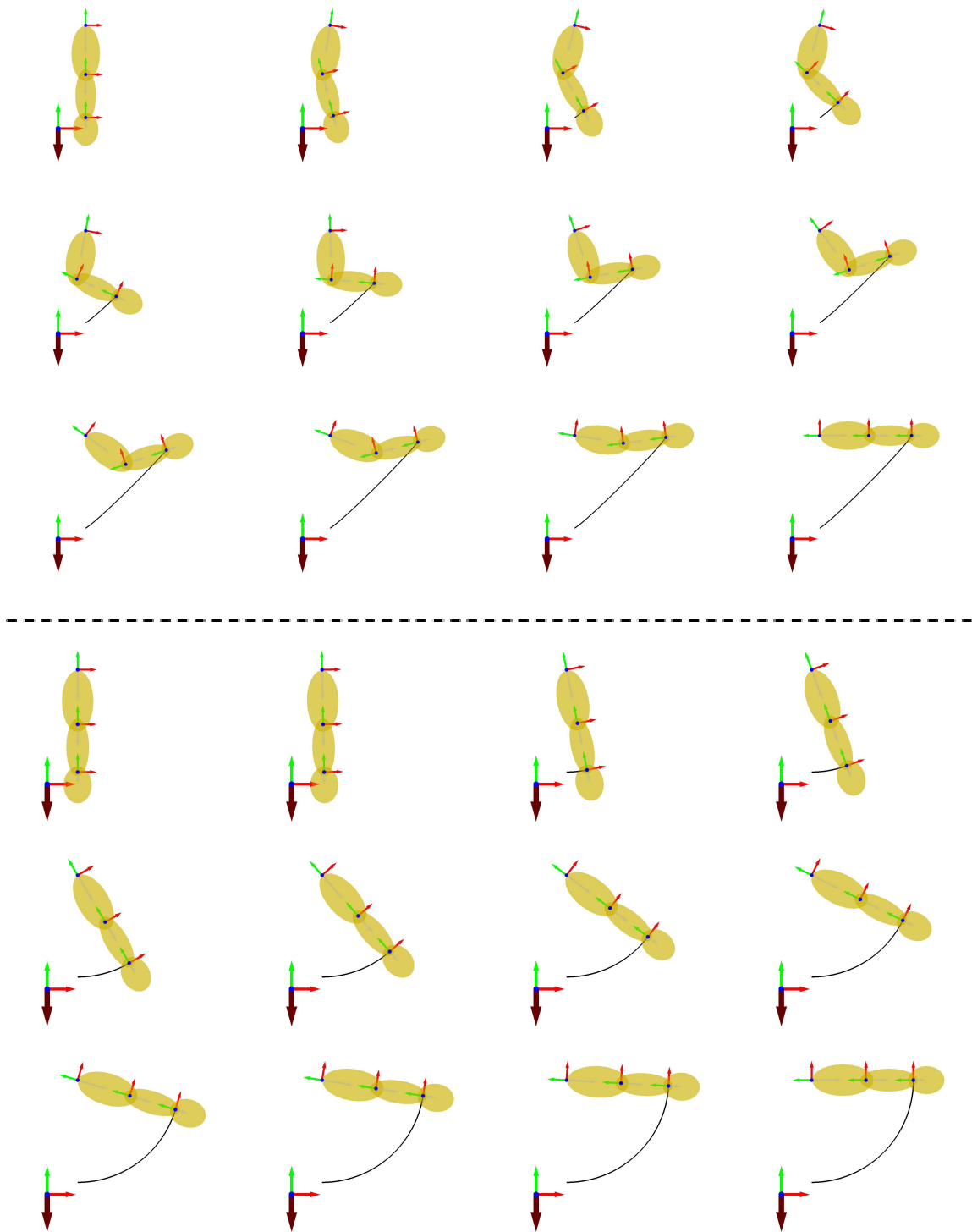


**Figure 5.3:** Results of a typical run in the pendulum task for mMhJM (top) and MAJM (bottom).

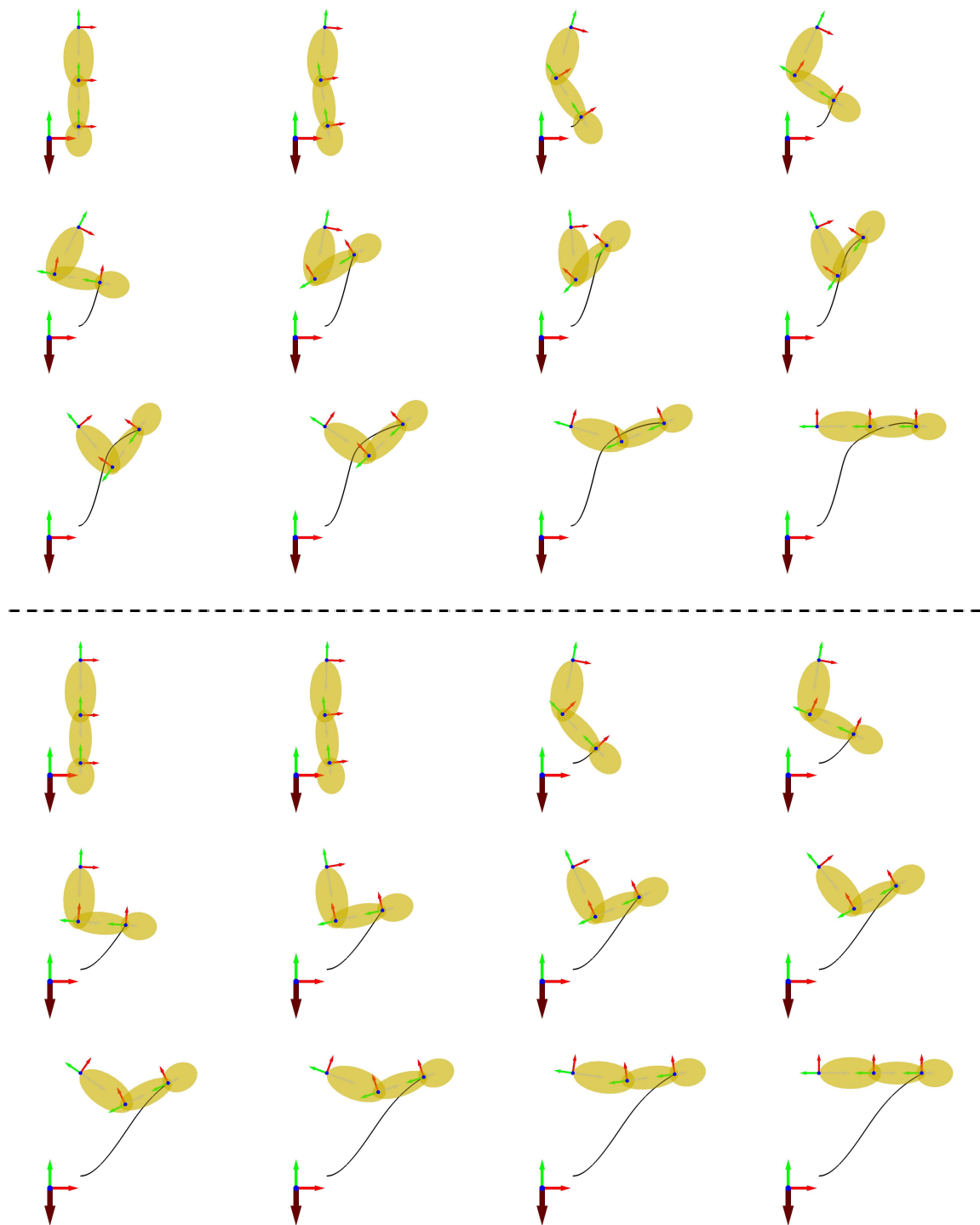


**Figure 5.4:** Results of a typical run in the pendulum task for MTM (top) and MTCM (bottom).

### 5.3.2 Target 1: Comparison of the measured and predicted trajectories

The results of the performance of the different optimal control models is presented as outlined in chapter 5.2.8.

#### 5.3.2.1 Qualitative analysis of measured and predicted trajectories

The results of the qualitative analysis of human and predicted trajectories are presented according to the simulation protocol shown in table 5.1.

##### 1 DOF optimized: Shoulder abduction/adduction

Representative hand paths are illustrated in figure 5.5. None of the models were able to precisely reproduce the measured hand movement in 3D space. In contrast to the other optimization models, MHJM produced straight hand paths. The hand paths generated by mMhJM, MAJM and MTCM were curved in all trials. The top middle plot in Figure 5.5 shows typical tangential velocity profiles of the hand. Again, none of the optimal control models were able to completely reproduce the measured tangential velocity profiles. However, the models were able to approximate the single-peak, nearly bell-shaped measured velocity profile. Across all trials, the peak velocity of MHJM and mMhJM were lower than the peak velocities of the subjects. In a few cases, the velocity profiles of mMhJM, MAJM and MTCM appeared slightly oscillating and the profiles showed some distortion at the end. On joint level, all three models reproduced the shoulder movement of the subjects with only small deviations (Fig. 5.5). MAJM generated a nearly straight path in joint space. In figure 5.5, representative angular velocities are plotted. Again, the three models were not able to completely reproduce the measured joint angle trajectories. The velocity profiles of MAJM were smooth, single-peak and bell-shaped in all trials. The shape of the trajectories of the joint angular velocities produced by mMhJM and MTCM were much more variable. Finally, MTCM was only rarely able to replicate the human torque profiles. In many cases, MTCM produced a large torque at the beginning of the movement that constantly decreased toward the end of the movement. The peak torque produced by MTCM was only occasionally larger than the peak torque produced by the subjects. Furthermore, all torque profiles were slightly oscillating (Fig. 5.5).

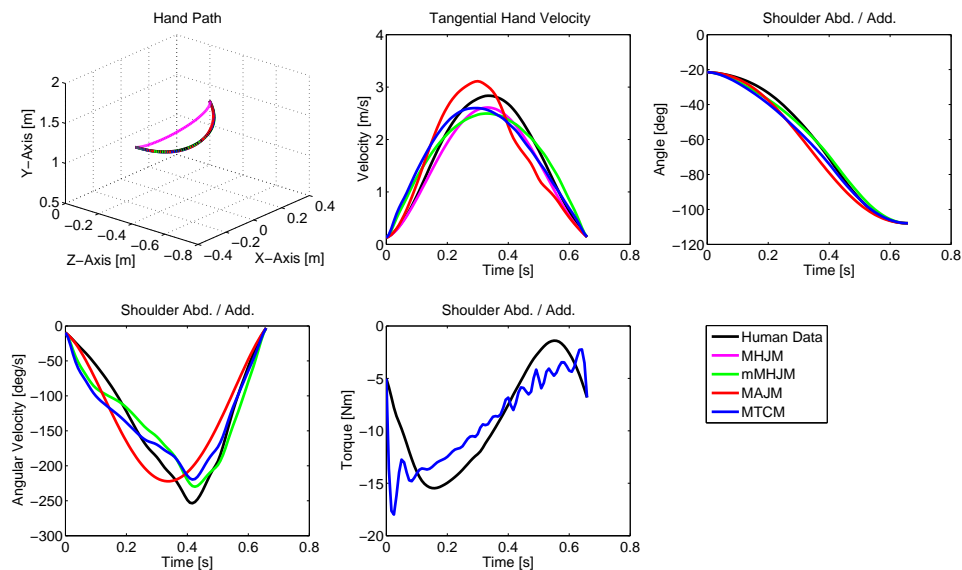


**Figure 5.5:** Representative trial for the optimization of shoulder abduction/adduction.

### 1 DOF optimized: Shoulder rotation

In figure 5.6 representative hand paths are illustrated. As before, none of the models were able to exactly reproduce the measured movement. Again, the MHJM produced straight hand paths. All other models generated curved paths. Moreover, all of the four optimal control models were able to emulate the single peaked and almost bell-shaped tangential velocity profiles of the subjects. None of the optimal control models were able to completely reproduce the measured tangential velocity profiles. Across all trials the peak velocity of the MHJM and the mMHJM were lower than the one produced by the subjects. Moreover, in a few cases the velocity profiles of the mMHJM, MAJM and the MTCM were slightly oscillating. On joint level the MAJM showed a close fit to the shoulder rotations of the subjects (Fig. 5.6), whereas the mMHJM and the MTCM exhibited larger deviations across the trials. Furthermore, in figure 5.6 representative angular velocities are illustrated. Again, none of the three models was able to completely reproduce the measured joint angle trajectories. The velocity profiles of the MAJM were highly stereotypical compared to the trajectories of the mMHJM and MTCM and showed in most cases a close fit. The MTCM reproduced the measured movement in torque space only incompletely, compared to the model fit in extrinsic and intrinsic kinematic spaces. Again the peak torque produced by the MTCM was in most cases comparable to the ones produced by the subjects. As before, all of the torque profiles were slightly oscillating (Fig. 5.6).

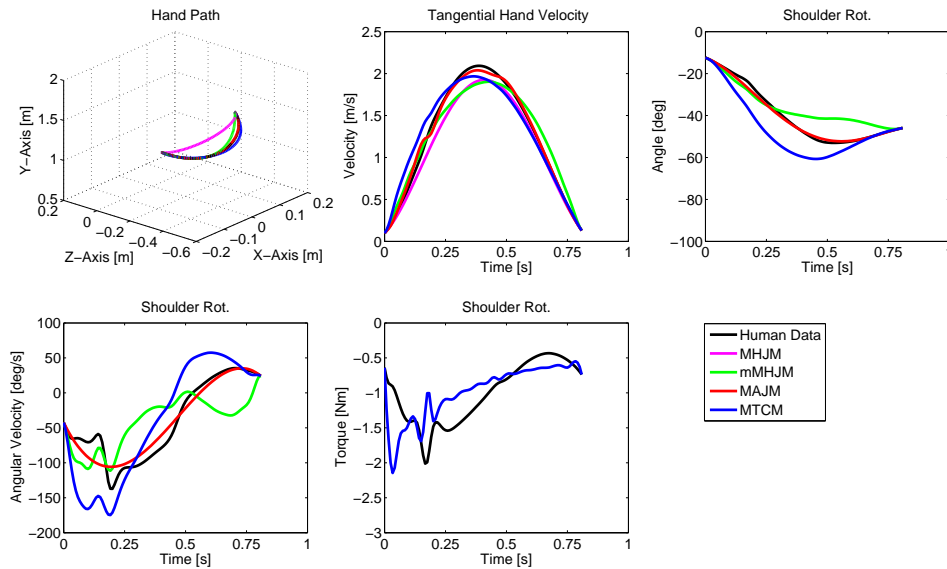


**Figure 5.6:** Representative trial for the optimization of shoulder rotation.

### 1 DOF optimized: Shoulder anteversion/retroversion

In figure 5.7 representative hand paths are displayed. The MHJM produced straight hand path across all trials. In contrast, the mMHJM, the MAJM and the MTCM generated across all trials curved hand paths. All in all, none of the models were able to reproduce the experimentally determined hand paths. The subjects tended to produce single peaked tangential velocities. However, the profiles were not exactly bell-shaped. In some cases the peak velocity was reached rather early during the movement as shown in figure 5.7. This kind of velocity profiles could not be reproduced by the MHJM (Fig. 5.7), but by the other three optimal control models. Across all trials the peak velocity of the MHJM was lower than the one produced by the subjects. On joint level the mMHJM and the MTCM showed larger deviations across the trials than the MAJM. None of the three models were able to reproduce the measured angular velocities. Again, the profiles of the MAJM were highly stereotypical compared to the trajectories of the mMHJM and MTCM. In comparison with the mMHJM and the MTCM the MAJM showed - across all trials - peak angular velocities that were close to those produced by the subjects. The MTCM was only rarely able to replicate the human torque profiles. The torque profiles did not exhibit large peak torques so that the profiles could be characterized by a minimal change in the torque course during the movement. In other words, there are no large torque spikes, although all of the torque profiles were slightly oscillating (Fig. 5.7).

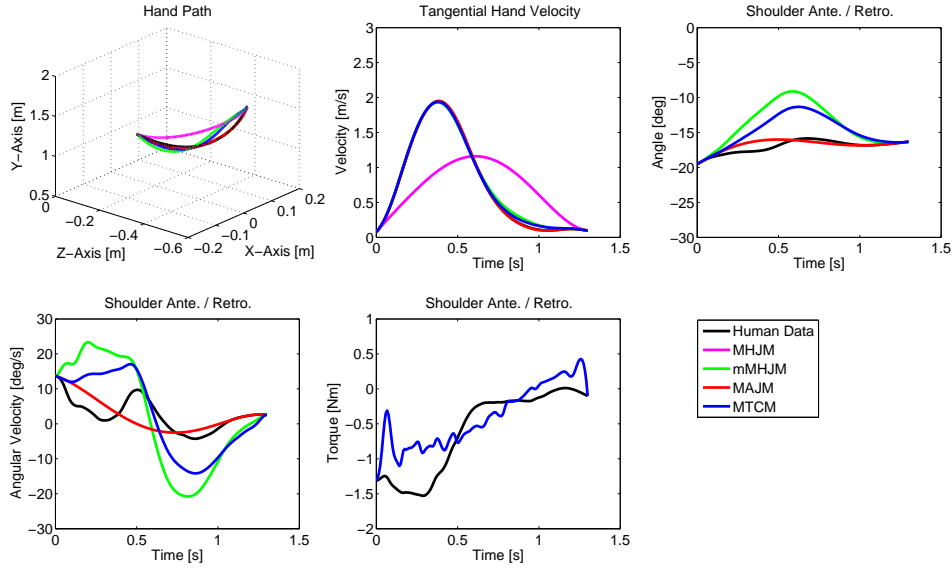


**Figure 5.7:** Representative trial for the optimization of shoulder anteversion/retroversion.

### 1 DOF optimized: Elbow flexion/extension

In figure 5.8 representative hand paths are displayed. The MHJM produced straight hand path across all trials. In contrast, the mMHJM, the MAJM and the MTCM generated curved hand paths across all trials. All in all, none of the models were able to emulate the measured hand movement in 3D-space. The subjects tended to produce single peaked tangential velocity profiles. These profiles could be approximated by all four optimal control models. Across all trials the peak velocity of the MHJM was lower than the one produced by the subjects. On joint level the mMHJM and the MTCM showed larger deviations across the trials than the MAJM. This corresponds to a larger flexion or extension in the elbow joint than the ones produced by the subjects. None of the three models were able to reproduce the measured angular velocities. Again, the profiles of the MAJM were highly stereotypical compared to the trajectories of the mMHJM and MTCM. In comparison with the mMHJM and MTCM the MAJM showed - across all trials - peak angular velocities close to those produced by the subjects. The MTCM reproduced the human torque profiles only incompletely. In most cases the model produced a large torque at the beginning of the movement, which was constantly reduced towards the end of the movement. Although the peak torques produced by the MTCM were only in a few cases considerably larger than the peak torques produced by the subjects. Furthermore, all of the torque profiles were slightly oscillating (Fig. 5.7).

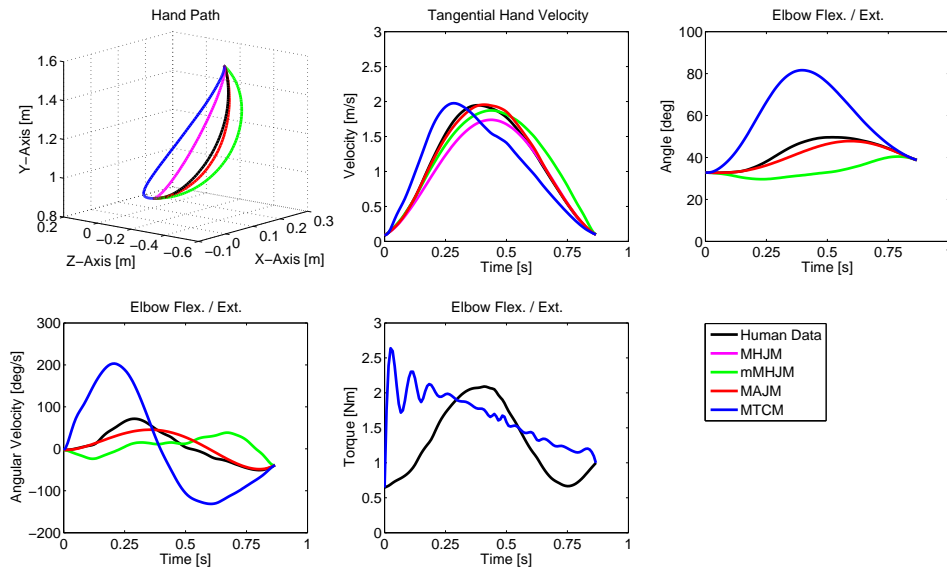


**Figure 5.8:** Representative trial for the optimization of elbow flexion/extension.

#### 4 DOFs optimized

In figure 5.9 representative hand paths are illustrated. The MHJM produced straight hand path across all trials. In contrast the mMHJM, the MAJM and the MTCM generated curved hand paths across all trials. All in all, none of the models were able to reproduce the experimentally determined hand paths. Furthermore, across all trials these three models seem to show larger deviations as before (1 DOF optimized). Especially the MTCM exhibited in a few cases large deviations. It was shown in the first study of this thesis (Fig. 4.1, 4.2) that the subjects produced single-peaked and almost bell-shaped velocity profiles. The MHJM produced in all cases single-peaked and bell-shaped velocity profiles with lower peak velocities than produced by the subjects. The other three optimal control models mostly produced single-peaked tangential velocity profiles with bell-like shapes. In some cases, however, the profiles exhibited distortions. To sum up, the increase of the number of joints to be optimized seem to increase the deviation from the measured movement in extrinsic coordinates of the hand. Nevertheless, all four optimal control models seem to be able to emulate the basic features of the measured hand trajectories in most test trials.

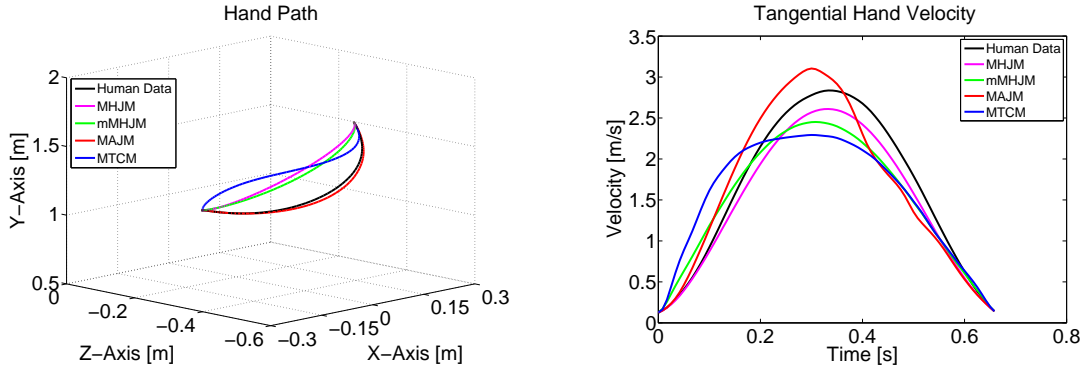


**Figure 5.9:** Representative hand paths and tangential velocity profiles for the optimization of shoulder abduction/adduction, shoulder rotation, shoulder anteversion/retroversion as well as elbow flexion/extension.

In the first row of figure 5.10 typical joint angle trajectories of the optimized DOFs are displayed. Across all trials the three optimal control models reproduced the angle profiles of the measured shoulder abduction best. Furthermore, the MAJM produced across the 4 DOFs the closest fit to the measured trajectories. In contrast, in the cases of the shoulder rotation, the shoulder anteversion/retroversion as well as elbow flexion/extension the trajectories of the mMHJM and the MTCM were more variable with larger movement ranges than the ones produced by the subjects. Moreover the angle profiles of the mMHJM were sometimes oscillating (Fig. 5.10, shoulder rot.). In the middle row of figure 5.10 the corresponding joint angular velocities are illustrated. The MAJM exhibited the closest fit across all 4 DOFs. The mMHJM and the MTCM reproduced the angular velocity profiles of the human shoulder abduction at least to some extent. In contrast, both models showed large deviations in the other three DOFs with large differences in the peak angular velocities. In the bottom row of figure 5.10 the corresponding joint torques are displayed. As before in the case of single degree optimization the MTCM showed a tendency to reproduce the measured torque profiles only incompletely across all the trials and all 4 DOFs. However, in a few cases the MTCM produced trajectories emulating the measured torque profiles to some extent (Fig. 5.10, shoulder rot.). The peak torques produced by the MTCM were only in a few cases larger than the peak torques produced by the subjects. Furthermore, all of the torque profiles were slightly oscillating.

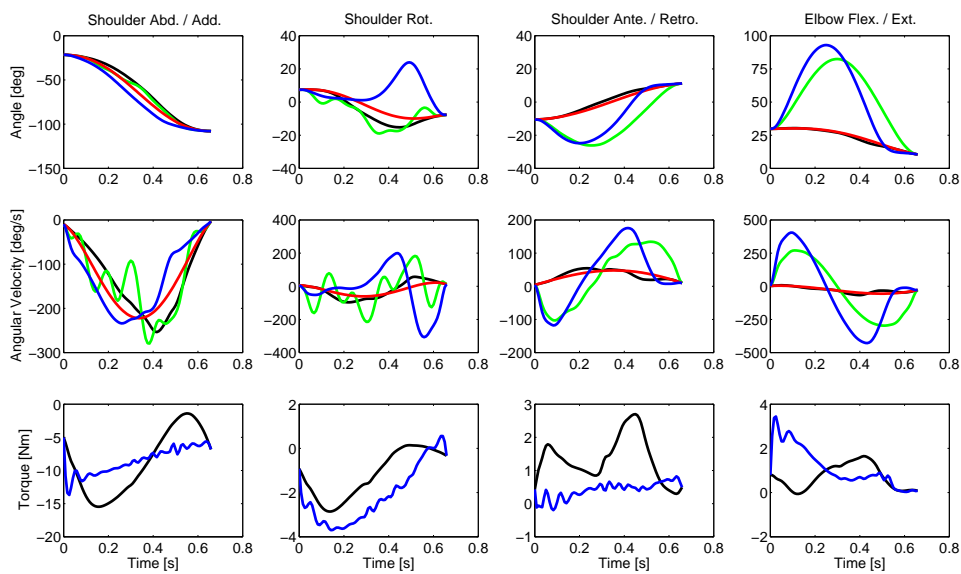


**Figure 5.10:** Representative angle, angular velocity and torque profiles for the optimization of shoulder abduction/adduction, shoulder rotation, shoulder anteversion/retroversion as well as elbow flexion/extension. As before, the human trajectories are black, the trajectories of the mMhJM are green, the trajectories of the MAJM are red and the trajectories of the MTCM are blue.

### 5.3.2.2 Variations between measured and predicted trajectories

The variations between the measured and predicted trajectories were analyzed based on equations 5.11, 5.12, 5.13 and 5.14. First, the performance of the different optimal control models across the optimized DOFs were analyzed (Chap. 5.3.2.2.1). Second, each optimal control model was examined separately to determine if there were performance differences across the four optimized DOFs. This step was carried out for the condition “1 DOF optimized” and for the condition “4 DOFs optimized” (Chap. 5.3.2.2.2). Finally, each of the optimal control models was tested to conclude if there were performance differences between the two conditions “1 DOF optimized” vs. “4 DOF optimized” across the four optimized DOFs (Chap. 5.3.2.2.3).

#### 5.3.2.2.1 Performance differences between different optimal control models

In this section, the performance of MHJM, mMHJM, MAJM and the MTCM are analyzed for the optimization of 1 DOF and 4 DOFs. The analysis was carried out according to the simulation protocol (Tab. 5.1).

##### 1 DOF optimized: Shoulder abduction/adduction

The results of the %RMSDs for the measured and the predicted hand paths (Fig. 5.11, top left) indicate that none of the four optimal control models were able to reproduce the measured hand movements in extrinsic coordinates. MAJM produced the smallest %RMSD followed by mMHJM, MTCM and finally MHJM. The repeated ANOVA yielded significant differences ( $F = 15.190, p \leq .001, \eta^2 = .280$ ) between the %RMSDs of the measured and predicted hand paths of the four optimal control models. Pairwise Bonferroni tests revealed significant differences between the %RMSDs of the measured and predicted hand paths of MHJM and mMHJM ( $p \leq .001$ ), MHJM and MAJM ( $p \leq .001$ ), mMHJM and MAJM ( $p \leq .001$ ), MAJM and MTCM ( $p \leq .01$ ). The Bonferroni tests yielded no significant differences between MHJM and MTCM ( $p = 1.000$ ) as well as between mMHJM and MTCM ( $p = .054$ ).

The results of the %RMSDs between the measured and predicted tangential velocities of the hand (Fig. 5.11, top right) show that MAJM produced the smallest %RMSD followed by mMHJM, MTCM and MHJM. The repeated ANOVA yielded significant differences ( $F = 10.698, p \leq .001, \eta^2 = .215$ ) between the %RMSDs of the measured and predicted tangential hand velocities of the four optimal control models. Pairwise Bonferroni tests revealed significant differences between the %RMSDs of the measured and predicted tangential hand velocities of MHJM and mMHJM ( $p \leq .001$ ), MHJM and MAJM ( $p \leq .001$ ), mMHJM and MAJM ( $p \leq .01$ ), MAJM and MTCM ( $p \leq .01$ ). The Bonferroni tests yielded no significant differences between MHJM and MTCM ( $p = 1.000$ ) as well as between mMHJM and MTCM ( $p = .094$ ).

The results of the %RMSDs between the measured and predicted shoulder angles (Fig. 5.11, bottom left) indicate that none of the three optimal control models were able to reproduce the measured joint angle trajectories. MAJM produced the

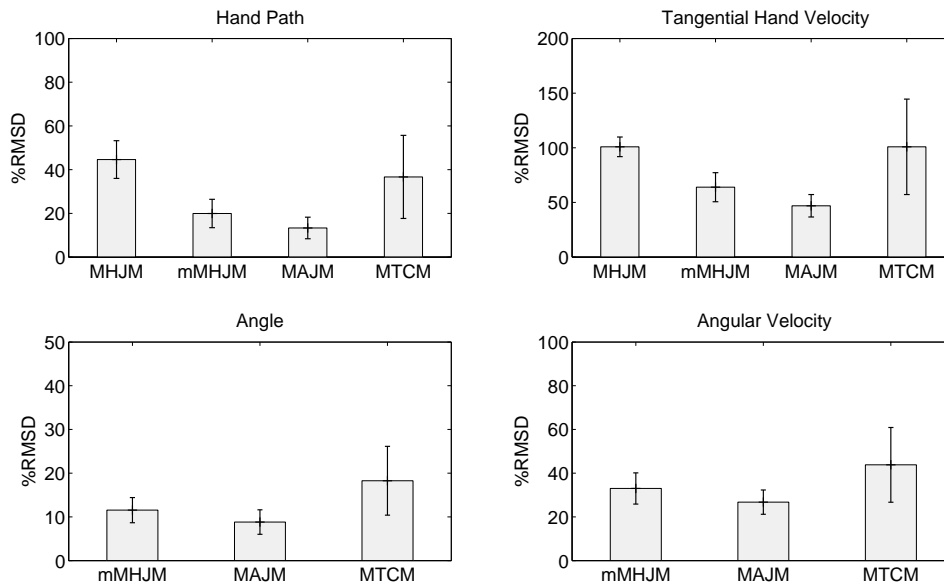


**Figure 5.11:** Mean of the %RMSDs between the measured and predicted hand paths, tangential hand velocities, angles and angular velocities for MHJM, mMHJM, MAJM and MTCM for the optimization of the DOF shoulder abduction/adduction. Error bars indicate the 99 % confidence intervals.

smallest %RMSD followed by mMHJM and MTCM. The repeated ANOVA yielded significant differences ( $F = 8.511, p \leq .01, \eta^2 = .179$ ) between the %RMSDs of the measured and predicted joint angles of the three optimal control models. Pairwise Bonferroni tests revealed significant differences between the %RMSDs of the measured and predicted joint angles of MAJM and MTCM ( $p \leq .01$ ). The Bonferroni tests yielded no significant differences between mMHJM and MAJM ( $p = .055$ ) or mMHJM and MTCM ( $p = .058$ ).

The results of the %RMSDs between the measured and predicted angular velocities (Fig. 5.11, bottom right) again show that the MAJM produced the smallest %RMSD followed by mMHJM and MTCM. The repeated ANOVA yielded no significant differences ( $F = 5.063, p = .021, \eta^2 = .115$ ) between the %RMSDs of the measured and predicted joint angular velocities of the three optimal control models.

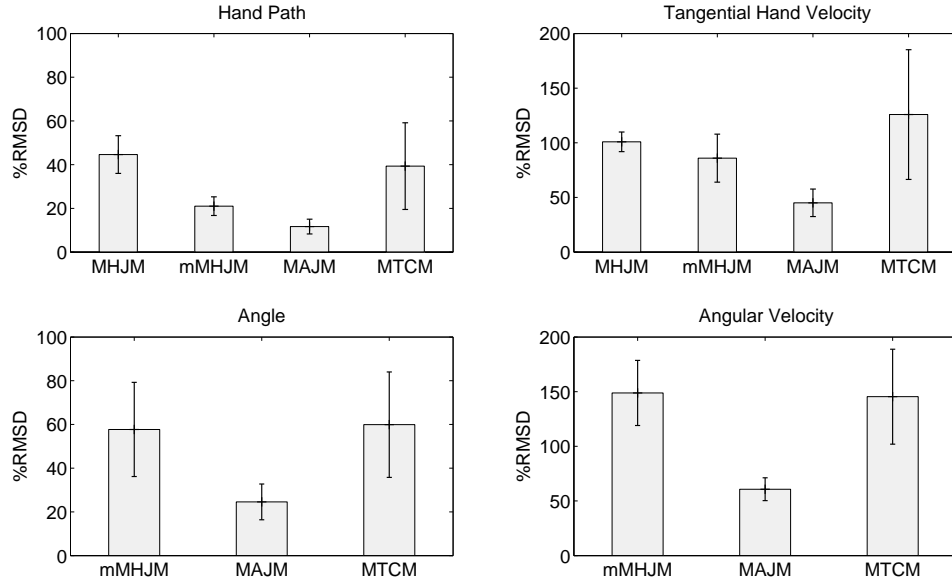


**Figure 5.12:** Mean of the %RMSDs between measured and predicted hand paths, tangential hand velocities, angles and angular velocities for MHJM, mMHJM, MAJM and MTCM for the optimization of the DOF shoulder rotation. Error bars indicate the 99 % confidence intervals.

### 1 DOF optimized: Shoulder rotation

The results of the %RMSDs for the measured and predicted hand paths (Fig. 5.12, top left) indicate that none of the four optimal control models were able to reproduce the measured hand movements in extrinsic coordinates. MAJM produced the smallest %RMSD followed by mMHJM, MTCM and finally MHJM. The repeated ANOVA yielded significant differences ( $F = 14.511, p \leq .001, \eta^2 = .271$ ) between the %RMSDs of the measured and predicted hand paths of the four optimal control models. Pairwise Bonferroni tests revealed significant differences between the %RMSDs of the measured and predicted hand paths of MHJM and mMHJM ( $p \leq .001$ ), MHJM and MAJM ( $p \leq .001$ ), mMHJM and MAJM ( $p \leq .001$ ), MAJM and MTCM ( $p \leq .01$ ). The Bonferroni tests yielded no significant differences between MHJM and MTCM ( $p = 1.000$ ) or mMHJM and MTCM ( $p = .100$ ).

The results of the %RMSDs between the measured and predicted tangential velocities of the hand (Fig. 5.12, top right) show that MAJM produced the smallest %RMSDs followed by mMHJM, MHJM and MTCM. The repeated ANOVA yielded significant differences ( $F = 8.743, p \leq .01, \eta^2 = .183$ ) between the %RMSDs of the measured and predicted tangential hand velocities of the four optimal control models. Pairwise Bonferroni tests revealed significant differences between the %RMSDs of the measured and predicted tangential hand velocities of MHJM and MAJM ( $p \leq .001$ ),

mMHJM and MAJM ( $p \leq .001$ ), MAJM and MTCM ( $p \leq .01$ ). The Bonferroni tests yielded no significant differences between MHJM and mMHJM ( $p = .365$ ), MHJM and MTCM ( $p = 1.000$ ) or mMHJM and MTCM ( $p = .439$ ).

The results of the %RMSDs between the measured and predicted shoulder angles (Fig. 5.12, bottom left) indicate that none of the three optimal control models were able to reproduce the measured joint angle trajectories. MAJM produced the smallest %RMSD followed by mMHJM and MTCM. The repeated ANOVA yielded significant differences ( $F = 12.903, p \leq .001, \eta^2 = .249$ ) between the %RMSDs of the measured and predicted joint angles of the three optimal control models. Pairwise Bonferroni tests revealed significant differences between the %RMSDs of the measured and predicted joint angles of mMHJM and MAJM ( $p \leq .001$ ) as well as MAJM and MTCM ( $p \leq .001$ ). The Bonferroni tests yielded no significant differences between mMHJM and MTCM ( $p = 1.000$ ).

The results of the %RMSDs between the measured and predicted angular velocities (Fig. 5.12, bottom right) show that MAJM produced the smallest %RMSD followed by MTCM and mMHJM. The repeated ANOVA yielded significant differences ( $F = 23.543, p \leq .001, \eta^2 = .376$ ) between the %RMSDs of the measured and predicted joint angular velocities of the three optimal control models. Pairwise Bonferroni tests revealed significant differences between the %RMSDs of the measured and predicted joint angles of mMHJM and MAJM ( $p \leq .001$ ) as well as between MAJM and MTCM ( $p \leq .001$ ). The Bonferroni tests yielded no significant differences between mMHJM and MTCM ( $p = 1.000$ ).

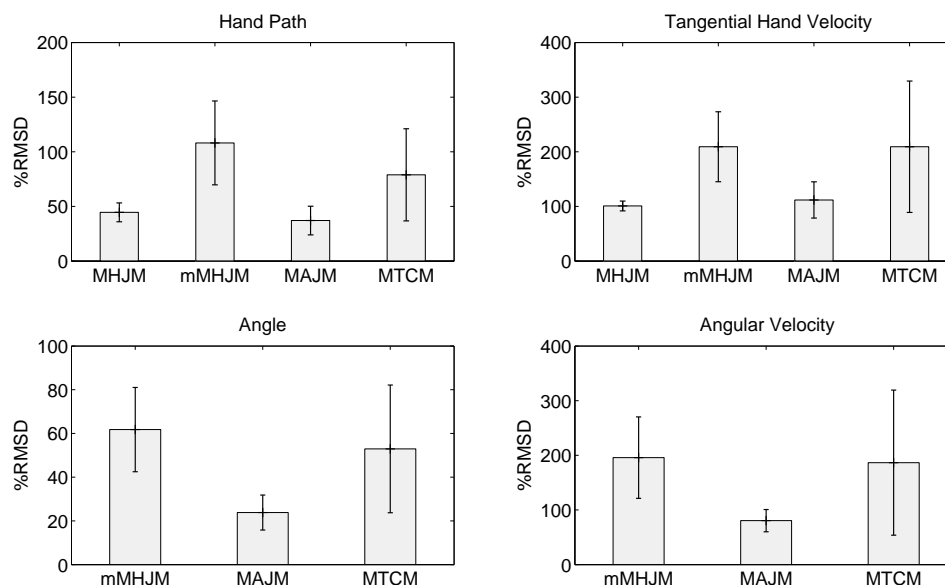


**Figure 5.13:** Mean of the %RMSDs between the measured and predicted hand paths, tangential hand velocities, angles and angular velocities for MHJM, mMhJM, MAJM and MTCM for the optimization of the DOF shoulder anteversion/retroversion. Error bars indicate the 99 % confidence intervals.

### 1 DOF optimized: Shoulder anteversion/retroversion

The results of the %RMSDs between the measured and predicted hand paths (Fig. 5.13, top left) indicate that none of the four optimal control models were able to reproduce the measured hand movements in extrinsic coordinates. MAJM produced the smallest %RMSD followed by MHJM, MTCM and finally mMhJM. The repeated ANOVA yielded significant differences ( $F = 9.587, p \leq .001, \eta^2 = .197$ ) between the %RMSDs of the measured and predicted hand paths of the four optimal control models. Pairwise Bonferroni tests revealed significant differences between the %RMSDs of the measured and predicted hand paths of MHJM and mMhJM ( $p \leq .001$ ) and between mMhJM and MAJM ( $p \leq .001$ ). The Bonferroni tests yielded no significant differences between MHJM and MAJM ( $p = .912$ ), MHJM and MTCM ( $p = .319$ ), mMhJM and MTCM ( $p = .598$ ) or MAJM and MTCM ( $p = .140$ ).

The results of the %RMSDs between the measured and predicted tangential velocities of the hand (Fig. 5.13, top right) show that MHJM produced the smallest %RMSD followed by MAJM, MTCM and mMhJM. The repeated ANOVA yielded significant differences ( $F = 5.725, p \leq .01, \eta^2 = .128$ ) between the %RMSDs of the measured and predicted tangential hand velocities of the four optimal control models. Pairwise Bonferroni tests revealed significant differences between the %RMSDs of the measured and predicted tangential hand velocities of MHJM and mMhJM ( $p \leq .001$ ).

as well as mMHJM and MAJM ( $p \leq .001$ ). The Bonferroni tests yielded no significant differences between MHJM and MAJM ( $p = 1.000$ ), MHJM and MTCM ( $p = .164$ ), mMHJM and MTCM ( $p = 1.000$ ) or MAJM and MTCM ( $p = .242$ ).

The results of the %RMSDs between the measured and predicted shoulder angles (Fig. 5.13, bottom left) indicate that none of the three optimal control models were able to reproduce the measured joint angle trajectories. MAJM produced the smallest %RMSD followed by MTCM and mMHJM. The repeated ANOVA yielded significant differences ( $F = 7.005, p \leq .01, \eta^2 = .152$ ) between the %RMSDs of the measured and predicted joint angles of the three optimal control models. Pairwise Bonferroni tests revealed significant differences between the %RMSD of the measured and predicted joint angles of mMHJM and MAJM ( $p \leq .001$ ). The Bonferroni tests yielded no significant differences between mMHJM and MTCM ( $p = 1.000$ ) or MAJM and MTCM ( $p = .059$ ).

The results of the %RMSDs between the measured and predicted angular velocities (Fig. 5.13, bottom right) also show that MAJM produced the smallest %RMSD followed by MTCM and mMHJM. The repeated ANOVA yielded no significant differences ( $F = 4.970, p = .018, \eta^2 = .113$ ) between the %RMSDs of the measured and predicted joint angular velocities of the three optimal control models. Since the repeated ANOVA was significant in trend, we conducted the pairwise Bonferroni tests. They revealed significant differences between the %RMSD of the measured and predicted joint angular velocities of mMHJM and MAJM ( $p \leq .001$ ) and no significant differences between mMHJM and MTCM ( $p = 1.000$ ) or MAJM and MTCM ( $p = .120$ ).

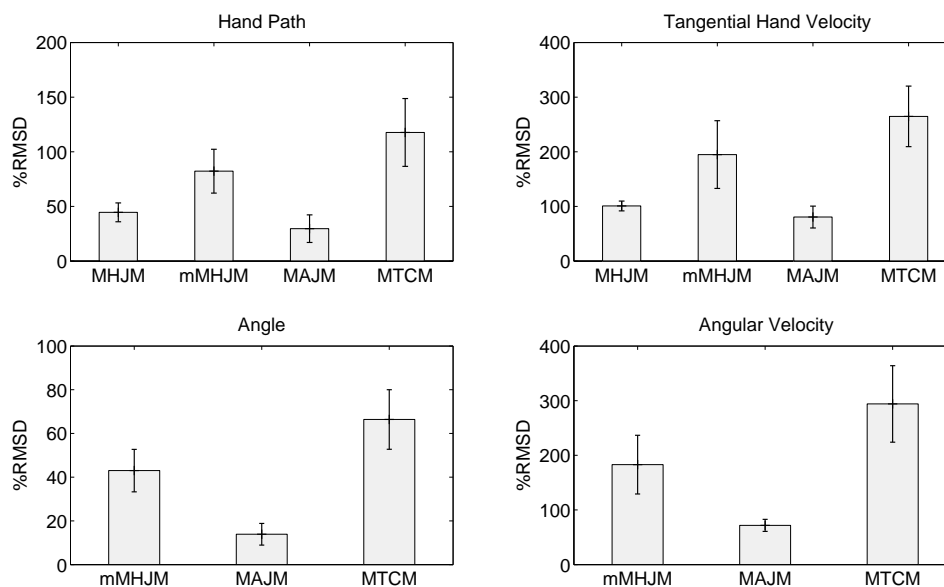


**Figure 5.14:** Mean of the %RMSDs between the measured and predicted hand paths, tangential hand velocities, angles and angular velocities for MHJM, mMHJM, MAJM and MTCM for the optimization of the DOF elbow flexion/extension. Error bars indicate the 99 % confidence intervals.

### 1 DOF optimized: Elbow flexion/extension

The results of the %RMSDs between the measured and predicted hand paths (Fig. 5.14, top left) indicate that none of the four optimal control models were able to reproduce the measured hand movements in extrinsic coordinates. MAJM produced the smallest %RMSD followed by MHJM, mMHJM and finally MTCM. The repeated ANOVA yielded significant differences ( $F = 36.289, p \leq .001, \eta^2 = .482$ ) between the %RMSDs of the measured and predicted hand paths of the four optimal control models. Pairwise Bonferroni tests revealed significant differences between the %RMSDs of the measured and predicted hand paths of MHJM and mMHJM ( $p \leq .001$ ), MHJM and MAJM ( $p \leq .01$ ), MHJM and MTCM ( $p \leq .001$ ), mMHJM and MAJM ( $p \leq .001$ ) as well as MAJM and MTCM ( $p \leq .001$ ). The Bonferroni tests yielded no significant differences between mMHJM and MTCM ( $p = .018$ ).

The results of the %RMSDs between the measured and predicted tangential velocities of the hand (Fig. 5.14, top right) show that MAJM produced the smallest %RMSD followed by MHJM, mMHJM and MTCM. The repeated ANOVA yielded significant differences ( $F = 36.015, p \leq .001, \eta^2 = .48$ ) between the %RMSDs of the measured and predicted tangential hand velocities of the four optimal control models. Pairwise Bonferroni tests revealed significant differences between the %RMSDs of the measured and predicted tangential hand velocities of MHJM and mMHJM

( $p \leq .01$ ), MHJM and MTCM ( $p \leq .001$ ), mMhJM and MAJM ( $p \leq .001$ ) as well as MAJM and MTCM ( $p \leq .001$ ). The Bonferroni tests yielded no significant differences between MHJM and MAJM ( $p = .076$ ) or mMhJM and MTCM ( $p = .028$ ).

The results of the %RMSDs between the measured and predicted elbow angles (Fig. 5.14, bottom left) indicate that none of the three optimal control models were able to reproduce the measured joint angle trajectories. MAJM produced the smallest %RMSD followed by mMhJM and MTCM. The repeated ANOVA yielded significant differences ( $F = 49.691, p \leq .001, \eta^2 = .560$ ) between the %RMSDs of the measured and predicted joint angles of the three optimal control models. Pairwise Bonferroni tests revealed significant differences between the %RMSDs of the measured and predicted joint angles of mMhJM and MAJM ( $p \leq .001$ ), mMhJM and MTCM ( $p \leq .01$ ) as well as MAJM and MTCM ( $p \leq .001$ ).

The results of the %RMSDs between the measured and predicted angular velocities (Fig. 5.14, bottom right) indicate that none of the three optimal control models were able to reproduce the measured joint angle trajectories. MAJM produced the smallest %RMSD followed by mMhJM and MTCM. The repeated ANOVA yielded significant differences ( $F = 39.782, p \leq .001, \eta^2 = .505$ ) between the %RMSDs of the measured and predicted joint angular velocities of the three optimal control models. Pairwise Bonferroni tests revealed significant differences between the %RMSDs of the measured and predicted joint angular velocities of mMhJM and MAJM ( $p \leq .001$ ), mMhJM and MTCM ( $p \leq .001$ ) as well as MAJM and MTCM ( $p \leq .001$ ).

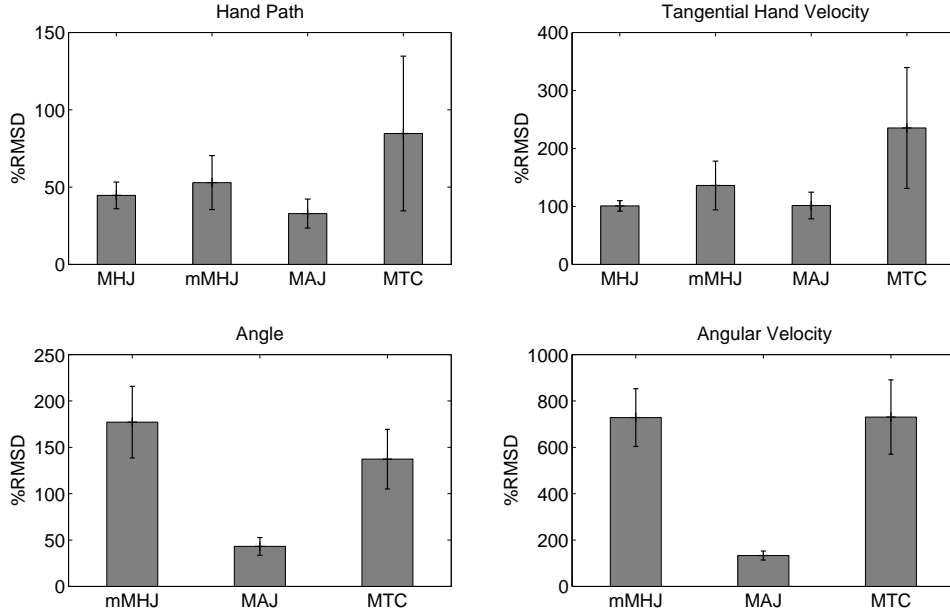


**Figure 5.15:** Mean of the %RMSDs between the measured and predicted hand paths, tangential hand velocities, angles and angular velocities for MHJM, mMHJM, MAJM and MTCM for the optimization of the shoulder abduction/adduction, shoulder rotation, shoulder anteversion/retroversion and elbow flexion/extension. Error bars indicate the 99 % confidence intervals.

#### 4 DOFs optimized

The results of the %RMSDs between the measured and predicted hand paths (Fig. 5.15, top left) indicate that none of the four optimal control models were able to reproduce the measured hand movements in extrinsic coordinates. MAJM produced the smallest %RMSD followed by MHJM, mMHJM and finally MTCM. The repeated ANOVA yielded no significant differences ( $F = 4.469, p = .031, \eta^2 = .103$ ) between the %RMSDs of the measured and predicted hand paths of the four optimal control models.

The results of the %RMSDs between the measured and predicted tangential velocities of the hand (Fig. 5.15, top right) show that MHJM produced the smallest %RMSD followed by MAJM, mMHJM and MTCM. The repeated ANOVA yielded significant differences ( $F = 8.406, p \leq .01, \eta^2 = .177$ ) between the %RMSDs of the measured and predicted tangential hand velocities of the four optimal control models. Pairwise Bonferroni tests revealed significant differences between the %RMSDs of the measured and predicted tangential hand velocities of MHJM and MTCM ( $p \leq .01$ ) as well as between MAJM and MTCM ( $p \leq .01$ ). The Bonferroni tests yielded no significant differences between MHJM and mMHJM ( $p = .269$ ), MHJM and MAJM

( $p = 1.000$ ), mMHJM and MAJM ( $p = .372$ ) and between mMHJM and MTCM ( $p = .177$ ).

The results of the %RMSDs between the measured and predicted elbow angles (Fig. 5.15, bottom left) indicate that none of the three optimal control models were able to reproduce the measured joint angle trajectories. MAJM produced the smallest %RMSD followed by mMHJM and MTCM. The repeated ANOVA yielded significant differences ( $F = 40.817, p \leq .001, \eta^2 = .511$ ) between the %RMSDs of the measured and predicted joint angles of the three optimal control models. Pairwise Bonferroni tests revealed significant differences between the %RMSD of the measured and predicted joint angles of mMHJM and MAJM ( $p \leq .001$ ) as well as MAJM and MTCM ( $p \leq .001$ ). The Bonferroni tests yielded no significant differences between mMHJM and MTCM ( $p = .127$ ).

The results of the %RMSDs between the measured and predicted angular velocities (Fig. 5.15, bottom right) indicate that none of the three optimal control models were able to reproduce the measured joint angle trajectories. MAJM produced the smallest %RMSD. MTCM and mMHJM produced comparable results. The repeated ANOVA yielded significant differences ( $F = 75.019, p \leq .001, \eta^2 = .658$ ) between the %RMSDs of the measured and predicted joint angular velocities of the three optimal control models. Pairwise Bonferroni tests revealed significant differences between the %RMSDs of the measured and predicted joint angular velocities of mMHJM and MAJM ( $p \leq .001$ ) as well as between MAJM and MTCM ( $p \leq .001$ ). The Bonferroni tests yielded no significant differences between mMHJM and MTCM ( $p = 1.000$ ).

### 5.3.2.2.2 Performance differences across the optimized DOFs

The performance differences across the optimized DOFs were calculated for MAJM and MTCM. In the case of mMhJM, the optimization was not conducted in intrinsic-kinematic coordinates but in extrinsic-kinematic coordinates of the hand. The limits of the individual joints were used as an additional boundary condition during the optimization.

#### MAJM

The results of the %RMSDs between the measured and the predicted hand paths across the four DOFs (Fig. 5.16) indicate that MAJM produced the smallest %RMSD when the DOF of shoulder rotation was optimized, followed by shoulder abduction/adduction, elbow flexion/extension and shoulder anteversion/retroversion. The repeated ANOVA yielded significant differences ( $F = 14.992, p \leq .001, \eta^2 = .278$ ) between the %RMSDs of the measured and predicted hand paths across the four DOFs. Pairwise Bonferroni tests revealed significant differences between the DOFs shoulder abduction/adduction and shoulder anteversion/retroversion ( $p \leq .001$ ), shoulder abduction/adduction and elbow flexion/extension ( $p \leq .01$ ), shoulder rotation and shoulder anteversion/retroversion ( $p \leq .001$ ) and shoulder rotation and elbow flexion/extension ( $p \leq .01$ ), respectively. The Bonferroni tests yielded no significant differences between the DOFs shoulder abduction/adduction and shoulder rotation ( $p = 1.000$ ) or shoulder anteversion/retroversion and elbow flexion/extension ( $p = .950$ ).

The results of the %RMSDs between the measured and predicted hand tangential velocities across the four DOFs (Fig. 5.16) indicate that MAJM produced the smallest %RMSD when the DOF of shoulder rotation was optimized, followed by shoulder abduction/adduction, elbow flexion/extension and shoulder anteversion/retroversion. The repeated ANOVA yielded significant differences ( $F = 22.248, p \leq .001, \eta^2 = .363$ ) between the %RMSDs of the measured and predicted hand tangential velocities across the four DOFs. Pairwise Bonferroni tests revealed significant differences between the DOFs shoulder abduction/adduction and shoulder anteversion/retroversion ( $p \leq .001$ ), shoulder abduction/adduction and elbow flexion/extension ( $p \leq .001$ ), shoulder rotation and shoulder anteversion/retroversion ( $p \leq .001$ ) and shoulder rotation and elbow flexion/extension ( $p \leq .001$ ). The Bonferroni tests yielded no significant differences between the DOFs shoulder abduction/adduction and shoulder rotation ( $p = 1.000$ ) or shoulder anteversion/retroversion and elbow flexion/extension ( $p = .019$ ).

The results of the %RMSDs between the measured and predicted joint angles for the four DOFs (Fig. 5.16) indicate that MAJM produced the smallest %RMSD when the DOF of shoulder abduction/adduction was optimized, followed by elbow flexion/extension, shoulder anteversion/retroversion and finally, shoulder rotation. The repeated ANOVA yielded significant differences ( $F = 10.444, p \leq .001, \eta^2 = .211$ ) between the %RMSDs of the measured and predicted joint angles for the

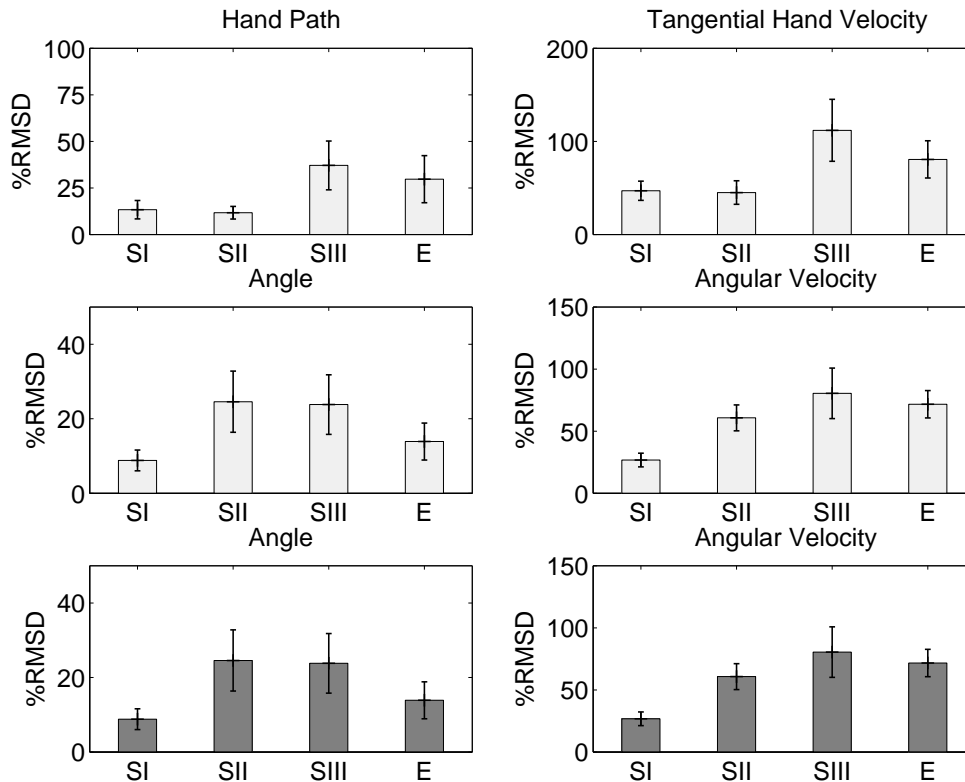


**Figure 5.16:** Mean of the %RMSDs of MAJM across the four DOFs under the optimization condition “1 DOF optimized” (light gray) and “4 DOFs optimized” (dark gray). Furthermore, the title SI indicates shoulder abduction/adduction, SII indicates shoulder rotation, SIII indicates shoulder anteversion/retroversion and E represents elbow flexion/extension. Error bars indicate the 99 % confidence intervals.

four DOFs. Pairwise Bonferroni tests revealed significant differences between the DOFs shoulder abduction/adduction and shoulder rotation ( $p \leq .001$ ) and shoulder abduction/adduction and shoulder anteversion/retroversion ( $p \leq .001$ ). The Bonferroni tests yielded no significant differences between the DOFs shoulder abduction/adduction and elbow flexion ( $p = .120$ ), shoulder rotation and shoulder anteversion/retroversion ( $p = 1.000$ ), shoulder rotation and elbow flexion ( $p = .032$ ) and shoulder anteversion/retroversion and elbow flexion/extension ( $p = .012$ ).

The results of the %RMSDs between the measured and predicted joint angular velocities for the four DOFs (Fig. 5.16) indicate that MAJM produced the smallest %RMSD when the DOF of shoulder abduction/adduction was optimized, followed by shoulder rotation, elbow flexion/extension and shoulder anteversion/retroversion. The repeated ANOVA yielded significant differences ( $F = 25.200, p \leq .001, \eta^2 =$

.393) between the %RMSDs of the measured and predicted joint angular velocities for the four DOFs. Pairwise Bonferroni tests revealed significant differences between the DOFs shoulder abduction/adduction and shoulder rotation ( $p \leq .001$ ), shoulder anteversion/retroversion ( $p \leq .001$ ) and elbow flexion/extension ( $p \leq .001$ ). The Bonferroni tests yielded no significant differences between the DOFs shoulder rotation and shoulder anteversion/retroversion ( $p = .239$ ), shoulder rotation and elbow flexion ( $p = .219$ ) and shoulder anteversion/retroversion and elbow flexion/extension ( $p = 1.000$ ).

When all four DOFs were optimized, the %RMSDs between the measured and predicted joint angles for the four DOFs (Fig. 5.16) indicate that MAJM produced the smallest %RMSD for the optimization of shoulder abduction/adduction, followed by the elbow flexion/extension, shoulder anteversion/retroversion and finally shoulder rotation. The repeated ANOVA yielded significant differences ( $F = 10.446, p \leq .001, \eta^2 = .211$ ) between the %RMSDs of the measured and predicted joint angles for the four DOFs. Pairwise Bonferroni tests revealed significant differences between the DOFs shoulder abduction/adduction and shoulder rotation ( $p \leq .001$ ) and shoulder abduction/adduction and shoulder anteversion/retroversion ( $p \leq .001$ ). The Bonferroni tests yielded no significant differences between the DOFs shoulder abduction/adduction and elbow flexion ( $p = .120$ ), shoulder rotation and shoulder anteversion/retroversion ( $p = 1.000$ ), shoulder rotation and elbow flexion ( $p = .032$ ) and shoulder anteversion/retroversion and elbow flexion/extension ( $p = .012$ ).

When all four DOFs were optimized the %RMSDs between the measured and predicted joint angular velocities for the four DOFs (Fig. 5.16) indicate that MAJM produced the smallest %RMSD for the optimization of shoulder abduction/adduction, followed by the shoulder rotation, elbow flexion/extension and finally shoulder anteversion/retroversion. The repeated ANOVA yielded significant differences ( $F = 25.200, p \leq .001, \eta^2 = .393$ ) between the %RMSDs of the measured and predicted joint angular velocities for the four DOFs. Pairwise Bonferroni tests revealed significant differences between the DOFs shoulder abduction/adduction and shoulder rotation ( $p \leq .001$ ), shoulder anteversion/retroversion ( $p \leq .001$ ) and elbow flexion/extension ( $p \leq .001$ ). The Bonferroni tests yielded no significant differences between the DOFs shoulder rotation and shoulder anteversion/retroversion ( $p = .239$ ), shoulder rotation and elbow flexion ( $p \leq .220$ ) and shoulder anteversion/retroversion and elbow flexion ( $p = 1.000$ ).

### MTCM

The results of the %RMSDs between the measured and predicted hand paths for the four DOFs (Fig. 5.17) indicate that MTCM produced the smallest %RMSD when the DOF of shoulder abduction/adduction was optimized, followed by shoulder rotation, shoulder anteversion/retroversion and elbow flexion/extension. The repeated ANOVA yielded significant differences ( $F = 18.840, p \leq .001, \eta^2 = .326$ ) between the %RMSDs of the measured and predicted hand paths for the four DOFs. Pairwise Bonferroni tests revealed significant differences between the DOFs shoulder abduction/adduction and shoulder anteversion/retroversion ( $p \leq .01$ ), shoulder abduction/adduction and elbow flexion/extension ( $p \leq .001$ ) and shoulder rotation and elbow flexion/extension ( $p \leq .001$ ). The Bonferroni tests yielded no significant differences between the DOFs shoulder abduction/adduction and shoulder rotation ( $p = 1.000$ ), shoulder rotation and shoulder anteversion/retroversion ( $p = .042$ ) and shoulder anteversion/retroversion and elbow flexion/extension ( $p = .254$ ).

The results of the %RMSDs between the measured and predicted hand tangential velocities across the four DOFs (Fig. 5.17) indicate that MTCM produced the smallest %RMSD when the DOF of shoulder abduction/adduction was optimized, followed by shoulder rotation, shoulder anteversion/retroversion and elbow flexion/extension. The repeated ANOVA yielded significant differences ( $F = 10.681, p \leq .001, \eta^2 = .215$ ) between the %RMSDs of the measured and predicted hand tangential velocities for the four DOFs. Pairwise Bonferroni tests revealed significant differences between the DOFs shoulder abduction/adduction and elbow flexion ( $p \leq .001$ ) and shoulder rotation and elbow flexion/extension ( $p \leq .001$ ). The Bonferroni tests yielded no significant differences between the DOFs shoulder abduction/adduction and shoulder rotation ( $p = .994$ ), shoulder abduction/adduction and shoulder anteversion/retroversion ( $p = .035$ ), shoulder rotation and shoulder anteversion/retroversion ( $p = .319$ ) and shoulder anteversion/retroversion and elbow flexion/extension ( $p = 1.000$ ), respectively.

The %RMSDs between the measured and predicted joint angles for the four DOFs (Fig. 5.17) indicate that MTCM produced the smallest %RMSD when the DOF of shoulder abduction/adduction was optimized, followed by shoulder anteversion/retroversion, shoulder rotation and elbow flexion/extension. The repeated ANOVA yielded significant differences ( $F = 7.995, p \leq .001, \eta^2 = .170$ ) between the %RMSD of the measured and predicted joint angles for the four DOFs. Pairwise Bonferroni tests revealed significant differences between the DOFs shoulder abduction/adduction and shoulder rotation ( $p \leq .001$ ), shoulder abduction/adduction and shoulder anteversion/retroversion ( $p \leq .01$ ) and shoulder abduction/adduction and elbow flexion ( $p \leq .001$ ). The Bonferroni tests yielded no significant differences between the DOFs shoulder rotation and shoulder anteversion/retroversion ( $p = 1.000$ ), shoulder rotation and elbow flexion/extension ( $p = 1.000$ ) and finally shoulder anteversion/retroversion and elbow flexion ( $p = 1.000$ ).

The results of the %RMSDs between the measured and predicted joint angular

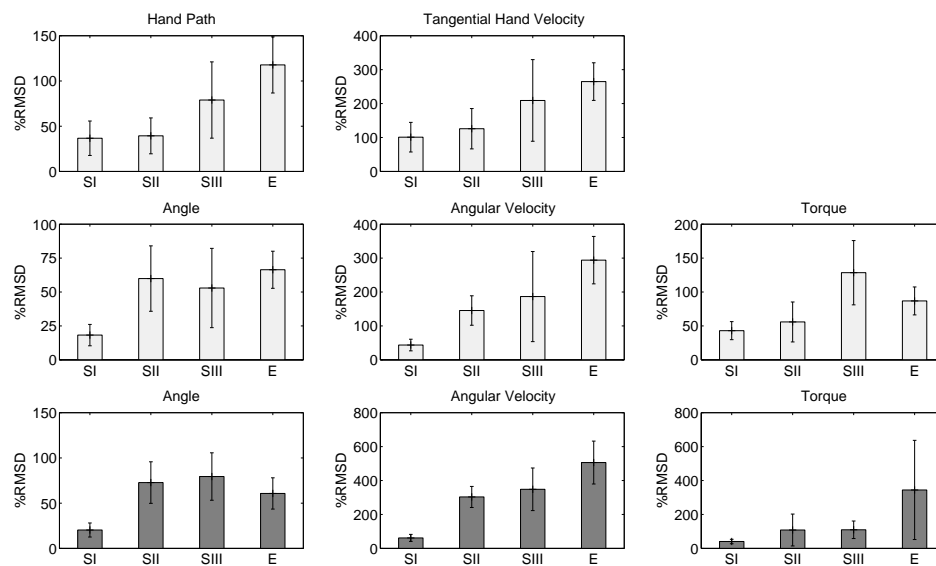


**Figure 5.17:** Mean of the %RMSDs of MTCM for the four DOFs under the optimization condition “1 DOF optimized” (light gray) and “4 DOFs optimized” (dark gray). Furthermore, the title SI indicates shoulder abduction/adduction, SII indicates shoulder rotation, SIII indicates shoulder anteversion/retroversion and E represents elbow flexion/extension. Error bars indicate the 99 % confidence intervals.

velocities for the four DOFs (Fig. 5.17) indicate that MTCM produced the smallest %RMSD when the DOF of shoulder abduction/adduction was optimized, followed by shoulder rotation, shoulder anteversion/retroversion and elbow flexion/extension. The repeated ANOVA yielded significant differences ( $F = 15.148, p \leq .001, \eta^2 = .280$ ) between the %RMSDs of the measured and predicted joint angular velocities for the four DOFs. Pairwise Bonferroni tests revealed significant differences between shoulder abduction/adduction and shoulder rotation ( $p \leq .001$ ), elbow flexion/extension ( $p \leq .001$ ) as well as the shoulder rotation and the elbow flexion/extension ( $p \leq .001$ ). The Bonferroni tests yielded no significant differences between shoulder abduction/adduction and shoulder anteversion/retroversion ( $p = .025$ ), shoulder rotation and shoulder anteversion/retroversion ( $p = 1.000$ ) and shoulder anteversion/retroversion and elbow flexion ( $p = .203$ ).

The results of the %RMSDs between the measured and predicted joint torques for the four DOFs (Fig. 5.17) indicate that MTCM produced the smallest %RMSD when the DOF of shoulder abduction/adduction was optimized, followed by shoulder rotation, elbow flexion/extension and shoulder anteversion/retroversion. The repeated ANOVA yielded significant differences ( $F = 12.847, p \leq .001, \eta^2 = .248$ ) between

the %RMSD of the measured and predicted joint torques across the four DOFs. Pairwise Bonferroni tests revealed significant differences between the DOFs shoulder abduction/adduction and shoulder anteversion/retroversion ( $p \leq .001$ ), shoulder abduction/adduction and elbow flexion/extension ( $p \leq .001$ ) and shoulder rotation and shoulder anteversion/retroversion ( $p \leq .001$ ). The Bonferroni tests yielded no significant differences between the DOFs shoulder abduction/adduction and shoulder rotation ( $p = 1.000$ ), shoulder rotation and elbow flexion/extension ( $p = .217$ ) and shoulder anteversion/retroversion and elbow flexion/extension ( $p = .290$ ).

When all four DOFs were optimized the %RMSDs between the measured and predicted joint angles for the four DOFs (Fig. 5.17) indicate that MTCM produced the smallest %RMSD for the optimization of shoulder abduction/adduction, followed by elbow flexion/extension, shoulder rotation and shoulder anteversion/retroversion. The repeated ANOVA yielded significant differences ( $F = 14.324, p \leq .001, \eta^2 = .269$ ) between the %RMSDs of the measured and predicted joint angles across the four DOFs. Pairwise Bonferroni tests revealed significant differences between the DOFs shoulder abduction/adduction and shoulder rotation ( $p \leq .001$ ), shoulder abduction/adduction and shoulder anteversion/retroversion ( $p \leq .001$ ) and shoulder abduction/adduction and elbow flexion ( $p \leq .001$ ). The Bonferroni tests yielded no significant differences between the DOFs shoulder rotation and shoulder anteversion/retroversion ( $p = 1.000$ ), shoulder rotation and elbow flexion ( $p = 1.000$ ) as well as shoulder anteversion/retroversion and elbow flexion ( $p = .261$ ).

When all four DOFs were optimized the %RMSDs between the measured and predicted joint angular velocities across the four DOFs (Fig. 5.17) indicate that the MTCM produced the smallest %RMSD for the optimization of shoulder abduction/adduction, followed by shoulder rotation, shoulder anteversion/retroversion and elbow flexion/extension. The repeated ANOVA yielded significant differences ( $F = 32.992, p \leq .001, \eta^2 = .458$ ) between the %RMSDs of the measured and predicted joint angular velocities across the four DOFs. Pairwise Bonferroni tests revealed significant differences between the DOFs shoulder abduction/adduction and shoulder rotation ( $p \leq .001$ ), shoulder abduction/adduction and shoulder anteversion/retroversion ( $p \leq .001$ ), shoulder abduction/adduction and elbow flexion/extension and shoulder rotation and elbow flexion/extension ( $p \leq .001$ ). The Bonferroni tests yielded no significant differences between the DOFs shoulder rotation and shoulder anteversion/retroversion ( $p = 1.000$ ) and shoulder anteversion/retroversion and elbow flexion ( $p \leq .064$ ).

When all four DOFs were optimized the %RMSDs between the measured and predicted joint torques for the four DOFs (Fig. 5.17) indicate that MTCM produced the smallest %RMSD for the optimization of shoulder abduction/adduction, followed by shoulder rotation, shoulder anteversion/retroversion and elbow flexion. The repeated ANOVA yielded no significant differences ( $F = 4.989, p = .023, \eta^2 = .113$ ) between the %RMSDs of the measured and predicted joint torques across the four DOFs. However, the 99 % confidence intervals in figure 5.17 indicate that there

might be significant differences between some DOFs. Therefore, we calculated the pairwise Bonferroni tests, which revealed significant differences between the DOFs shoulder abduction/adduction and shoulder anteversion/retroversion ( $p \leq .01$ ). The Bonferroni tests yielded no significant differences between the DOFs shoulder abduction/adduction and shoulder rotation ( $p \leq .451$ ), shoulder abduction/adduction and elbow flexion ( $p = .056$ ), shoulder rotation and shoulder anteversion/retroversion ( $p = 1.000$ ), shoulder rotation and elbow flexion/extension ( $p = .329$ ) and shoulder anteversion/retroversion and elbow flexion ( $p = .256$ ).

### 5.3.2.2.3 Performance differences between the two conditions “1 DOF optimized” and “4 DOFs optimized”

In this section, the performance of MHJM, mMHJM, MAJM and MTCM between the two conditions “1 DOF optimized” vs. “4 DOFs optimized” for the four DOFs is analyzed separately. The analysis was carried out according to the simulation protocol (Tab. 5.1).

#### 1 DOF optimized versus 4 DOFs optimized: Shoulder abduction/adduction

The results of the %RMSDs between the two optimization conditions (Fig. 5.18, top left) indicate that when the DOFs to be optimized were increased the %RMSDs for the hand paths increased for all three models. In other words, the deviations between the measured movements and the movements generated by different optimal control models increased when fewer joints were driven by experimental data. However, paired two-sample t-tests revealed significant differences for mMHJM ( $T = -4.575, p \leq .001$ ), MAJM ( $T = -6.365, p \leq .001$ ) and MTCM ( $T = -3.559, p \leq .001$ ).

The results of the %RMSDs between the two optimization conditions (Fig. 5.18, top right) indicate that when the DOFs to be optimized were increased the %RMSDs for the tangential hand velocities increased for all three models. Paired two-sample t-tests revealed significant differences for mMHJM ( $T = -4.172, p \leq .001$ ), MAJM ( $T = -7.177, p \leq .001$ ) and MTCM ( $T = -4.865, p \leq .001$ ).

The results of the %RMSDs between the two optimization conditions indicate that when the DOFs to be optimized were increased the %RMSDs for the joint angles increased for mMHJM and MTCM and remained the same for MAJM (Fig. 5.18, bottom left). Paired two-sample t-tests revealed no significant differences for mMHJM ( $T = -2.002, p = .052$ ), MAJM ( $T = .523, p = .604$ ) and MTCM ( $T = -.624, p = .536$ ).

The results of the %RMSDs between the two optimization conditions indicate that when the DOFs to be optimized were increased the %RMSDs for the joint angular velocities increased for mMHJM and MTCM and remained the same for the MAJM (Fig. 5.18, bottom right). Paired two-sample t-tests revealed significant differences for mMHJM ( $T = -6.785, p \leq .001$ ) and MTCM ( $T = -2.754, p \leq .01$ ). The paired two-sample t-tests revealed no significant differences for MAJM ( $T = .919, p = .364$ ).

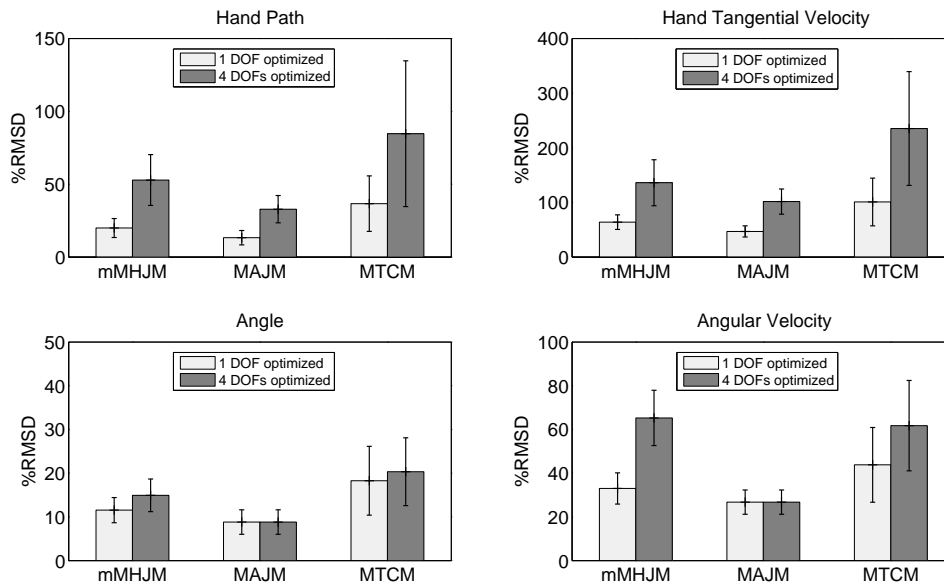


**Figure 5.18:** Mean of the %RMSDs for shoulder abduction/adduction under two different optimization conditions (“1 DOF optimized” and “4 DOFs optimized”). Error bars indicate the 99 % confidence intervals.

### 1 DOF optimized versus 4 DOFs optimized: Shoulder rotation

The results of the %RMSDs between the two optimization conditions (Fig. 5.19, top left) indicate that when the DOFs to be optimized were increased the %RMSDs for the hand paths increased for all three models. Paired two-sample t-tests revealed significant differences for mMHJM ( $T = -4.549, p \leq .001$ ), MAJM ( $T = -5.622, p \leq .001$ ) and MTCM ( $T = -2.820, p \leq .01$ ).

The results of the %RMSDs between the two optimization conditions (Fig. 5.19, top right) indicate that when the DOFs to be optimized were increased the %RMSDs for the tangential hand velocities increased for all three models. Paired two-sample t-tests revealed significant differences for mMHJM ( $T = -2.813, p \leq .01$ ), MAJM ( $T = -6.527, p \leq .001$ ) and MTCM ( $T = -3.312, p \leq .01$ ).

The results of the %RMSDs between the two optimization conditions (Fig. 5.19, bottom left) indicate when the DOFs to be optimized were increased the %RMSDs for the joint angles decreased for mMHJM, remained the same for MAJM and increased for MTCM. Paired two-sample t-tests revealed no significant differences for mMHJM ( $T = .069, p = .946$ ), MAJM ( $T = .131, p = .896$ ) and MTCM ( $T = -1.047, p = .302$ ).

The results of the %RMSDs between the two optimization conditions (Fig. 5.19, bottom right) exhibit that when the DOFs to be optimized were increased the %RMSDs for the joint angular velocities increased for mMHJM and MTCM and

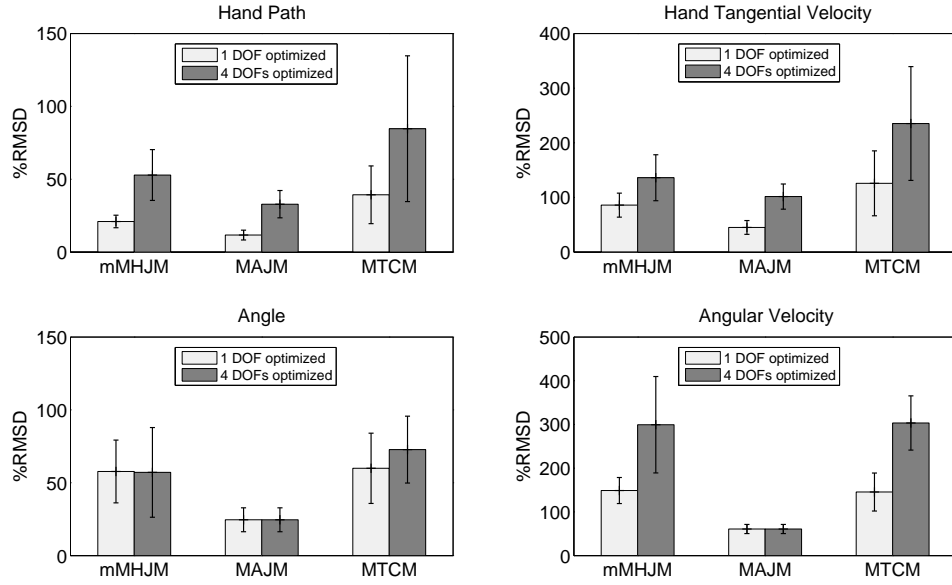


**Figure 5.19:** Mean of the %RMSDs for shoulder rotation under two different optimization conditions. Error bars indicate the 99 % confidence intervals.

remained the same for MAJM. Paired two-sample t-tests revealed significant differences for mMHJM ( $T = -3.841, p \leq .001$ ) and MTCM ( $T = -5.845, p \leq .001$ ). The paired two-sample t-tests revealed no significant differences for MAJM ( $T = -.026, p = .980$ ).

### 1 DOF optimized vs. 4 DOFs optimized: Shoulder anteversion/retroversion

The results of the %RMSDs between the two optimization conditions (Fig. 5.20, top left) exhibit that when the DOFs to be optimized were increased the %RMSDs for the hand paths for mMHJM and MAJM decreased. In contrast the %RMSDs of the hand paths of MTCM increased. Paired two-sample t-tests revealed significant differences for mMHJM ( $T = 3.635, p \leq .001$ ) and no the significant differences for MAJM ( $T = 1.337, p = .189$ ) and MTCM ( $T = -.437, p = .665$ ).

The results of the %RMSDs between the two optimization conditions (Fig. 5.20, top right) exhibit that when the DOFs to be optimized were increased the %RMSDs for the tangential hand velocities of mMHJM and MAJM decreased. In contrast the %RMSD of the tangential velocities of MTCM increased. Paired two-sample t-tests revealed no significant differences for mMHJM ( $T = 2.531, p = .016$ ), MAJM ( $T = 1.205, p = .235$ ) and MTCM ( $T = -.646, p = .522$ ).

The results of the %RMSDs between the two optimization conditions (Fig. 5.20, bottom left) exhibit that when the DOFs to be optimized were increased the %RMSDs for the joint angles increased for mMHJM and MTCM and remained the same for

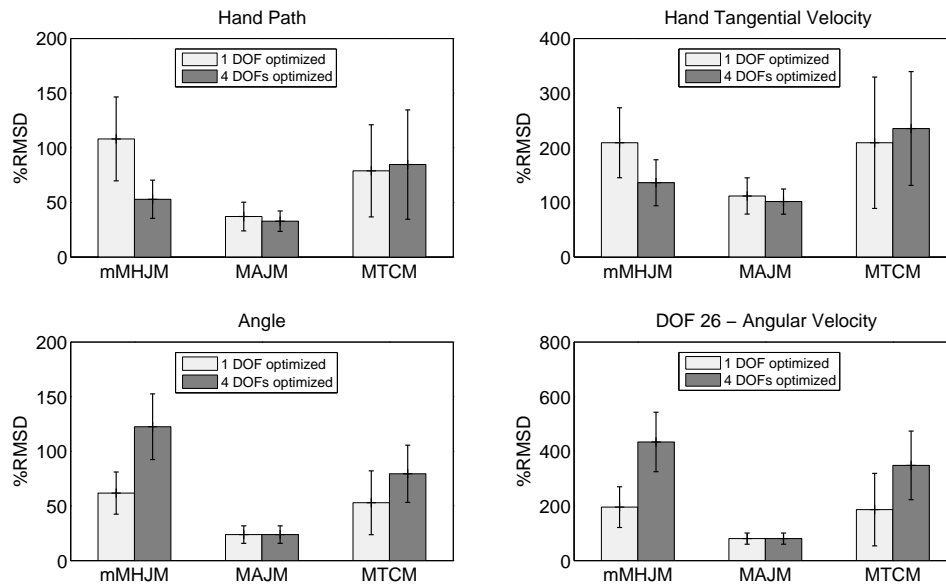


**Figure 5.20:** Mean of the %RMSDs for shoulder anteversion/retroversion under two different optimization conditions. Error bars indicate the 99 % confidence intervals.

MAJM. Paired two-sample t-tests revealed significant differences for mMHJM ( $T = -4.727, p \leq .001$ ) and no significant differences for MTCM ( $T = -2.306, p \leq .027$ ) and MAJM ( $T = .772, p = .445$ ).

The results of the %RMSDs between the two optimization conditions (Fig. 5.20, bottom right) exhibit that when the DOFs to be optimized were increased the %RMSDs for the joint angular velocities increased for mMHJM and MTCM and remained the same for MAJM. Paired two-sample t-tests revealed significant differences for mMHJM ( $T = -6.981, p \leq .001$ ) and MTCM ( $T = -3.572, p \leq .001$ ). The paired two-sample t-tests revealed no significant differences for MAJM ( $T = -.150, p = .881$ ).

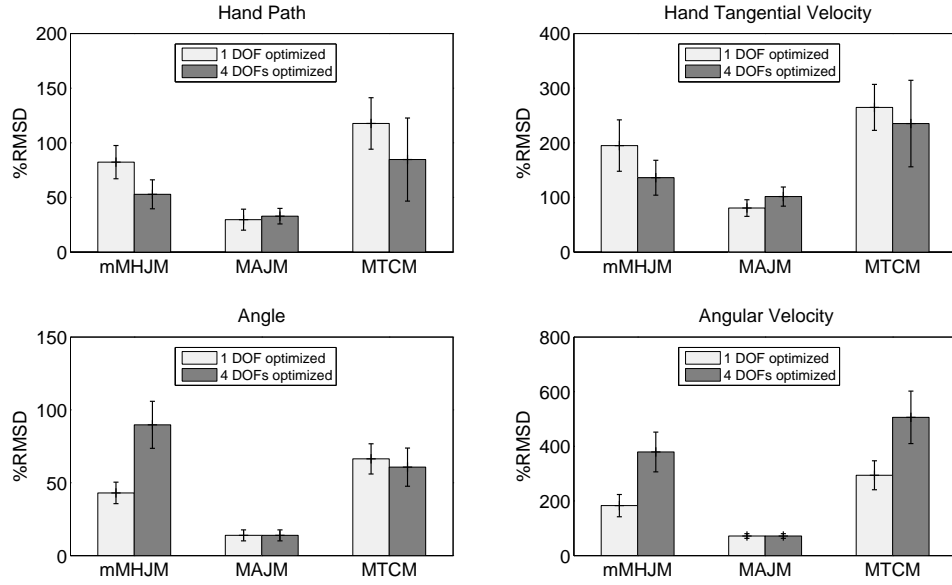


**Figure 5.21:** Mean of the %RMSDs for elbow flexion/extension under two different optimization conditions. Error bars indicate the 99 % confidence intervals.

### 1 DOF optimized vs. 4 DOFs optimized: Elbow flexion/extension

The results of the %RMSDs between the two optimization conditions (Fig. 5.21, top left) exhibit that when the DOFs to be optimized were increased the %RMSDs for the hand paths for mMHJM and MTCM decreased. In contrast the %RMSDs of the hand paths for the MAJM increased. Paired two-sample t-tests revealed significant differences for mMHJM ( $T = 2.756, p \leq .01$ ) and no significant differences for MAJM ( $T = -.696, p = .491$ ) and MTCM ( $T = 1.642, p = .109$ ).

The results of the %RMSDs between the two optimization conditions (Fig. 5.21, top right) exhibit that when the DOFs to be optimized were increased the %RMSDs for the tangential hand velocities for mMHJM and MTCM decreased. In contrast the %RMSDs of the tangential hand velocities for MAJM increased. Paired two-sample t-tests revealed no significant differences for mMHJM ( $T = 1.999, p = .053$ ), MAJM ( $T = -2.555, p = .015$ ) and MTCM ( $T = .781, p = .440$ ).

The results of the %RMSDs between the two optimization conditions (Fig. 5.21, bottom left) exhibit that when the DOFs to be optimized were increased the %RMSDs for the joint angles increased for mMHJM, decreased for MTCM and remained the same for MAJM. Paired two-sample t-tests revealed significant differences for mMHJM ( $T = -5.428, p \leq .001$ ) and no significant differences for MAJM ( $T = -1.036, p = .307$ ) and MTCM ( $T = .668, p = .508$ ).

The %RMSDs between the two conditions (Fig. 5.21, bottom right) exhibit that when the DOFs to be optimized were increased the %RMSDs for the joint angular ve-

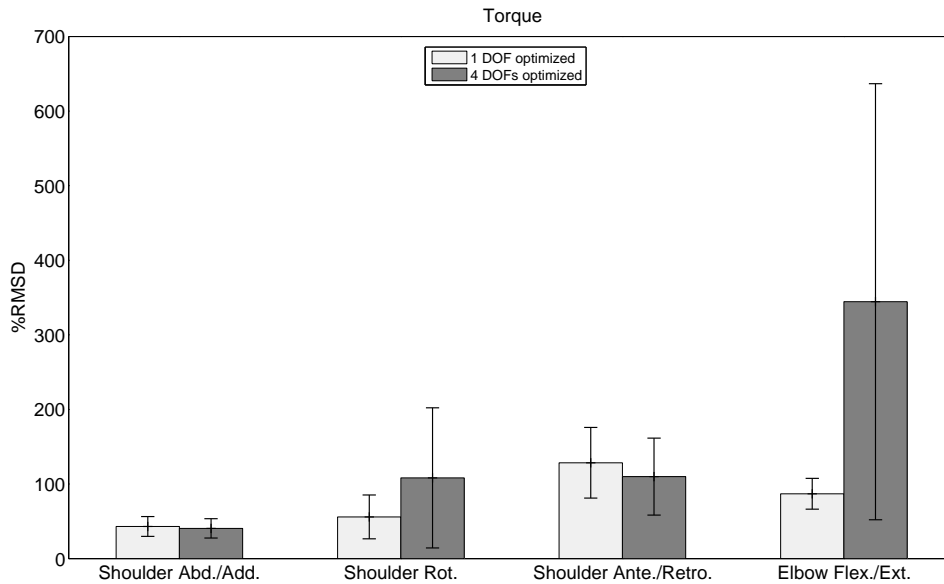


**Figure 5.22:** Mean of the %RMSDs of torques for MTCM across the four DOFs under different optimization conditions. Error bars indicate the 99 % confidence intervals.

locities increased for mMHJM and MTCM and remained the same for MAJM. Paired two-sample t-tests revealed significant differences for mMHJM ( $T = -5.871, p \leq .001$ ) and MTCM ( $T = -5.805, p \leq .001$ ). The paired two-sample t-tests revealed no significant differences for MAJM ( $T = 1.044, p = .303$ ).

#### 1 DOF optimized vs. 4 DOFs optimized: Torques

The results of the %RMSDs between the two optimization conditions (Fig. 5.22) exhibit that when the DOFs to be optimized were increased the %RMSDs of the torques of MTCM were decreased for the shoulder abduction/adduction as well as the shoulder anteversion/retroversion and increased for the shoulder rotation and the elbow flexion/extension. Paired two-sample t-tests revealed no significant differences for the shoulder abduction/adduction ( $T = -.651, p = .519$ ), the shoulder rotation ( $T = -1.356, p = .183$ ), the shoulder anteversion/retroversion ( $T = .995, p = .326$ ) and the elbow flexion/extension ( $T = -2.322, p = .026$ ).

### 5.3.2.3 Similarities between the measured and predicted trajectories

In this section, the similarities between the measured and predicted trajectories are analyzed based on the approach described in section 5.2.8. First, the similarity coefficient  $sim$  (Eq. 5.16) for each optimized DOF was analyzed separately (Chap. 5.3.2.3.1). The optimization condition “1 DOF optimized” and “4 DOFs optimized” are shown in one table. The second step involved the analysis of the similarity coefficients  $SIM$  (Eq. 5.17) for the optimization condition “4 DOFs optimized” (Chap. 5.3.2.3.2).

#### 5.3.2.3.1 Similarities between the measured and predicted trajectories of single DOFs

In this section, the similarities between the measured and predicted trajectories of MHJM, mMHJM, MAJM and MTCM under the two conditions “1 DOF optimized” vs. “4 DOFs optimized” are discussed for each of the four DOFs. The analysis was carried out according to the simulation protocol (Tab. 5.1).

##### Shoulder abduction/adduction

The results (Tab. 5.3) for the hand paths ( $R$ ) revealed only small differences in similarity coefficients between the different optimal control models for both optimization conditions. Moreover, the similarity coefficients of the four optimal control models for the tangential hand velocities ( $Rp$ ) were smaller than the similarity coefficients for the hand paths. MTCM showed the smallest values for the tangential hand velocities under both optimization conditions. MHJM and MAJM performed similarly. Collectively, the simulations reveal that in extrinsic kinematic coordinates of the hand ( $R$  and  $Rp$ ) only small differences in the similarity coefficients between the two optimization conditions “1 DOF optimized” and “4 DOFs optimized” exist. In the case of joint angles ( $q$ ), only small differences within and between the two optimization conditions were observed in the performances of the three optimal control models. Moreover, MAJM shows the highest similarity coefficients between the measured and predicted joint angular velocity profiles ( $qp$ ), followed by mMHJM and MTCM. The similarity coefficients of mMHJM and MTCM were much smaller under the condition “4 DOFs optimized” than under the condition “1 DOF optimized”. In addition, the coefficients for the joint angular velocities are substantially smaller than the coefficients for the joint angles. Finally, the similarity coefficients for the joint torques ( $T$ ) are comparable between the two optimization conditions but much smaller than the coefficients of the extrinsic and intrinsic kinematic coordinates.

**Table 5.3:** Mean of the similarity coefficients between the measured and predicted trajectories ( $N = 40$ ) of MHJM, mMHJM, MAJM and MTCM for shoulder abduction/adduction under two optimization conditions.  $R$  corresponds to the hand paths in 3D space,  $Rp$  to the tangential velocities of the hand,  $q$  to joint angles,  $qp$  to joint angular velocities and  $T$  to joint torques.

	“1 DOF optimized”				“4 DOFs optimized”			
	MHJM	mMHJM	MAJM	MTCM	MHJM	mMHJM	MAJM	MTCM
$R$	.9963	.9961	.9975	.9936	.9963	.9930	.9977	.9944
$Rp$	.9632	.9424	.9697	.9201	.9632	.9332	.9685	.9165
$q$	-	.9920	.9959	.9886	-	.9887	.9959	.9823
$qp$	-	.8642	.9170	.8380	-	.7943	.9170	.6750
$T$	-	-	-	.5456	-	-	-	.5635

### Shoulder rotation

The results (Tab. 5.4) for the hand paths ( $R$ ) exhibited only small differences in the similarity coefficients between the different optimal control models within each optimization condition. Furthermore, under the condition “4 DOFs optimized” the similarity coefficients of the hand paths were smaller than under the condition “1 DOF optimized”. The similarity coefficients of the four optimal control models for the tangential hand velocities ( $Rp$ ) were smaller than the similarity coefficients for the hand paths. Moreover, the coefficients were smaller under the condition “4 DOFs optimized” than under the condition “1 DOF optimized”. All in all, MAJM produced the highest coefficients in extrinsic kinematic coordinates. On joint level, again, MAJM produced the closest fit to the measured data ( $q$  and  $qp$ ). The mMHJM and MTCM exhibited much smaller values than MAJM in the intrinsic kinematic coordinates. Furthermore, the similarity coefficients of the intrinsic kinematic coordinates were substantial smaller for shoulder rotation (Tab. 5.4) as for shoulder abduction/adduction (Tab. 5.3). Finally, the similarity coefficients of the joint torques ( $T$ ) were under the condition “4 DOFs optimized” substantial smaller than under the condition “1 DOF optimized”. Moreover, these coefficients were smaller than the coefficients of the quantities defined in extrinsic and intrinsic kinematic coordinates.

**Table 5.4:** Mean of the similarity coefficients between the measured and predicted trajectories ( $N = 40$ ) of MHJM, mMHJM, MAJM and MTCM for shoulder rotation under two optimization conditions.  $R$  corresponds to the hand paths in 3D space,  $Rp$  to the tangential velocities of the hand,  $q$  to joint angles,  $qp$  to joint angular velocities and  $T$  to joint torques.

	“1 DOF optimized”				“4 DOFs optimized”			
	MHJM	mMHJM	MAJM	MTCM	MHJM	mMHJM	MAJM	MTCM
$R$	.9963	.9984	.9996	.9988	.9963	.9930	.9977	.9944
$Rp$	.9632	.9760	.9943	.9808	.9632	.9332	.9685	.9165
$q$	-	.6643	.9548	.8044	-	.7904	.9548	.6705
$qp$	-	-.0007	.7612	.3646	-	.2218	.7612	.2994
$T$	-	-	-	.6071	-	-	-	.3635

### Shoulder anteversion/retroversion

The results (Tab. 5.5) for the hand paths ( $R$ ) exhibited only small differences in the similarity coefficients between the different optimal control models and between the two optimization conditions. The similarity coefficients of the hand tangential velocities ( $Rp$ ) were under the optimization condition “4 DOFs optimized” smaller than under the optimization condition “1 DOF optimized”. Furthermore, the differences between the similarity coefficients of the optimal control models for the tangential hand velocities and the hand paths were under the condition “4 DOFs optimized” larger than under the condition “1 DOF optimized”. On joint level ( $q$ ), MTCM produced the highest similarity coefficient under the condition “1 DOF optimized” followed by MAJM and mMHJM. In contrast, if 4 DOFs were optimized MAJM showed the closest fit to the measured joint angles. Under the optimization condition “1 DOF optimized” MTCM revealed the highest similarity to the measured joint angular velocity profiles ( $qp$ ) followed by mMHJM and MAJM. In contrast, MAJM showed the closest fit to the measured joint angular velocity profiles under the optimization condition “4 DOFs optimized”. The similarity coefficients of the joint torques ( $T$ ) were comparable between the two optimization conditions. Moreover, these coefficients were in same range as the coefficients for the quantities defined in intrinsic kinematic coordinates but much smaller than the coefficients of the quantities defined in extrinsic kinematic coordinates.

**Table 5.5:** Mean of the similarity coefficients between the measured and predicted trajectories ( $N = 40$ ) of MHJM, mMHJM, MAJM and MTCM for shoulder anteversion/retroversion under two optimization conditions.  $R$  corresponds to the hand paths in 3D space,  $Rp$  to the tangential velocities of the hand,  $q$  to joint angles,  $qp$  to joint angular velocities and  $T$  to joint torques.

	“1 DOF optimized”				“4 DOFs optimized”			
	MHJM	mMHJM	MAJM	MTCM	MHJM	mMHJM	MAJM	MTCM
$R$	.9963	.9999	1.0000	1.0000	.9963	.9930	.9977	.9944
$Rp$	.9632	.9981	.9998	.9993	.9632	.9332	.9685	.9165
$q$	-	.8687	.9133	.9224	-	.5326	.9133	.7151
$qp$	-	.7781	.6020	.8563	-	.1369	.6020	.4692
$T$	-	-	-	.6225	-	-	-	.6550

### Elbow flexion/extension

The results (Tab. 5.6) for the hand paths ( $R$ ) exhibited only small differences in the similarity coefficients between the different optimal control models within each optimization condition and between the two optimization conditions. The similarity coefficients of the hand tangential velocities ( $Rp$ ) were under the optimization condition “4 DOFs optimized” smaller than under the optimization condition “1 DOF optimized”. Furthermore, the differences between the similarity coefficients of the optimal control models for the tangential hand velocities and the hand paths were under the condition “4 DOFs optimized” larger than under the condition “1 DOF optimized”. Collectively, MAJM produced the highest coefficients in extrinsic kinematic coordinates. On joint level ( $q$  and  $qp$ ), MAJM produced the highest similarity coefficients in intrinsic kinematic coordinates. The similarity coefficients for the joint torques ( $T$ ) were comparable between the two optimization conditions. Moreover, these coefficients were smaller than the coefficients of the quantities defined in kinematic coordinates as well as the coefficients of the joint torques of the shoulder joint (Tab. 5.3, 5.4, 5.5).

**Table 5.6:** Mean of the similarity coefficients between the measured and predicted trajectories ( $N = 40$ ) of MHJM, mMHJM, MAJM and MTCM for elbow flexion/extension under two optimization conditions.  $R$  corresponds to the hand paths in 3D space,  $Rp$  to the tangential velocities of the hand,  $q$  to joint angles,  $qp$  to joint angular velocities and  $T$  to joint torques.

	"1 DOF optimized"				"4 DOFs optimized"			
	MHJM	mMHJM	MAJM	MTCM	MHJM	mMHJM	MAJM	MTCM
$R$	.9963	.9995	1.0000	.9977	.9963	.9930	.9977	.9944
$Rp$	.9632	.9922	.9990	.9785	.9632	.9332	.9685	.9165
$q$	-	.6322	.9063	.6940	-	.7620	.9063	.3408
$qp$	-	.3938	.7071	.5741	-	.6737	.7071	.2650
$T$	-	-	-	.2242	-	-	-	.1752

### 5.3.2.3.2 Similarities between the measured and predicted trajectories of multiple DOFs

The results (Tab. 5.7) of the similarity coefficients between measured and predicted trajectories of multiple DOFs revealed that on joint level ( $q$  and  $qp$ ) the MAJM showed the closest fit to the human data. The similarity coefficients of the joint torques ( $T$ ) were comparable to the one's presented in chapter 5.3.2.3.1.

**Table 5.7:** Mean of similarities coefficients between multiple (4 DOFs) measured and predicted joint angles, joint angular velocities and joint torques ( $N = 40$ ) of mMHJM, MAJM and MTCM. Thereby,  $q$  corresponds to joint angles,  $qp$  to joint angular velocities and  $T$  to joint torques.

	mMHJM	MAJM	MTCM
$q$	.7109	.9112	.6411
$qp$	.4393	.6935	.3769
$T$	-	-	.3999

### 5.3.3 Target 3: Comparison of the measured and predicted trajectories

The performance results of the different optimal control models are presented as outlined in chapter 5.2.8.

#### 5.3.3.1 Qualitative analysis of the measured and predicted trajectories

The results of the qualitative analysis of measured and predicted trajectories are presented according to the simulation protocol shown in table 5.1.

##### 1 DOF optimized: Shoulder abduction/adduction

In figure 5.23 representative hand paths are illustrated. However, none of the four optimal control models were able to exactly reproduce the measured hand movements. In contrast to the other optimization models, MHJM produced straight hand paths. The hand paths generated by mMHJM, MAJM and MTCM were curved across all trials. Furthermore, none of the four models were able to completely reproduce the measured tangential velocity profiles of the subjects. Notwithstanding the models were able to approximate the single-peaked, almost bell-shaped measured velocity profiles. Some of the generated velocity profiles, however, were slightly distorted like the MAJ-profile in figure 5.23. In contrast, the MHJM generated single peaked and bell-shaped velocity profiles across all trials. The peak velocities of the MHJM and the mMHJM were in all cases smaller than the ones produced by the subjects. On joint level all of the three models could reproduce the shoulder movements of the subjects with only small deviations (Fig. 5.23). Across all the trials MAJM showed the closest fit. None of the three models were able to completely reproduce the measured joint angular velocities. The velocity profiles of MAJM were in all of the trials smooth, single peaked and almost bell shaped. The shape of the joint angular velocities profiles produced by mMHJM and MTCM were much more variable. Moreover, MTCM was only occasionally able to replicate the measured torque profiles. In most cases the model produced a more or less large torque at the beginning of the movement, which was constantly reduced towards the end of the movement. The peak torque produced by MTCM, however, was only in a few cases larger than the peak torques produced by the subjects. Moreover, all of the torque profiles were slightly oscillating (Fig. 5.23).

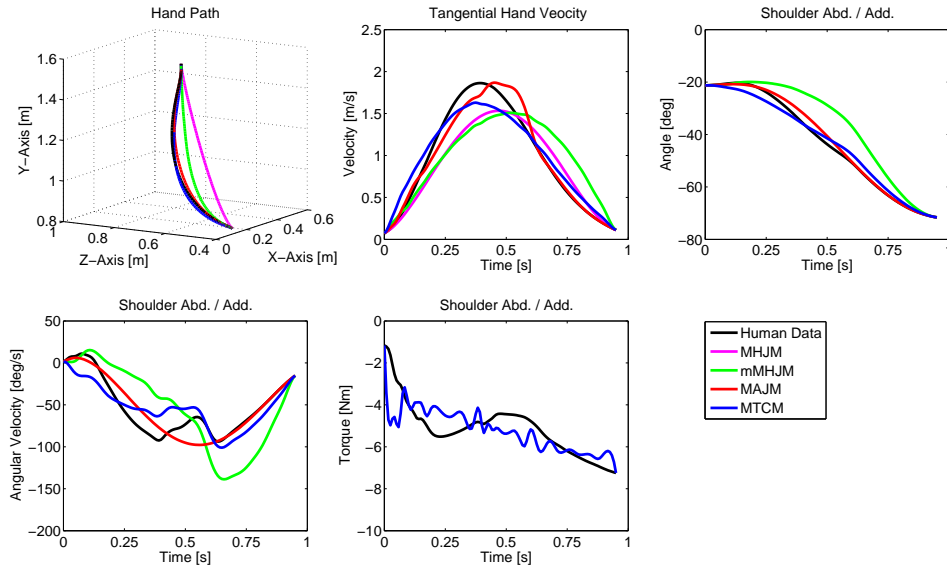


**Figure 5.23:** Representative trial for the optimization of shoulder abduction/adduction.

### 1 DOF optimized: Shoulder rotation

In figure 5.24 representative hand paths are illustrated. As before, none of the four optimal control models were able to exactly reproduce the human movement. Again, MHJM generated straight hand paths. All other models generated curved paths. In most of the cases all models were able to emulate the single peaked and almost bell-shaped human tangential velocity profiles. However, in a few cases the velocity profiles revealed a small plateau as shown by MAJM. Moreover, in some cases the models tended to show slightly oscillating velocity profiles as adumbrated by MTCM (Fig. 5.24). On the joint level, MAJM showed a close fit to the shoulder rotations of the subjects (Fig. 5.24), whereas the joint angular trajectories of mMHJM and MTCM were much more variable with larger deviations across the trials. Furthermore, in figure 5.24 representative angular velocities are illustrated. Again, none of the three models were able to completely reproduce the human angular velocity profiles. MAJM exhibited single peaked and bell-shaped velocity profiles. These profiles were stereotypically reproduced across the trials by MAJM. MTCM reproduced the measured movement in torque space only incompletely. The peak torques produced by MTCM were mostly smaller than the peak torques produced by the subjects. As before, all of the torque profiles were slightly oscillating (Fig. 5.24).

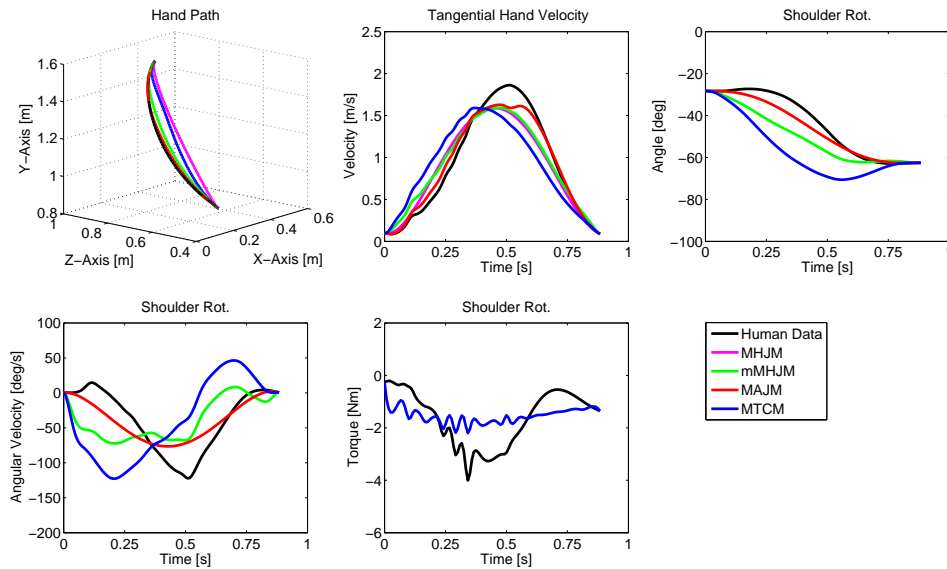


**Figure 5.24:** Representative trial for the optimization of shoulder rotation.

### 1 DOF optimized: Shoulder anteversion/retroversion

Figure 5.25 shows representative hand paths. MHJM produced across all trials straight hand paths. In contrast, mMHJM, MAJM and MTCM generated curved hand paths across all trials. None of the models were able to exactly reproduce the experimentally determined measured hand paths. The subjects tended to produce single peaked tangential velocities. However, the profiles were not exactly bell-shaped. In most cases all models were able to reconstruct the basic shape of the velocity profiles, although in some cases especially MTCM produced deviations from the measured profiles. On joint level mMHJM and MTCM showed partly large deviations across the trials. In contrast, MAJM generated rather straight angular trajectories that showed a close fit to the measured data in most cases (Fig. 5.25). Neither mMHJM nor MAJM or MTCM were able to reproduce the measured angular velocities. Again, the profiles of MAJM were highly stereotypical compared to the trajectories of mMHJM and MTCM. In comparison with the two last-named models MAJM showed peak angular velocities that were close to those produced by the subjects across all trials. The MTCM reproduced the measured torque profiles only incompletely. The torque profiles were characterized by a minimal change in the torque course during the movement. In other words, there occurred no large torque spikes, although all of the torque profiles were slightly oscillating (Fig. 5.25).

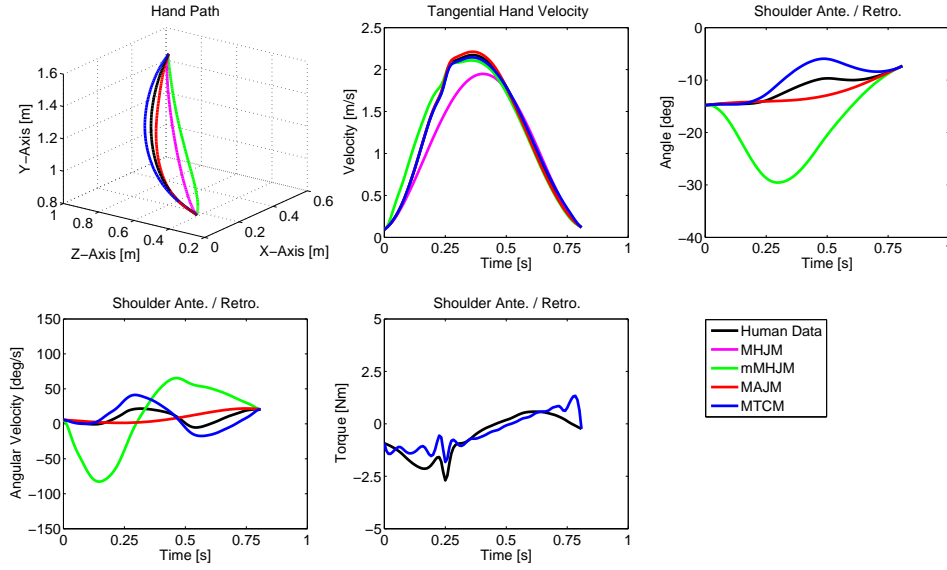


**Figure 5.25:** Representative trial for the optimization of shoulder anteversion/retroversion.

### 1 DOF optimized: Elbow flexion/extension

In figure 5.26 representative hand paths are displayed. MHJM produced straight hand path across all trials. In contrast, MAJM and MTCM generated curved hand paths across all trials. mMHJM generated in some cases nearly straight hand paths and some cases curved ones. None of the models were able to completely reproduce the experimentally determined hand paths. The subjects tended to produce single peaked tangential velocity profiles. These profiles could be approximated by all four optimal control models (Fig. 5.26). MHJM generated highly stereotypical single peaked, bell-shaped tangential velocity profiles across all trials. The other three models showed in some cases larger deviations. The peak velocities of MHJM were in all cases smaller than the ones produced by the subjects. On joint level mMHJM and MTCM showed larger deviations across the trials than the MAJM. Thereby, MTCM produced in all cases a flexion/extension movement in the elbow joint with larger movement amplitudes than the subjects. mMHJM tended to produce in most cases an extension/flexion movement. MAJM generated flexion/extension movements with small movement amplitudes (Fig. 5.26). Although different movement strategies were used by the subjects (Chap. 4.3.1), MAJM showed across all trials the closest fit to the measured elbow movements. Furthermore, none of the three models were able to reproduce the angular velocity profiles of the subjects. Again, the profiles of MAJM were highly stereotypical compared to the trajectories of mMHJM and MTCM. In comparison with the two last-named models, MAJM showed across all

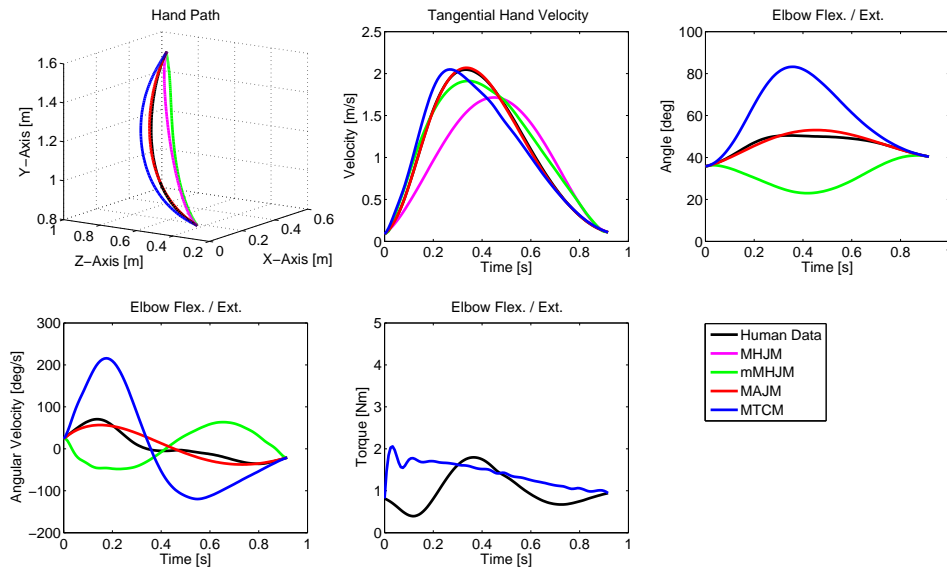


**Figure 5.26:** Representative trial for the optimization of elbow flexion/extension.

trials peak angular velocities that were close to those produced by the subjects. MTCM reproduced the measured torque profiles only incompletely. In most cases the model produced a more or less large torque at the beginning of the movement, which was constantly reduced during the movement with only small changes. The peak torques produced by MTCM, however, were in most cases comparable to the peak torques produced by the subjects. Furthermore, all of the torque profiles were slightly oscillating (Fig. 5.26).

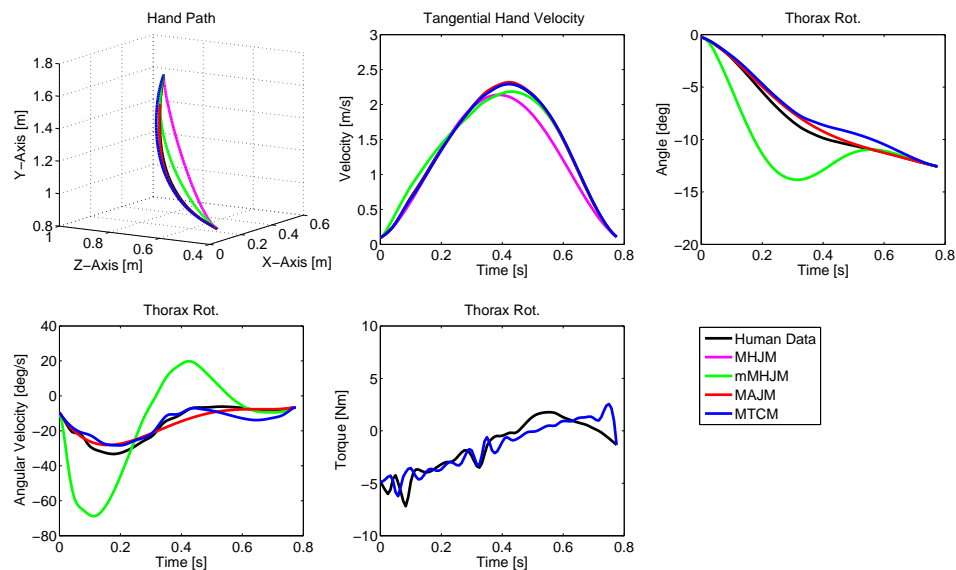


**Figure 5.27:** Representative trial for the optimization of thorax rotation.

### 1 DOF optimized: Thorax rotation

In figure 5.27 representative hand paths are displayed. MHJM produced straight hand path across all trials. In contrast, mMhJM, MAJM and MTCM generated curved hand paths across all trials. None of the models were able to reproduce the experimentally determined hand paths. The subjects tended to produce single peaked tangential velocity profiles. These profiles could be approximated by all four optimal control models (Fig. 5.27). MHJM generated highly stereotypical single peaked, bell-shaped tangential velocity profiles across all trials. The peak velocities of MHJM were in all cases smaller than the ones produced by the subjects. The other three models showed in a few cases some distortions leading to larger deviations from the measured velocity profiles. On joint level mMhJM showed the largest deviations. Both, MTCM and MAJM showed a close fit to experimentally determined data and tended to produce comparable results. mMhJM exhibited large deviations from the measured angular velocity profiles of the subjects. Both, MAJM and MTCM showed a good data fit. Furthermore, the two last named models showed peak angular velocities that were close to those produced by the subjects across most trials. MTCM reproduced the measured torque profiles only incompletely. The peak torque produced by MTCM, however, were in most cases comparable to the peak torques produced by the subjects. Furthermore, all of the torque profiles were slightly oscillating (Fig. 5.27).

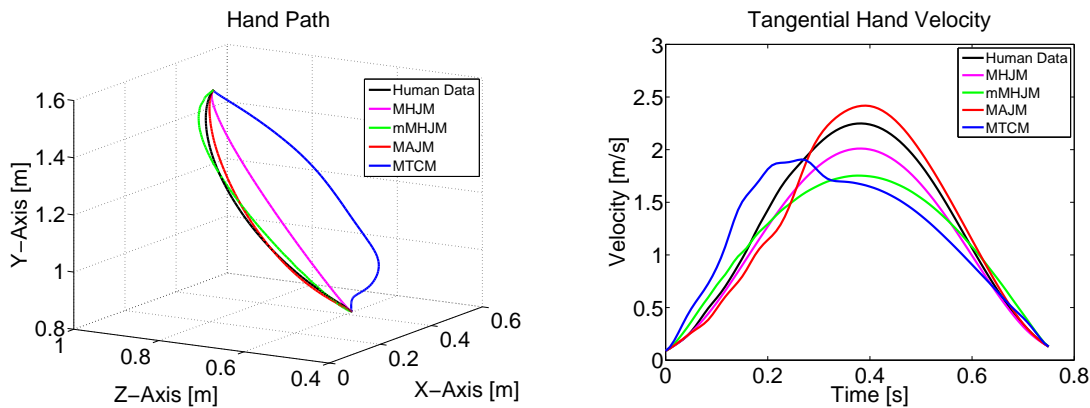


**Figure 5.28:** Representative hand paths and tangential velocity profiles for the optimization of shoulder abduction/adduction, shoulder rotation, shoulder anteversion/retroversion, elbow flexion/extension and thorax rotation.

### 5 DOF optimized

In figure 5.28 representative hand paths are illustrated. MHJM produced straight hand path across all trials. In contrast mMhJM and MAJM generated curved hand paths across all trials. MTCM showed the largest deviations from the measured data. None of the models were able to completely reproduce the experimentally determined hand paths. MAJM, however, showed a close fit to the measured data in most cases. It was shown in the first study of this thesis (Fig. 4.2) that the subjects produced single-peaked and almost bell-shaped velocity profiles. MHJM produced in all cases single-peaked and bell-shaped velocity profiles with lower peak velocities than the ones produced by the subjects. The other three optimal control models produced in most cases single-peaked tangential velocity profiles with bell-like shapes. The profiles of mMhJM and MTCM, however, exhibited in some cases distortions. To sum up, the increase of the number of joints to be optimized seemed to increase the deviations from the measured movements in extrinsic kinematic coordinates of the hand. Nevertheless, all four optimal control models seemed to be able to emulate the basic features of the measured hand trajectories in most of the test trials.

In the first column of figure 5.29 typical joint angle trajectories of the five optimized DOFs are displayed. MAJM produced across all five DOFs the closest fit to the measured trajectories. In contrast, the trajectories of mMhJM and MTCM showed a higher variability with larger movement ranges than the ones produced by the subjects. Moreover the angle profiles of mMhJM and MTCM were sometimes oscillating (Fig. 5.29). In the second column of figure 5.29 the corresponding joint angular velocities are illustrated. Since joint angular velocities are not independent from joint angular courses, the joint angular velocities of the MAJM should exhibit a closer fit to the joint angular velocity profiles of the subjects than mMhJM and MTCM. However, the data confirm this assumption. MAJM showed the closest fit

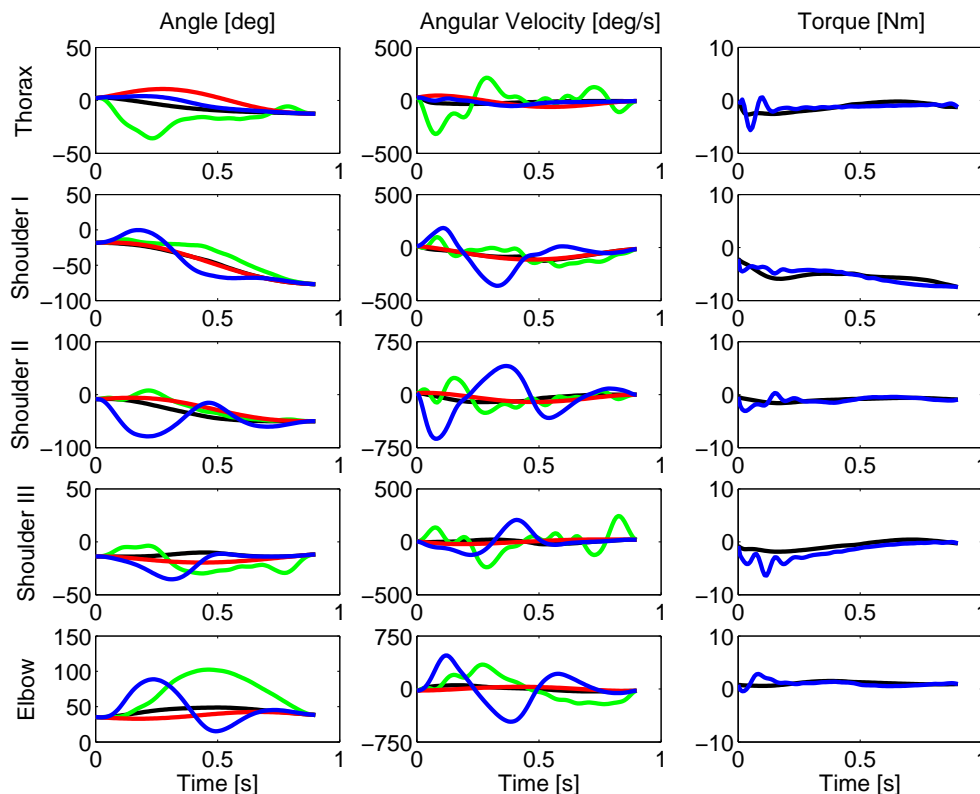


**Figure 5.29:** Representative angle, angular velocity and torque profiles for the optimization of thorax rotation, shoulder abduction/adduction, shoulder rotation, shoulder anteversion/retroversion and elbow flexion/extension. As before measured trajectories are black, trajectories of mMHJM are green, trajectories of MAJM are red and trajectories of MTCM are blue.

across all five DOFs. mMHJM and MTCM produced trajectories with large velocity ranges and large differences in the peak angular velocities compared to the peak angular velocities of the subjects. In the third column of figure 5.29 the corresponding joint torques are displayed. As before in the case of single degree optimization, MTCM showed a tendency to reproduce the measured torque profiles across all the trials and all five DOFs only incompletely. However, in a few cases the MTCM produced trajectories that emulated the measured torque profiles to some extent (Fig. 5.29). In most cases the model produced the peak torque at the beginning of the movement. This torque level was constantly reduced during the movement with only small changes. All of the torque profiles were slightly oscillating.

### 5.3.3.2 Variations between the measured and predicted trajectories

The variations between the measured and predicted trajectories were analyzed based on equations 5.11, 5.12, 5.13 and 5.14. The analysis is carried out in three steps: First, according to the simulation protocol the performance of the different optimal control models across the optimized DOFs were analyzed (Chap. 5.3.3.2.1). Second, each optimal control model was examined separately to determine, if there were performance differences across the five optimized DOFs. This step was carried out for the condition “1 DOF optimized” and for the condition “5 DOFs optimized” (Chap. 5.3.3.2.2). Finally, each of the optimal control models was tested to conclude if there were performance differences between the two conditions “1 DOF optimized” vs. “5 DOFs optimized” across the five optimized DOFs (Chap. 5.3.3.2.3).

#### 5.3.3.2.1 Performance differences between different optimal control models

In this section the performance of MHJM, mMHJM, MAJM and MTCM were analyzed for the optimization of 1 DOF and 5 DOFs. Thereby, the analysis was carried out according to the simulation protocol (Tab. 5.1).

##### 1 DOF optimized: Shoulder abduction/adduction

The results of the %RMSDs for the measured and predicted hand paths (Fig. 5.30, top left) indicate that none of the four optimal control models were able to reproduce the measured hand movements in extrinsic coordinates. MAJM produced the smallest %RMSD followed by mMHJM, MHJM and finally MTCM, which produced the highest %RMSD. The repeated ANOVA yielded significant differences ( $F = 11.391, p \leq .001, \eta^2 = .226$ ) between the %RMSDs of the measured and predicted hand paths of the four optimal control models. Pairwise Bonferroni tests revealed significant differences between the %RMSDs of the measured and predicted hand paths of MHJM and mMHJM ( $p \leq .001$ ), MHJM and MAJM ( $p \leq .001$ ) as well as MAJM and MTCM ( $p \leq .01$ ). The Bonferroni tests yielded no significant differences between MHJM and MTCM ( $p = 1.000$ ), mMHJM and MAJM ( $p = .962$ ) as well as mMHJM and MTCM ( $p = .021$ ).

The results of the %RMSDs for the measured and predicted tangential velocities of the hand (Fig. 5.30, top right) exhibit that MAJM produced the smallest %RMSD followed by mMHJM, MHJM and MTCM. The repeated ANOVA yielded significant differences ( $F = 10.953, p \leq .001, \eta^2 = .219$ ) between the %RMSDs of the measured and predicted tangential hand velocities of the four optimal control models. Pairwise Bonferroni tests revealed significant differences between the %RMSDs of the measured and predicted tangential hand velocities of MHJM and mMHJM ( $p \leq .001$ ), MHJM and MAJM ( $p \leq .001$ ) as well as MAJM and MTCM ( $p \leq .01$ ). The Bonferroni tests yielded no significant differences between MHJM and MTCM ( $p = .391$ ), mMHJM and MAJM ( $p = 1.000$ ) and mMHJM and MTCM ( $p = .011$ ).

The results of the %RMSDs for the measured and predicted shoulder angles (Fig.

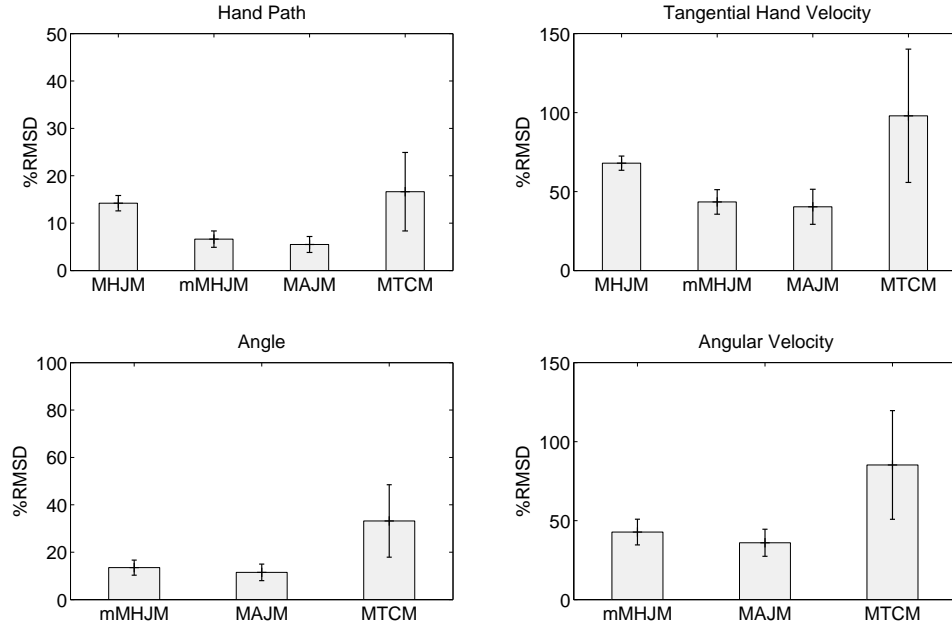


**Figure 5.30:** Mean of the %RMSDs between the measured and predicted hand paths, tangential hand velocities, angles and angular velocities for MHJM, mMHJM, MAJM and MTCM for the optimization of the DOF shoulder abduction/adduction. Error bars indicate the 99 % confidence intervals.

5.30, bottom left) indicate that none of the three optimal control models were able to reproduce the measured joint angle trajectories. MAJM produced the smallest %RMSDs followed by mMHJM and MTCM. The repeated ANOVA yielded significant differences ( $F = 12.539, p \leq .001, \eta^2 = .243$ ) between the %RMSDs of the measured and predicted joint angles of the three optimal control models. Pairwise Bonferroni tests revealed significant differences between the %RMSDs of the measured and predicted joint angles of mMHJM and MTCM ( $p \leq .01$ ) and MAJM and MTCM ( $p \leq .001$ ). The Bonferroni tests yielded no significant differences between mMHJM and MAJM ( $p = .811$ ).

The results of the %RMSDs for the measured and predicted angular velocities (Fig. 5.30, bottom right) show that MAJM produced the smallest %RMSD followed by mMHJM and MTCM. The repeated ANOVA yielded significant differences ( $F = 12.937, p \leq .001, \eta^2 = .249$ ) between the %RMSDs of the measured and predicted joint angular velocities of the three optimal control models. Pairwise Bonferroni tests revealed significant differences between the %RMSDs of the measured and predicted joint angular velocities of mMHJM and MTCM ( $p \leq .01$ ) and MAJM and MTCM ( $p \leq .01$ ). The Bonferroni tests yielded no significant differences between mMHJM and MAJM ( $p = .463$ ).

### 1 DOF optimized: Shoulder rotation

The results of the %RMSDs for the measured and predicted hand paths (Fig. 5.31, top left) indicate that none of the four optimal control models were able to reproduce the hand movement of the subjects in extrinsic coordinates. MAJM produced the smallest %RMSD followed by mMHJM, MHJM and finally MTCM, which produced the highest %RMSD. The repeated ANOVA yielded significant differences ( $F = 17.704, p \leq .001, \eta^2 = .312$ ) between the %RMSDs of the measured and predicted hand paths of the four optimal control models. Pairwise Bonferroni tests revealed significant differences between the %RMSDs of the measured and predicted hand paths of MHJM and mMHJM ( $p \leq .001$ ), MHJM and MAJM ( $p \leq .001$ ), mMHJM and MAJM ( $p \leq .001$ ), MAJM and MTCM ( $p \leq .001$ ). The Bonferroni tests yielded no significant differences between MHJM and MTCM ( $p = 1.000$ ) and between mMHJM and MTCM ( $p = .065$ ).

The results of the %RMSDs for the measured and predicted tangential velocities of the hand (Fig. 5.31, top right) denote that MAJM produced the smallest %RMSD followed by mMHJM, MTCM and MHJM. The repeated ANOVA yielded significant differences ( $F = 20.539, p \leq .001, \eta^2 = .345$ ) between the %RMSDs of the measured and predicted tangential hand velocities of the four optimal control models. Pairwise Bonferroni tests revealed significant differences between the %RMSDs of the measured and predicted tangential hand velocities of the MHJM and mMHJM ( $p \leq .001$ ), MHJM and MAJM ( $p \leq .001$ ), mMHJM and MAJM ( $p \leq .001$ ) as well as between MAJM and MTCM ( $p \leq .001$ ). The Bonferroni tests yielded no significant differences between MHJM and MTCM ( $p = 1.000$ ) and between mMHJM and MTCM ( $p = .072$ ).

The results of the %RMSDs for the measured and predicted shoulder angles (Fig. 5.31, bottom left) indicate that none of the three optimal control models were able to reproduce the human joint angle trajectories. MAJM produced the smallest %RMSD followed by mMHJM and MTCM. The repeated ANOVA yielded significant differences ( $F = 11.598, p \leq .001, \eta^2 = .229$ ) between the %RMSDs of the measured and predicted joint angles of the three optimal control models. Pairwise Bonferroni tests revealed significant differences between the %RMSDs of the measured and predicted joint angles of mMHJM and MAJM ( $p \leq .001$ ) as well as between MAJM and MTCM ( $p \leq .01$ ). The Bonferroni tests yielded no significant differences between mMHJM and MTCM ( $p = .127$ ).

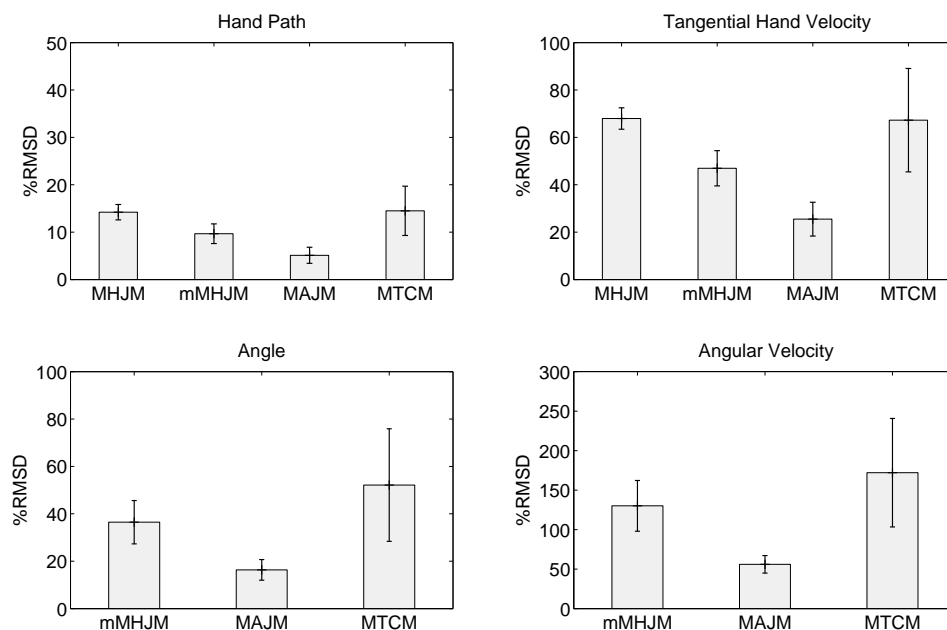


**Figure 5.31:** Mean of the %RMSDs between the measured and predicted hand paths, tangential hand velocities, angles and angular velocities for MHJM, mMHJM, MAJM and MTCM for the optimization of the DOF shoulder rotation. Error bars indicate the 99 % confidence intervals.

The results of the %RMSDs for the measured and predicted angular velocities (Fig. 5.31, bottom right) show as before that MAJM produced the smallest %RMSD followed by mMHJM and MTCM. The repeated ANOVA yielded significant differences ( $F = 15.885, p \leq .001, \eta^2 = .289$ ) between the %RMSDs of the measured and predicted joint angular velocities of the three optimal control models. Pairwise Bonferroni tests revealed significant differences between the %RMSDs of the measured and predicted joint angles of mMHJM and MAJM ( $p \leq .001$ ) and between MAJM and MTCM ( $p \leq .001$ ). The Bonferroni tests yielded no significant differences between mMHJM and MTCM ( $p = .100$ ).

### 1 DOF optimized: Shoulder anteversion/retroversion

The results of the %RMSDs for the measured and predicted hand paths (Fig. 5.32, top left) indicate that none of the four optimal control models were able to reproduce the measured hand movements in extrinsic coordinates. MAJM produced the smallest %RMSD followed by MHJM, mMHJM and finally MTCM, which produced the highest %RMSD. The repeated ANOVA yielded significant differences ( $F = 10.126, p \leq .001, \eta^2 = .206$ ) between the %RMSDs of the measured and predicted hand paths of the four optimal control models. Pairwise Bonferroni tests

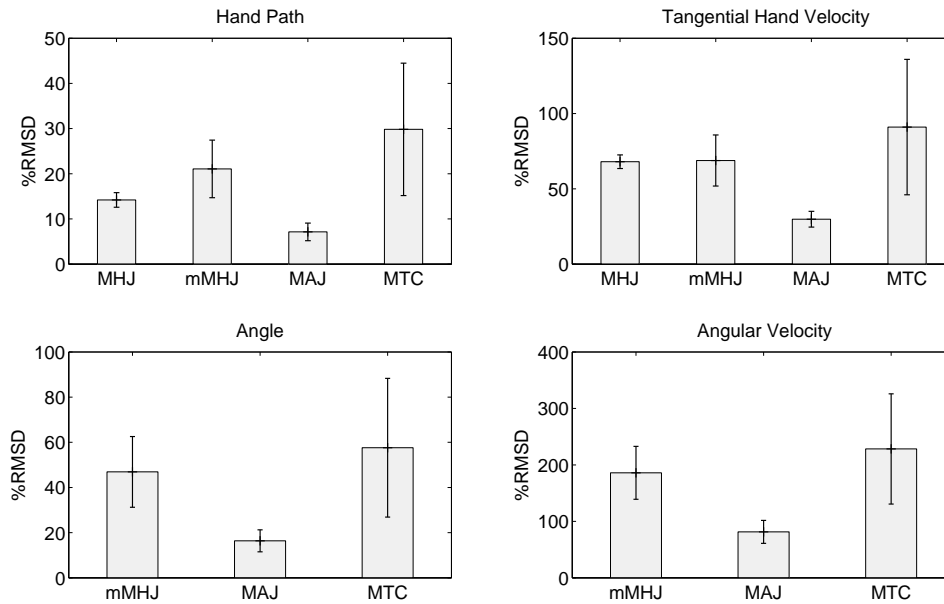


**Figure 5.32:** Mean of the %RMSDs between the measured and predicted hand paths, tangential hand velocities, angles and angular velocities for MHJM, mMhJM, MAJM and MTCM for the optimization of the DOF shoulder anteversion/retroversion. Error bars indicate the 99 % confidence intervals.

revealed significant differences between the %RMSDs of the measured and predicted hand paths of MHJM and MAJM ( $p \leq .001$ ), mMhJM and MAJM ( $p \leq .001$ ) as well as between MAJM and MTCM ( $p \leq .001$ ). The Bonferroni tests yielded no significant differences between MHJM and mMhJM ( $p = .066$ ), MHJM and MTCM ( $p = .052$ ) and between mMhJM and MTCM ( $p = .891$ ).

The results of the %RMSDs for the measured and predicted tangential velocities of the hand (Fig. 5.32, top right) show that MAJM produced the smallest %RMSD followed by MHJM, mMhJM and MTCM. The repeated ANOVA yielded significant differences ( $F = 7.563, p \leq .01, \eta^2 = .162$ ) between the %RMSDs of the measured and predicted tangential hand velocities of the four optimal control models. Pairwise Bonferroni tests revealed significant differences between the %RMSDs of the measured and predicted tangential hand velocities of MHJM and MAJM ( $p \leq .001$ ), mMhJM and MAJM ( $p \leq .001$ ) as well as MAJM and MTCM ( $p \leq .01$ ). The Bonferroni tests yielded no significant differences between MHJM and mMhJM ( $p = 1.000$ ), MHJM and MTCM ( $p = 1.000$ ) and mMhJM and MTCM ( $p = 1.000$ ).

The results of the %RMSDs for the measured and predicted shoulder angles (Fig. 5.32, bottom left) indicate that none of the three optimal control models were able to reproduce the human joint angle trajectories. MAJM produced the smallest %RMSD followed by mMHJM and MTCM. The repeated ANOVA yielded significant differences ( $F = 7.574, p \leq .01, \eta^2 = .163$ ) between the %RMSDs of the measured and predicted joint angles of the three optimal control models. Pairwise Bonferroni tests revealed significant differences between the %RMSDs of the measured and predicted joint angles of mMHJM and MAJM ( $p \leq .001$ ) and between MAJM and MTCM ( $p \leq .01$ ). The Bonferroni tests yielded no significant differences between mMHJM and MTCM ( $p = 1.000$ ).

The results of the %RMSDs for the measured and predicted angular velocities (Fig. 5.32, bottom right) show that MAJM produced the smallest %RMSDs followed by mMHJM and MTCM. The repeated ANOVA yielded significant differences ( $F = 9.885, p \leq .001, \eta^2 = .202$ ) between the %RMSDs of the measured and predicted joint angular velocities of the three optimal control models. Pairwise Bonferroni tests revealed significant differences between the %RMSDs of the measured and predicted joint angular velocities of mMHJM and MAJM ( $p \leq .001$ ) and between MAJM and MTCM ( $p \leq .001$ ). The Bonferroni tests yielded no significant differences between mMHJM and MTCM ( $p = .929$ ).

### **1 DOF optimized: Elbow flexion/extension**

The results of the %RMSDs for the measured and predicted hand paths (Fig. 5.33, top left) indicate that none of the four optimal control models were able to reproduce the hand movement of the subjects in extrinsic coordinates of the hand. MAJM produced the smallest %RMSD followed by MHJM, mMHJM and finally MTCM, which produced in highest %RMSD. The repeated ANOVA yielded significant differences ( $F = 16.005, p \leq .001, \eta^2 = .291$ ) between the %RMSDs of the measured and predicted hand paths of the four optimal control models. Pairwise Bonferroni tests revealed significant differences between the %RMSDs of the measured and predicted hand paths of MHJM and MAJM ( $p \leq .01$ ), MHJM and MTCM ( $p \leq .001$ ) and MAJM and MTCM ( $p \leq .001$ ). The Bonferroni tests yielded no significant differences between MHJM and mMHJM ( $p = 1.000$ ), mMHJM and MAJM ( $p = .047$ ) as well as mMHJM and MTCM ( $p = .030$ ).

The results of the %RMSDs for the measured and predicted tangential velocities of the hand (Fig. 5.33, top right) show that MAJM produced the smallest %RMSD followed by mMHJM, MHJM and MTCM. The repeated ANOVA yielded significant differences ( $F = 20.183, p \leq .001, \eta^2 = .341$ ) between the %RMSDs of the measured and predicted tangential hand velocities of the four optimal control models. Pairwise Bonferroni tests revealed significant differences between the %RMSDs of the measured and predicted tangential hand velocities of MHJM and mMHJM ( $p \leq .01$ ), MHJM and MAJM ( $p \leq .001$ ), mMHJM and MTCM ( $p \leq .01$ ), as well as between MAJM and MTCM ( $p \leq .001$ ). The Bonferroni tests yielded no significant differ-

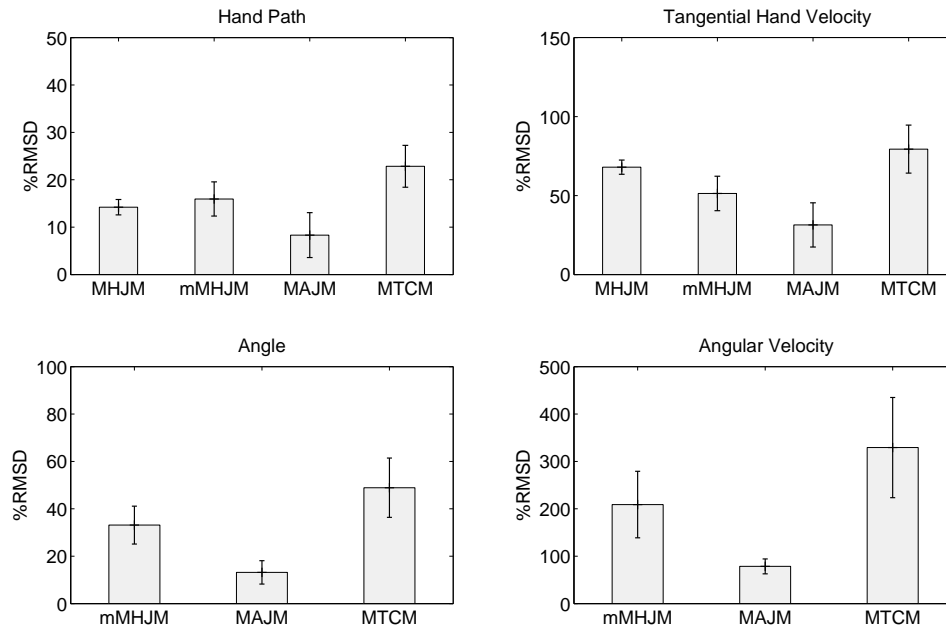


**Figure 5.33:** Mean of the %RMSDs between the measured and predicted hand paths, tangential hand velocities, angles and angular velocities for MHJM, mMHJM, MAJM and MTCM for the optimization of the DOF elbow flexion/extension. Error bars indicate the 99 % confidence intervals.

ences between MHJM and MTCM ( $p = .507$ ) and between mMHJM and MAJM ( $p = .112$ ).

The results of the %RMSDs for the measured and predicted elbow angles (Fig. 5.33, bottom left) indicate that none of the three optimal control models were able to reproduce the human joint angle trajectories. MAJM produced the smallest %RMSD followed by mMHJM and MTCM. The repeated ANOVA yielded significant differences ( $F = 26.008, p \leq .001, \eta^2 = .400$ ) between the %RMSDs of the measured and predicted joint angles of the three optimal control models. Pairwise Bonferroni tests revealed significant differences between the %RMSDs of the measured and predicted joint angles of mMHJM and MAJM ( $p \leq .001$ ) and between MAJM and MTCM ( $p \leq .001$ ). The Bonferroni tests yielded no significant differences between mMHJM and MTCM ( $p = .025$ ).

The results of the %RMSDs for the measured and predicted angular velocities (Fig. 5.33, bottom right) indicate that none of the three optimal control models were able to reproduce the human joint angular velocities. MAJM produced the smallest %RMSD followed by mMHJM and MTCM. The repeated ANOVA yielded significant differences ( $F = 26.086, p \leq .001, \eta^2 = .401$ ) between the %RMSDs of the measured and predicted joint angular velocities of the three optimal control models.

Pairwise Bonferroni tests revealed significant differences between the %RMSDs of the measured and predicted joint angular velocities of mMHJM and MAJM ( $p \leq .001$ ), mMHJM and MTCM ( $p \leq .01$ ) and the MAJM and the MTCM ( $p \leq .001$ ).

### 1 DOF optimized: Thorax rotation

The results of the %RMSDs for the measured and predicted hand paths (Fig. 5.34, top left) indicate that none of the four optimal control models were able to reproduce the human hand movements in extrinsic coordinates. MTCM produced the smallest %RMSD followed by MAJM, MHJM and finally mMTHM, which produced the highest %RMSD. The repeated ANOVA yielded significant differences ( $F = 23.632, p \leq .001, \eta^2 = .377$ ) between the %RMSDs of the measured and predicted hand paths of the four optimal control models. Pairwise Bonferroni tests revealed significant differences between the %RMSDs of the measured and predicted hand paths of MHJM and MAJM ( $p \leq .001$ ), MHJM and MTCM ( $p \leq .001$ ), mMHJM and MAJM ( $p \leq .001$ ) and between mMHJM and MTCM ( $p \leq .001$ ). The Bonferroni tests yielded no significant differences between MHJM and mMHJM ( $p = .203$ ) and between MAJM and MTCM ( $p = 1.000$ ).

The results of the %RMSDs for the measured and predicted tangential velocities of the hand (Fig. 5.34, top right) show that MTCM produced the smallest %RMSD followed by MAJM, mMHJM and MHJM. The repeated ANOVA yielded significant differences ( $F = 53.642, p \leq .001, \eta^2 = .579$ ) between the %RMSDs of the measured and predicted tangential hand velocities of the four optimal control models. Pairwise Bonferroni tests revealed significant differences between the %RMSDs of the measured and predicted hand paths of MHJM and MAJM ( $p \leq .001$ ), MHJM and MTCM ( $p \leq .001$ ), mMHJM and MAJM ( $p \leq .001$ ) and between mMHJM and MTCM ( $p \leq .001$ ). The Bonferroni tests yielded no significant differences between MHJM and mMHJM ( $p = 1.000$ ) and between MAJM and MTCM ( $p = 1.000$ ).

The results of the %RMSDs for the measured and predicted thorax angles (Fig. 5.34, bottom left) indicate that none of the three optimal control models were able to reproduce the human joint angle trajectories. MTCM produced the smallest %RMSD followed by MAJM and mMHJM. The repeated ANOVA yielded significant differences ( $F = 35.889, p \leq .001, \eta^2 = .479$ ) between the %RMSDs of the measured and predicted joint angles of the three optimal control models. Pairwise Bonferroni tests revealed significant differences between the %RMSDs of the measured and predicted joint angles of mMHJM and MAJM ( $p \leq .001$ ) and mMHJM and MTCM ( $p \leq .001$ ) and no significant differences between MAJM and MTCM ( $p = .665$ ).

The results of the %RMSDs for the measured and predicted angular velocities (Fig. 5.34, bottom right) indicate that none of the three optimal control models were able to reproduce the human joint angular velocities. MTCM produced the smallest %RMSD followed by MAJM and mMHJM. The repeated ANOVA yielded significant differences ( $F = 45.566, p \leq .001, \eta^2 = .539$ ) between the %RMSDs of the measured and predicted joint angular velocities of the three optimal control models.

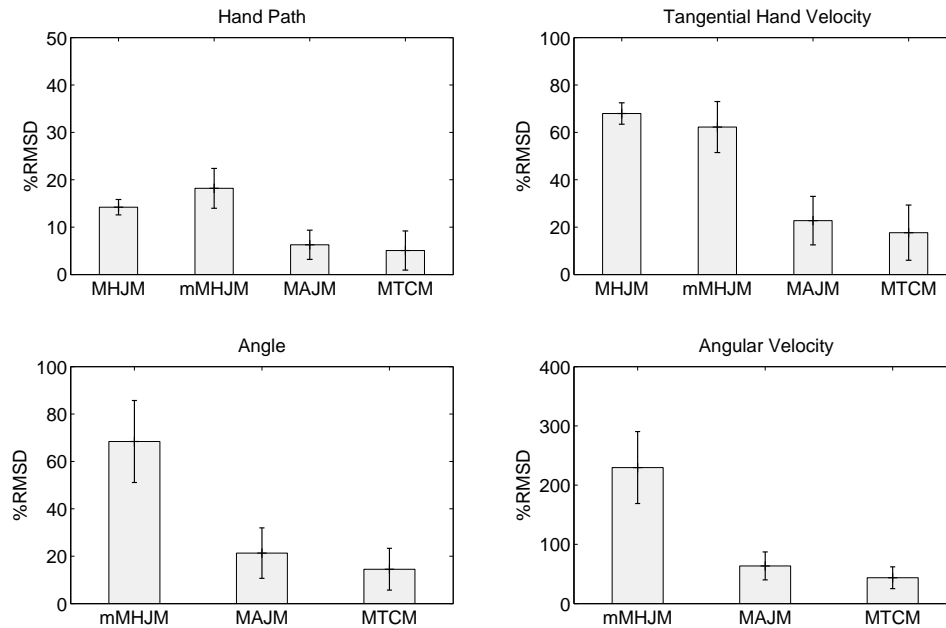


**Figure 5.34:** Mean of the %RMSDs between the measured and predicted hand paths, tangential hand velocities, angles and angular velocities for MHJM, mMHJM, MAJM and MTCM for the optimization of the DOF thorax rotation. Error bars indicate the 99 % confidence intervals.

Pairwise Bonferroni tests revealed significant differences between the %RMSDs of the measured and predicted joint angular velocities of mMHJM and MAJM ( $p \leq .001$ ) as well as mMHJM and MTCM ( $p \leq .001$ ) and no significant differences between MAJM and MTCM ( $p = .252$ ).

### 5 DOFs optimized

The results of the %RMSDs for the measured and predicted hand paths (Fig. 5.35, top left) indicate that none of the four optimal control models were able to reproduce the human hand movement of the subjects in extrinsic coordinates of the hand. MAJM produced the smallest %RMSD followed by MHJM, mMHJM and finally MTCM. The repeated ANOVA yielded significant differences ( $F = 18.894$ ,  $p \leq .001$ ,  $\eta^2 = .326$ ) between the %RMSDs of the measured and predicted hand paths of the four optimal control models. Pairwise Bonferroni tests revealed significant differences between the %RMSDs of the measured and predicted hand paths of MHJM and mMHJM ( $p \leq .001$ ), MHJM and MTCM ( $p \leq .001$ ), mMHJM and MAJM ( $p \leq .001$ ) and between MAJM and MTCM ( $p \leq .001$ ). The Bonferroni tests yielded no significant differences between MHJM and MAJM ( $p = .206$ ) and mMHJM and MTCM ( $p = .013$ ).

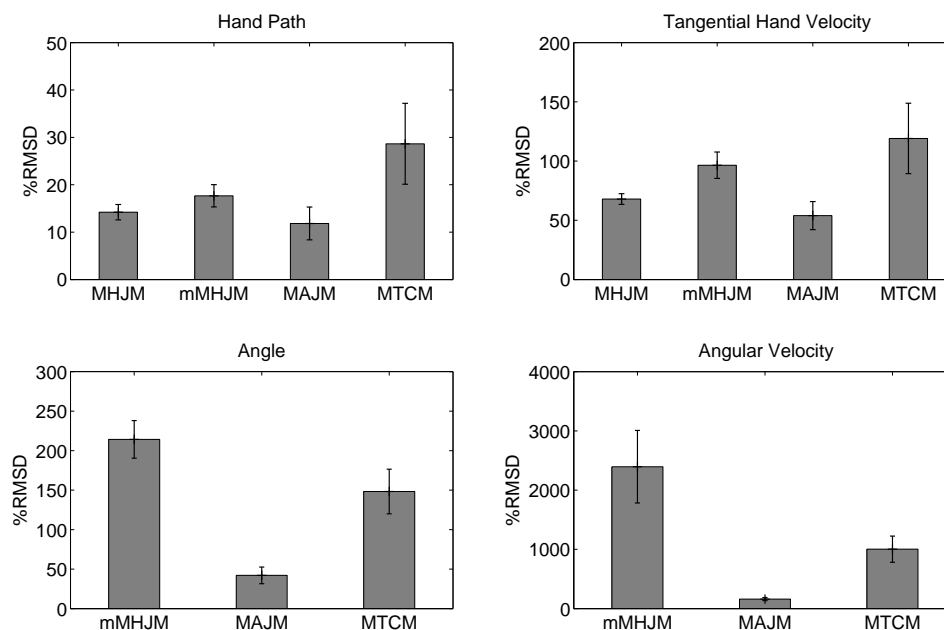


**Figure 5.35:** Mean of the %RMSDs between the measured and predicted hand paths, tangential hand velocities, angles and angular velocities for MHJM, mMHJM, MAJM and MTCM for the optimization of the DOF of shoulder abduction/adduction, shoulder rotation, shoulder anteversion/retroversion, elbow flexion/extension and thorax rotation. Error bars indicate the 99 % confidence intervals.

The results of the %RMSDs for the measured and predicted tangential velocities of the hand (Fig. 5.35, top right) show that MAJM produced the smallest %RMSD followed by MHJM, mMHJM and MTCM. The repeated ANOVA yielded significant differences ( $F = 22.784, p \leq .001, \eta^2 = .369$ ) between the %RMSDs of the measured and predicted tangential hand velocities of the four optimal control models. Pairwise Bonferroni tests revealed significant differences between the %RMSDs of the measured and predicted tangential hand velocities of MHJM and mMHJM ( $p \leq .001$ ), MHJM and MAJM ( $p \leq .01$ ), MHJM and MTCM ( $p \leq .001$ ), mMHJM and MAJM ( $p \leq .001$ ) as well as between MAJM and MTCM ( $p \leq .001$ ). The Bonferroni tests yielded no significant differences between mMHJM and MTCM ( $p = .389$ ).

The results of the %RMSDs for the measured and predicted joint angles (Fig. 5.35, bottom left) indicate that none of the three optimal control models were able to reproduce the measured joint angle trajectories. MAJM produced the smallest %RMSD followed by MTCM and mMHJM. The repeated ANOVA yielded significant differences ( $F = 108.960, p \leq .001, \eta^2 = .736$ ) between the %RMSDs of the measured and predicted joint angles of the three optimal control models. Pairwise

Bonferroni tests revealed significant differences between the %RMSDs of the measured and predicted joint angles of mMHJM and MAJM ( $p \leq .001$ ), mMHJM and MTCM ( $p \leq .001$ ) and between MAJM and MTCM ( $p \leq .001$ ).

The results of the %RMSDs for the measured and predicted angular velocities (Fig. 5.35, bottom right) indicate that none of the three optimal control models were able to reproduce the measured joint angular velocities. MAJM produced the smallest %RMSD followed by MTCM and mMHJM. The repeated ANOVA yielded significant differences ( $F = 60.454, p \leq .001, \eta^2 = .608$ ) between the %RMSDs of the measured and predicted joint angular velocities of the three optimal control models. Pairwise Bonferroni tests revealed significant differences between the %RMSDs of the measured and predicted joint angular velocities of mMHJM and MAJM ( $p \leq .001$ ), mMHJM and MTCM ( $p \leq .001$ ) and MAJM and MTCM ( $p \leq .001$ ).

### 5.3.3.2.2 Performance differences across the optimized DOFs

The performance differences across the optimized DOFs were calculated for MAJM and MTCM. In the case of mMhJM the optimization was not conducted in intrinsic kinematic coordinates but in extrinsic kinematic coordinates of the hand. The limits of the individual joints were used as an additional boundary condition during the optimization.

#### MAJM

The results of the %RMSDs for the measured and predicted hand paths across the five DOFs (Fig. 5.36) indicate that MAJM produced the smallest %RMSD when the DOF of shoulder rotation was optimized, followed by shoulder abduction/adduction, thorax rotation, shoulder anteversion/retroversion and elbow flexion/extension. The repeated ANOVA yielded no significant differences ( $F = 1.652, p = .200, \eta^2 = .041$ ) between the %RMSDs of the measured and predicted hand paths across the five DOFs.

The results of the %RMSDs for the measured and predicted hand tangential velocities across the five DOFs (Fig. 5.36) indicate that MAJM produced the smallest %RMSD when the DOF of thorax rotation was optimized, followed by shoulder rotation, shoulder anteversion/retroversion, elbow flexion/extension and shoulder abduction/adduction. The repeated ANOVA yielded no significant differences ( $F = 3.753, p = .020, \eta^2 = .088$ ) between the %RMSDs of the measured and predicted hand tangential velocities across the five DOFs. However, since the results of the repeated ANOVA are significant in tendency, we checked the post-hoc Bonferroni tests. These revealed significant differences between the DOFs shoulder abduction/adduction and shoulder rotation ( $p \leq .01$ ). The Bonferroni tests yielded no significant differences between the DOFs thorax rotation and shoulder abduction/adduction ( $p = .026$ ), thorax rotation and shoulder rotation ( $p = 1.000$ ), thorax rotation and shoulder anteversion/retroversion ( $p = .660$ ), thorax rotation and elbow flexion/extension ( $p = 1.000$ ), shoulder abduction/adduction and shoulder anteversion/retroversion ( $p = .253$ ), shoulder abduction/adduction and elbow flexion/extension ( $p = 1.000$ ), shoulder rotation and shoulder anteversion/retroversion ( $p = .958$ ), shoulder rotation and elbow flexion ( $p = 1.000$ ) and shoulder anteversion/retroversion and elbow flexion/extension ( $p = 1.000$ ), respectively.

The results of the %RMSDs for the measured and predicted joint angles across the five DOFs (Fig. 5.36) indicate that MAJM produced the smallest %RMSD when the DOF of shoulder abduction/adduction was optimized, followed by elbow flexion/extension, shoulder rotation, shoulder anteversion/retroversion and thorax rotation. The repeated ANOVA yielded no significant differences ( $F = 2.934, p = .065, \eta^2 = .070$ ) between the %RMSDs of the measured and predicted joint angles across the five DOFs.

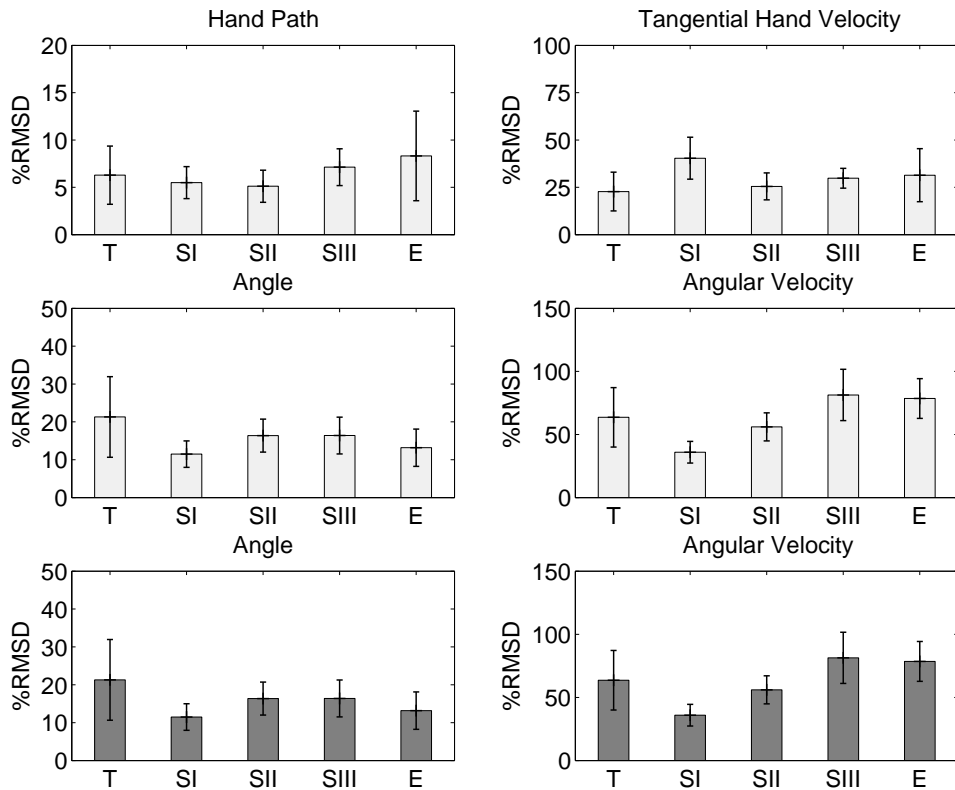


**Figure 5.36:** Mean of the %RMSDs of MAJM across the five DOFs under the optimization condition “1 DOF optimized” (light gray) and “5 DOFs optimized” (dark gray). Furthermore, the title T indicates thorax rotation, SI indicates shoulder abduction/adduction, SII indicates shoulder rotation, SIII indicates shoulder anteversion/retroversion and E represents elbow flexion/extension. Error bars indicate the 99 % confidence intervals.

The results of the %RMSDs for the measured and predicted joint angular velocities across the five DOFs (Fig. 5.36) indicate that MAJM produced the smallest %RMSD when the DOF of shoulder abduction/adduction was optimized, followed by shoulder rotation, thorax rotation, elbow flexion/extension and shoulder anteversion/retroversion. The repeated ANOVA yielded significant differences ( $F = 9.382, p \leq .001, \eta^2 = .194$ ) between the %RMSDs of the measured and predicted joint angular velocities across the five DOFs. Pairwise Bonferroni tests revealed significant differences between the DOFs shoulder abduction/adduction and shoulder rotation ( $p \leq .001$ ), shoulder anteversion/retroversion ( $p \leq .001$ ) as well as elbow flexion/extension ( $p \leq .001$ ). The Bonferroni tests yielded no significant differences between the DOFs thorax rotation and shoulder abduction/adduction ( $p = .046$ ),

thorax rotation and shoulder rotation ( $p = 1.000$ ), thorax rotation and shoulder anteversion/retroversion ( $p = .331$ ), thorax rotation and elbow flexion ( $p = 1.000$ ), shoulder rotation and shoulder anteversion/retroversion ( $p = .084$ ), shoulder rotation and elbow flexion ( $p = .036$ ) and shoulder anteversion/retroversion and elbow flexion/extension ( $p = 1.000$ ).

When all five DOFs were optimized the %RMSDs for the measured and predicted joint angles across the five DOFs (Fig. 5.36) indicate that MAJM produced the smallest %RMSD when the DOF of shoulder abduction/adduction was optimized, followed by elbow flexion/extension, shoulder rotation, shoulder anteversion/retroversion and thorax rotation. The repeated ANOVA yielded no significant differences ( $F = 2.934, p = .065, \eta^2 = .070$ ) between the %RMSDs of the measured and predicted joint angles across the five DOFs.

When all five DOFs were optimized the %RMSDs for the measured and predicted joint angular velocities across the five DOFs (Fig. 5.36) indicate that MAJM produced the smallest %RMSD when the DOF of shoulder abduction/adduction was optimized, followed by the shoulder rotation, thorax rotation, elbow flexion/extension and finally shoulder anteversion/retroversion. The repeated ANOVA yielded significant differences ( $F = 9.382, p \leq .001, \eta^2 = .194$ ) between the %RMSDs of the measured and predicted joint angular velocities across the five DOFs. Pairwise Bonferroni tests revealed significant differences between the DOFs shoulder abduction/adduction and shoulder rotation ( $p \leq .001$ ), shoulder anteversion/retroversion ( $p \leq .001$ ) and elbow flexion/extension ( $p \leq .001$ ). The Bonferroni tests yielded no significant differences between the DOFs thorax rotation and shoulder abduction/adduction ( $p = .046$ ), thorax rotation and shoulder rotation ( $p = 1.000$ ), thorax rotation and shoulder anteversion/retroversion ( $p = .331$ ), thorax rotation and elbow flexion/extension ( $p = 1.000$ ), shoulder rotation and shoulder anteversion/retroversion ( $p = .084$ ), shoulder rotation and elbow flexion/extension ( $p = .036$ ) and shoulder anteversion/retroversion and elbow flexion/extension ( $p = 1.000$ ).

### **MTCM**

The results of the %RMSDs for the measured and predicted hand paths across the five DOFs (Fig. 5.37) indicate that MTCM produced the smallest %RMSD when the DOF of thorax rotation was optimized, followed by shoulder rotation, shoulder abduction/adduction, elbow flexion and shoulder anteversion/retroversion. The repeated ANOVA yielded significant differences ( $F = 10.089, p \leq .001, \eta^2 = .206$ ) between the %RMSDs of the measured and predicted hand paths across the five DOFs. Pairwise Bonferroni tests revealed significant differences between the DOFs thorax rotation and shoulder abduction/adduction ( $p \leq .01$ ), shoulder rotation ( $p \leq .01$ ), shoulder anteversion/retroversion ( $p \leq .001$ ), elbow flexion/extension ( $p \leq .001$ ) and shoulder rotation and elbow flexion ( $p \leq .01$ ). The Bonferroni tests yielded no significant differences between the DOFs shoulder abduction/adduction and shoulder rotation ( $p = 1.000$ ), shoulder abduction/adduction and shoulder anteversion/retroversion

( $p = .212$ ), shoulder abduction/adduction and elbow flexion ( $p = .812$ ), shoulder rotation and shoulder anteversion/retroversion ( $p = .058$ ) and shoulder anteversion/retroversion and elbow flexion/extension ( $p = 1.000$ ).

The results of the %RMSDs for the measured and predicted hand tangential velocities across the five DOFs (Fig. 5.37) indicate that MTCM produced the smallest %RMSD when the DOF of thorax rotation was optimized, followed by shoulder rotation, elbow flexion/extension, shoulder anteversion/retroversion and finally shoulder abduction/adduction. The repeated ANOVA yielded significant differences ( $F = 9.116, p \leq .001, \eta^2 = .189$ ) between the %RMSDs of the measured and predicted hand tangential velocities across the five DOFs. Pairwise Bonferroni tests revealed significant differences between the DOFs thorax rotation and shoulder abduction/adduction ( $p \leq .001$ ), shoulder rotation ( $p \leq .001$ ), shoulder anteversion/retroversion ( $p \leq .001$ ) and elbow flexion ( $p \leq .001$ ). The Bonferroni tests yielded no significant differences between the DOFs shoulder abduction/adduction and shoulder rotation ( $p = .945$ ), shoulder abduction/adduction and shoulder anteversion/retroversion ( $p = 1.000$ ), shoulder abduction/adduction and elbow flexion/extension ( $p = 1.000$ ), shoulder rotation and shoulder anteversion/retroversion ( $p = 1.000$ ), shoulder rotation and elbow flexion/extension ( $p = 1.000$ ) and shoulder anteversion/retroversion and elbow flexion/extension ( $p = 1.000$ ).

The results of the %RMSDs for the measured and predicted joint angles across the five DOFs (Fig. 5.37) indicate that MTCM produced the smallest %RMSD when the DOF of thorax rotation was optimized, followed by shoulder abduction/adduction, elbow flexion/extension, shoulder rotation and shoulder anteversion/retroversion. The repeated ANOVA yielded significant differences ( $F = 5.757, p \leq .01, \eta^2 = .129$ ) between the %RMSDs of the measured and predicted joint angles across the five DOFs. Pairwise Bonferroni tests revealed significant differences between the DOFs thorax rotation and shoulder rotation ( $p \leq .01$ ), thorax rotation and shoulder anteversion/retroversion ( $p \leq .01$ ) as well as thorax rotation and elbow flexion/extension ( $p \leq .001$ ). The Bonferroni tests yielded no significant differences between the DOFs thorax rotation and shoulder abduction/adduction ( $p = .020$ ), shoulder abduction and shoulder rotation ( $p = .978$ ), shoulder abduction/adduction and shoulder anteversion/retroversion ( $p = .303$ ), shoulder abduction/adduction and elbow flexion/extension ( $p = .312$ ), shoulder rotation and shoulder anteversion/retroversion ( $p = 1.000$ ), shoulder rotation and elbow flexion/extension ( $p = 1.000$ ) as well as shoulder anteversion/retroversion and elbow flexion/extension ( $p = 1.000$ ).

The results of the %RMSDs for the measured and predicted joint angular velocities across the five DOFs (Fig. 5.37) indicate that MTCM produced the smallest %RMSD when the DOF of thorax rotation was optimized, followed by shoulder abduction/adduction, shoulder rotation, shoulder anteversion/retroversion and elbow flexion/extension. The repeated ANOVA yielded significant differences ( $F = 18.751, p \leq .001, \eta^2 = .325$ ) between the %RMSDs of the measured and predicted joint angular velocities across the five DOFs. Pairwise Bonferroni tests revealed

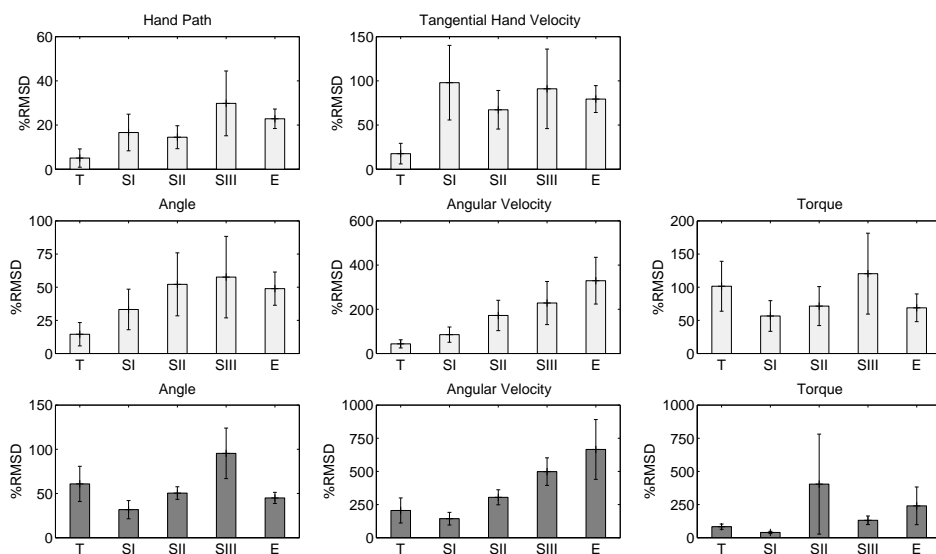


**Figure 5.37:** Mean of the %RMSDs of MTCM for the five DOFs under the optimization condition “1 DOF optimized” (light gray) and “5 DOFs optimized” (dark gray). Furthermore, the title T indicates thorax rotation, SI indicates shoulder abduction/adduction, SII indicates shoulder rotation, SIII indicates shoulder anteversion/retroversion and E represents elbow flexion/extension. Error bars indicate the 99 % confidence intervals.

significant differences between the DOFs of thorax rotation and shoulder abduction/adduction ( $p \leq .01$ ), thorax rotation and shoulder rotation ( $p \leq .001$ ), thorax rotation and shoulder anteversion/retroversion ( $p \leq .001$ ), thorax rotation and elbow flexion/extension ( $p \leq .001$ ), shoulder abduction/adduction and shoulder anteversion/retroversion ( $p \leq .001$ ) and shoulder abduction/adduction and elbow flexion/extension ( $p \leq .001$ ). The Bonferroni tests yielded no significant differences between the DOFs shoulder abduction/adduction and shoulder rotation ( $p = .050$ ), shoulder rotation and shoulder anteversion/retroversion ( $p = 1.000$ ), shoulder rotation and elbow flexion/extension ( $p = .025$ ) as well as shoulder anteversion/retroversion and elbow flexion ( $p = .301$ ).

The results of the %RMSDs between the measured and predicted joint torques across the five DOFs (Fig. 5.37) indicate that MTCM produced the smallest %RMSD when the DOF of shoulder abduction/adduction was optimized, followed by elbow flexion/extension, shoulder rotation, thorax rotation and shoulder anteversion/retroversion. The repeated ANOVA yielded no significant differences ( $F = 3.630, p = .022, \eta^2 = .085$ ) between the %RMSD of the measured and predicted joint torques across the five DOFs.

When all five DOFs were optimized the %RMSDs for the measured and predicted

joint angles across the five DOFs (Fig. 5.37) indicate that MTCM produced the smallest %RMSD when the DOF of shoulder abduction/adduction was optimized, followed by elbow flexion/extension, shoulder rotation, thorax rotation and shoulder anteversion/retroversion. The repeated ANOVA yielded significant differences ( $F = 16.235, p \leq .001, \eta^2 = .294$ ) between the %RMSDs of the measured and predicted joint angles across the five DOFs. Pairwise Bonferroni tests revealed significant differences between the DOFs thorax rotation and shoulder abduction/adduction ( $p \leq .001$ ), shoulder abduction/adduction and shoulder rotation ( $p \leq .001$ ), shoulder abduction/adduction and shoulder anteversion/retroversion ( $p \leq .001$ ), shoulder rotation and shoulder anteversion/retroversion ( $p \leq .01$ ) and shoulder anteversion/retroversion and elbow flexion/extension ( $p \leq .001$ ). The Bonferroni tests yielded no significant differences between the DOFs thorax rotation and shoulder rotation ( $p = 1.000$ ), thorax rotation and shoulder anteversion/retroversion ( $p = .013$ ), thorax rotation and elbow flexion ( $p = .700$ ), shoulder abduction/adduction and elbow flexion/extension ( $p = .046$ ) as well as shoulder rotation and elbow flexion ( $p = 1.000$ ).

When all five DOFs were optimized the %RMSDs for the measured and predicted joint angular velocities across the five DOFs (Fig. 5.37) indicate that MTCM produced the smallest %RMSD when the DOF of shoulder abduction/adduction was optimized, followed by thorax rotation, shoulder rotation, shoulder anteversion/retroversion and elbow flexion/extension. The repeated ANOVA yielded significant differences ( $F = 25.017, p \leq .001, \eta^2 = .391$ ) between the %RMSDs of the measured and predicted joint angular velocities across the five DOFs. Pairwise Bonferroni tests revealed significant differences between the DOFs thorax rotation and shoulder anteversion/retroversion ( $p \leq .001$ ), thorax rotation and elbow flexion/extension ( $p \leq .001$ ), shoulder abduction/adduction and shoulder rotation ( $p \leq .001$ ), shoulder abduction/adduction and shoulder anteversion/retroversion ( $p \leq .001$ ), shoulder abduction/adduction and elbow flexion/extension ( $p \leq .001$ ), shoulder rotation and shoulder anteversion/retroversion ( $p \leq .001$ ) and shoulder rotation elbow flexion/extension ( $p \leq .001$ ). The Bonferroni tests yielded no significant differences between the DOFs thorax rotation and shoulder abduction/adduction ( $p = .863$ ), thorax rotation and shoulder rotation ( $p = .070$ ) as well as shoulder anteversion/retroversion and elbow flexion/extension ( $p = .548$ ).

When all five DOFs were optimized the %RMSDs for the measured and predicted joint torques across the five DOFs (Fig. 5.37) indicate that MTCM produced the smallest %RMSD when the DOF of shoulder abduction/adduction was optimized, followed by thorax rotation, shoulder anteversion/retroversion, elbow flexion and shoulder rotation. The repeated ANOVA yielded no significant differences ( $F = 3.031, p = .083, \eta^2 = .072$ ) between the %RMSDs of the measured and predicted joint torques across the five DOFs. However, figure 5.37 indicates that pairwise post-hoc tests may reveal significant differences. Furthermore more, the large variance in the simulation results of the shoulder rotation and elbow flexion/extension could be

a reason for a strong adjustment of the Greenhouse-Geiser procedure. Therefore, we checked the pairwise Bonferroni tests. As indicated by figure 5.37, the Bonferroni tests revealed significant results for thorax rotation and shoulder abduction ( $p \leq .001$ ), thorax rotation and shoulder anteversion/retroversion ( $p \leq .01$ ), shoulder abduction/adduction and shoulder anteversion/retroversion ( $p \leq .001$ ) as well as shoulder abduction/adduction and elbow flexion/extension ( $p \leq .01$ ). The Bonferroni tests yielded no significant differences between the DOFs thorax rotation and shoulder rotation ( $p = .800$ ), thorax rotation and elbow flexion/extension ( $p = .041$ ), shoulder abduction/adduction and shoulder rotation ( $p = .043$ ), shoulder rotation and shoulder anteversion/retroversion ( $p = 1.000$ ), shoulder rotation and elbow flexion/extension ( $p = 1.000$ ) as well as shoulder anteversion/retroversion and elbow flexion/extension ( $p = .402$ ).

### 5.3.3.2.3 Performance differences between the two conditions “1 DOF optimized” and “5 DOFs optimized”

In this section the performance of MHJM, mMHJM, MAJM and MTCM between the two conditions “1 DOF optimized” vs. “5 DOFs optimized” for the five DOFs was analyzed separately. The analysis was carried out according to the simulation protocol (Tab. 5.1).

#### 1 DOF optimized vs. 5 DOFs optimized: Shoulder abduction/adduction

The results of the %RMSDs between the two conditions (Fig. 5.38, top left) indicate that when the DOFs to be optimized were increased the %RMSDs for the hand path increased across all three models. In other words, when less joints were driven by measured data the deviations between measured movements and movements generated by different optimal control models raised. However, paired two-sample t-tests revealed significant differences for mMHJM ( $T = -9.322, p \leq .001$ ), MAJM ( $T = -5.635, p \leq .001$ ) and MTCM ( $T = -3.428, p \leq .001$ ).

The results of the %RMSDs between the two conditions (Fig. 5.38, top right) indicate that when the DOFs to be optimized were increased the %RMSDs for the tangential hand velocities increased across all three models. Paired two-sample t-tests revealed significant differences for mMHJM ( $T = -10.396, p \leq .001$ ) and MAJM ( $T = -3.921, p \leq .001$ ). Paired two-sample t-tests revealed no significant differences for MTCM ( $T = -1.563, p = .126$ ).

The results of the %RMSDs between the two conditions (Fig. 5.38, bottom left) indicate that when the DOFs to be optimized were increased the %RMSDs for the joint angles increased for mMHJM and decreased for MTCM. The %RMSD for MAJM remained the same. Paired two-sample t-tests revealed significant differences for mMHJM ( $T = -5.211, p \leq .001$ ) and no significant differences for MAJM ( $T = -1.290, p = .205$ ) and MTCM ( $T = .255, p = .800$ ).

The results of the %RMSDs between the two conditions (Fig. 5.38, bottom right) indicate that when the DOFs to be optimized were increased the %RMSDs for the

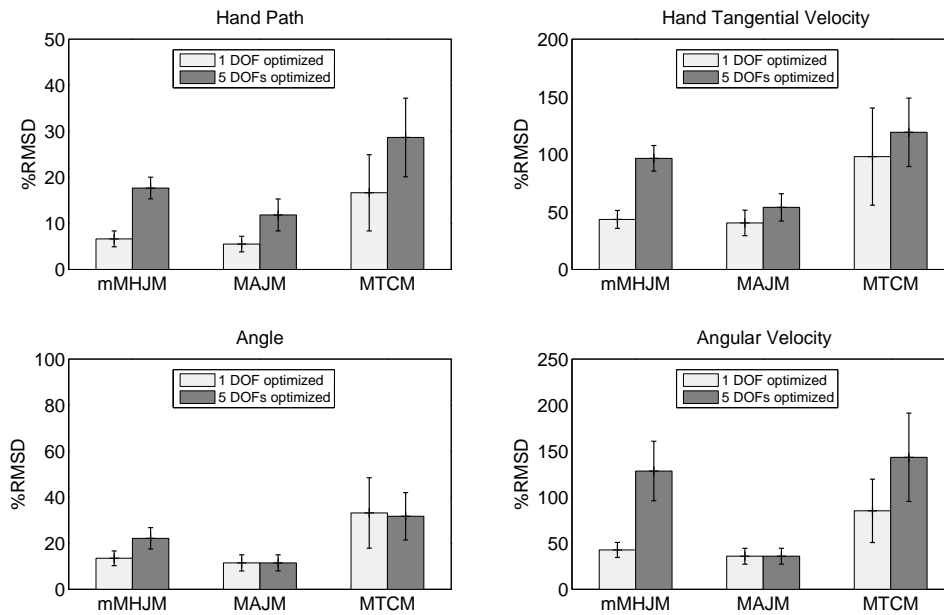


**Figure 5.38:** Mean of the %RMSDs for shoulder abduction/adduction under two different optimization conditions. Error bars indicate the 99 % confidence intervals.

joint angular velocities increased for mMHJM and MTCM. The %RMSD for MAJM remained the same. Paired two-sample t-tests revealed significant differences for mMHJM ( $T = -7.171, p \leq .001$ ) and MTCM ( $T = -3.582, p \leq .001$ ). The paired two-sample t-tests revealed no significant differences for MAJM ( $T = -.795, p = .431$ ).

### 1 DOF optimized vs. 5 DOFs optimized: Shoulder rotation

The results of the %RMSDs between the two conditions (Fig. 5.39, top left) indicate that when the DOFs to be optimized were increased the %RMSDs for the hand path increased across all three models. Paired two-sample t-tests revealed significant differences for mMHJM ( $T = -7.083, p \leq .001$ ), MAJM ( $T = -5.724, p \leq .001$ ) and MTCM ( $T = -4.501, p \leq .001$ ).

The results of the %RMSDs between the two conditions (Fig. 5.39, top right) indicate that when the DOFs to be optimized were increased the %RMSDs for the tangential hand velocities increased across all three models. Paired two-sample t-tests revealed significant differences for mMHJM ( $T = -11.346, p \leq .001$ ), MAJM ( $T = -7.234, p \leq .001$ ) and MTCM ( $T = -4.716, p \leq .001$ ).

The results of the %RMSDs between the two conditions (Fig. 5.39, bottom left) show that when the DOFs to be optimized were increased the %RMSDs for the joint angles increased for mMHJM, remained the same for MAJM and decreased

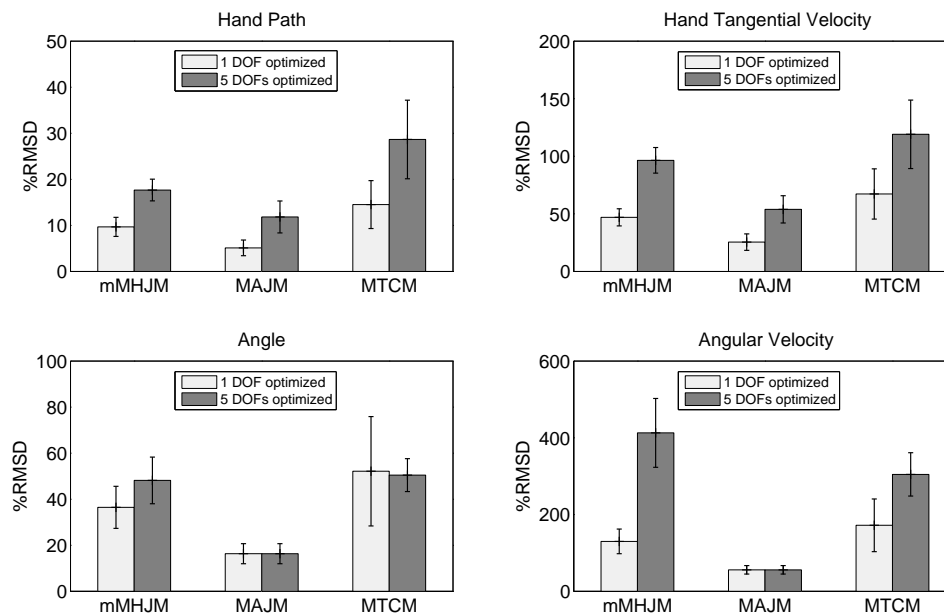


**Figure 5.39:** Mean of the %RMSDs for shoulder rotation under two different optimization conditions. Error bars indicate the 99 % confidence intervals.

for MTCM. Paired two-sample t-tests revealed significant differences for mMHJM ( $T = -3.477, p \leq .001$ ) and no significant differences for MAJM ( $T = .458, p = .650$ ) and MTCM ( $T = .182, p = .857$ ).

The results of the %RMSDs between the two conditions (Fig. 5.39, bottom right) exhibit that when the DOFs to be optimized were increased the %RMSDs for the joint angular velocities increased for mMHJM and MTCM and remained the same for MAJM. Paired two-sample t-tests revealed significant differences for mMHJM ( $T = -9.294, p \leq .001$ ) and MTCM ( $T = -4.392, p \leq .001$ ). The paired two-sample t-tests revealed no significant differences for MAJM ( $T = .611, p = .545$ ).

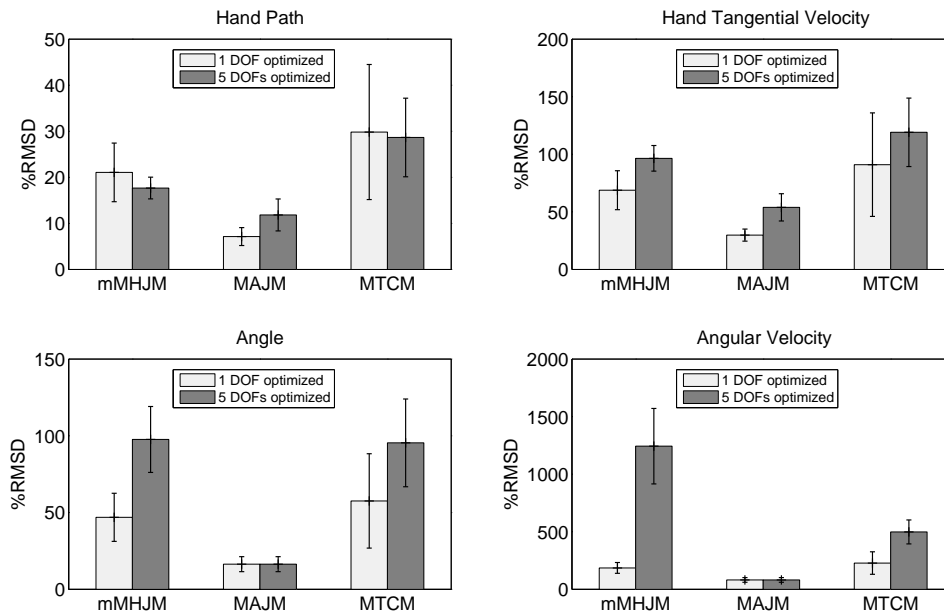


**Figure 5.40:** Mean of the %RMSDs for shoulder anteversion/retroversion under two different optimization conditions. Error bars indicate the 99 % confidence intervals.

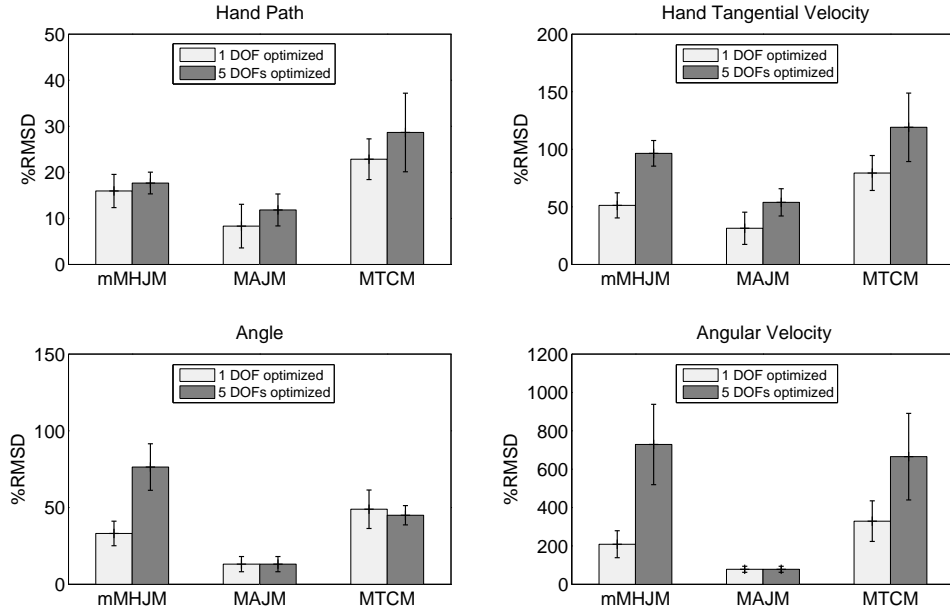
### 1 DOF optimized vs. 5 DOFs optimized: Shoulder anteversion/retroversion

The results of the %RMSDs between the two conditions (Fig. 5.40, top left) exhibit that when the DOFs to be optimized were increased the %RMSDs of the hand paths of mMHJM and MTCM were decreased. In contrast the %RMSDs of the hand paths of MAJM were increased. Paired two-sample t-tests revealed significant differences for MAJM ( $T = -4.320, p \leq .001$ ) and no significant differences for mMHJM ( $T = 1.270, p = .211$ ) and MTCM ( $T = .240, p = .812$ ).

The results of the %RMSDs between the two conditions (Fig. 5.40, top right) exhibit that when the DOFs to be optimized were increased the %RMSDs of the tangential hand velocities of all three optimal control models were increased. Paired two-sample t-tests revealed significant differences for mMHJM ( $T = -3.629, p \leq .001$ ), MAJM ( $T = -6.089, p \leq .001$ ) and no significant differences for MTCM ( $T = -2.038, p = .048$ ).

The results of the %RMSDs between the two conditions (Fig. 5.40, bottom left) exhibit that when the DOFs to be optimized were increased the %RMSDs of the joint angles increased for mMHJM and for MTCM and remained the same for MAJM. Paired two-sample t-tests revealed significant differences for mMHJM ( $T = -6.107, p \leq .001$ ) and no significant differences for MTCM ( $T = -2.247, p = .030$ ) and MAJM ( $T = -1.136, p = .263$ ).

The results of the %RMSDs between the two conditions (Fig. 5.40, bottom right)



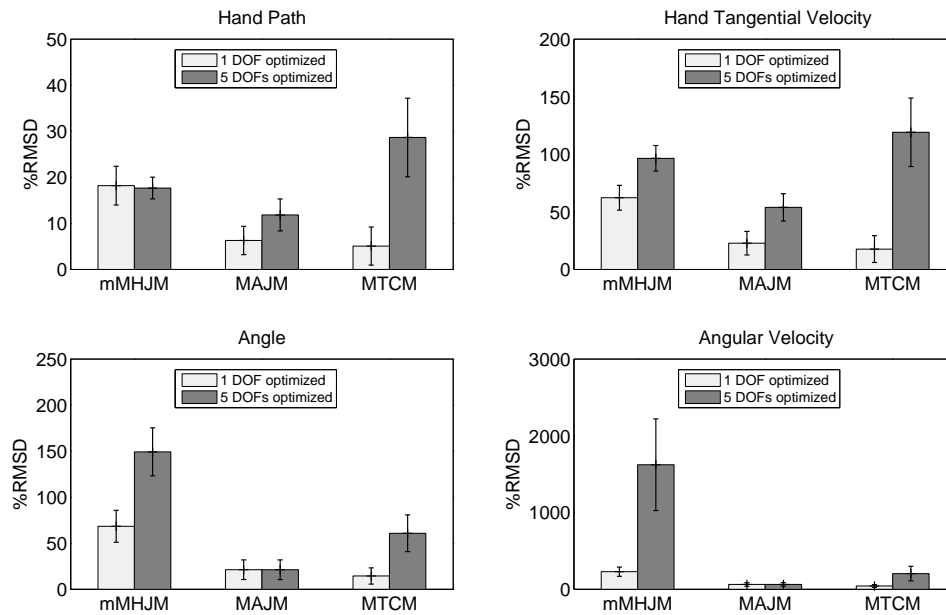
**Figure 5.41:** Mean of the %RMSDs for elbow flexion/extension under two different optimization conditions. Error bars indicate the 99 % confidence intervals.

exhibit that when the DOFs to be optimized were increased the %RMSDs for the joint angular velocities increased for mMHJM and MTCM and remained the same for MAJM. Paired two-sample t-tests revealed significant differences for mMHJM ( $T = -8.662, p \leq .001$ ) and MTCM ( $T = -5.462, p \leq .001$ ). The paired two-sample t-tests revealed no significant differences for MAJM ( $T = -.994, p = .326$ ).

### 1 DOF optimized vs. 5 DOFs optimized: Elbow flexion/extension

The results of the %RMSDs between the two conditions (Fig. 5.41, top left) exhibit that when the DOFs to be optimized were increased the %RMSDs of the hand paths of mMHJM, MAJM and MTCM were increased. Paired two-sample t-tests revealed no significant differences for MAJM ( $T = 2.606, p = .012$ ), mMHJM ( $T = -.943, p = .351$ ) and MTCM ( $T = -1.778, p = .083$ ).

The results of the %RMSDs between the two conditions (Fig. 5.41, top right) exhibit that when the DOFs to be optimized were increased the %RMSDs of the tangential hand velocities of all three optimal control models were increased. Paired two-sample t-tests revealed significant differences for mMHJM ( $T = -7.405, p \leq .001$ ), MAJM ( $T = -4.993, p \leq .001$ ) and MTCM ( $T = -3.523, p \leq .001$ ).



**Figure 5.42:** Mean of the %RMSDs for thorax rotation under two different optimization conditions. Error bars indicate the 99 % confidence intervals.

The results of the %RMSDs between the two conditions (Fig. 5.41, bottom left) exhibit that when the DOFs to be optimized were increased the %RMSDs of the joint angles increased for mMHJM, decreased for MTCM and remained the same for MAJM. Paired two-sample t-tests revealed significant differences for mMHJM ( $T = -8.669, p \leq .001$ ) and no significant differences for MAJM ( $T = -1.297, p = .202$ ) and MTCM ( $T = .728, p = .471$ ).

The %RMSDs between the two conditions (Fig. 5.41, bottom right) exhibit that when the DOFs to be optimized were increased the %RMSDs for the joint angular velocities increased for mMHJM and MTCM and remained the same for MAJM. Paired two-sample t-tests revealed significant differences for mMHJM ( $T = -8.590, p \leq .001$ ) and MTCM ( $T = -4.834, p \leq .001$ ). The paired two-sample t-tests revealed no significant differences for MAJM ( $T = 1.374, p = .177$ ).

### 1 DOF optimized vs. 5 DOFs optimized: Thorax rotation

The results of the %RMSDs between the two conditions (Fig. 5.42, top left) exhibit that when the DOFs to be optimized were increased the %RMSDs of the hand paths of mMHJM were decreased and for MAJM as well as MTCM were increased. Paired two-sample t-tests revealed significant differences for MAJM ( $T = -3.712, p \leq .001$ ) and MTCM ( $T = -7.020, p \leq .001$ ) and no significant differences for mMHJM ( $T = .269, p = .789$ ).

The results of the %RMSDs between the two conditions (Fig. 5.42, top right) exhibit that when the DOFs to be optimized were increased the %RMSDs of the tangential hand velocities of all three optimal control models were increased. Paired two-sample t-tests revealed significant differences for mMHJM ( $T = -6.259, p \leq .001$ ), MAJM ( $T = -6.106, p \leq .001$ ) and MTCM ( $T = -9.997, p \leq .001$ ).

The results of the %RMSDs between the two conditions (Fig. 5.42, bottom left) exhibit that when the DOFs to be optimized were increased the %RMSDs of the joint angles increased for mMHJM and MTCM and remained the same for MAJM. Paired two-sample t-tests revealed significant differences for mMHJM ( $T = -7.324, p \leq .001$ ) and MTCM ( $T = -5.474, p \leq .001$ ) and no significant differences for MAJM ( $T = -1.290, p = .205$ ).

The results of the %RMSDs between the two conditions (Fig. 5.42, bottom right) exhibit that when the DOFs to be optimized were increased the %RMSDs for the joint angular velocities were increased for mMHJM and MTCM and remained the same for MAJM. Paired two-sample t-tests revealed significant differences for mMHJM ( $T = -6.452, p \leq .001$ ) and MTCM ( $T = -4.357, p \leq .001$ ). The paired two-sample t-tests revealed no significant differences for MAJM ( $T = 1.248, p = .219$ ).

### **1 DOF optimized vs. 5 DOFs optimized: Torques**

The results of the %RMSDs between the two conditions (Fig. 5.43) exhibit that when the DOFs to be optimized were increased the %RMSDs of the torques of MTCM were decreased for thorax rotation and shoulder abduction/adduction and increased for shoulder rotation, shoulder anteversion/retroversion and elbow flexion/extension. Paired two-sample t-tests revealed significant differences for elbow flexion/extension ( $T = -3.052, p \leq .01$ ) and no significant differences for thorax rotation ( $T = 1.799, p = .080$ ), shoulder abduction/adduction ( $T = 2.099, p = .042$ ), shoulder rotation ( $T = -1.841, p = .073$ ) and shoulder anteversion/retroversion ( $T = -.441, p = .661$ ).

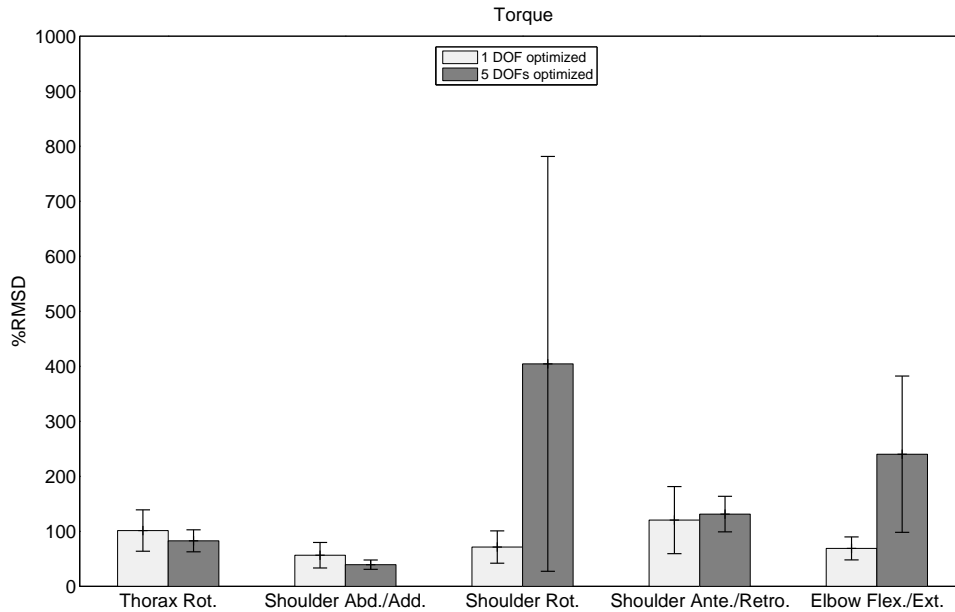


**Figure 5.43:** Mean of the %RMSDs of torques for MTCM across the five DOFs under different optimization conditions. Error bars indicate the 99 % confidence intervals.

### 5.3.3.3 Similarities between the measured and predicted trajectories

In this section the similarities between the measured and predicted trajectories are analyzed based on the approach described in section 5.2.8. First, the similarity coefficients  $sim$  (Eq. 5.16) for each optimized DOF was analyzed separately (Chap. 5.3.3.3.1). The optimization condition “1 DOF optimized” and “5 DOFs optimized” are respectively shown in one table. The second step involved the analysis of the similarity coefficients  $SIM$  (Eq. 5.17) for the optimization condition “5 DOFs optimized” (Chap. 5.3.3.3.2).

#### 5.3.3.3.1 Similarities between the measured and predicted trajectories of single DOFs

In this section the similarities between the measured and predicted trajectories of MHJM, mMHJM, MAJM and MTCM under the two conditions “1 DOF optimized” and “5 DOFs optimized” are discussed for each of the five DOFs. The analysis was carried out according to the simulation protocol (Tab. 5.1).

**Table 5.8:** Mean of the similarity coefficients between the measured and predicted trajectories ( $N = 40$ ) of MHJM, mMHJM, MAJM and MTCM for shoulder abduction/adduction under two optimization conditions.  $R$  corresponds to the hand paths in 3D space,  $Rp$  to the tangential velocities of the hand,  $q$  to joint angles,  $qp$  to joint angular velocities and  $T$  to joint torques.

	“1 DOF optimized”				“5 DOFs optimized”			
	MHJM	mMHJM	MAJM	MTCM	MHJM	mMHJM	MAJM	MTCM
$R$	.9956	.9958	.9980	.9918	.9956	.9904	.9979	.9916
$Rp$	.9588	.9469	.9787	.9132	.9588	.8531	.9729	.8834
$q$	-	.9850	.9934	.9739	-	.9692	.9934	.9402
$qp$	-	.7788	.8846	.7286	-	.6430	.8846	.5543
$T$	-	-	-	.5264	-	-	-	.5372

### Shoulder abduction/adduction

The results (Tab. 5.8) for the hand paths ( $R$ ) exhibited only small differences in the similarity coefficients between the different optimal control models for both optimization conditions. When 1 DOF was optimized MAJM revealed the highest similarity coefficient for the tangential hand velocities ( $Rp$ ) followed by MHJM, mMHJM and MTCM. If 5 DOFs were optimized MAJM exhibited the highest coefficient followed by MHJM, MTCM and mMHJM. Furthermore, the coefficients were smaller under the condition “5 DOFs optimized” than under the condition “1 DOF optimized”. Finally, the coefficients of the tangential hand velocities were smaller than the coefficients of the hand paths. For the joint angles ( $q$ ) the optimal control models exhibited only small differences in the similarity coefficients under the condition “1 DOF optimized”. These differences increased when 5 DOFs were optimized. Thereby, MAJM showed the closest fit to the measured trajectories followed by mMHJM and MTCM. In the case of joint angular velocities ( $qp$ ) MAJM revealed the highest coefficients under both optimization conditions. The similarity coefficients for the joint torques ( $T$ ) were comparable between the two optimization conditions.

**Table 5.9:** Mean of the similarity coefficients between the measured and predicted trajectories ( $N = 40$ ) of MHJM, mMHJM, MAJM and MTCM for shoulder rotation under two optimization conditions.  $R$  corresponds to the hand paths in 3D space,  $Rp$  to the tangential velocities of the hand,  $q$  to joint angles,  $qp$  to joint angular velocities and  $T$  to joint torques.

	“1 DOF optimized”				“5 DOFs optimized”			
	MHJM	mMHJM	MAJM	MTCM	MHJM	mMHJM	MAJM	MTCM
$R$	.9956	.9976	.9996	.9976	.9956	.9904	.9979	.9916
$Rp$	.9588	.9624	.9915	.9608	.9588	.8531	.9729	.8834
$q$	-	.7676	.9704	.8077	-	.6641	.9704	.6887
$qp$	-	.0659	.8413	.4117	-	.0996	.8413	.3346
$T$	-	-	-	.5356	-	-	-	.1911

### Shoulder rotation

The results (Tab. 5.9) for the hand paths ( $R$ ) revealed only small differences in the similarity coefficients between the different optimal control models for both optimization conditions. When 1 DOF was optimized MAJM showed the highest similarity coefficient for the tangential hand velocities ( $Rp$ ). The coefficients for MHJM, mMHJM and MTCM were comparable. When 5 DOFs were optimized MAJM exhibited the highest coefficient followed by MHJM, MTCM and mMHJM. Moreover, the coefficients were smaller under the condition “5 DOFs optimized” than under the condition “1 DOF optimized”. Finally, the coefficients of the tangential hand velocities were smaller than the coefficients of the hand paths. In joint space ( $q$  and  $qp$ ) MAJM showed the closest fit to the measured data followed by MTCM and mMHJM. Furthermore, these similarity coefficients were much smaller than the coefficients of shoulder abduction/adduction. The similarity coefficients for the joint torques ( $T$ ) were substantially higher when 1 DOF was optimized than when 5 DOFs were optimized.

**Table 5.10:** Mean of the similarity coefficients between the measured and predicted trajectories ( $N = 40$ ) of MHJM, mMHJM, MAJM and MTCM for shoulder anteversion/retroversion under two optimization conditions.  $R$  corresponds to the hand paths in 3D space,  $Rp$  to the tangential velocities of the hand,  $q$  to joint angles,  $qp$  to joint angular velocities and  $T$  to joint torques.

	"1 DOF optimized"				"5 DOFs optimized"			
	MHJM	mMHJM	MAJM	MTCM	MHJM	mMHJM	MAJM	MTCM
$R$	.9956	.9999	1.0000	.9999	.9956	.9904	.9979	.9916
$Rp$	.9588	.9916	.9987	.9948	.9588	.8531	.9729	.8834
$q$	-	.6113	.9008	.7681	-	.2669	.9008	.4921
$qp$	-	.3138	.5175	.6428	-	.0664	.5175	.3514
$T$	-	-	-	.7190	-	-	-	.6271

### Shoulder anteversion/retroversion

The results (Tab. 5.10) for the hand paths ( $R$ ) exhibited only small differences in the similarity coefficients between the different optimal control models for both optimization conditions. If 1 DOF was optimized the coefficients for the tangential hand velocities ( $Rp$ ) of mMHJM, MAJM and MTCM were comparable, whereas the coefficient of MHJM was smaller. If 5 DOFs were optimized MAJM exhibited the highest coefficient followed by MHJM, MTCM and mMHJM. Moreover, the coefficients were smaller under the condition "5 DOFs optimized" than under the condition "1 DOF optimized". Finally, the coefficients of the tangential hand velocities were smaller than the coefficients of the hand paths. In joint space ( $q$ ) MAJM showed the closest fit to the measured joint angles followed by MTCM and mMHJM. MTCM revealed the closest fit to the measured joint angular velocity profiles ( $qp$ ) under the condition "1 DOF optimized" followed by MAJM and mMHJM. In contrast, when 5 DOFs were optimized MAJM exhibited the highest similarity coefficients followed by MTCM and mMHJM. The similarity coefficients for the joint torques ( $T$ ) were higher when 1 DOF was optimized than when 5 DOFs were optimized.

**Table 5.11:** Mean of the similarity coefficients between the measured and predicted trajectories ( $N = 40$ ) of MHJM, mMHJM, MAJM and MTCM for elbow flexion/extension under two optimization conditions.  $R$  corresponds to the hand paths in 3D space,  $Rp$  to the tangential velocities of the hand,  $q$  to joint angles,  $qp$  to joint angular velocities and  $T$  to joint torques.

	“1 DOF optimized”				“5 DOFs optimized”			
	MHJM	mMHJM	MAJM	MTCM	MHJM	mMHJM	MAJM	MTCM
$R$	.9956	.9995	.9999	.9999	.9956	.9904	.9979	.9916
$Rp$	.9588	.9936	.9991	.9811	.9588	.8531	.9729	.8834
$q$	-	.5528	.8946	.7178	-	.6999	.8946	.3455
$qp$	-	.3948	.7447	.6658	-	.5750	.7447	.3179
$T$	-	-	-	.1054	-	-	-	.0834

### Elbow flexion/extension

The results (Tab. 5.11) for the hand paths ( $R$ ) revealed only small differences in the similarity coefficients between the different optimal control models for both optimization conditions. When 1 DOF was optimized the coefficients for the tangential hand velocities ( $Rp$ ) of mMHJM, MAJM and MTCM were comparable, whereas the coefficient of MHJM was smaller. When 5 DOFs were optimized MAJM exhibited the highest coefficient followed by MHJM, MTCM and mMHJM. Moreover, the coefficients were smaller under the condition “5 DOFs optimized” than under the condition “1 DOF optimized”. Finally, the coefficients of the tangential hand velocities were smaller than the coefficients of the hand paths. In joint space ( $q$  and  $qp$ ) MAJM showed the closest fit to the measured data. The similarity coefficients for the joint torques ( $T$ ) were comparable between the two optimization conditions and rather small in both cases.

**Table 5.12:** Mean of the similarity coefficients between the measured and predicted trajectories ( $N = 40$ ) of MHJM, mMHJM, MAJM and MTCM for the thorax rotation under two optimization conditions.  $R$  corresponds to the hand paths in 3D space,  $Rp$  to the tangential velocities of the hand,  $q$  to joint angles,  $qp$  to joint angular velocities and  $T$  to joint torques.

	“1 DOF optimized”				“5 DOF optimized”			
	MHJM	mMHJM	MAJM	MTCM	MHJM	mMHJM	MAJM	MTCM
$R$	.9956	.9998	1.0000	1.0000	.9956	.9904	.9979	.9916
$Rp$	.9588	.9912	.9996	.9998	.9588	.8531	.9729	.8834
$q$	-	.6243	.9826	.9887	-	.3889	.9826	.8689
$qp$	-	.3372	.8377	.8685	-	.0970	.8377	.3975
$T$	-	-	-	.6845	-	-	-	.6099

### Thorax rotation

The results (Tab. 5.12) for the hand paths ( $R$ ) revealed only small differences in the similarity coefficients between the different optimal control models for both optimization conditions. When 1 DOF was optimized the similarity coefficients of the tangential hand velocities ( $Rp$ ) between mMHJM, MAJM and MTCM were comparable, whereas the coefficient for MHJM was smaller. When 5 DOFs were optimized MAJM exhibited the highest coefficient followed by MHJM, MTCM and mMHJM. The coefficients were smaller under the condition “5 DOFs optimized” than under the condition “1 DOF optimized”. Furthermore, the coefficients of the tangential hand velocities were smaller than the coefficients of the hand paths. In joint space ( $q$  and  $qp$ ) MTCM revealed the highest coefficient followed by MAJM and mMHJM under the condition “1 DOF optimized”. In contrast, when 5 DOFs were optimized MAJM exhibited the closest fit to the measured movement followed by MTCM and mMHJM. In joint space the values for mMHJM and MTCM were smaller when more DOFs were optimized. The similarity coefficients for the joint torques ( $T$ ) were higher when 1 DOF was optimized than when 5 DOFs were optimized.

**Table 5.13:** Mean of similarities coefficients between multiple measured and predicted joint angles, joint angular velocities and joint torques ( $N = 40$ ) of the mMHJM, the MAJM and the MTCM for the shoulder abduction/adduction, shoulder rotation, shoulder anteversion/retroversion, elbow flexion/extension and thorax rotation. Thereby,  $q$  corresponds to joint angles,  $qp$  to joint angular velocities and  $T$  to joint torques.

	mMHJM	MAJM	MTCM
$q$	.5409	.9064	.5775
$qp$	.2707	.6769	.3236
$T$	-	-	.4714

### 5.3.3.3.2 Similarities between the measured and predicted trajectories of multiple DOFs

The results (Tab. 5.13) of the similarity coefficients between the measured and predicted trajectories of multiple DOFs revealed that in intrinsic kinematic coordinates ( $q$  and  $qp$ ) MAJM showed the closest fit to the measured data. The performance of mMHJM and MTCM was comparable but considerably worse than the performance of MAJM. The similarity coefficient for the joint torques ( $T$ ) was comparable to the coefficient for target 1 (Tab. 5.7).

## 5.4 Discussion

The results outlined above are discussed with respect to the introduced theoretical assumptions of biological motor control and the development of humanoid robots that move in a human-like way. Additionally, the applied methods are discussed.

### 5.4.1 Biological motor control

Movement generation in biological systems is ill-posed in the sense that the task requirements can generally be met by an infinite number of different movements. Despite the complexity of the human motor system (Chap. 2.2, 2.4.1.2), behavioral research has discovered various regularities in human goal-directed movements (Chap. 2.3.3.1, 4). These regularities are key issues in understanding the coordination of human movements as they seem to indicate some fundamental organizational principles of the CNS. Optimal control models can reproduce behavioral regularities on multiple levels (Todorov, 2004). Although these models have been established in technical literature for some years, a quantitative comparison between the performance of these models for multi-joint movements in 3D space is a fairly new concept (Admiraal et al., 2004; Kaphle and Eriksson, 2008; Gielen, 2009b). Therefore, the purpose of this study was to quantitatively examine if optimal control models can reproduce multi-joint pointing movements in 3D space. Optimal control models can be grouped into open-loop and closed-loop models (Chap. 2.3.3.1). In this study, we concentrated on open-loop or feed-forward control. It should be recognized that open-loop models cannot model all types of human movements. The CNS uses feed-forward control presumably in the context of fast or highly practiced movements (Heuer and Konczak, 2003). In this context, pointing to distal visual targets, which are in the visual field of the subjects, is a potential candidate for feed-forward control. However, it is a difficult task to find the optimal control policy that the CNS may use to overcome the excessive number of DOFs and choose one movement from the infinite number of possible movements. Therefore, it is not surprising that in technical literature different optimal control models are discussed (Kawato, 1996; Todorov, 2004). Besides the question of which optimization principle the CNS may use to solve the introduced ill-posed problems of movement generation, it should be asked on which levels in the sensorimotor system these principles work. Expressly, in which coordinate frame or space are human movements planned. As outlined in chapters 2.3.3.1 and 5.1, it is currently impossible to identify the space in which human movements are planned. We addressed the problem of motor redundancy and the problem of planning spaces together by comparing trajectories predicted by optimal control models defined in different planning spaces and using experimentally determined trajectories. We focused on extrinsic-kinematic space, intrinsic-kinematic space and intrinsic-dynamic-mechanic space (Fig. 5.1) and tested a minimum hand jerk model (Flash and Hogan, 1985), a minimum angle jerk model (Wada et al.,

2001) and a minimum torque change model (Uno et al., 1989). Furthermore, we developed an optimal control model, referred to as the modified hand jerk model, which works on both an extrinsic and intrinsic kinematic level. Many studies indicate a planning in extrinsic coordinates of the hand (Chap. 2.3.3.1). However, planning purely in extrinsic coordinates without any consideration of joint limits seems debatable. Although this model is still in an early stage of development, we examined the performance of the model compared to the established models discussed in this study. It should be noted that the experimental design presented here is based on the assumption that actual trajectories are close to planned trajectories, although this assumption is generally considered valid (Osu et al., 1997; Nakano et al., 1999).

### **Target 1**

The results of the %RMSDs between the measured and predicted trajectories revealed that none of the optimal control models were able to completely reproduce human movements. Computer simulations indicate that MAJM has the closest fit to the measured hand paths. MAJM generated the smallest %RMSDs for all four DOFs, although in the case of the shoulder anteversion/retroversion, no significant differences to MHJM and MTCM were observed. MHJM and MTCM produced the second and third smallest %RMSDs, respectively. For the optimization of elbow flexion/extension, no significant differences between the %RMSD of the measured and predicted tangential hand velocities of MAJM and MHJM were noted. The comparison of the measured and predicted hand trajectories indicate a planning in intrinsic kinematic coordinates. However, if one understands motor control as a cascade of sensorimotor transformations (Fig. 2.2), the transformation from extrinsic kinematic coordinates to intrinsic kinematic coordinates would be omitted. In other words, it appears the CNS developed a strategy to avoid at least one of the ill-posed transformations (Chap. 2.2). If this assumption is correct, MAJM should also achieve the best results on joint level. The results show that MAJM produced the smallest %RMSDs in intrinsic kinematic coordinates for all four DOFs (Chap. 5.3.2.2.1). For the optimization of shoulder rotation and elbow flexion, MAJM generated significantly smaller %RMSDs than the other models. For the optimization of shoulder abduction/adduction, no significant differences between the measured and predicted joint angles of MAJM and mMhJM were observed. mMhJM produced the second smallest %RMSD. Furthermore, no significant differences for the joint angular velocities were detected. In the case of the shoulder anteversion/retroversion, the differences in the %RMSDs between MAJM and MTCM were not significant. In addition to the %RMSDs, we calculated similarity coefficients between the measured and predicted trajectories. MAJM generated the highest coefficients for the optimization of the DOFs of shoulder abduction/adduction, shoulder rotation and elbow flexion/extension. In the case of the shoulder anteversion/retroversion, MAJM produced the highest coefficients for the quantities defined in extrinsic kinematic coordinates. In contrast, MTCM generated the highest coefficients for the quantities

defined in intrinsic kinematic coordinates. In addition, it should be noted that the differences between the coefficients in extrinsic kinematic coordinates are sometimes small. In summary, during the optimization of one DOF, MAJM showed the best performance across the four DOFs. Based on these findings, a planning in intrinsic kinematic coordinates seems the most reasonable. Additionally, the 99 % confidence intervals displayed in figures 5.11, 5.12, 5.13 and 5.14 exhibit large variations of the means for MTCM. These variations can presumably be attributed to the applied optimization method (Chap. 5.4.3). Because the optimization process is the most complex in intrinsic dynamic coordinates, it is conceivable that the optimization algorithm did not converge in all cases.

The results indicate that although MAJM produced the smallest %RMSDs in all cases, it is not significantly superior to the remaining optimal control models in all cases. The mean values of the different optimal control models in figures 5.11, 5.12, 5.13 and 5.14, reveal partly large differences in the %RMSDs for the different DOFs. This suggests that the CNS may not use one optimization principle in the process of motor planning, but several models or different combinations of models. Moreover, it is conceivable that the CNS may use different control strategies for different DOFs. For example, in shoulder abduction/adduction, the CNS may adopt a minimum jerk strategy, whereas in the elbow joint, the preferred strategy may be a minimization of torque change. In this case, it would have to be expected that the performances of an optimal control model differs for the four DOFs. We therefore tested MAJM and MTCM to determine if significant differences in the performance for the four DOFs exist within each model.

In intrinsic kinematic coordinates, MAJM exhibited the smallest %RMSDs between the measured and predicted joint angles for shoulder abduction/adduction, followed by elbow flexion/extension, shoulder anteversion/retroversion and shoulder rotation (Fig. 5.16). Statistical analysis revealed significant differences between shoulder abduction/adduction and shoulder anteversion/retroversion and shoulder rotation. MAJM revealed the smallest %RMSDs between the measured and predicted joint angular velocities for shoulder abduction/adduction, followed by shoulder rotation, elbow flexion/extension and shoulder anteversion/retroversion. Statistical analysis showed that MAJM produced significantly smaller %RMSDs between the measured and predicted joint angular velocities for shoulder abduction/adduction than for all other DOFs. Based on these results, a MAJ-strategy seems the most plausible for shoulder abduction/adduction. A coordinate transformation in extrinsic kinematic coordinates exhibited the smallest %RMSDs for shoulder rotation, followed by shoulder abduction/adduction, elbow flexion/extension and shoulder anteversion/retroversion (Fig. 5.16). The statistical analysis yielded significant differences between shoulder rotation and elbow flexion/extension as well as shoulder anteversion/retroversion. Moreover, significant differences between shoulder abduction/adduction and elbow flexion/extension, and the shoulder anteversion/retroversion were observed. These results indicate that in extrinsic kinematic co-

ordinates, a MAJ-strategy appears to be more feasible for shoulder abduction/adduction and shoulder rotation, than for the shoulder anteversion/retroversion and elbow flexion/extension. Several explanations exist to explain the performance differences of MAJM in extrinsic and intrinsic kinematic coordinates for the four DOFs. If the results for hand paths and joint angles are compared, MAJM produced the lowest %RMSD for shoulder rotation in the extrinsic kinematic coordinates and the highest %RMSD in intrinsic kinematic coordinates for the four DOFs. One explanation could be that a rotation in the shoulder joint does not have a large effect on the hand path in this movement task. In summary, there are differences in the performance of MAJM between the individual DOFs and between extrinsic and intrinsic space. Although MAJM reproduced the human shoulder abduction/adduction best, different movement tasks should be tested in future studies to aid in the improvement of the understanding of the relationship between movement tasks and planning strategies.

The %RMSDs between the measured and predicted torques of shoulder abduction/adduction were significantly smaller than the %RMSDs of the shoulder anteversion/retroversion and elbow flexion/extension. MTCM produced significantly smaller %RMSDs between the measured and predicted torques during shoulder rotation than during shoulder anteversion/retroversion. Therefore, a MTC-strategy seems more likely for shoulder abduction/adduction than for the shoulder anteversion/retroversion or elbow flexion/extension. In addition, a MTC-strategy seems more probable for shoulder rotation than for the shoulder anteversion/retroversion. However, due to the intersegmental dynamics, it is difficult to determine in which DOF a MTC-strategy would be most suitable. A coordinate transformation from intrinsic dynamic to intrinsic kinematic space shows that MTCM yielded significantly smaller %RMSDs for shoulder abduction/adduction than for all other DOFs. A coordinate transformation from intrinsic-kinematic to extrinsic-kinematic space exhibited the smallest %RMSDs for shoulder abduction/adduction, followed by shoulder rotation, shoulder anteversion/retroversion and elbow flexion/extension (Fig. 5.17). Statistical analysis yielded significant differences between the %RMSDs of the measured and predicted hand paths of shoulder abduction/adduction and shoulder anteversion/retroversion as well as elbow flexion/extension. Shoulder rotation generated significantly smaller %RMSDs than elbow flexion/extension. Furthermore, the %RMSDs of the measured and predicted tangential hand velocities of shoulder abduction/adduction were significantly smaller than the %RMSDs of elbow flexion/extension. MTCM generated significantly smaller %RMSDs during shoulder rotation than during elbow flexion/extension. As before, there are differences in performance of the tested optimal control model between the individual DOFs for the three coordinate frames. Possible explanations for these differences have been discussed above in the context of MAJM. In summary, MTCM generated the smallest %RMSDs for shoulder abduction/adduction in extrinsic kinematic coordinates, intrinsic kinematic coordinates and intrinsic-dynamic coordinates. In 11 of 15 comparisons, MTCM produced significantly smaller %RMSDs for shoulder abduc-

tion/adduction than for the other DOFs. Therefore, a MTC-strategy seems the most likely for shoulder abduction/adduction. Furthermore, a MTC-strategy does not seem possible for the shoulder anteversion/retroversion or elbow flexion/extension. However, as previously stated, due to the complex intersegmental dynamics, it is difficult to determine in which DOF a MTC-strategy would best be suited because the torque generation is influenced by the torque generation in neighboring joints.

In addition to the simulations involving one DOF, we conducted simulations with four DOFs. The results of the %RMSDs between the measured and predicted trajectories revealed that none of the optimal control models were able to completely reproduce the measured hand trajectories (Fig. 5.15). In extrinsic kinematic space, MAJM produced the smallest %RMSDs between the measured and predicted hand paths, followed by MHJM, mMHJM and MTCM. However, statistical analysis revealed no significant differences in the model performance. MAJM also produced the smallest %RMSDs between the measured and predicted tangential hand velocities, followed by MHJM, mMHJM and MTCM. Statistical analysis revealed significant differences in %RMSDs between MAJM and MTCM, and between MHJM and MTCM. In intrinsic kinematic coordinates, MAJM produced significantly smaller %RMSDs than the other optimal control models. In addition to these results, the 99 % confidence intervals of the MTC-trajectories show large variations of the means. This could be an indication of numerical problems of the optimization algorithm during the simulations (Chap. 5.4.3). MAJM generated the smallest %RMSDs in extrinsic and intrinsic coordinates, although statistical analysis yielded no significant differences between the measured and predicted hand paths of the four optimal control models. These results can be explained by the fact that one single human hand path can be the consequence of different joint angle sequences due to the mechanical redundancy on joint level. In other words, the measured and predicted joint angle sequences can differ significantly in intrinsic kinematic coordinates and at the same time result in similar hand paths if transformed into extrinsic kinematic coordinates. Besides the %RMSDs, we calculated similarity coefficients between the measured and predicted trajectories. When multiple DOFs were optimized, MAJM generated the highest coefficients in extrinsic kinematic coordinates (e.g. Tab. 5.3) and intrinsic kinematic coordinates (Tab. 5.7). It should be noted that the differences between the coefficients of the hand paths were sometimes small. In summary, MAJM produced the closest fit to the measured data, indicating a planning in intrinsic kinematic coordinates.

In the case of multi-joint optimization, the %RMSD is the result of an optimization of multiple joints. Tests conducted in this study were used to determine if there are performance differences for the different DOFs. Large differences could be a sign that the CNS uses different optimization principles for the DOFs of the human body. As before, we examined MAJM and MTCM to determine if significant differences in the approximation of human movements across the four DOFs exist.

In intrinsic kinematic coordinates, MAJM exhibited the smallest %RMSDs between the measured and predicted joint angles for shoulder abduction/adduction, followed by elbow flexion/extension, shoulder anteversion/retroversion and shoulder rotation. Statistical analysis revealed significant differences between shoulder abduction/adduction and shoulder anteversion/retroversion as well as shoulder rotation. MAJM revealed the smallest %RMSDs between the measured and predicted joint angular velocities for shoulder abduction/adduction, followed by shoulder rotation, elbow flexion/extension and shoulder anteversion/retroversion. Statistical analysis showed that MAJM produced significantly smaller %RMSDs between the measured and predicted joint angular velocities for shoulder abduction/adduction than for all other DOFs. These results correspond to the results of the condition “1 DOF optimized”. Because in intrinsic kinematic coordinates each DOF is optimized separately, these results indicate a correct performance of the computational framework. Furthermore, these results suggest that it is more likely that the CNS uses a MAJ-strategy for movement planning in the DOF of shoulder abduction/adduction than in the other tested DOFs.

MTCM produced the smallest %RMSDs for shoulder abduction/adduction, followed by shoulder rotation, shoulder anteversion/retroversion and elbow flexion/extension in intrinsic dynamic coordinates. Statistical analysis revealed significant differences between the %RMSDs of shoulder abduction/adduction and the shoulder anteversion/retroversion. MTCM showed significantly smaller %RMSDs in intrinsic kinematic coordinates for shoulder abduction/adduction than for the other DOFs. These results indicate that a MTC-strategy appears most likely for shoulder abduction/adduction. In addition, the 99 % confidence intervals indicate large deviations of the means that may be explained by numerical problems in the optimization algorithm during the simulation (Chap. 5.4.3). In summary, a MTC-strategy appears most plausible for shoulder abduction/adduction.

Two results were robust across the two conditions “1 DOF optimized” and “4 DOF optimized”. Firstly, MAJM showed the closest fit to the measured data in both extrinsic kinematic coordinates and intrinsic kinematic coordinates, indicating that motor planning may take place in intrinsic kinematic coordinates. Secondly, significant differences across the optimized DOFs were found for MAJM and MTCM, indicating that the CNS may use more than one optimization principle to reduce the available DOFs. However, under both optimization conditions and for both optimal control models, the optimization of shoulder abduction/adduction exhibited the closest fit to the measured data. It should be noted that MAJM produced

significantly smaller %RMSDs between the measured and predicted joint angles under both conditions than MTCM. Moreover, MTCM showed high mean values for the %RMSDs with large confidence intervals. The results do not necessarily indicate that MTCM cannot reproduce measured movements nor do they suggest that this is a strategy the CNS does not use. Because the optimization on torque level is very complex and the results indicate that the optimization algorithm did not converge in all cases, the poor results may in some cases be attributable to methodological problems.

### **Target 3**

The results of the %RMSDs between the measured and predicted trajectories revealed that none of the optimal control models were able to completely reproduce the measured movements. MAJM generated significantly smaller %RMSDs in extrinsic kinematic coordinates across all five DOFs than the other models (Fig. 5.30, 5.31, 5.32, 5.33, 5.34), with two exceptions. For shoulder abduction/adduction, mMHJM exhibited a comparable performance for the tangential hand velocities and for thorax rotation, MTCM produced comparable results. Moreover, MTCM showed relatively high mean values for the %RMSDs with large confidence intervals, which can most likely be explained by methodological problems. The comparison of the measured and predicted hand trajectories indicate a planning in intrinsic kinematic coordinates. In the case of thorax rotation, a planning in intrinsic dynamic coordinates appears to be possible. As before, these results likely indicate that the CNS uses different optimization principles or combinations of optimization principles. These interpretations are corroborated by the findings on the joint level. MAJM produced significantly smaller %RMSDs across all five DOFs in intrinsic kinematic coordinates than all other models (Fig. 5.30, 5.31, 5.32, 5.33, 5.34). As before, the statistical analysis revealed two exceptions. Comparable results were produced for both shoulder abduction/adduction by mMHJM and thorax rotation by MTCM. In addition to the %RMSDs, similarity coefficients between the measured and predicted trajectories were calculated. MAJM generated the highest coefficients for the optimization of the DOFs of shoulder abduction/adduction, shoulder rotation and elbow flexion/extension. In the case of the shoulder anteversion/retroversion, MAJM produced the highest coefficients for the quantities defined in extrinsic kinematic coordinates and for the joint angular profiles, whereas MTCM exhibited the highest coefficients for the joint angular velocity profiles. In the case of thorax rotation, MAJM generated the highest coefficients for the hand paths, whereas MTCM exhibited the highest coefficients for the tangential hand velocities, the joint angular profiles and the joint angular velocity profiles. It should be noted that the differences between the coefficients are sometimes small. The 99 % confidence intervals of the %RMSDs of joint angle trajectories displayed in figures 5.30, 5.31, 5.32, 5.33 exhibit large variations of the means for MTCM compared to mMHJM and MAJM. However, these variations likely indicate that the optimization algorithm did not converge in all cases. In summary, during the optimization of one

DOF, MAJM showed the best performance across the five DOFs. Based on these findings, a planning in intrinsic kinematic coordinates seems the most feasible.

The results indicate that although MAJM produced, in most cases, the smallest %RMSDs, it is not in any case superior to the other optimal control models. Furthermore, the mean values of the different optimal control models in figures 5.30, 5.31, 5.32, 5.33, 5.34 reveal moderately large differences in the %RMSDs across the different DOFs. These findings indicate that the CNS may not use a single optimization principle in the process of motor planning but different planning strategies for different DOFs. We therefore tested MAJM and MTCM to determine if there are significant differences in the performance across the five DOFs.

In extrinsic kinematic coordinates, the statistical analysis for MAJM across the five DOFs yielded no significant differences between the %RMSDs of the measured and predicted hand paths and the tangential hand velocities (Fig. 5.36). Moreover, no significant differences for the five DOFs between %RMSDs of the measured and predicted joint angles were found. In contrast, statistical analysis revealed significant differences across the five DOFs between %RMSDs of the measured and predicted joint angular velocities. MAJM produced the smallest %RMSD for shoulder abduction/adduction, which is significantly smaller than the %RMSDs of shoulder rotation, shoulder anteversion/retroversion and elbow flexion. These findings suggest that MAJM is able to approximate the measured angle paths across the five DOFs in a similar quality, but not the joint angular velocity profiles. Based on the results, it seems apparent that the CNS does not use only a MAJ-strategy to reduce the available DOFs. However, in extrinsic kinematic coordinates no differences across the individual DOFs were found.

MTCM showed no significant differences across the five DOFs (Fig. 5.37) in intrinsic dynamic coordinates. In intrinsic and extrinsic kinematic coordinates, statistical analysis yielded significantly smaller %RMSDs for thorax rotation than for all other DOFs, with one exception. Although the %RMSD between the measured and predicted joint angles of thorax rotation is smaller than that of shoulder abduction/adduction, the differences are only significant in trend. These findings indicate that at least for the kinematics, a MTC-strategy appears to be the most likely model for thorax rotation. However, this result cannot be confirmed on torque level because there were no significant differences between the five DOFs. As previously noted, due to the complex intersegmental dynamics, it is difficult to determine in which DOF a MTC-strategy would be most feasible because torque generation is influenced by the torque generation in neighboring joints.

In addition to the optimizations for one DOF, we conducted simulations for five DOFs. MAJM produced the smallest %RMSDs in intrinsic kinematic coordinates and extrinsic kinematic coordinates (Fig 5.35). In intrinsic kinematic coordinates, MAJM was superior to all other optimal control models. Furthermore, MAJM generated significantly smaller %RMSDs between the measured and predicted hand paths than mMHJM and MTCM. Statistical analysis yielded no significant differences be-

tween the %RMSDs of the measured and predicted hand paths of MAJM and MHJM. Moreover, MAJM produced smaller %RMSDs between the measured and predicted hand tangential velocities than all other optimal control models. In addition to the %RMSDs, similarity coefficients between the measured and predicted trajectories were calculated. When multiple DOFs were optimized, MAJM generated the highest coefficients in extrinsic kinematic coordinates (e.g. Tab. 5.8) and intrinsic kinematic coordinates (Tab. 5.13). It should be noted that the differences between the coefficients of the hand paths were sometimes small. In summary, MAJM produced the closest fit to the measured data, suggesting a planning in intrinsic kinematic coordinates. However, mMhJM was developed because an exclusive planning in extrinsic kinematic coordinates likely results in a trajectory that cannot be reproduced in intrinsic kinematic coordinates due to joint limits. MHJM was therefore modified to also consider joint limits as a boundary condition during the planning process. Thus, while the optimization takes place in extrinsic kinematic coordinates and is subject to joint limits, mMhJM has no restrictions in the intrinsic kinematic coordinates. Therefore, it had to be expected that under the condition “5 DOF optimized”, mMhJM would produce high %RMSDs in intrinsic kinematic coordinates. In future studies, additional constraints in intrinsic kinematic coordinates should be incorporated.

In the case of multi-joint optimization, the %RMSD is the result of an optimization of multiple joints. We tested performance differences across different joints. Large differences may indicate that the CNS does not use a single optimization principle in the process of motor planning, but several principles, combinations of principles or different principles for different joints. As before, we examined MAJM and MTCM to determine if there were significant differences in the approximation of the measured movements across the five DOFs.

We found no significant differences across the five DOFs between %RMSDs of the measured and predicted joint angles by MAJM (Fig. 5.36). In contrast, statistical analysis revealed significant differences across the five DOFs between %RMSDs of the measured and predicted joint angular velocities. MAJM produced the smallest %RMSD for the angular velocities of shoulder abduction/adduction, which is significantly smaller than the %RMSDs of shoulder rotation, shoulder anteversion/retroversion and elbow flexion/extension. These results correspond to the results of the condition “1 DOF optimized”. In the case of MAJM, each DOF is optimized separately and the results indicate that the optimization algorithm works correctly. The findings suggest that MAJM is able to approximate the measured angle paths across the five DOFs in a similar quality, but is not able to predict the measured joint angular velocity profiles. Based on the results, it appears that the CNS does not exclusively use a MAJ-strategy to reduce the available DOFs.

MTCM produced the smallest %RMSDs between the measured and predicted joint torques for shoulder abduction/adduction followed by thorax rotation, shoulder anteversion/retroversion, elbow flexion and shoulder rotation (Fig. 5.37).

The %RMSDs for shoulder abduction/adduction were significantly smaller than the %RMSDs of thorax rotation, shoulder anteversion/retroversion and elbow flexion/extension. There were no significant differences between shoulder abduction/adduction and shoulder rotation. The extremely large mean value and the large deviation of the 99 % confidence interval of the %RMSDs of shoulder rotation suggest the occurrence of numerical problems during the optimization process. An inspection of the simulation data confirms this assumption. In a few cases, the optimization algorithm did not converge. A coordinate transformation to intrinsic kinematic coordinates yielded the result that MTCM produced the smallest %RMSDs between the measured and predicted joint angles for shoulder abduction/adduction followed by elbow flexion/extension, shoulder rotation, thorax rotation and shoulder anteversion/retroversion. Moreover, the %RMSD of shoulder abduction/adduction was significantly smaller than the %RMSDs of shoulder rotation, thorax rotation and the shoulder anteversion/retroversion. Statistical analysis yielded significant differences by trend between shoulder abduction/adduction and elbow flexion. MTCM produced the smallest %RMSDs between the measured and predicted joint angular velocities for shoulder abduction/adduction followed by thorax rotation, shoulder rotation, shoulder anteversion/retroversion and elbow flexion/extension. The %RMSDs of shoulder abduction/adduction were significantly smaller than the %RMSDs of shoulder rotation, shoulder anteversion/retroversion and elbow flexion/extension. The statistical analysis yielded no significant differences between shoulder abduction/adduction and thorax rotation. When five DOFs are optimized, a MTC-strategy appears to be most likely for shoulder abduction/adduction.

In summary, despite several inhomogeneous results, two findings were consistent across the two conditions “1 DOF optimized” and “5 DOFs optimized”. First, MAJM showed the closest fit to the measured data in extrinsic kinematic coordinates and intrinsic kinematic coordinates, indicating that motor planning may take place in intrinsic kinematic coordinates. Second, several differences for MAJM and MTCM across the optimized DOFs were found, indicating that the CNS may use different optimization principles in different DOFs to reduce the available DOFs. The results of MTCM indicate differences between the measured trajectories and MTC-trajectories that appear to be a result of the optimization method.

### **Overall discussion of the results**

The purpose of this study was to examine if optimal control models can reproduce measured multi-joint movements in 3D space. In testing different optimal control models assigned to different planning spaces, we also examined on which level these principles may work in the CNS. The results showed that none of the optimal control models could precisely reproduce the measured trajectories. However, due to noise in the sensorimotor system (Faisal et al., 2008), the complex intersegmental dynamics during movement production (Flash et al., 2003) and some methodological problems (Chap. 5.4.3), planned and executed movements will always differ to a certain extent. MAJM exhibited the closest fit to the measured data across both movement tasks. Based on the results of this study, it is most likely a planning in intrinsic kinematic coordinates occurs. However, due to the fact that MAJM did not fully reproduce the measured trajectories, an exclusive planning in intrinsic kinematic coordinates based on a MAJ-principle appears to be debatable.

MHJM produced straight hand paths with single-peaked, bell-shaped velocity profiles for all trials. Our analysis revealed that humans produce curved hand paths with single-peaked, nearly bell-shaped velocity profiles (Chap. 4). However, it is conceivable that the CNS plans straight trajectories that are distorted during execution due to the complex intersegmental dynamics (Dean et al., 1995; Flash et al., 2003).

MTCM exhibited large mean values for the %RMSDs with large confidence intervals. These results do not necessarily indicate that MTCM cannot reproduce measured trajectories or that the CNS does not use this strategy. Because the optimization on torque level is very complex and the results partly indicated that the optimization algorithm did not converge, the poor results of MTCM may to some extent be explained by methodological problems (Chap. 5.4.3).

Although MAJM showed a relatively close fit to the measured trajectories, it gave no explanation as to why the smoothness of movement is important. It is debatable whether the CNS is able to estimate such complex quantities. Furthermore, some authors (Feldman, 2006) even doubt that the CNS has direct access to these quantities. An alternative to MAJM is the minimum variance model by Harris and Wolpert (1998). This model assumes there is noise in the motor command and that the amount of noise is proportional to the magnitude of the motor command. There are several important ramifications associated with this model. First, non-smooth movements require larger motor commands than smooth movements and consequently generate an increase in noise. In the case of goal-directed movements, smoothness leads to accuracy but is not a specific goal of its own right. Second, signal-dependent noise inherently imposes a trade off between movement duration and final accuracy in the endpoint of the movement, consistent with Fitts law (Chap. 2.3.1.1). Third, the minimum variance model provides a biologically plausible theoretical underpinning for goal-directed movements. This is possible because such costs are directly available to the CNS and the optimal trajectory could be learned from the experi-

ence of repeated movements (Jordan and Wolpert, 1999). Our results indicate that the CNS may combine different optimization strategies in motor planning. In other words, depending on the task or the DOF to be optimized, the CNS may choose the appropriate principle or combination of principles. mMhJM is a first attempt at implementing this idea. A task dependent selection of optimization principles has been implemented in the optimal stochastic feedback control approach of Todorov and Jordan (2002). The study tried to develop a model that captures the remarkable property of biological movement systems to accomplish complex movement tasks in the presence of noise, delays and unpredictable changes in the environment. In this context, open-loop models are suboptimal. What is needed is an elaborate feedback control scheme that generates intelligent adjustments online. Such a control scheme would enable biological systems to solve a control problem repeatedly rather than repeating a single solution (Bernstein, 1967). This idea was recently realized by Todorov and Jordan (2002) in terms of an optimal feedback controller. In a closed-loop optimization model, the controller is fully programmable. That is, it constructs the best possible transformation from states of the body and environment into control signals. The idea is that the controller does not rely on preconceived notions of what control principle the sensorimotor system may use, but does what is required to accomplish the task. In other words, optimal feedback control allows the task and the plant to dictate the control scheme which best fit. In an isometric task, this may be a force control scheme and in a postural task where a target limb position is specified, this may be a position control scheme. Due to the fact that the state of the plant is only observable through delayed and noisy sensors, the controller is only optimal if the state estimator is optimal. Although the minimum variance approach and the optimal stochastic feedback control approach are more feasible in physiological terms, until now, no studies have been conducted where these approaches are tested for multi-joint movements in 3D space. Furthermore, the optimal feedback control approach does not have an answer as to how the CNS chooses one or more adequate optimization principles and how these principles are weighed.

### 5.4.2 Robotics

As outlined in chapter 4.1, the fields of biological motor control and robotics are related (Schaal and Schweighofer, 2005; Ijspeert, 2006) and by now an exchange of ideas has begun to take place (Hollerbach, 1982; Beer et al., 1998; Sternad and Schaal, 1999; Piazzi and Visioli, 2000; Atkeson et al., 2000; Sun and Scassellati, 2005; Konczak, 2005; Stein et al., 2006). Thus, the field of robotics has proved to be a useful field for developing and testing hypotheses about biological motor control. In other words, models of biological motor control can be corroborated or discarded by testing them on robots. Furthermore, breakthroughs in understanding certain aspects of human motor control have often been brought about by computational studies (Flash and Hogan, 1985; Bullock and Grossberg, 1988; Uno et al., 1989;

Hoff and Arbib, 1993; Shadmehr and Mussa-Ivaldi, 1994; Harris and Wolpert, 1998; Todorov and Jordan, 2002). These studies are more or less based on classical fields of engineering such as cybernetics (Wiener, 1948), optimal control (Bellman, 1957) and control theory (Slotine and Li, 1991). On the other hand, the capabilities of biological systems by far surpass those of artificial systems (Flash et al., 2004). Therefore, it is likely the body of knowledge gained in the field of biological motor control could help engineers develop hardware and software components for humanoid robots used to generate human-like movements and for operating in an environment built for humans. The field of *computational neuroscience* still is and will continue to be an important interface between the field of biological motor control and robotics.

The computational framework for movement generation presented in this thesis is transferable to humanoid robots. However, it should be examined whether the engines of the robot can generate the calculated torques and therefore the calculated movements. If the required torques are unattainable, the maximum capacity of the different robotic engines may be used as another boundary condition during the optimization process, similar to the maximum movement amplitudes of the different joints. A more serious problem to be considered is the required computing time of the different optimal control models. In this context, one must distinguish between the multibody algorithm of the biomechanical model and the optimization algorithm. Furthermore, different optimal control models have different computing times. For example, a trajectory generated by a MHJM requires only a few seconds, whereas a trajectory generated by a MTCM may take minutes to several hours on a standard workstation. In case of optimal control models defined in intrinsic kinematic (MAJM) or dynamic coordinates (MTCM), the number of DOFs to be optimized has an impact on the computing time. Solutions for the problem of computing time must be considered on different levels. First, the computing power of workstations will grow in the coming years and consequently, the required computing time of optimal control models will decrease. In addition to computing power, it is necessary to determine if optimization algorithms exist with a lower computational complexity (see *applied methods*). In this study, the multibody algorithm and the optimization algorithm have been implemented in Matlab. A translation of the Matlab code to C/C++ code would likely improve computing time. Another solution to the online movement generation problem may be the creation of look-up tables. Movements for certain tasks may be calculated offline and stored in a data table. However, in using this method, the problem of computing time is transferred to a data storage problem. Furthermore, the constraints of the precomputed trajectories need to be fulfilled to be able to use those precomputed trajectories in future situations. This approach is comparable to early concepts of motor programs in biological motor control (Keele, 1968). It was assumed that the human CNS stores motor programs in the brain and plays them like tapes to control movements. However, in the context of biological motor control, the precomputation of movements seems rather implausible because muscular torques at each joint depend on the moment of inertia, length,

mass and center of mass of each segment. In contrast to robots, these parameters change constantly during the ontogenesis in biological systems. Therefore, all motor programs would need to be reprogrammed permanently.

Based on the discussion of the results of this study, the model best suited to approximate measured movement behavior appears to be MAJM. The application of a MAJM in robotics would have the advantage of solving the inverse kinematics problem (Chap. 2.2) because the motor planning takes place in intrinsic kinematic coordinates. Furthermore, in contrast to human motor control, the science of robotics does not have to address the question of why the CNS should use a minimum angle jerk principle in movement generation. In robotics, this strategy can be used as a black box model provided it generates human-like trajectories.

The use of optimal control models in robotics is a contemporary issue (Piazzini and Visioli, 2000; Gasparetto and Zanotto, 2008). Some authors are of the opinion that the “reverse engineering” problem for finding the correct optimal control model that results in human-like behavior cannot be solved. Thus, in robotics research, the problem of trajectory planning is addressed with alternative methods like the dynamic movement primitives approach (Hoffmann et al., 2009; Pastor et al., 2009).

### 5.4.3 Applied methods

It has become more and more challenging to establish links between the different research areas in human motor control focusing on *neural control*, the *musculoskeletal mechanics* or *motor behavior* (Fig. 2.20). For the development of a cohesive framework incorporating the results from different levels of analysis, motor control models must be constructed. Certain details of such models can be tested by carefully designed experiments. However, whether or not the overall model works usually relies on the intuition of the modeler, which may be wrong. Therefore, a promising way of integrating the three levels appears to be the construction of a computational model of human motor control. Given a certain movement task, the computational model can be used to generate movements via computer simulation. The results of the computer simulations can then be compared to the results of biomedical or biomechanical experiments and thus, the functionality of the computational model can be tested. In this thesis, this approach was used to address the problem of motor redundancy (Chap. 2.2). The computational framework consists of a biomechanical multibody model and different optimal control models. The optimal control models are a combination of an optimization criterion (e.g. minimum angle jerk) and an optimization method. The biomechanical model was discussed in chapter 4.4 and the suitability of different optimization criteria in the context of biological motor control was discussed above. Hence, in connection with the developed computational framework, the following discussion will focus on the optimization method. In addition, the methodological approach of optimizing some DOFs and driving others with experimental data will be analyzed. Furthermore, the methods used to compare the

experimentally determined trajectories with the trajectories predicted by the different optimal control models shall be discussed. The movement tasks used to test the different optimal control models are discussed below.

### **Test data**

To understand the functionality of the human motor system, it is reasonable to work on goal-directed daily-life movements like pointing gestures that are less complex than most movements in sports, but are still ecologically valid. This is an important issue because artificial labor tasks sometimes require movements not used by humans in their daily routine. In future studies, the different optimal control models should to be examined with respect to new movement tasks. For instance, movement tasks of different complexity need to be analyzed, including movements with different DOFs and a different number of DOFs. Furthermore, the movement tasks should be accomplished with different movement strategies like movements with flexed and extended arms. In addition, subjects should perform these movements under pressure of time or pressure of accuracy. It is known from Fitt's law (Fitts, 1954) that humans cannot move as fast as possible and as accurately as possible at the same time. Such test data may help to enhance the understanding in which situations the CNS chooses which principle or combination of principles.

### **Optimization method**

Mathematically, the optimization problem to be solved involves the optimization of a general nonlinear cost function with nonlinear constraints, bounds for the optimized variables and boundary conditions for the start and target time. The optimization method used in this thesis was introduced in chapter 5.2.6. The reader is referred to the thesis of Simonidis (2010) for a more detailed description of the method. A pilot study was conducted to validate the algorithm prior to the application of the optimization method. Therefore, we used a less complex task than the one the method was originally developed for. The idea was to use tasks where the solution is well known and therefore, the behavior of the optimization method could be judged. In the case under consideration, the optimization method was validated with a two-joint pendulum. The results revealed that the algorithm works correctly (Chap. 5.3.1). In the main study, the optimization algorithm converged towards an optimum in most cases. However, the results of the means and 99 % confidence intervals indicate that in a few cases, the optimization algorithm was not able to find an optimal solution (e.g. Fig. 5.22, elbow flexion/extension and Fig. 5.43). In the cases where the optimization method did not achieve satisfactory results, a problem-specific adaptation would be necessary. We transformed the optimization problem into an unconstrained quadratic parameter optimization problem. The trajectories were discretized into a parameter dependent set of trajectories using a temporal finite element method (Eriksson, 2008). At equidistant time instances, nodes were chosen and values between these nodes were interpolated by piecewise Hermite splines. There are two

possibilities to improve the performance of the splines. First, the number of nodes can be changed and second, splines of a different order or different type can be used. Preliminary tests showed that both elements have an impact on the performance of the optimization algorithm. We chose a configuration of the algorithm that yielded acceptable results in most cases. In future studies, more intensive pretests should be conducted to better adapt the algorithm to the problem at hand. Furthermore, automation of this process should be considered.

Most practically relevant optimization problems are extremely complex. The corresponding solution spaces are characterized by complex topographical structures, which tend to have multiple local optima (Fig. 5.44). In other words, if an optimum identified by an optimization algorithm corresponds to the global optimum cannot be determined with certainty. In the case under consideration, we are dealing precisely with this problem. One way to resolve this issue is to run the optimization algorithm with different numbers of nodes and different types of splines. A comparison of the results may help to enhance the performance of the algorithm and assess the quality of the solutions. Another possibility is to use a second optimization method and compare the results of both methods. Numerous optimization algorithms are discussed in technical literature (Lu and Antoniou, 2007). Given a complex optimization problem, the algorithm must incorporate two techniques to be able to find an optimum. First, the algorithm has to be able to explore new and unknown areas of the solution space. Second, the algorithm has to make use of knowledge found at points previously visited to find better solutions in future iterations. The first technique is called *exploration* and the second is referred to as *exploitation*. These two techniques are contradictory and therefore, an optimum trade off that can change during the search process has to be found. A class of optimization methods incorporating these two techniques are evolutionary algorithms. The different types of evolutionary algorithms are well described in the book of Baeck et al. (1997). Wiemeyer and Friederich (2001) showed that optimization criteria and genetic algorithms can be combined in optimal control models.

### **Simulation design**

One of the major challenges in the examination of human motor control is the expansion of the analysis to daily-life multi-joint movements in 3D space and to evaluate if the theories developed for 2D movements remain valid. The computational frameworks needed for this purpose are very complex. Development of the frameworks is usually an iterative process in which the level of complexity gradually increases. On each level of development, experiments need to be conducted to validate the current status of the computational framework, and for each validation, additional experiments need to be performed. Therefore, a data set that can be used during the process of model building for validation purposes is required. In the process of model building, the complexity of the calculations has to be increased gradually. Therefore, in our experiments only some of the joints are optimized while others are driven by

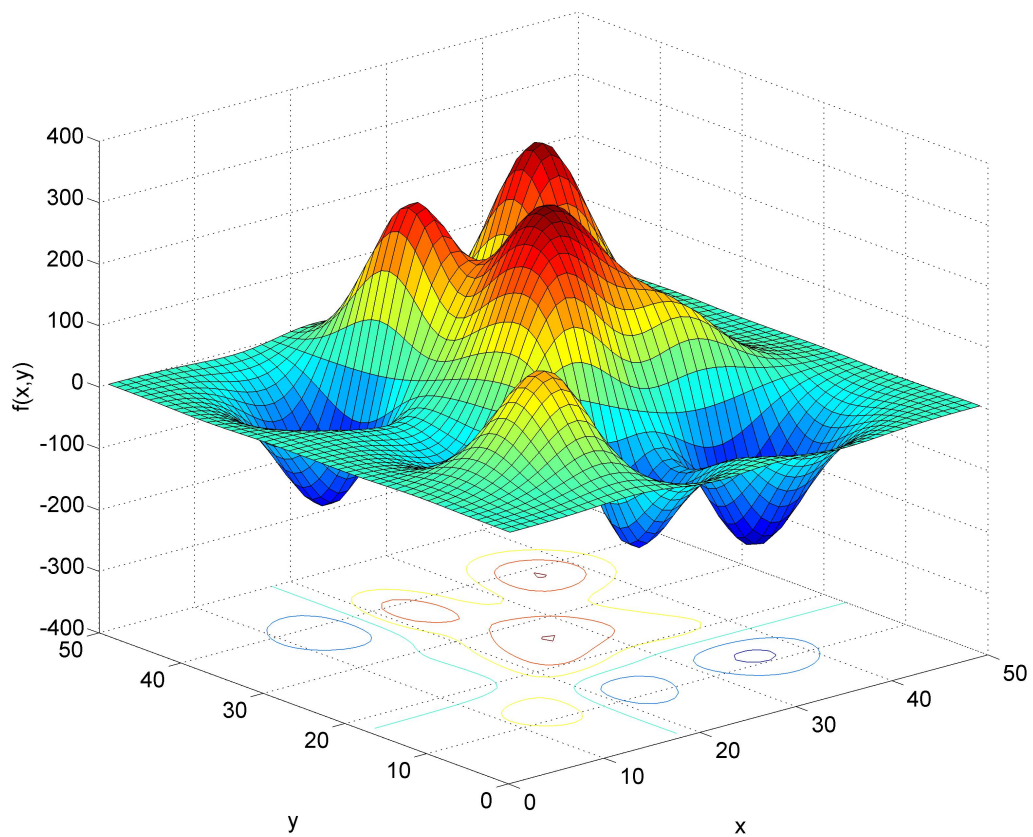


**Figure 5.44:** Hypothetical solution space of an optimization problem with several local optima. In the case of a maximization problem, the optimization algorithm has to find the dark red area of the highest peak and in the case of a minimization problem, the optimization algorithm has to find the dark blue area of the deepest valley.

experimentally determined data. For this reason, we examined whether an increase in the number of DOFs to be optimized has an effect on performance of mMhJM, MAJM and MTCM (Chap. 5.3.2.2.3, 5.3.2.3.1, 5.3.3.2.3, 5.3.2.3.1).

In the case of mMhJM, the optimization was conducted on hand level (extrinsic coordinates of the hand). As an additional boundary condition during the optimization, the limits of the individual DOFs were fixed. Therefore, during the optimization, some of the joint movements were driven by experimental data and while other joints (DOFs) were released, meaning that the optimization method can use this DOF within the joint limits to find a minimum hand jerk trajectory. The question to be answered is whether an increase in the released DOFs has an effect on the performance of mMhJM in extrinsic kinematic coordinates. The results of the %RMSDs of the hand paths and the tangential velocities of the hand are for both targets inhomogeneous, indicating that the results are highly dependent on the individual DOF that is released for the optimization. In contrast, the similarity coefficients clearly show that with an increase in the DOFs to be released, the similarity between the measured and predicted trajectories decreases.

The results of the %RMSDs and the similarity coefficients of MAJM indicate no differences between the two optimization conditions in intrinsic kinematic coordinates for either target. This result was expected because each joint is optimized in isolation. A calculation of the forward kinematics showed that an increase in the DOFs to be optimized has, in most cases, an effect on the differences and similarities between the measured and predicted trajectories of the hand, and the tangential velocity profiles. The effects are difficult to predict because of the kinematic redundancy of the human body.

In case of MTCM, the optimization was conducted on torque level. In the first movement task (target 1), we found no significant differences between the %RMSDs of the two optimization conditions. In the second movement task (target 3), we found no significant differences in the shoulder joint and thorax rotation. However, our calculations for the elbow joint revealed significant differences between the two optimization conditions. The differences in intrinsic kinematic coordinates after the calculation of the forward dynamics and the differences in extrinsic kinematic coordinates after the calculation of the forward kinematics can not be predicted. As previously discussed, the optimization on torque level is very complex and the results indicate that the optimization algorithm did not converge in all cases. Therefore, a quality improvement of the optimization method may influence the described results.

In the case of mMhJM and MTCM, the results are difficult to interpret because methodological problems remain. However, the results indicate that for the optimal control models defined in intrinsic coordinates, the transformation from one coordinate frame to another coordinate frame (e.g. forward kinematics or forward dynamics) is nonlinear. In other words, small differences between the two optimization conditions in intrinsic kinematic coordinates can lead to large differences in extrinsic kinematic coordinates and vice versa. Therefore, future studies should include a data

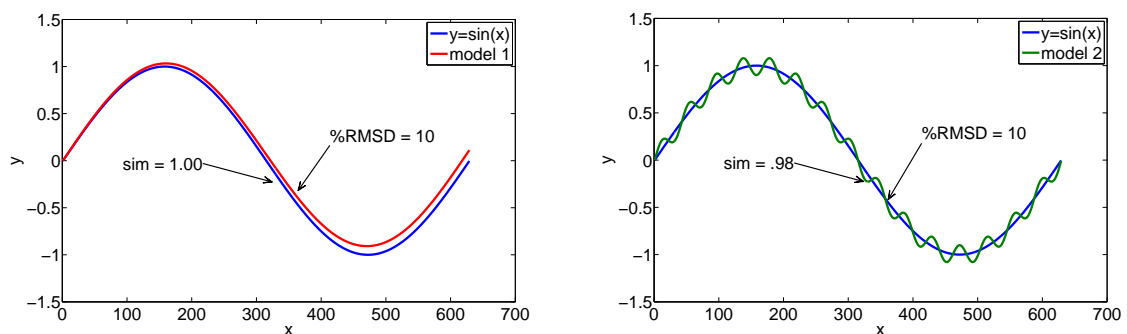


**Figure 5.45:** The blue trajectory is a sinusoidal oscillation  $y = \sin(x)$  with equidistant time instances  $i = 0.01$  on the interval  $x = [0, \dots, 2\pi]$ . The red and green trajectories indicate two hypothetical approximations of this oscillation by two different models. Each of them has a %RMSD of 10 but different similarity coefficients (sim).

set (see section “Test data”) that consists of different movement tasks of different complexity, e.g. movements with different DOFs and a different number of DOFs.

### Determination of model quality

It was shown in chapter 2.3.3.1 that in the context of optimal control models, a lot of research has been conducted on simple 2D movements. In contrast, the use of those models is still in an investigate phase for multi-joint movements in 3D space (Flash et al., 2003; Hermens and Gielen, 2004; Admiraal et al., 2004; Gielen, 2009b). Consequently, the purpose of this study was to quantitatively examine if optimal control models can reproduce multi-joint movements in 3D space. However, a problem arising when analyzing multi-joint movements in 3D space is the choice of metric for quantitative comparison the different models (Gielen, 2009b). We developed a three step process to compare experimentally determined trajectories with trajectories predicted by different optimal control models. In the first step, the results of all simulation runs were qualitatively examined for a first impression of the behavior of the models. The variations and similarities between the measured and predicted movement data were of specific interest. Because the development of a computational model is an iterative process, beginning with a qualitative analysis of the results is very important to be able to detect potential errors as early in the development process as possible. If the computational model has achieved a certain quality and can be used for hypothesis testing, quantitative analysis should then to be carried out. Therefore, we quantitatively analyzed the differences between the measured and predicted movement data as a second step. We specified the differences between two time series by the %RMSD. Because the %RMSD is a discrete value, it can be used as a quantity for the model fit. In addition, the differences in the %RMSDs between the measured and predicted movement data of different optimal control models can

be analyzed using methods from inferential statistics. However, figure 5.45 indicates that an exclusive comparison of different optimal control models on the basis of the %RMSD is insufficient for the determination of the best fit model. Both models in figure 5.45 produced a %RMSD of 10. However, the second model shows strong oscillations indicating a large number of submovements, which are uncommon in human trajectories. Because of that, we calculated a similarity coefficient between the measured and predicted trajectories in a third step. The results from the calculations show that the similarity coefficient is able to detect the differences in similarity of the two hypothetical model outputs. Although this three step procedure appears to be adequate, future studies should quantitatively analyze amplitudes and peak values of trajectories for assessing the quality of the different optimal control models more comprehensively.



## 6 Summary

This thesis is a culmination of the author's work in the CRC 588 "Humanoid Robots - Learning and Cooperating Multimodal Robots" project over the past five years. Within the field of robotics humanoid robots have been constructed that are able to deal with a large number of degrees of freedom (DOFs) (Fig. 1.1). This redundancy is advantageous because it enables robots to avoid obstacles and joint limits (Atkeson et al., 2000). However, this flexibility leads to a control problem. Which particular movement among the large number of possible movements should be chosen in a given situation? Similar problems exist in biological motor control. Imagine sitting in front of a glass of water. Take a drink from the glass would require grasping the glass and directing it toward the mouth. However, when you feel thirsty, you simply grasp the glass and take a drink without much thought. In doing so, we are controlling perhaps one of the most complex systems ever created by nature. The human movement system consists of billions of interconnected neurons, approximately 800 muscles and over 200 mechanical DOFs. This highly redundant system enables us to achieve movement tasks, such as the one just described, in countless ways. How exactly the CNS overcomes this redundancy and chooses one movement from of the many possible movements is still unknown. In *chapter 1*, it was shown that the fields of biological motor control and robotics have already begun to interact (Schaal and Schweighofer, 2005; Ijspeert, 2006) and exchanged ideas (Hollerbach, 1982; Beer et al., 1998; Sternad and Schaal, 1999; Piazzini and Visioli, 2000; Atkeson et al., 2000; Sun and Scassellati, 2005; Konczak, 2005; Stein et al., 2006). The field of robotics has proved to be a useful environment for developing and testing hypotheses about biological motor control. In other words, models of biological motor control can be corroborated or discarded by testing them on robots. On the other hand, the capabilities of biological systems by far surpass those of artificial systems (Flash et al., 2004). Therefore, the body of knowledge gained in the field of biological motor control may help engineers develop hardware and software components for humanoid robots that generate human-like movements and operate in future human environments. In this context, the research objective for this thesis was to address the motor redundancy problem. While this thesis was inspired by robotics research, it is founded in biology. Consequently, the results of both studies are discussed in the context of biological motor control and the generation of human-like movements by humanoid robots.

*Chapter 2* began with an introduction to the field of human motor control. In the following section, a thorough introduction to the redundancy problem was given. Then, existing models from three different scientific paradigms dealing with the prob-

lem of motor redundancy were presented and discussed. Based on the review of existing models, a computational approach was developed. This approach was based on the idea that results from neurophysiological studies, studies on the physics of the musculoskeletal system and behavioral studies should be linked in computational models of human motor control. Moreover, it was suggested that computational models should be used to examine multi-joint daily life movements in 3D space. For the implementation of this approach, the development of a biomechanical model and the collection of human movement data were necessary.

*Chapter 3* included a description of the methods used in the two studies (Chap. 4 and 5). A detailed description of the biomechanical data acquisition and data processing was outlined. In addition, a brief introduction to the multibody algorithm MKD-tools that was used for the calculation of joint angles and joint torques in the two studies was given.

The first of the two studies was presented in *chapter 4*. This study was based on the idea that information about the process of movement planning and control can be deduced from behavioral regularities (Bernstein, 1967). A large number of such regularities have been reported in literature (Goodman and Gottlieb, 1995), however the analysis of multi-joint movements of daily life in 3D space is uncommon. Thus, the purpose of the first study was to analyze different multi-joint pointing movements in 3D space with respect to the selection of regularities, with the goal to provide an initial idea of how humans reduce available DOFs in complex movements of daily life.

The second study, presented in *chapter 5*, was based on the work presented in chapters 2, 3 and 4. Different approaches to the problem of motor redundancy have been discussed in the literature (Chap. 2). Previous studies have shown that optimal control models can reproduce movement regularities on multiple levels (Todorov, 2004). In optimal control models, a unique trajectory is selected by adding additional constraints on the task and thus reducing the effective DOFs. This is usually done by selecting a cost function to be optimized (Engelbrecht, 2001). While optimal control models have been established in the technical literature for some years, a quantitative comparison between the performance of these models for multi-joint movements in 3D space is a fairly new concept (Flash et al., 2003; Admiraal et al., 2004; Hermens and Gielen, 2004; Kaphle and Eriksson, 2008; Gielen, 2009b). The purpose of the second study was to quantitatively examine the performance of different optimal control models in reproducing human multi-joint pointing movements in 3D space. The optimal control models were tested and the results were examined to determine if these models reproduce the regularities found in the first study (Chap. 2).

In the concluding chapter (Chap. 6), the results of this thesis are summarized and suggestions for future research are given. This chapter includes a discussion of the theoretical considerations (Chap. 2), the methods (Chap. 3), and the results of the two studies (Chap. 4 and 5).

## 6.1 Results

- After nearly 100 years of extensive multidisciplinary research, the interest in understanding human movements is still growing. The primary principles used for movement generation in humans are still largely unknown, and solutions for overcoming the problem of motor redundancy in human motor control research are poorly understood.
- During the last 100 years, many studies have been conducted with the goal to understand how the CNS solves the problem of motor redundancy. These studies can be categorized into three different areas of research (Fig. 2.20) including neurophysiological studies, studies on the physics of the musculoskeletal system and behavioral studies. As research continues to grow in each of the three areas, it becomes increasingly challenging to establish links between research conducted on the different levels of motor control. For the development of a cohesive framework to incorporate the results, models of motor control must be constructed. Specific details of such a model can be tested through carefully designed experiments; however, the overall working of the model usually relies on the intuition of the modeler, which may be incorrect. Therefore, a promising way of integrating the approaches used in the three areas seems to be the construction of a computational model of human motor control. Given a movement task, the computational model can be used to generate movements via computer simulation. The results of the computer simulations can then be compared to the results of biomedical or biomechanical experiments, and thus the functionality of the computational model can be tested. The next step would involve the implementation of the computational model on the robot platform because simulations are likely to oversimplify the problem. Furthermore, by testing computational models on robots, problems not foreseen during a simulation may emerge (Hoffmann, 2008).
- Three scientific frameworks currently exist within human motor control research: the motor approach, the dynamical systems approach and the computational neuroscience approach (Chap. 2.3). Each framework has specific concepts to handle the problem of motor redundancy. Computational neuroscience, in conjunction with the use of optimal control models and internal models, utilizes two concepts that best address the above presented considerations. Furthermore, these models have a great potential of integration. For example, open-loop optimization criteria can be interpreted as attractors. In the dynamical systems approach, these are favorable, attractive system states that a system progresses to (Chap. 2.3.2.1). It is conceivable that the motor system is attracted in the perceptual-motor workspace by system states represented by minimum jerk or minimum torque change principles. Furthermore,

the concept of internal models is used in current approaches of cognitive psychology (Hossner, 2004; Konczak, 2008). Moreover, optimal feedback control is related to the dynamical systems view (Chap. 2.3.2.1) in the sense that the coupling of the optimal feedback controller together with the controlled plant generates a specific dynamical systems model in the context of a given task. Finally, the minimum intervention principle is related to the uncontrolled manifold concept (Chap. 2.3.2.3).

- The purpose of the first study was to analyze multi-joint pointing movements in 3D space with respect to the selection of regularities. Based on the pioneering work of Morasso (1981) and Shadmehr and Mussa-Ivaldi (1994), an important assumption of motor psychophysics is as follows: Represented movement features differ from non-represented features in the *criterion of simplicity* and the *criterion of invariance*. A comparison of the pointing movements in extrinsic and intrinsic coordinates revealed that the trajectories of the hand in extrinsic coordinates were much simpler than the joint angle trajectories in joint space. Furthermore, in contrast to the joint angle trajectories, the trajectories of the hand were highly invariant across different movement tasks. When information about the process of movement planning and control can be deduced from these two criteria, the results of this study indicate that the CNS uses rather extrinsic than intrinsic coordinates in the process of movement planning. Furthermore, the CNS may use a compensatory control strategy on the joint level to assure the planned trajectory is achieved.
- It has been suggested in robotics research that humanoid robots should use human-like movements to promote man-machine interaction (Wank et al., 2004; Khatib et al., 2004; Schaal, 2007a). Hence, based on an analysis of human pointing gestures, humanoid robots should generate pointing gestures with curved hand paths and single-peak, nearly bell-shaped velocity profiles with a peak velocity of 1.5 – 2.0 *m/s*. The results of the first study showed that humans use different coordination strategies and that the coordination strategies of different subjects provide the chance to select the kinematics that can best be mapped to the humanoid robot of interest. Depending on the chosen kinematics, the motors of the robot should be able to produce angular velocities of up to 150 *deg/s* in the shoulder and elbow joints.
- The purpose of the second study was to determine if optimal control models can reproduce human multi-joint movements in 3D space. The results of this study indicate that none of the optimal control models analyzed could precisely reproduce the human trajectories. However, because of noise in the sensorimotor system (Faisal et al., 2008), the complex intersegmental dynamics during movement production (Flash et al., 2003), and methodological problems (Chap. 5.4.3), planned and executed movements will always differ to some extent. The

MAJM exhibited the closest fit to the human data for both movement tasks. Based on the results of the study, movement planning most likely occurs in intrinsic kinematic coordinates. However, these results contradict the results of the first study, which indicated that motor planning may take place in extrinsic kinematic coordinates of the hand. Because of the fact that the MAJM did not fully reproduce the human trajectories and was not significantly superior in all cases to the other optimal control models analyzed, an exclusive planning in intrinsic kinematic coordinates based on a MAJ-principle seems unlikely. The MHJM produced straight hand paths with single-peak, bell-shaped velocity profiles in all trials. Our study revealed that humans produced curved hand paths with single-peak, bell-shaped velocity profiles in all trials (Chap. 4). However, it is conceivable that the CNS plans straight trajectories that are distorted during execution because of the complex intersegmental dynamics (Dean et al., 1995; Flash et al., 2003). The MTCM exhibited large mean values for the %RMSDs with large confidence intervals. These results do not necessarily indicate that the MTCM cannot reproduce measured trajectories or that the CNS does not use this strategy to complete a task. Since the optimization on torque level is very complex and the results indicated that the optimization algorithm did not converge in all cases, the poor results of the MTCM may be explained by methodological problems (Chap. 5.4.3).

- The results of the second study indicate that the MAJM provided the best fit to the measured trajectories. The application of a MAJM in robotics has the advantage of solving the inverse kinematics problem (Chap. 2.2) because motor planning takes place in intrinsic kinematic coordinates. The question of why the CNS should use a minimum angle jerk principle in movement generation does not have to be addressed. In robotics, this principle can be used as a black box model provided it generates human-like trajectories. However, the use of optimal control models in robotics is a contemporary issue (Piazzini and Visioli, 2000; Gasparetto and Zanotto, 2008). Some authors in robotics believe that the “reverse engineering” problem of finding the correct optimal control model to reproduce human movements cannot be solved. Thus, in robotics research, the problem of trajectory planning is addressed with alternative methods like the dynamic movement primitives approach (Hoffmann et al., 2009; Pastor et al., 2009).

## 6.2 Further research

- To understand the functionality of the human motor system, it is reasonable to work on goal-directed movements of daily life including pointing gestures that are less complex than most movements in sports but are still ecologically valid. In other words, movements that are used by humans in their daily life should be analyzed. This is an important issue because artificial labor tasks sometimes require movements that humans do not regularly use in their daily routines. In future studies, different optimal control models should be examined with regards to new movement tasks. Movement tasks of different complexity should be analyzed such as, for instance, movements that involve the use of different numbers and combinations of DOFs. In addition, subjects should carry out these movements under pressure of time or pressure of accuracy. It is known from Fitt's law (Fitts, 1954) that humans cannot move as fast as possible and as accurately as possible at the same time. Such movement tasks may help to enhance the understanding of which principle or combination of principles the CNS chooses in different situations.
- New test trials should be analyzed in the context of movement synergies as introduced in chapter 2.3.2.2. The sharing component of synergies could be addressed with *principal component analysis* (Mah et al., 1994) or more sophisticated *matrix factorization methods* (Tresch et al., 2006). Furthermore, the flexibility/stability (error compensation) component could be addressed with the concept of the UCM (Schöner and Scholz, 2007; Latash et al., 2007; Latash, 2008b). These analyses would enhance the understanding of how the CNS coordinates multi-joint movements in 3D space.
- Although the MAJM showed a relatively close fit to measured human trajectories, it does not provide an explanation of why the CNS should produce smooth movements. It is also debatable whether the CNS is able to estimate such complex quantities, and some authors (Feldman, 2006) doubt that the CNS has direct access to these quantities. Hence, future studies should include the analysis of models that are physiologically more feasible than the models tested in this thesis. Possible candidates are the minimum variance model by Harris and Wolpert (1998) or the optimal feedback control model by Todorov and Jordan (2002). The optimal feedback control model by Todorov and Jordan (2002) is of special interest because it enables the incorporation of feedback processes in the computational framework.
- Based on the results of this thesis, it is conceivable that the CNS uses different optimization principles in context-specific combinations. Accordingly, context-specific combinations of optimal control principles should be analyzed in future studies. The mMHJM is an initial attempt to implement this concept.

- Based on the enhancements on the neurophysiological level of the computational framework, future studies will require the incorporation of muscles in the biomechanical model.
- The optimization algorithm should be enhanced in future studies. For example, an automated adaptation of the algorithm to the problem at hand should be implemented. In addition to the developed optimization method, a second optimization method could be incorporated into the computational framework. The class of optimization methods supplementing the method used in this thesis is referred to as evolutionary algorithms. A comparison of the performance of both methods may help in understanding the impact of the optimization method on the results.



## References

- [Abend et al. 1982] ABEND, W. ; BIZZI, E. ; MORASSO, P.: Human arm trajectory formation. In: *Brain* 105 (1982), p. 331–348
- [Adams 1971] ADAMS, J.A.: A closed-loop theory of motor learning. In: *Journal of Motor Behaviour* 3 (1971), No. 2, p. 111–149
- [Admiraal et al. 2004] ADMIRAAL, M. A. ; KUSTERS, M.J.M.A.M. ; GIELEN, S.C.A.M.: Modeling kinematics and dynamics of human arm movements. In: *Motor Control* 8 (2004), p. 312–338
- [Albers et al. 2006] ALBERS, A. ; BRUDNIOK, S. ; OTTNAD, J. ; SAUTER, C. ; SEDCHAICHARN, K.: ARMAR III - Design of the upper body. In: *Human-Centered Robotic Systems (HCRS 06)*, 2006
- [Alexander and Crutcher 1990] ALEXANDER, G.E. ; CRUTCHER, M.D.: Neural representation of the target (goal) of visually guided arm movements in three areas of the monkey. In: *Journal of Neurophysiology* 64 (1990), p. 164–178
- [Allen and Tsukahara 1974] ALLEN, G. ; TSUKAHARA, N.: Cerebrocerebellar Communication Systems. In: *Physiological Reviews* 54 (1974), p. 957–1006
- [Amirikian and Georgopoulos 2003] AMIRIKIAN, B. ; GEORGOPOULOS, A.P.: Motor cortex: Coding and decoding of directional operations. In: ARBIB, M.A. (Ed.): *The Handbook of Brain Theory and Neural Networks*. 2nd ed. MIT Press, 2003, p. 690–696
- [Andersen et al. 2004] ANDERSEN, R. ; MEEKER, D. ; PESARAN, B. ; BREZHEN, B. ; BUNEO, C. ; SCHERBERGER, H.: Sensorimotor transformations in the posterior parietal cortex. In: GAZZANIGA, M.S. (Ed.): *The Cognitive Neuroscience III*. 3rd ed. Cambridge, MA : MIT Press, 2004, Chapter 34, p. 463–475
- [Anglin and Wyss 2000] ANGLIN, C. ; WYSS, U.P.: Review of arm motion analyses. In: *Journal of Engineering in Medicine* 214 (2000), No. 5, p. 541–555
- [Arbib 2003] ARBIB, M.A. (Ed.): *The Handbook of Brain Theory and Neural Networks*. 2nd ed. MIT Press, 2003
- [Asfour 2003] ASFOUR, T.: *Sensomotorische Bewegungskoordination zur Handlungsausführung eines humanoiden Roboters (Sensorimotor coordination for action control of humanoid robots)*. Herdecke : GCA-Verlag, 2003

- [Asfour et al. 2008] ASFOUR, T. ; AZAD, P. ; VAHRENKAMP, N. ; REGENSTEIN, K. ; BIERBAUM, A. ; WELKE, K. ; SCHRDER, J. ; DILLMANN, R.: Toward humanoid manipulation in human-centred environments. In: *Robotics and Autonomous Systems* 56 (2008), p. 54–65
- [Ashe 1997] ASHE, J.: Force and the motor cortex. In: *Behavioural Brain Research* 87 (1997), p. 255–269
- [Atkeson et al. 2000] ATKESON, C.G. ; HALE, J. ; POLLICK, F. ; RILEY, M. ; KOTOSAKA, S. ; SCHAAL, S. ; SHIBATA, T. ; TEVATIA, G. ; VIJAYAKUMAR, S. ; UDE, A. ; KAWATO, M.: Using humanoid robots to study human behavior. In: *IEEE Intelligent Systems: Special Issue on Humanoid Robotics* 15 (2000), No. 4, p. 46–56
- [Atkeson and Hollerbach 1985] ATKESON, C.G. ; HOLLERBACH, J.M.: Kinematic features of unrestrained vertical arm movements. In: *Journal of Neuroscience* 5 (1985), No. 9, p. 2318–2330
- [Bae and Haug 1987] BAE, D. ; HAUG, E.: A recursive formulation for constrained mechanical system dynamics. Part I: Open-loop systems. In: *Mechanics Based Design of Structures and Machines* 15 (1987), No. 3, p. 359–382
- [Baeck et al. 1997] BAECK, T. (Ed.) ; FOGEL, D. B. (Ed.) ; MICHALEWICZ, Z. (Ed.): *Handbook of Evolutionary Computation*. Inst of Physics Pub, 1997
- [Battaglia-Mayer et al. 2000] BATTAGLIA-MAYER, A. ; FERRAINA, S. ; MITSUDA, T. ; MARCONI, B. ; GENOVESIO, A. ; ONORATI, P. ; LACQUANITI, F. ; CAMINITI, R.: Early coding of reaching in the parietooccipital cortex. In: *Journal of Neurophysiology* 83 (2000), p. 2374–2391
- [Becher et al. 2004] BECHER, R. ; STEINHAUS, P. ; DILLMANN, R.: The Collaborative Research Center 588: Humanoid Robots - Learning and Cooperation of Multimodal Robots. In: *International Journal on Humanoid Robotics* 1 (2004), No. 3, p. 429–448
- [Beer et al. 1998] BEER, R.D. ; CHIEL, H.J. ; QUINN, R.D. ; RITZMANN, R.E.: Biorobotic approaches to the study of motor systems. In: *Current Opinion in Neurobiology* 8 (1998), p. 777–782
- [Bellman 1957] BELLMAN, R.: *Dynamic programming*. Princeton University Press, 1957
- [Berkinblit and Feldman 1988] BERKINBLIT, M.B. ; FELDMAN, A.G.: Some problems of motor control. In: *Journal of Motor Behavior* 20 (1988), p. 369–373

- 
- [Berkinblit et al. 1986] BERKINBLIT, M.B. ; FELDMAN, A.G. ; FUKOSON, O.I.: Adaptability of innate motor patterns and motor control mechanisms. In: *Behavioral and Brain Sciences* 9 (1986), p. 585–638
- [Bernstein 1967] BERNSTEIN, N.A.: *The coordination and regulation of movement*. Oxford : Pergamon Press, 1967
- [Bernstein 1996] BERNSTEIN, N.A.: On dexterity and its development. In: LATASH, M.L. (Ed.) ; TURVEY, M.T. (Ed.): *Dexterity and its development*. New Jersey : Erlbaum, 1996, p. 1–244
- [Betts 1998] BETTS, J.T.: Survey of numerical methods for trajectory optimization. In: *Journal of Guidance, Control and Dynamics* 21 (1998), No. 2, p. 193–207
- [Birklbauer 2006] BIRKLBAUER, J.: *Modelle der Motorik (Models of motor control and motor learning)*. Meyer, 2006
- [Bizzi et al. 1982] BIZZI, E. ; ACCORNERO, N. ; CHAPPLE, W. ; HOGAN, N.: Arm trajectory formation in monkeys. In: *Experimental Brain Research* 46 (1982), p. 139–143
- [Bizzi et al. 1984] BIZZI, E. ; ACCORSERO, N. ; CHAPPLE, W. ; HOGAN, N.: Posture control and trajectory formation during arm movements. In: *Journal of Neuroscience* 4 (1984), p. 2738–2744
- [Bizzi et al. 1978] BIZZI, E. ; DEV, P. ; MORASSO, P. ; POLIT, A.: Effect of load disturbances during centrally initiated movements. In: *Journal of Neurophysiology* 41 (1978), p. 542–556
- [Bizzi et al. 1992] BIZZI, E. ; HOGAN, N. ; MUSSA-IVALDI, F.A. ; GISZTER, S.: Does the nervous system use equilibrium point control to guide single and multiple joint movements? In: *Behavioral and Brain Sciences* 15 (1992), No. 4, p. 603–613
- [Bizzi and Mussa-Ivaldi 2004] BIZZI, E. ; MUSSA-IVALDI, F.A.: Toward a neurobiology of coordinate transformations. In: GAZZANIGA, M.S. (Ed.): *The Cognitive Neuroscience III*. 3rd. ed. Cambridge, MA : MIT Press, 2004, Chapter 30, p. 413–425
- [Bizzi et al. 2000] BIZZI, E. ; TRESCH, M.C. ; SALTIEL, P. ; D’AVELLA, A.: New perspectives on spinal motor systems. In: *Nature Reviews Neuroscience* 1 (2000), p. 101–108
- [Blakemore et al. 2002] BLAKEMORE, S.-J. ; WOLPERT, D.M. ; FRITH, C.D.: Abnormalities in the awareness of action. In: *Trends in Cognitive Sciences* 6 (2002), No. 6, p. 237–242

- [Blakemore et al. 1999] BLAKEMORE, S.J. ; FRITH, C.D. ; WOLPERT, D.M.: Spatio-Temporal Prediction Modulates the Perception of Self-Produced Stimuli. In: *Journal of Cognitive Neuroscience* 11 (1999), p. 551–559
- [Boesnach et al. 2006a] BOESNACH, I. ; KÖHLER, H. ; GEHRIG, D. ; STELZNER, G. ; SIMONIDIS, C. ; FISCHER, A. ; STEIN, T.: A large-scale database of human movements to humanize robot motion. In: *Proceedings of the French-German Workshop on Humanoid and Legged Robots (HRL 2006)*, 2006
- [Boesnach et al. 2006b] BOESNACH, I. ; MOLDENHAUER, J. ; FISCHER, A. ; STEIN, T.: Context oriented motion generation: A new scheme for humanoid robot control. In: *Proceedings of the IEEE Int'l. Symposium on Robot and Human Interactive Communication (RO-MAN 2006)*. Hertfordshire, Grobritannien, 2006
- [de Boor and Swartz 1973] BOOR, C. de ; SWARTZ, B.: Collocation at Gaussian points. In: *SIAM Journal on Numerical Analysis* 2 (1973), No. 4, p. 582–606
- [Bortz 1999] BORTZ, J.: *Statistik für Sozialwissenschaftler (Statistics for social scientists)*. 5th ed. Springer, 1999
- [Bös 2002] BÖS, K. (Ed.): *Handbuch sportmotorische Tests (Handbook of sport-motor tests)*. 2nd ed. Göttingen : Hogrefe, 2002
- [Brock et al. 2005] BROCK, O. ; FAGG, A. ; GRUPEN, R. ; PLATT, R. ; ROSENSTEIN, M. ; SWEENEY, J.: A framework for learning and control in intelligent humanoid robots. In: *International Journal of Humanoid Robotics* 2 (2005), No. 3, p. 301–336
- [Brooks 2007] BROOKS, R.: *MIT Artificial Intelligence Laboratory - Humanoid Robotics Group*. <http://www.ai.mit.edu/projects/humanoid-robotics-group>. Version: 2007. – download on 14.01.07
- [Brown and Rosenbaum 2002] BROWN, L. E. ; ROSENBAUM, D. A.: Motor control: Models. In: NADEL, L. (Ed.): *Encyclopedia of Cognitive Science*. London : Macmillan, 2002
- [Buckley et al. 1996] BUCKLEY, M.A. ; YARDLEY, A. ; JOHNSON, G.R. ; CARUS, D.A.: Dynamics of the upper limb during performance of the tasks of every day living: A review of the current knowledge base. In: *Journal of Engineering in Medicine* 210 (1996), p. 241–247
- [Bullock and Grossberg 1988] BULLOCK, D. ; GROSSBERG, S.: Neural dynamics of planned arm movements: Emergent invariants and speed-accuracy properties during trajectory formation. In: *Psychological Review* 95 (1988), No. 1, p. 49–90

- 
- [Buneo et al. 2002] BUNEO, C.A. ; JARVIS, M.R. ; BATISTA, A.P. ; ANDERSON, R.A.: Direct visuomotor transformations for reaching. In: *Nature* 416 (2002), p. 632–636
- [Bursztyn et al. 2006] BURSZTYN, L.L. ; GANESH, G. ; IMAMIZU, H. ; KAWATO, M. ; FLANAGAN, J.R.: Neural correlates of internal-model loading. In: *Current Biology* 16 (2006), p. 2440–2445
- [Caminiti et al. 1991] CAMINITI, R. ; JOHNSON, P. ; GALLI, C. ; FERRAINA, S. ; BURNOD, Y.: Making arm movements within different parts of space: The premotor and motor cortical representation of a coordinate system for reaching to visual targets. In: *Journal of Neurophysiology* 11 (1991), p. 1182–1197
- [Caminiti et al. 1990] CAMINITI, R. ; JOHNSON, P. ; URBANO, A.: Making arm movements within different parts of space: Dynamic aspects in the primate motor cortex. In: *Journal of Neurophysiology* 10 (1990), p. 2039–2058
- [Campbell et al. 2002] CAMPBELL, M. ; HOANE, A. J. ; HSU, F.-H.: Deep blue. In: *Artificial Intelligence* 134 (2002), p. 57–83
- [Cappozzo et al. 1995] CAPPOZZO, A. ; CATANI, F. ; DELLA CROCE, U. ; LEARDINI, A.: Position and orientation of bones during movement: Anatomical frame definition and determination. In: *Clinical Biomechanics* 10 (1995), p. 171–178
- [Cappozzo et al. 2005] CAPPOZZO, A. ; CROCE, U. ; LEARDINI, A. ; CHIARI, L.: Human movement analysis using stereophotogrammetry. Part 1: Theoretical background. In: *Gait and Posture* 21 (2005), p. 186–196
- [Cisek 2005] CISEK, P.: Neural representation of motor plans, desired trajectories, and controlled objects. In: *Cognitive Processing* 6 (2005), p. 15–24
- [Cisek and Kalaska 2005] CISEK, P. ; KALASKA, J.F.: Neural correlates of reaching decisions in dorsal premotor cortex: Specification of multiple direction choices and final selection of action. In: *Neuron* 45 (2005), p. 801–814
- [Cloutier et al. 1995] CLOUTIER, B. ; PAI, D. ; ASCHER, U.: The formulation stiffness of forward dynamics algorithms and implications for robot simulation. In: *IEEE International Conference on Robotics and Automation*, 1995
- [Cohn et al. 2000] COHN, J.V. ; DIZIO, P. ; LACKNER, J.R.: Reaching during virtual rotation: Context specific compensations for expected coriolis forces. In: *Journal of Neurophysiology* 83 (2000), p. 3230–3240
- [Conditt and Mussa-Ivaldi 1999] CONDITT, M.A. ; MUSSA-IVALDI, F.A.: Central representation of time during motor learning. In: *Proc. Natl. Acad. Sci.* 96 (1999), p. 11625–11630

- [Corbetta and Vereijken 1999] CORBETTA, D. ; VEREIJKEN, B.: Understanding development and learning of motor coordination in sport: The contribution of dynamic systems theory. In: *International Journal of Sport Psychology* 30 (1999), p. 507–530
- [Corradini et al. 1993] CORRADINI, M.L. ; FIORETTI, S. ; LEO, T.: Numerical differentiation in movement analysis: how to standardise the evaluation of techniques. In: *Medical & Biological Engineering & Computing* 31 (1993), p. 187–197
- [Courtney and Fetz 1973] COURTNEY, K.R. ; FETZ, E.E.: Unit responses recorded from cervical spinal cord of awake monkey. In: *Brain Research* 52 (1973), p. 445–450
- [Craig 2005] CRAIG, J.J.: *Introduction to robotics: Mechanics and control*. 3rd ed. New Jersey : Pearson Prentice Hall, 2005
- [Criscimagna-Hemminger et al. 2003] CRISCIMAGNA-HEMMINGER, S.E. ; DONCHIN, O. ; GAZZANIGA, M.S. ; SHADMEHR, R.: Learned dynamics of reaching movements generalize from dominant to nondominant arm. In: *Journal of Neurophysiology* 1 (2003), p. 168–176
- [Croce et al. 2005] CROCE, U. ; LEARDINI, A. ; CHIARI, L. ; CAPPOZZO, A.: Human Movement Analysis Using Stereophotogrammetry: Part 4: Assessment of Anatomical Landmark Misplacement and its Effects on Joint Kinematics. In: *Gait and Posture* 21 (2005), p. 226–237
- [Daug's 1994] DAUGS, R.: Motorische Kontrolle als Informationsverarbeitung: Vom Auf- und Niedergang eines Paradigmas (Motor control as information processing: The rise and the fall of a paradigm). In: BLASER, P. (Ed.) ; STUCKE, C. (Ed.) ; WITTE, K. (Ed.): *Steuer- und Regelvorgänge der menschlichen Motorik*. Sankt Augustin : Academia, 1994, p. 13–38
- [Davidson and Wolpert 2005] DAVIDSON, P.R. ; WOLPERT, D.M.: Widespread access to predictive models in the motor system: A short review. In: *Journal of Neural Engineering* 2 (2005), p. 313–319
- [De Leva 1996] DE LEVA, P.: Adjustments to Zatsiorsky-Seluyanov's segment inertia parameters. In: *Journal of Biomechanics* 29 (1996), No. 9, p. 1223–1230
- [Dean et al. 1995] DEAN, J. ; CRUSE, H. ; BRÜWER, M. ; STEINKÜHLER, U.: Kontrollstrategien für einen Manipulator mit redundanten Freiheitsgraden am Beispiel des menschlichen Arms (Control strategies for a manipulator with redundant degrees of freedom). In: JÄNCKE, L. (Ed.) ; HEUER, H. (Ed.): *Interdisziplinäre Bewegungsforschung*. Lengerich : Pabst, 1995, p. 349–396

- 
- [DeLong 1973] DELONG, M.R.: Putamen: Activity of single units during slow and rapid arm movements. In: *Science* 179 (1973), p. 1240–1242
- [Delp et al. 2007] DELP, S.L. ; ANDERSON, F.C. ; ARNOLD, A.S. ; LOAN, P. ; HABIB, A. ; JOHN, C.T. ; GUENDELMAN, E. ; THELEN, D.G.: OpenSim: Open-source software to create and analyze dynamic simulations of movement. In: *IEEE Transactions on Biomedical Engineering* 54 (2007), No. 11, p. 1940–1950
- [Delp and Loan 1995] DELP, S.L. ; LOAN, J.P.: A graphics-based software system to develop and analyze models of musculoskeletal structures. In: *Computers in Biology and Medicine* 25 (1995), p. 21–34
- [Delp and Loan 2000] DELP, S.L. ; LOAN, J.P.: A computational framework for simulating and analyzing human and animal movement. In: *Computing in Science & Engineering* 2 (2000), No. 5, p. 46–55
- [Desmurget and Grafton 2000] DESMURGET, M. ; GRAFTON, S.: Forward modelling allows feedback control for fast reaching movements. In: *Trends in Cognitive Sciences* 4 (2000), No. 11, p. 423–431
- [Desmurget et al. 1997] DESMURGET, M. ; JORDAN, M. ; PRABLANC, C. ; JEANNEROD, M.: Constrained and unconstrained movements involve different control strategies. In: *Journal of Neurophysiology* 77 (1997), p. 1644–1650
- [Desmurget et al. 1998] DESMURGET, M. ; PLISSON, D. ; ROSSETTI, Y. ; PRABLANC, C.: From eye to hand: Planning goal-directed movements. In: *Neuroscience and Biobehavioral Reviews* 22 (1998), No. 6, p. 761–788
- [Desmurget and Prablanc 1997] DESMURGET, M. ; PRABLANC, C.: Postural Control of Three-Dimensional Prehension Movements. In: *Journal of Neurophysiol.* 77 (1997), p. 452–464
- [Desmurget et al. 1996] DESMURGET, M. ; PRABLANC, C. ; ARZI, M. ; ROSSETTI, Y. ; PAULIGNAN, Y. ; URQUIZAR, C.: Integrated control of hand transport and orientation during prehension movements. In: *Experimental Brain Research* 110 (1996), p. 265–278
- [Dewhurst 1967] DEWHURST, D.J.: Neuromuscular control system. In: *IEEE Transactions on Biomedical Engineering* 14 (1967), p. 167–171
- [Dum and Strick 1991] DUM, R.P. ; STRICK, P.L.: The origin of corticospinal projections from premotor areas in the frontal lobe. In: *Journal of Neuroscience* 11 (1991), p. 667–689

- [Elsner 2006] ELSNER, W. B. and P. B. and Prinz: Psychologische Modelle der Handlungssteuerung (Psychological models of action control). In: KARNATH, H.-O. (Ed.) ; THIER, P. (Ed.): *Neuropsychologie*. 2nd. ed. Heidelberg : Springer, 2006, p. 286–295
- [Engelbrecht 2001] ENGELBRECHT, S.E.: Minimum principles in motor control. In: *Journal of Mathematical Psychology* 45 (2001), p. 497–542
- [Eriksson 2008] ERIKSSON, A.: Optimization in target movement simulations. In: *Comput. Methods Appl. Mech. Engrg.* 197 (2008), p. 4207–4215
- [Evarts 1968] EVARTS, E.V.: Relation of pyramidal tract activity to force exerted during voluntary movement. In: *Journal of Neurophysiology* 31 (1968), No. 1, p. 14–27
- [Evarts 1969] EVARTS, E.V.: Activity of pyramidal tract neurons during postural fixation. In: *Journal of Neurophysiology* 32 (1969), No. 3, p. 375–385
- [Faisal et al. 2008] FAISAL, A.A. ; SELEN, L.P.J. ; WOLPERT, D.M.: Noise in the nervous system. In: *Nature Reviews Neuroscience* 9 (2008), p. 292–303
- [Featherstone 2008] FEATHERSTONE, R.: *Rigid Body Dynamics Algorithms*. Springer, 2008
- [Feldman 1986] FELDMAN, A. G.: Once more on the equilibrium-point hypothesis (lambda model) for motor control. In: *Journal of Motor Behavior* 18 (1986), p. 17–54
- [Feldman 1966] FELDMAN, A.G.: Functional tuning of the nervous system with control of movement or maintenance of a steady posture. In: *Biophysics* 11 (1966), p. 565–578
- [Feldman 2006] FELDMAN, A.G.: The nature of voluntary control of motor actions. In: LATASH, M.L. (Ed.) ; LESTIENNE, F. (Ed.): *Motor Control and Learning*. Springer, 2006, Chapter 1, p. 3–8
- [Feldman et al. 1995] FELDMAN, A.G. ; ADAMOVICH, S.V. ; LEVIN, M.F.: The relationship between control, kinematic and electromyographic variables in fast single-joint movements in humans. In: *Experimental Brain Research* 103 (1995), p. 440–450
- [Feldman and Latash 2005] FELDMAN, A.G. ; LATASH, M.L.: Testing hypotheses and the advancement of science: Recent attempts to falsify the equilibrium point hypothesis. In: *Experimental Brain Research* 161 (2005), p. 91–103

- 
- [Feldman and Levin 1995] FELDMAN, A.G. ; LEVIN, M.F.: The origin and use of positional frames of reference in motor control. In: *Behavioral and Brain Sciences* 18 (1995), p. 723–806
- [Feldman and Levin 2009] FELDMAN, A.G. ; LEVIN, M.F.: The equilibrium-point hypothesis - past, present and future. In: STERNAD, D. (Ed.): *Progress in Motor Control - A Multidisciplinary Perspective*. Springer, 2009, p. 699–726
- [Ferrein 2005] FERREIN, A.: Specifying soccer moves with golog. In: SEIFRIZ, F. (Ed.) ; MESTER, J. (Ed.) ; PERL, J. (Ed.) ; SPANIOL, O. (Ed.) ; WIEMEYER, J. (Ed.): *Book of Abstracts - 1st International Working Conference IT and Sport & 5th Conference dvs-Section Computer Science in Sport*. DSHS, 2005, p. 161–165
- [Fischer et al. 2009a] FISCHER, A. ; GEHRIG, D. ; STEIN, T. ; SCHULTZ, T. ; SCHWAMEDER, H.: Recognition and estimation of human locomotion with hidden markov models. In: HARRISON, A.J. (Ed.) ; ANDERSON, R. (Ed.) ; KENNY, I. (Ed.): *Proceedings of the 27th Conference on Biomechanics in Sports*, University of Limerick, 2009, p. 112
- [Fischer et al. 2005] FISCHER, A. ; STEIN, T. ; BÖS, K. ; WANK, V. ; BOESNACH, I. ; MOLDENHAUER, J. ; BETH, T.: Guidelines for motion planning of humanoid robots: Analysis of intra- and inter-individual variations in human movements. In: *Proceedings of the 5th International Symposium Computer Science in Sport*. Hvar, Kroatien, 2005, p. 41
- [Fischer et al. 2009b] FISCHER, A. ; STEIN, T. ; GEHRIG, D. ; SCHULTZ, T. ; SCHWAMEDER, H.: Bewegungserkennung mit Hidden Markov Modellen (Movement recognition with hidden markov models). In: BAUMGÄRTNER, S. (Ed.) ; HÄNSEL, F. (Ed.) ; WIEMEYER, J. (Ed.): *Informations- und Kommunikationstechnologien in der Sportmotorik*. Hamburg : Druckerei der Techniker Krankenkasse, 2009, p. 179–181
- [Fischer et al. 2010] FISCHER, A. ; STEIN, T. ; GEHRIG, D. ; SCHULTZ, T. ; SCHWAMEDER, H.: Training und Erkennung mit Hidden Markov Modellen bei unterschiedlichen Geh- und Laufgeschwindigkeiten (Training and recognition of different walking and running speeds using hidden markov models). In: WANK, V. (Ed.): *Biomechanik - Grundlagenforschung und Anwendung*. Hamburg : Czwalina, 2010. – in print
- [Fitch et al. 1982] FITCH, H.I. ; TULLER, B. ; TURVEY, M.T.: The Bernstein perspective III: Tuning of coordinate structures with special reference to perception. In: KELSO, J.A.S. (Ed.): *Human motor behavior*. Ney York : Erlbaum, 1982, p. 271–281

- [Fitts 1954] FITTS, P.M.: The information capacity of the human motor system in controlling the amplitude of movement. In: *Journal of Experimental Psychology* 47 (1954), p. 381–391
- [Flanagan and Ostry 1990] FLANAGAN, J.R. ; OSTRY, D.J.: Trajectories for human multi-joint arm movements: evidence of joint level planning. In: HAYWARD, V. (Ed.) ; KHATIB, O. (Ed.): *Experimental Robotics 1, Lecture Notes in Control and Information Science*. Springer, 1990, p. 594–613
- [Flanagan and Rao 1995] FLANAGAN, J.R. ; RAO, A.K.: Trajectory adaptation to a nonlinear visuomotor transformation: Evidence of motion planning in visually perceived space. In: *Journal of Neurophysiology* 74 (1995), p. 2174–2178
- [Flanagan and Wing 1997] FLANAGAN, J.R. ; WING, A.M.: The role of internal models in motion planning and control: Evidence from grip force adjustments during movements of hand-held loads. In: *The Journal of Neuroscience* 17 (1997), No. 4, p. 1519–1528
- [Flanders et al. 1992] FLANDERS, M. ; HELMS-TILLERY, S.I. ; SOECHTING, J.F.: Early stages in a sensorimotor transformation. In: *Behavioral and Brain Sciences* 15 (1992), p. 309–362
- [Flash and Hogan 1985] FLASH, T. ; HOGAN, N.: The coordination of arm movements: an experimentally confirmed mathematical model. In: *Journal of Neuroscience* 5 (1985), p. 1688–1703
- [Flash et al. 2003] FLASH, T. ; HOGAN, N. ; RICHARDSON, M.J.E.: Optimization principles in motor control. In: ARBIB, M.A. (Ed.): *The handbook of brain theory and neural networks*. 2nd ed. MIT Press, 2003, p. 827–831
- [Flash et al. 2004] FLASH, T. ; RICHARDSON, M.E. ; HANDZEL, A.A. ; LIEBERMANN, D.G.: Computational models and geometric approaches in arm trajectory control studies. In: LATASH, M.L. (Ed.) ; LEVIN, M. F. (Ed.): *Progress in Motor Control III: Effects of Age, Disorder, and Rehabilitation* Bd. III. Human Kinetics, 2004, Chapter 2, p. 35–54
- [Flash and Sejnowski 2001] FLASH, T. ; SEJNOWSKI, J.T.: Computational approaches to motor control. In: *Current Opinion in Neurobiology* 11 (2001), p. 655–662
- [Fong et al. 2003] FONG, T. ; NOURBAKHSI, I. ; DAUTENHAHN, K.: A survey of socially interactive robots. In: *Robotics and Autonomous Systems* 42 (2003), p. 143–166

- 
- [Gandolfo et al. 1996] GANDOLFO, F. ; MUSSA-IVALDI, F.A. ; BIZZI, E.: Motor learning by field approximation. In: *Proc. Natl. Acad. Sci.* 93 (1996), p. 3843–3846
- [Gasparetto and Zanotto 2008] GASPARETTO, A. ; ZANOTTO, V.: A technique for time-jerk optimal planning of robot trajectories. In: *Robotics and Computer-Integrated Manufacturing* 24 (2008), p. 415–426
- [Gehrig et al. 2008] GEHRIG, D. ; FISCHER, A. ; KÜHNE, H. ; STEIN, T. ; WÖRNER, A. ; SCHWAMEDER, H. ; SCHULTZ, T.: Online recognition of daily-life movements. In: *Proceedings of the IEEE-RAS International Conference on Humanoid Robots*, 2008
- [Gentile 2000] GENTILE, A.M.: Skill acquisition: Action, movement, and neuromotor processes. In: CARR, J.H. (Ed.) ; SHEPHERD, R.B. (Ed.): *Movement science: Foundations for physical therapy*. Aspen, 2000, p. 111–187
- [Gentner 1987] GENTNER, D.R.: Timing of skilled motor performance: tests of the proportional duration model. In: *Psychological Review* 94 (1987), p. 255–276
- [Georgopoulos 1996a] GEORGOPOULOS, A.P.: Arm movements in monkeys: Behavior and neurophysiology. In: *J Comp Physiol A* 179 (1996), p. 603–612
- [Georgopoulos 1996b] GEORGOPOULOS, A.P.: On the translation of directional motor cortical commands to activation of muscles via spinal interneuronal systems. In: *Cognitive Brain Research* 3 (1996), p. 151–155
- [Georgopoulos and Ashe 2000] GEORGOPOULOS, A.P. ; ASHE, J.: One motor cortex, two different views. In: *Nature Neuroscience* 3 (2000), p. 963–964
- [Georgopoulos et al. 1983] GEORGOPOULOS, A.P. ; CAMINITI, R. ; KALASKA, J.F. ; MASSEY, J.T.: Spatial coding of movement: A hypothesis concerning the coding of movement direction by motor cortical populations. In: *Experimental Brain Research Res Suppl.* 7 (1983), p. 327–336
- [Georgopoulos et al. 1982] GEORGOPOULOS, A.P. ; KALASKA, J.F. ; CAMINITI, R. ; MASSEY, J.T.: On the relations between the direction of two-dimensional arm movements and cell discharge in primate motor cortex. In: *Journal of Neuroscience* 2 (1982), p. 1527–1537
- [Georgopoulos et al. 1986] GEORGOPOULOS, A.P. ; SCHWARTZ, A.B. ; KETTNER, R.E.: Neuronal population coding of movement direction. In: *Science* 233 (1986), p. 1416–1419

- [Ghez and Krakauer 2000] GHEZ, C. ; KRAKAUER, J.: The organization of movement. In: KANDEL, E. R. (Ed.) ; SCHWARTZ, J. H. (Ed.) ; JESSELL, T. (Ed.): *Principles of Neuroscience*. 4th ed. McGraw-Hill, 2000, Chapter 33, p. 652–673
- [Gielen et al. 1995] GIELEN, C.C.A.M. ; BOLHUIS, B.M. van ; THEEUWEN, M.: On the control of biologically and kinematically redundant manipulators. In: *Human Movement Science* 14 (1995), p. 487–509
- [Gielen 2009a] GIELEN, S.: Bridging of models for complex movements in 3D. In: STERNAD, D. (Ed.): *Progress in Motor Control: A Multidisciplinary Perspective*. Springer, 2009, p. 479–483
- [Gielen 2009b] GIELEN, S.: Review of models for the generation of multijoint movements in 3D. In: STERNAD, D. (Ed.): *Progress in Motor Control: A Multidisciplinary Perspective*. Springer, 2009, p. 523–552
- [Gill et al. 1981] GILL, P. ; MURRAY, W. ; WRIGHT, M.: *Practical optimization*. San Diego : Academic Press, 1981
- [Giszter et al. 2000] GISZTER, S.F. ; MOXON, K.A. ; CHAPIN, J.K.: A neurobiological perspective on humanoid robot design. In: *IEEE Intelligent Systems* (2000), No. 4, p. 64–69
- [Giszter et al. 1993] GISZTER, S.F. ; MUSSA-IVALDI, F.A. ; BIZZI, E.: Convergent force fields organized in the frog’s spinal cord. In: *Journal of Neurophysiology* 13 (1993), p. 467–491
- [Gollhofer 2008] GOLLHOFER, A.: Muscle mechanics and neural control. In: HONG, Y. (Ed.) ; BARTLETT, R. (Ed.): *Handbook of Biomechanics and Human Movement Science*. Routledge, 2008, p. 83–92
- [Gomi and Kawato 1996] GOMI, H. ; KAWATO, M.: Equilibrium-point hypothesis examined by measured arm stiffness during multijoint movement. In: *Science* 272 (1996), p. 117–120
- [Goodbody and Wolpert 1998] GOODBODY, S.J. ; WOLPERT, D.M.: Temporal and amplitude generalization in motor learning. In: *Journal of Neurophysiology* 79 (1998), p. 1825–1838
- [Goodman and Gottlieb 1995] GOODMAN, S.R. ; GOTTLIEB, G.L.: Analysis of kinematic invariances of multijoint reaching movement. In: *Biological Cybernetics* 73 (1995), p. 311–322
- [Gordon et al. 1994] GORDON, J. ; GHILARDI, M.F. ; GHEZ, C.: Accuracy of planar reaching movements. In: *Experimental Brain Research* 99 (1994), p. 97–111

- 
- [Greene 1972] GREENE, P.H.: Problems of organization of motor systems. In: ROSEN, R. (Ed.) ; SNELL, F.M. (Ed.): *Progress in theoretical biology*. New York : Academic Press, 1972
- [Gribble et al. 1998] GRIBBLE, P.L. ; OSTRY, D.J. ; SANGUINETI, V. ; LABOISSIERE, R.: Are complex control signals required for human arm movements? In: *Journal of Neurophysiology* 79 (1998), p. 1409–1424
- [Grush 2004] GRUSH, R.: The emulation theory of representation: Motor control, imagery, and perception. In: *Behavioral and Brain Sciences* 27 (2004), p. 377–442
- [Günther and Ruder 2003] GÜNTHER, M. ; RUDER, H.: Synthesis of two-dimensional human walking: A test of the lambda-model. In: *Biological Cybernetics* 89 (2003), p. 89–106
- [Haggard et al. 1995] HAGGARD, P. ; HUTCHINSON, K. ; STEIN, J.: Patterns of coordinated multi-joint movement. In: *Experimental Brain Research* 107 (1995), p. 254–266
- [Haken 2004] HAKEN, H.: *Synergetics: Introduction and Advanced topics*. 3rd ed. Berlin : Springer, 2004
- [Haken et al. 1985] HAKEN, H. ; KELSO, J.A.S. ; BUNZ, H.: A theoretical model of phase transitions in human hand movements. In: *Biological Cybernetics* 51 (1985), p. 347–356
- [Harris 1998] HARRIS, C.M.: On the optimal control of behaviour: A stochastic perspective. In: *Journal of Neuroscience Methods* 83 (1998), p. 73–88
- [Harris and Wolpert 1998] HARRIS, C.M. ; WOLPERT, D.M.: Signal-dependent noise determines motor planning. In: *Nature* 394 (1998), p. 780–784
- [Hart and Giszter 2004] HART, C.B. ; GISZTER, S.F.: Modular premotor drives and unit bursts as primitives for frog motor behaviors. In: *Journal of Neurosciences* 24 (2004), p. 5269–5282
- [Haruno et al. 2001] HARUNO, M. ; WOLPERT, D.M. ; KAWATO, M.: MOSAIC model for sensorimotor learning and control. In: *Neural Computation* 13 (2001), p. 2201–2220
- [Hawking 2002] HAWKING, S. W.: *Das Universum in der Nuschale (The Universe in a nutshell)*. Hoffmann, 2002

- [He et al. 1993] HE, S.Q. ; DUM, R.P. ; STRICK, P.L.: Topographic organization of corticospinal projections from the frontal lobe: Motor areas on the lateral surface of the hemisphere. In: *Journal of Neuroscience* 13 (1993), No. 3, p. 952–980
- [Henneman 1965] HENNEMAN, E.: Recruitment of motoneurons: The size principle. In: *Journal of Neurophysiologie* 28 (1965), p. 560–580
- [Henry and Rogers 1960] HENRY, F.M. ; ROGERS, D.E.: Increased response latency for complicated movements and a memory drum theory of neuromotor reaction. In: *Research Quarterly* 31 (1960), p. 448–458
- [Hermens and Gielen 2004] HERMENS, F. ; GIELEN, S.: Posture-based or trajectory-based movement planning: A comparison of direct and indirect pointing movements. In: *Experimental Brain Research* 159 (2004), p. 340–348
- [Heuer 1991] HEUER, H.: Invariant relative timing in motor-program theory. In: FAGARD, J. (Ed.) ; WOLFF, P.H. (Ed.): *The development of timing control and temporal organization in coordinated action. Invariant relative timing, rhythms, and coordination*. North-Holland, 1991, p. 37–68
- [Heuer and Konczak 2003] HEUER, H. ; KONCZAK, J.: Bewegungssteuerung Bewegungskoordination (Motor control - motor coordination). In: MECHLING, H. (Ed.) ; MUNZERT, J. (Ed.): *Handbuch Bewegungswissenschaft Bewegungslehre*. Hofmann, 2003, p. 105–129
- [Hick 1952] HICK, W.E.: On the rate of gain of information. In: *Quarterly Journal of Experimental Psychology* 4 (1952), p. 11–26
- [Hildreth and Hollerbach 1987] HILDRETH, E.C. ; HOLLERBACH, J.M.: Artificial intelligence: Computational approach to vision and motor control. In: PLUM, F. (Ed.): *Handbook of Physiology: The Nervous System*. American Physiological Society, 1987, p. 605–642
- [Hinder and Milner 2003] HINDER, M. R. ; MILNER, T. E.: The case for an internal dynamics model versus equilibrium point control in human movement. In: *Journal of Physiology* 549 (2003), p. 953–963
- [Hoff and Arbib 1993] HOFF, B. ; ARBIB, M.A.: Models of trajectory formation and temporal interaction of reach and grasp. In: *Journal of Motor Behavior* 25 (1993), p. 175–192
- [Hoffmann 2008] HOFFMANN, H.: *Unsupervised Learning of Visuomotor Associations*, Technische Fakultät der Universität Bielefeld, Diss., 2008

- 
- [Hoffmann et al. 2009] HOFFMANN, H. ; PASTOR, P. ; PARK, D.-H. ; SCHAAL, S.: Biologically-inspired dynamical systems for movement generation: Automatic real-time goal adaptation and obstacle avoidance. In: *Proceedings of the International Conference on Robotics and Automation (ICRA2009)*, 2009
- [Hoffmann 1993] HOFFMANN, J.: *Vorhersage und Erkenntnis (Prediction and knowledge)*. Göttingen : Hogrefe, 1993
- [Hogan et al. 1987] HOGAN, N. ; BIZZI, E. ; MUSSA-IVALDI, F.A. ; FLASH, T.: Controlling multijoint motor behavior. In: *Excercise and Sport Science Reviews* 15 (1987), p. 153–190
- [Hogan and Flash 1987] HOGAN, N. ; FLASH, T.: Moving gracefully: Quantitative theories of motor coordination. In: *Trends in Neurosciences* 10 (1987), No. 4, p. 170–174
- [Hollerbach 1982] HOLLERBACH, J.M.: Computers, brains and the control of movement. In: *Trends in Neuroscience* 5 (1982), p. 189–192
- [Hollerbach 1990a] HOLLERBACH, J.M.: Fundamentals of motor behaviour. In: OSHERSON, D.N. (Ed.) ; KOSSLYN, S.M. (Ed.) ; HOLLERBACH, J.M. (Ed.): *Visual Cognition and Action*. Cambridge, Massachusetts : MIT Press, 1990, p. 153–182
- [Hollerbach 1990b] HOLLERBACH, J.M.: Planing of arm movements. In: OSHERSON, D.N. (Ed.) ; KOSSLYN, S.M. (Ed.) ; HOLLERBACH, J.M. (Ed.): *Visual Action and Cognition*. Cambridge, Massachusetts : MIT Press, 1990, p. 183–211
- [Hollerbach and Atkeson 1984] HOLLERBACH, J.M. ; ATKESON, C.G.: Characterization of joint-interpolated arm movements. In: *Soc. Neurosci. Abstr.* 10 (1984), p. 338
- [Hollerbach and Atkeson 1985] HOLLERBACH, J.M. ; ATKESON, C.G.: Characterization of joint-interpolated arm movements / MIT, AI-Lab and Center for Biological Information Processing. 1985. – Technical Report
- [Hollerbach and Atkeson 1987] HOLLERBACH, J.M. ; ATKESON, C.G.: Deducing planning variables from experimental arm trajectories: Pitfalls and possibilities. In: *Biological Cybernetics* 56 (1987), p. 279–292
- [Hommel 2008] HOMMEL, B.: Planung und executive Kontrolle von Handlungen (Planning and executive control of actions). In: MÜSSELER, J (Ed.): *Allgemeine Psychologie*. 2nd ed. Berlin : Springer, 2008, Chapter 16, p. 684–738

- [Hommel and Elsner 2009] HOMMEL, B. ; ELSNER, B.: Acquisition, representation, and control of action. In: MORSELLA, E. (Ed.) ; BARGH, J. A. (Ed.) ; GOLLWITZER, P. M. (Ed.): *Oxford handbook of human action*. New York : Oxford University Press, 2009, Chapter 18, p. 371–398
- [Hommel et al. 2001] HOMMEL, B. ; MSSELER, J. ; ASCHERSLEBEN, G. ; PRINZ, W.: The theory of event coding (TEC): A framework for perception and action planning. In: *Behavioral and Brain Sciences* 24 (2001), p. 849–937
- [Hossner 2004] HOSSNER, E.J.: *Bewegende Ereignisse. Ein Versuch über die menschliche Motorik (Moving events. An essay on the human motor system)*. Schorndorf : Hofmann, 2004
- [Ijspeert 2006] IJSPEERT, A.J.: Dynamical principles in neural systems and robotics. In: *Biological Cybernetics* 95 (2006), p. 517–518
- [Ijspeert et al. 2002] IJSPEERT, A.J. ; NAKANISHI, J. ; SCHAAL, S.: Movement imitation with nonlinear dynamical systems in humanoid robots. In: *IEEE International Conference on Robotics and Automation*. New York, 2002, p. 1398–1403
- [James 1890] JAMES, W: *The principles of psychology*. New York : Dover Publications, 1890
- [Jaric et al. 1999] JARIC, S. ; MILANOVIC, S. ; BLEZIC, S. ; LATASH, M.L.: Changes in movement kinematics during single-joint movements against expectedly and unexpectedly changed inertial loads. In: *Human Movement Science* 18 (1999), p. 49–66
- [Jobbagy and Furnee 1994] JOBBAGY, A. ; FURNEE, E.H.: Marker centre estimation algorithms in CCD camera-based motion analysis. In: *Medical & Biological Engineering & Computing* 32 (1994), p. 85–91
- [Jordan and Wolpert 1999] JORDAN, M.I. ; WOLPERT, D.M.: Computational motor control. In: GAZZANIGA, M. (Ed.): *The Cognitive Neurosciences*. Cambridge, MA : MIT Press, 1999
- [Kahnemann 1973] KAHNEMANN, D.: *Attention and Effort*. Englewood Cliffs (N.J.) : Prentice-Hall, 1973
- [Takei et al. 2001] TAKEI, S. ; HOFFMAN, D.S. ; STRICK, P.L.: Direction of action is represented in the ventral premotor cortex. In: *Nature Neuroscience* 4 (2001), p. 1020–1025

- 
- [Kakei et al. 1999] KAKEI, S. ; S., Hoffman D. ; STRICK, P. L.: Muscle and movement representations in the primary motor cortex. In: *Science* 285 (1999), p. 2136–2139
- [Kalaska 2009] KALASKA, J.F.: From intention to action: Motor cortex and the control of reaching movements. In: STERNAD, D. (Ed.): *Progress in Motor Control: A Multidisciplinary Perspective*. New York : Springer, 2009, p. 139–178
- [Kalaska et al. 1989] KALASKA, J.F. ; COHEN, D.A.D. ; HYDE, M.L. ; PRUD’HOMME, M.: A comparison of movement direction-related versus load direction-related activity in primate motor cortex using a two-dimensional reaching task. In: *Journal of Neurophysiology* 9 (1989), No. 6, p. 2080–2102
- [Kalaska et al. 1990] KALASKA, J.F. ; COHEN, D.A.D. ; PRUD’HOMME, M. ; HYDE, M.L.: Parietal area 5 neuronal activity encodes movement kinematics, not movement dynamics. In: *Experimental Brain Research* 80 (1990), p. 351–364
- [Kalaska et al. 1998] KALASKA, J.F. ; SERGIO, L.E. ; CISEK, P.: Cortical control of wholearm motor tasks. In: GLICKSTEIN, M. (Ed.): *Sensory guidance of movement*. Wiley, 1998, p. 176–201
- [Kaminski and Gentile 1986] KAMINSKI, T. ; GENTILE, A.M.: Joint control strategies and hand trajectories in multijoint pointing movements. In: *Journal of Motor Behavior* 18 (1986), No. 3, p. 261–278
- [Kaphle and Eriksson 2008] KAPHLE, M. ; ERIKSSON, A.: Optimality in forward dynamics simulations. In: *Journal of Biomechanics* 41 (2008), p. 1213–1221
- [Kawato 1996] KAWATO, M.: Trajectory formation in arm movements: Minimization principles and procedures. In: ZELAZNIK, H.N. (Ed.): *Advances in motor learning and control*. Champaign : Human Kinetics, 1996, p. 225–258
- [Kawato 1999] KAWATO, M.: Internal models for motor control and trajectory planning. In: *Current Opinion in Neurobiology* 9 (1999), p. 718–727
- [Kawato 2008a] KAWATO, M.: Brain controlled robots. In: *HFSP Journal* 2 (2008), No. 3, p. 136–142
- [Kawato 2008b] KAWATO, M.: From ’understanding the brain by creating the brain’ towards manipulative neuroscience. In: *Phil. Trans. R. Soc.* 363 (2008), p. 2201–2214
- [Kawato et al. 2003] KAWATO, M. ; KURODA, T. ; IMAMIZU, H. ; NAKANO, E. ; MIYAUCHI, S. ; YOSHIOKA, T.: Internal forward models in the cerebellum:

- fMRI study on grip force and load force coupling. In: C. PRABLANC, D. P. (Ed.) ; ROSSETTI, Y. (Ed.): *Progress in Brain Research*. Elsevier Science B.V., 2003, Chapter 11, p. 171–188
- [Kawato et al. 1990] KAWATO, M. ; MAEDA, Y. ; UNO, Y. ; SUZUKI, R.: Trajectory formation of arm movement by cascade neural network model based on minimum torque-change criterion. In: *Biological Cybernetics* 62 (1990), p. 275–288
- [Keele 1968] KEELE, S.W.: Movement control in skilled performance. In: *Psychological Bulletin* 70 (1968), p. 387–403
- [Keele and Posner 1968] KEELE, S.W. ; POSNER, M.I.: Processing visual feedback in rapid movements. In: *Journal of Experimental Psychology* 77 (1968), p. 155–158
- [Kelso et al. 1998] KELSO, J. A. S. ; FUCHS, A. ; LANCASTER, R. ; HOLROYD, T. ; CHEYNE, D. ; WEINBERG, H.: Dynamic cortical activity in the human brain reveals motor equivalence. In: *Nature* 392 (1998), p. 814–818
- [Kelso 1995] KELSO, J.A.S.: *Dynamic patterns: The self organisation of brain and behaviour*. Cambridge : MIT Press, 1995
- [Kelso 2009] KELSO, J.A.S.: Synergies: Atoms of brain and behavior. In: STERNAD, D. (Ed.): *Progress in Motor Control: A Multidisciplinary Perspective*. Springer, 2009 (Advances in Experimental Medicine and Biology 629), p. 83–91
- [Khatib et al. 2004] KHATIB, O. ; SENTIS, L. ; PARK, J. ; WARREN, J.: Whole body dynamic behaviour and control of human-like robots. In: *International Journal of Humanoid Robotics* 1 (2004), No. 1, p. 29–43
- [Knuth 1999] KNUTH, D. E.: *The Art of Computer Programming (I-III)*. Bd. fourth edition. Amsterdam : Addison-Wesley, 1999
- [Konczak 1996] KONCZAK, J.: Benutzt das Gehirn Motorische Programme zur Steuerung von Bewegung (Does the brain use " motor programs " to control movements). In: DAUGS, R. (Ed.) ; BLISCHKE, K. (Ed.): *Kognition und Motorik*. Sankt Augustin : Academia, 1996, p. 37–51
- [Konczak 2005] KONCZAK, J.: On the notion of motor primitives in humans and robots. In: BERTHOUSSE, L. (Ed.) ; KAPLAN, F. (Ed.) ; KOZIMA, H. (Ed.) ; YANO, Y. (Ed.) ; KONCZAK, J. (Ed.) ; METTA, G. (Ed.) ; NADEL, J. (Ed.) ; SANDINI, G. (Ed.) ; STOJANOV, G. (Ed.) ; BALKENIUS, C. (Ed.): *Proceedings of the fifth international workshop on epigenetic robotics: Modeling cognitive development in robotic systems.*, 2005 (Lund University Cognitive Studies), p. 47–53

- 
- [Konczak 2008] KONCZAK, J.: Motorische Kontrolle (Motor control). In: MSSELER, J. (Ed.): *Allgemeine Psychologie*. 2nd. ed. Berlin : Springer, 2008, Chapter 17, p. 738–764
- [Konczak et al. 1999] KONCZAK, J. ; BROMMANN, K. ; KALVERAM, K.T.: Identification of time-varying stiffness, damping, and equilibrium position in human forearm movements. In: *Motor Control* 3 (1999), p. 394–413
- [Körding 2007] KÖRDING, K.: Decision Theory: What ”should” the nervous system do? In: *Science* 318 (2007), p. 606–610
- [Körding and Wolpert 2006] KÖRDING, K.P. ; WOLPERT, D.M.: Bayesian decision theory in sensorimotor control. In: *Trends in Cognitive Science* 10 (2006), No. 7, p. 319–326
- [Krakauer and Ghez 2000] KRAKAUER, J. ; GHEZ, C.: Voluntary Movement. In: KANDEL, E. R. (Ed.) ; SCHWARTZ, J. H. (Ed.) ; JESSELL, T. (Ed.): *Principles of Neuroscience*. fourth edition. McGraw-Hill, 2000, Chapter 38, p. 756–781
- [Krakauer et al. 1999] KRAKAUER, J.W. ; GHILARDI, M.-F. ; GHEZ, C.: Independent learning of internal models for kinematic and dynamic control of reaching. In: *Nature Neuroscience* 2 (1999), No. 11, p. 1026–1031
- [Kuhn 1962] KUHN, T.S.: *The structure of scientific revolutions*. Chicago : University of Chicago Press, 1962
- [Kuo 1995] KUO, A. D.: An optimal control model for analyzing human postural balance. In: *IEEE Transactions on Biomedical Engineering* 42 (1995), p. 87–101
- [Lackner and Dizio 1994] LACKNER, J.R. ; DIZIO, P.: Rapid adaptation to Coriolis force perturbations of arm trajectory. In: *Journal of Neurophysiology* 72 (1994), p. 299–313
- [Lackner and Dizio 1998] LACKNER, J.R. ; DIZIO, P.: Gravitational force background level affects adaptation to Coriolis force perturbations of reaching movements. In: *Journal of Neurophysiology* 80 (1998), p. 546–553
- [Lackner and DiZio 2005] LACKNER, J.R. ; DIZIO, P.: Motor control and learning in altered dynamic environments. In: *Current Opinion in Neurobiology* 15 (2005), p. 653–659
- [Lacquaniti 1997] LACQUANITI, F.: Frames of reference in sensorimotor coordination. In: BOLLER, F. (Ed.) ; GRAFMAN, J. (Ed.): *Handbook of Neurophysiology*. Elsevier, 1997, Chapter 3, p. 27–64

- [Lacquaniti and Soechting 1982] LACQUANITI, F. ; SOECHTING, J.F.: Coordination of arm and wrist motion during a reaching task. In: *The Journal of Neuroscience* 4 (1982), No. 2, p. 399–408
- [Landers and Arent 2001] LANDERS, D.M. ; ARENT, S.M.: Arousal-performance relationships. In: WILLIAMS, J.M. (Ed.): *Applied sport psychology: Personal growth to peak performance*. Mountain View, C.A. : Mayfield, 2001, p. 206–228
- [Lashley 1917] LASHLEY, K.S.: The accuracy of movement in the absence of excitation from the moving organ. In: *American Journal of Physiology* 43 (1917), p. 169–194
- [Latash 1993] LATASH, M.L. ; LATASH, M.L. (Ed.): *Control of human movement*. Champaign : Human Kinetics, 1993
- [Latash 1996] LATASH, M.L.: The Bernstein Problem: How does the CNS make its choices? In: LATASH, M.L. (Ed.) ; TURVEY, M.T. (Ed.): *Dexterity and its development*. Lawrence Erlbaum, 1996, p. 277–303
- [Latash 2008a] LATASH, M.L.: *Neurophysiological Basis of Movement*. 2nd edition. Champaign : Human Kinetics, 2008
- [Latash 2008b] LATASH, M.L.: *Synergy*. Oxford University Press, 2008
- [Latash et al. 2004] LATASH, M.L. ; DANION, F. ; SCHOLZ, J.F. ; SCHÖNER, G.: Coordination of multielement motor systems based on motor abundance. In: LATASH, M.L. (Ed.) ; LEVIN, M.F. (Ed.): *Progress in Motor Control - Volume 3: Effects of Age, Disorder, and Rehabilitation*. Human Kinetics, 2004, Chapter 5, p. 97–124
- [Latash and Gottlieb 1991] LATASH, M.L. ; GOTTLIEB, G.L.: Reconstruction of shifting elbow joint compliant characteristics during fast and slow movements. In: *Neuroscience* 43 (1991), p. 697–712
- [Latash et al. 2007] LATASH, M.L. ; SCHOLZ, J.P. ; SCHÖNER, G.: Toward a new theory of motor synergies. In: *Motor Control* 11 (2007), p. 276–308
- [Latash and Zatsiorsky 2001] LATASH, M.L. ; ZATSIORSKY, V.M. ; LATASH, M.L. (Ed.) ; ZATSIORSKY, V.M. (Ed.): *Classics in Movement Science*. Champaign : Human Kinetics, 2001
- [Leardini et al. 2005] LEARDINI, A. ; CHIARI, L. ; CROCE, U. ; CAPPOZZO, A.: Human movement analysis using stereophotogrammetry. Part 3: Soft tissue artifact assessment and compensation. In: *Gait and Posture* 21 (2005), p. 212–225

- 
- [Lu and Antoniou 2007] LU, W.-S. ; ANTONIOU, A.: *Practical optimization: Algorithms and engineering applications*. Berlin : Springer, 2007
- [Magill 2001] MAGILL, R.A. ; MAGILL, R.A. (Ed.): *Motor learning concepts and applications*. 6. Auflage. Boston, Mass. : McGraw-Hill, 2001
- [Mah et al. 1994] MAH, C.D. ; HULLINGER, M. ; LEE, R.G. ; O'CALLAGHAN, I.: Quantitative analysis of human movement synergies: Constructive pattern analysis for gait. In: *Journal of Motor Behavior* 26 (1994), p. 83–102
- [Mah and Mussa-Ivaldi 2003] MAH, C.D. ; MUSSA-IVALDI, F.A.: Evidence for a specific internal representation of motion-force relationships during object manipulation. In: *Biological Cybernetics* 88 (2003), p. 60–72
- [Malfait et al. 2002] MALFAIT, N. ; SHILLER, D.M. ; OSTRY, D.J.: Transfer of motor learning across arm configurations. In: *Journal of Neurophysiology* 22 (2002), p. 9656–9660
- [Martin 2005] MARTIN, V.: *A dynamical systems account of the uncontrolled manifold and motor equivalence in human pointing movements*, Ruhr Universität Bochum, Institut für Neuroinformatik, Diss., 2005
- [Matthews 1959] MATTHEWS, P.B.C.: The dependence of tension upon extension in the stretch reflex of the soleus muscle of the decerebrated cat. In: *Journal of Physiology* 147 (1959), p. 521–546
- [Meijer and Roth 1988] MEIJER, O.G. ; ROTH, K. ; MEIJER, O.G. (Ed.) ; ROTH, K. (Ed.): *Complex movement behaviour. The motor-action controversy*. Amsterdam : North-Holland, 1988
- [Merfeld et al. 1999] MERFELD, D.M. ; ZUPAN, L. ; PETERKA, R.J.: Humans use internal models to estimate gravity and linear accelerations. In: *Nature* 398 (1999), p. 615–618
- [Miall 2003] MIALL, R.C.: Motor control, biological and theoretical. In: M.A., Arbib (Ed.): *The Handbook of Brain Theory and Neural Networks*. 2nd ed. Cambridge (MA) : MIT Press, 2003, p. 686–689
- [Miall and Haggard 1995] MIALL, R.C. ; HAGGARD, P.N.: The curvature of human arm movements in the absence of visual experience. In: *Experimental Brain Research* 103 (1995), p. 421–428
- [Moldenhauer et al. 2006] MOLDENHAUER, J. ; BOESNACH, I. ; STEIN, T. ; FISCHER, A.: Composition of complex motion models from elementary human motions. In: PERALES, F.J. (Ed.) ; FISHER, R.B. (Ed.): *Articulated Motion*

- and Deformable Objects*. Berlin : Springer, 2006 (Lectures Notes in Computer Science), p. 68–77
- [Moran 1996] MORAN, A.P.: *The Psychology of Concentration in Sport Performers - A Cognitive Analysis*. Erlbaum (UK) : Taylor & Francis, 1996
- [Moran and Schwartz 2000] MORAN, D.W. ; SCHWARTZ, A.B.: One motor cortex, two different views. In: *Nature Neuroscience* 3 (2000), p. 963
- [Morasso 1981] MORASSO, P.: Spatial control of arm movements. In: *Experimental Brain Research* 42 (1981), p. 223–227
- [Morasso and Sanguineti 2004] MORASSO, P.G. ; SANGUINETI, V.: Modelling motor control paradigms. In: FENG, J. (Ed.): *Computational Neuroscience: A comprehensive approach*. London : Chapman & Hall/CRC, 2004, p. 535–574
- [Müller and Sternad 2009] MÜLLER, H. ; STERNAD, D.: Motor learning: Changes in the structure of variability in a redundant task. In: STERNAD, D. (Ed.): *Progress in Motor Control: A Multidisciplinary Perspective*. New York : Springer, 2009, p. 439–456
- [Mussa Ivaldi et al. 1988] MUSSA IVALDI, F.A. ; MORASSO, P. ; ZACCARIA, R.: Kinematic networks: A distributed model for representing and regularizing motor redundancy. In: *Biological Cybernetics* 60 (1988), p. 1–16
- [Muybridge 1957] MUYBRIDGE, E.: *The Human Figure in Motion*. New York : Dover Press, 1957
- [Nakano et al. 1999] NAKANO, E. ; IMAMIZU, H. ; OSU, R. ; UNO, Y. ; GOMI, H. ; YOSHIOKA, T. ; KAWATO, M.: Quantitative examinations of internal representations for arm trajectory planning: Minimum commanded torque change model. In: *Journal of Neurophysiology* 81 (1999), p. 2140–2155
- [Neumann 1993] NEUMANN, O.: Psychologie der Informationsverarbeitung: Aktuelle Tendenzen und einige Konsequenzen für die Aufmerksamkeitsforschung (Psychology of information processing: Current trends and some consequences for the research on attention). In: DAUGS, R. (Ed.) ; BLISCHKE, K. (Ed.): *Aufmerksamkeit und Automatisierung in der Sportmotorik*. St. Augustin : Academia, 1993, p. 56–78
- [Newell 1986] NEWELL, K.M.: Constraints on the development of coordination. In: WADE, M.G. (Ed.) ; WHITING, H.T.A. (Ed.): *Motor development in children: Aspects of coordination and control*. Nijhoff, 1986, p. 341–360

- 
- [Newell 2003] NEWELL, K.M.: Schema Theory (1975): Retrospectives and prospectives. In: *Research Quarterly for Exercise and Sport* 74 (2003), No. 4, p. 383–388
- [Nezafat et al. 2001] NEZAFAT, R. ; SHADMEHR, R. ; HOLCOMB, H.H.: Long-term adaptation on dynamics of reaching movements: A PET study. In: *Experimental Brain Research* 140 (2001), p. 66–76
- [Nigg and Herzog 2007] NIGG, B.M. (Ed.) ; HERZOG, W. (Ed.): *Biomechanics of the Musculo-skeletal System*. 3rd ed. Wiley, 2007
- [Ostry and Feldman 2003] OSTRY, D.J. ; FELDMAN, A.G.: A critical evaluation of the force control hypothesis in motor control. In: *Experimental Brain Research* 153 (2003), p. 275–288
- [Osui et al. 1997] OSU, R. ; UNO, Y. ; KOIKE, Y. ; KAWATO, M.: Possible explanations for trajectory curvature in multijoint arm movements. In: *Journal of Experimental Psychology: Human Perception and Performance* 23 (1997), No. 3, p. 890–913
- [Oztop et al. 2004] OZTOP, E. ; CHAMINADE, T. ; FRANKLIN, D.W.: Human-humanoid interaction: Is a humanoid robot perceived as a human? In: *Humanoids 2004*, 2004
- [Park et al. 2005] PARK, W. ; MARTIN, B. ; CHOE, S. ; D., Chaffin ; REED, M.: Representing and identifying alternative movement techniques for goal-directed manual tasks. In: *Journal of Biomechanics* 38 (2005), p. 519–527
- [Pastor et al. 2009] PASTOR, P. ; HOFFMANN, H. ; ASFOUR, T. ; SCHAAL, S.: Learning and generalization of motor skills by learning from demonstration. In: *Proceedings of the International Conference on Robotics and Automation (ICRA2009)*, 2009
- [Piazzi and Visioli 2000] PIAZZI, A. ; VISIOLI, A.: Global minimum-jerk trajectory planning of robot manipulators. In: *IEEE Transaction on Industrial Electronics* 47 (2000), p. 140–149
- [Piek 1998] PIEK, J.P. ; PIEK, J.P. (Ed.): *Motor Behaviour and Human Skill: A Multidisciplinary Approach*. Champaign : Human Kinetics, 1998
- [Pigeon et al. 2003] PIGEON, P. ; BORTOLAMI, S.B. ; DIZIO, P. ; LACKNER, J.R.: Coordinated turn-and-rach movements. I. Anticipatory compensation for self-generated Coriolis and interaction torques. In: *Journal of Neurophysiology* 89 (2003), p. 276–289

- [Prinz and Müsseler 2008] PRINZ, W. ; MÜSSELER, J.: Einleitung: Psychologie als Wissenschaft (Introduction: Psychology as a science). In: MÜSSELER, J. (Ed.): *Allgemeine Psychologie*. 2nd. ed. Berlin : Springer, 2008, Chapter 1, p. 1–11
- [Prochazka et al. 2000] PROCHAZKA, A. ; CLARAC, F. ; LOEB, G.E. ; ROTHWELL, J.C. ; WOLPAW, J.R.: What do reflex and voluntary mean? Modern views on an ancient debate. In: *Experimental Brain Research* 130 (2000), p. 417–432
- [Rack and Westbury 1969] RACK, P.M.H. ; WESTBURY, D.R.: The effects of length and stimulus rate on tension in the isometric cat soleus muscle. In: *Journal of Physiology* 204 (1969), p. 443–460
- [Raibert 1977] RAIBERT, M.H.: Motor control and learning by the the state space model. / MIT, Artificial Intelligence Laboratory. 1977. – Technical Report
- [Rau et al. 2000] RAU, G. ; DISSELHORST-KLUG, C. ; SCHMIDT, R.: Movement biomechanics goes upwards: From the leg to the arm. In: *Journal of Biomechanics* 33 (2000), p. 1207–1216
- [Reimer and Hatsopoulos 2009] REIMER, J. ; HATSOPOULOS, N.G.: The problem of parametric neural coding in the motor system. In: STERNAD, D. (Ed.): *Progress in Motor Control: A multidisciplinary perspective*. Springer, 2009, p. 243–259
- [Requin 1992] REQUIN, J.: From Action representation to movement control. In: STELMACH, G. (Ed.) ; REQUIN, J. (Ed.): *Tutorials in Motor Behavior II*. Amsterdam : North-Holland, 1992, p. 159–179
- [Richardson and Flash 2002] RICHARDSON, M.J.E. ; FLASH, T.: Comparing smooth arm movements with two-thirds power law and the related segmented-control hypothesis. In: *Journal of Neuroscience* 22 (2002), No. 18, p. 8201–8211
- [Rose 1997] ROSE, D.J.: *A multilevel approach to the study of motor control and learning*. Needham Heights, MA : Allyn & Bacon, 1997
- [Rosenbaum 1980] ROSENBAUM, D.A.: Human movement initiation: Specification of arm, direction, and extent. In: *Journal of Experimental Psychology: General* 109 (1980), p. 444–474
- [Rosenbaum 1991] ROSENBAUM, D.A. ; ROSENBAUM, D.A. (Ed.): *Human Motor Control*. San Diego, 1991
- [Rosenbaum 2002] ROSENBAUM, D.A.: Motor Control. In: PASHLER, H. (Ed.) ; YANTIS, S. (Ed.): *Steven’s handbook of experimental psychology, Vol. 1: Sensation and perception*. 3rd. Wiley, 2002, Chapter 8, p. 315–339

- 
- [Rosenbaum et al. 2006] ROSENBAUM, D.A. ; COHEN, R.G. ; MEULENBROEK, R.G. ; VAUGHAN, J.: Plans for grasping objects. In: LATASH, M. (Ed.) ; LESTIENNE, F. (Ed.): *Motor control and learning over the lifespan*. Springer, 2006, p. 9–25
- [Rosenbaum et al. 1983] ROSENBAUM, D.A. ; KENNY, S.B. ; DERR, M.A.: Hierarchical control of rapid movement sequences. In: *Journal of Experimental Psychology: Human Perception and Performance* 9 (1983), p. 86–102
- [Roth 2000] ROTH, G.: The evolution and ontogeny of consciousness. In: METZINGER, T. (Ed.): *Neural correlates of consciousness: Empirical and conceptual question*. Cambridge, MA : MIT Press, 2000, p. 77–97
- [Roth 1989] ROTH, K.: *Taktik im Sportspiel (Tactics in sports game)*. Schorndorf : Hofmann, 1989
- [Roth 1999] ROTH, K.: Die fähigkeitsorientierte Betrachtungsweise (Differential approaches). In: ROTH, K. (Ed.) ; WILLIMCZIK, K. (Ed.): *Bewegungswissenschaft*. Reinbeck : Rowohlt, 1999, p. 227–287
- [Roth and Hossner 1999] ROTH, K. ; HOSSNER, E.J.: Informationsverarbeitungsansätze [motor approaches]. In: ROTH, K. (Ed.) ; WILLIMCZIK, K. (Ed.): *Bewegungswissenschaft*. Rowohlt, 1999, p. 176–211
- [Sabes 2000] SABES, P.N.: The planning and control of reaching movements. In: *Current Opinion in Neurobiology* 10 (2000), p. 740–746
- [Sakagami et al. 2002] SAKAGAMI, Y. ; WATANABE, R. ; AOYAMA, C. ; MATSUNAGA, S. ; HIGAKI, N. ; FUJIMURA, K.: The intelligent ASIMO: System overview and integration. In: *Proceedings of IEEE International Conference on Intelligent Robots and Systems*. Lausanne, Switzerland, 2002, p. 2478–2483
- [Saltzman 1979] SALTZMAN, E.: Levels of sensorimotor representation. In: *Journal of Mathematical Psychology* 20 (1979), p. 91–163
- [Sandercock et al. 2003] SANDERCOCK, T.G. ; LIN, D.C. ; RYMER, W.Z.: Muscle Models. In: ARBIB, M. A. (Ed.): *The Handbook of Brain Theory and Neural Networks*. 2nd ed. Cambridge : MIT Press, 2003, p. 711–715
- [Schaal 2007a] SCHAAL, S.: The computational neurobiology of reaching and pointing - a foundation for motor learning. In: *Network: Computation in Neural Systems* 18 (2007), p. 1–3
- [Schaal 2007b] SCHAAL, S.: The new robotics - towards human-centered machines. In: *HFSP Journal* 1 (2007), No. 2, p. 115–126

- [Schaal et al. 2003] SCHAAL, S. ; IJSPEERT, A. ; BILLARD, A.: Computational approaches to motor learning by imitation. In: *Philosophical Transactions: Biological Sciences* 358 (2003), p. 537–547
- [Schaal and Schweighofer 2005] SCHAAL, S. ; SCHWEIGHOFER, N.: Computational motor control in humans and robots. In: *Current Opinion in Neurobiology* 15 (2005), p. 675–682
- [Schieber 2001] SCHIEBER, M.H.: Constraints on somatotopic organization in the primary motor cortex. In: *Journal of Neurophysiology* 86 (2001), p. 2125–2143
- [Schmidt 1975] SCHMIDT, R.A.: A schema theory of discrete motor skill learning. In: *Psychological Review* 82 (1975), p. 225–260
- [Schmidt 1982] SCHMIDT, R.A.: The schema concept. In: KELSO, J.A.S. (Ed.): *Human Motor Behavior*. Hillsdale : Erlbaum, 1982, p. 219–235
- [Schmidt 1985] SCHMIDT, R.A.: The search for invariance in skilled movement behaviour. In: *Research Quarterly for Exercise and Sport* 56 (1985), No. 2, p. 188–200
- [Schmidt 2003] SCHMIDT, R.A.: Motor schema theory after 27 years: Reflections and implications for a new theory. In: *Research Quarterly for Exercise and Sport* 74 (2003), No. 4, p. 366–375
- [Schmidt and Lee 2005] SCHMIDT, R.A. ; LEE, T.D. ; SCHMIDT, R.A. (Ed.) ; LEE, T.D. (Ed.): *Motor control and learning: a behavioral emphasis*. 4rd ed. Champaign : Human Kinetics, 2005
- [Schmidt and McGown 1980] SCHMIDT, R.A. ; MCGOWN, C.A.: Terminal accuracy of unexpectedly loaded rapid movements. Evidence for mass-spring mechanisms in programming. In: *Journal of Motor Behavior* 12 (1980), p. 149–161
- [Schmidt and Wrisberg 2004] SCHMIDT, R.A. ; WRISBERG, C.A.: *Motor Learning and Performance. A problem-based learning approach*. 3rd Edition. Champaign : Human Kinetics, 2004
- [Schöllhorn 1998] SCHÖLLHORN, W.: *Systemdynamische Betrachtung komplexer Bewegungsmuster im Lernprozess (System dynamic observations of complex movement patterns during the learning process)*. Frankfurt am Main u.a. : Peter Lang, 1998
- [Scholz and Schöner 1999] SCHOLZ, J.P. ; SCHÖNER, G.: The uncontrolled manifold concept: Identifying control variables for a functional task. In: *Experimental Brain Research* 126 (1999), p. 289–306

- 
- [Schöner 1995] SCHÖNER: Recent developments and problems in human movement science and their conceptual implications. In: *Ecological Psychology* 7 (1995), No. 4, p. 291–314
- [Schöner 1990] SCHÖNER, G.: A dynamic theory of coordination of discrete movements. In: *Biological Cybernetics* 63 (1990), p. 257–270
- [Schöner and Scholz 2007] SCHÖNER, G. ; SCHOLZ, J.P.: Analyzing variance in multi-degree-of-freedom movements: Uncovering structure versus extracting correlations. In: *Motor Control* 11 (2007), p. 259–275
- [Schwartz 1993] SCHWARTZ, A.B.: Motor cortical activity during drawing movements: Population representation during sinusoid tracing. In: *Journal of Neurophysiology* 70 (1993), p. 28–36
- [Scott 2000a] SCOTT, S.H.: One motor cortex, two different views. In: *Nature Neuroscience* 3 (2000), p. 964–965
- [Scott 2000b] SCOTT, S.H.: Population vectors and motor cortex: Neural coding or epiphenomenon. In: *Nature Neuroscience* 3 (2000), No. 4, p. 307–308
- [Scott 2000c] SCOTT, S.H.: Role of motor cortex in coordinating multi-joint movements: Is it time for a new paradigm? In: *Canadian Journal of Physiology and Pharmacology* 78 (2000), p. 923–933
- [Scott 2002] SCOTT, S.H.: Optimal strategies for movement: Success with variability. In: *Nature Neuroscience* 5 (2002), No. 11, p. 1110–1111
- [Scott 2003] SCOTT, S.H.: The role of primary motor cortex in goal-directed movements: Insights from neurophysiological studies on non-human primates. In: *Current Opinion in Neurobiology* 13 (2003), p. 671–677
- [Scott 2004] SCOTT, S.H.: Optimal feedback control and the neural basis of volitional motor control. In: *Nature Reviews Neuroscience* 5 (2004), p. 532–546
- [Scott 2005] SCOTT, S.H.: Conceptual frameworks for interpreting motor cortical function: New insights from a planar multiple-joint paradigm. In: RIEHLE, A. (Ed.) ; VAADIA, E. (Ed.): *Motor Cortex In Voluntary Movements*. London : CRC Press, 2005, Chapter 6, p. 157–180
- [Scott and Kalaska 1997] SCOTT, S.H. ; KALASKA, J.F.: Reaching movements with similar hand paths but different arm orientations. I. Activity of individual cells in motor cortex. In: *Journal of Neurophysiology* 77 (1997), p. 826–852

- [Scott and Norman 2003] SCOTT, S.H. ; NORMAN, K.E.: Computational approaches to motor control and their potential role for interpreting motor dysfunction. In: *Current Opinion in Neurology* 16 (2003), p. 693–698
- [Sergio and Scott 1998] SERGIO, L.E. ; SCOTT, S.H.: Hand and joint paths during reaching movements with and without vision. In: *Experimental Brain Research* 122 (1998), p. 157–164
- [Shadmehr and Brashers-Krug 1997] SHADMEHR, R. ; BRASHERS-KRUG, T.: Functional stages in the formation of human long-term motor memory. In: *Journal of Neuroscience* 17 (1997), No. 1, p. 409–419
- [Shadmehr and Mussa-Ivaldi 1994] SHADMEHR, R. ; MUSSA-IVALDI, F.A: Adaptive representation of dynamics during learning of a motor task. In: *The Journal of Neuroscience* 14 (1994), No. 5, p. 3208–3224
- [Shadmehr and Wise 2005] SHADMEHR, R. ; WISE, S.P.: *The computational neurobiology of reaching and pointing. A foundation for motor learning.* Cambridge : MIT Press, 2005
- [Shumway-Cook and Woollacott 2007] SHUMWAY-COOK, A. ; WOOLLACOTT, M.H.: *Motor Control - Translating research into clinical practice.* 3rd Edition. Philadelphia : Lippincott Williams & Wilkins, 2007
- [Simonidis 2010] SIMONIDIS, C.: *Methoden zur Analyse und Synthese menschlicher Bewegungen unter Anwendung von Mehrköpersystemen und Optimierungsverfahren (Analysis and synthesis of human movements by multibody systems and optimization methods)*, Universität Karlsruhe: Institut für Technische Mechanik, Diss., 2010
- [Simonidis et al. 2009a] SIMONIDIS, C. ; STEIN, T. ; BAUER, F. ; FISCHER, A. ; SCHWAMEDER, H. ; SEEMANN, W.: Determining principles of human motion by combining motion analysis and motion synthesis. In: *Proceedings of the IEEE-RAS International Conference on Humanoid Robots.* Paris (France), 2009
- [Simonidis et al. 2009b] SIMONIDIS, C. ; STEIN, T. ; BAUER, F. ; FISCHER, A. ; SCHWAMEDER, H. ; SEEMANN, W.: Solving optimal control problems with recursive multibody systems and motion capture to understand the principles of human motion. In: *Proceedings of the XII International Symposium on Computer Simulation in Biomechanics.* Cape Town (Africa), 2009
- [Simonidis et al. 2010] SIMONIDIS, C. ; STEIN, T. ; FISCHER, A. ; BAUER, F. ; SCHWAMEDER, H. ; SEEMANN, W.: Mkd-Tools: Ein Mehrkörperalgorithmus zur Analyse und Synthese menschlicher Bewegungen (Mkd-Tools: A multibody

- algorithm for the analysis and synthesis of human movements). In: WANK, V. (Ed.): *Biomechanik - Grundlagenforschung und Anwendung*. Hamburg : Czwalina, 2010. – in print
- [Slater-Hammel 1960] SLATER-HAMMEL, A.T.: Reliability, accuracy and refractoriness of a transit reaction. In: *Research Quarterly* 31 (1960), p. 217–228
- [Slotine and Li 1991] SLOTINE, J.-J.E. ; LI, W.: *Applied Nonlinear Control*. Prentice Hall, 1991
- [Smith and Thelen 1993] SMITH, L.B. (Ed.) ; THELEN, E. (Ed.): *A dynamical systems approach to development: Applications*. Cambridge : MIT Press, 1993
- [Smith and Thelen 1994] SMITH, L.B. (Ed.) ; THELEN, E. (Ed.): *A dynamical systems approach to the development of cognition and action*. Cambridge : MIT Press, 1994
- [Soechting and Flanders 1992] SOECHTING, J.F. ; FLANDERS, M.: Moving in three-dimensional space: Frames of reference, vectors and coordinate systems. In: *Annual Review of Neuroscience* 15 (1992), p. 167–191
- [Soechting and Flanders 1998] SOECHTING, J.F. ; FLANDERS, M.: Movement planning: Kinematics, dynamics, both or neither. In: HARRIS, L.R. (Ed.) ; JENKIN, M. (Ed.): *Vision and Action*. Cambridge : Cambridge University Press, 1998, Chapter 16, p. 332–349
- [Soechting and Lacquaniti 1981] SOECHTING, J.F. ; LACQUANITI, F.: Invariant characteristics of a pointing movement in man. In: *The Journal of Neuroscience* 1 (1981), No. 7, p. 710–720
- [Soechting and Lacquaniti 1983] SOECHTING, J.F. ; LACQUANITI, F.: Modification of trajectory of a pointing movement in response to a change in target location. In: *Journal of Neurophysiology* 49 (1983), p. 548–564
- [St-Onge and Feldman 2004] ST-ONGE, N. ; FELDMAN, A.G.: Referent configuration of the body: A global factor in the control of multiple skeletal muscles. In: *Experimental Brain Research* 155 (2004), p. 291–300
- [Stachowiak 1973] STACHOWIAK, H. ; STACHOWIAK, H. (Ed.): *Allgemeine Modelltheorie (General model theory)*. Wien : Springer, 1973
- [Stein et al. 2008a] STEIN, T. ; FISCHER, A. ; BOESNACH, I. ; GEHRIG, D. ; KÖHLER, H. ; SCHWAMEDER, H.: Kinematische Analyse menschlicher Alltagsbewegungen für die Mensch-Maschine-Interaktion (Kinematic analysis of daily-life movements for man-machine interaction). In: EDELMANN-NUSSER, J. (Ed.) ;

- MORITZ, E. F. (Ed.) ; SENNER, V. (Ed.) ; WITTE, K. (Ed.): *Sporttechnologie zwischen Theorie und Praxis V*. Aachen : Shaker, 2008
- [Stein et al. 2006] STEIN, T. ; FISCHER, A. ; BÖS, K. ; WANK, V. ; BOESNACH, I. ; MOLDENHAUER, J.: Guidelines for motion control of humanoid robots: Analysis and modeling of human movements. In: *International Journal of Computer Science in Sport* 5 (2006), No. 1, p. 15–30
- [Stein et al. 2005] STEIN, T. ; FISCHER, A. ; BÖS, K. ; WANK, V. ; BOESNACH, I. ; MOLDENHAUER, J. ; BETH, T.: Erfassung und Analyse menschlicher Basisbewegungen zur Bewegungsplanung für humanoide Roboter (Tracking and analysis of human movements in the context of movement planning of humanoid robots). In: HUBER, G. (Ed.) ; SCHNEIDER, E. (Ed.) ; MORLOCK, M. (Ed.) ; Deutschen Gesellschaft für Biomechanik (Veranst.): *Tagungsband der Jahrestagung der Deutschen Gesellschaft für Biomechanik - biomechanica V*. Hamburg : TU Hamburg-Harburg, Arbeitsbereich Biomechanik, 2005, p. 112
- [Stein et al. 2009a] STEIN, T. ; FISCHER, A. ; SIMONIDIS, C. ; BAUER, W. A. S. A. Seemann ; SCHWAMEDER, H.: The coordination of multi-joint pointing movements in 3D-space. In: LOLAND, S. (Ed.) ; BO, K. (Ed.) ; FASTING, K. (Ed.) ; HALLN, J. (Ed.) ; OMMUNDSEN, Y. (Ed.) ; ROBERTS, G. (Ed.) ; TSO-LAKIDIS, E. (Ed.): *Proceedings of the 14th Annual Congress of the European College of Sport Science*, Gamlebyen Grafiske AS, 2009, p. 372
- [Stein et al. 2008b] STEIN, T. ; FISCHER, A. ; SIMONIDIS, C. ; STELZNER, G. ; SEEMANN, W. ; SCHWAMEDER, H.: Kinematic analysis of human pointing gestures. In: WASSINK, R. (Ed.): *Proceedings of the 10th International Symposium on 3D Analysis of Human Movements - Fusion Works*, 2008, p. 50
- [Stein et al. 2009b] STEIN, T. ; SIMONIDIS, C. ; FISCHER, A. ; BAUER, F. ; SEEMANN, W. ; SCHWAMEDER, H.: Bewegungssteuerung in Systemen mit redundanten Freiheitsgraden (Coordination in redundant movement system). In: PFEFFER, I. (Ed.) ; ALFERMANN, D. (Ed.): *Menschen in Bewegung - Sportpsychologie zwischen Tradition und Zukunft*. Hamburg : Czwalina, 2009, p. 145
- [Stein et al. 2009c] STEIN, T. ; SIMONIDIS, C. ; FISCHER, A. ; SEEMANN, W. ; SCHWAMEDER, H.: Komputationale Modelle der Bewegungsplanung (Computational models of motor planning). In: BAUMGÄRTNER, S. (Ed.) ; HÄNSEL, F. (Ed.) ; WIEMEYER, J. (Ed.): *Informations- und Kommunikationstechnologien in der Sportmotorik*. Hamburg : Druckerei der Techniker Krankenkasse, 2009, p. 106–109
- [Stein et al. 2010] STEIN, T. ; SIMONIDIS, C. ; FISCHER, A. ; SEEMANN, W. ; SCHWAMEDER, H.: Trajektoriengenerierung mit Hilfe von Optimierungsansätzen (Trajectory formation based on optimization approaches).

- 
- In: WANK, V. (Ed.): *Biomechanik - Grundlagenforschung und Anwendung*. Czwalina, 2010. – in Press
- [Stelzle et al. 1995] STELZLE, W. ; KECESKEMETHY, A. ; HILLER, M.: A comparative study of recursive methods. In: *Archive of Applied Mechanics* 66 (1995), No. 1, p. 9–19
- [Stelzner 2008] STELZNER, G.: *Zur Modellierung und Simulation biomechanischer Mehrkörpersysteme (Modeling and simulation of biomechanical multibody systems)*, Universität Karlsruhe: Institut für Technische Mechanik, Diss., 2008. <http://digbib.ubka.uni-karlsruhe.de/volltexte/1000010134>
- [Sternad and Schaal 1999] STERNAD, D. ; SCHAAL, S.: Segmentation of endpoint trajectories does not imply segmented control. In: *Experimental Brain Research* 124 (1999), p. 118–136
- [Stryk 1998] STRYK, O.: Optimal control of multibody systems in minimal coordinates. In: *Zeitschrift für Angewandte Mathematik und Mechanik* 78 (1998), No. 3, p. 1117
- [Summers 1992] SUMMERS, J. ; SUMMERS, J. (Ed.): *Approaches to the study of motor control and learning*. Amsterdam, 1992
- [Summers and Anson 2009] SUMMERS, J.J. ; ANSON, J.G.: Current status of the motor program: Revisited. In: *Human Movement Science* (2009). <http://dx.doi.org/doi:10.1016/j.humov.2009.01.002>. – DOI doi:10.1016/j.humov.2009.01.002
- [Sun and Scasselati 2005] SUN, G. ; SCASSELLATI, B.: Exploiting vestibular output during learning results in naturally curved reaching trajectories. In: BERTHOUBE, L. (Ed.) ; KAPLAN, F. (Ed.) ; KOZIMA, H. (Ed.) ; YANO, Y. (Ed.) ; KONCZAK, J. (Ed.) ; METTA, G. (Ed.) ; NADEL, J. (Ed.) ; SANDINI, G. (Ed.) ; STOJANOV, G. (Ed.) ; BALKENIUS, C. (Ed.): *Proceedings of the Fifth International Workshop on Epigenetic Robotics: Modeling Cognitive Development in Robotic Systems*, 2005 (Lund University Cognitive Studies), p. 71–77
- [Tanie 2003] TANIE, K.: Humanoid robot and its application possibility. In: *Proceedings of the IEEE Conference on Multisensor Fusion and Integration for Intelligent Systems*, 2003
- [Thach 1970a] THACH, W.T.: Discharge of cerebellar neurons related to two maintained postures and two prompt movements. II. Purkinje cell output and input. In: *Journal of Neurophysiology* 33 (1970), p. 537–547

- [Thach 1970b] THACH, W.T.: Discharge of cerebellar neurons related to two maintained postures and two prompt movements. I. Nuclear cell output. In: *Journal of Neurophysiology* 33 (1970), p. 527–536
- [Thoroughman and Shadmehr 1999] THOROUGHMAN, K.A. ; SHADMEHR, R.: Electromyographic correlates of learning an internal model of reaching movements. In: *Journal of Neuroscience* 19 (1999), No. 19, p. 8573–8588
- [Thoroughman and Shadmehr 2000] THOROUGHMAN, K.A. ; SHADMEHR, R.: Learning through adaptive combination of motor primitives. In: *Nature* 407 (2000), p. 742–747
- [Thoroughman et al. 2007] THOROUGHMAN, K.A. ; WANG, W. ; TOMOV, D.N.: Influence of viscous loads on motor planning. In: *Journal of Neurophysiology* 98 (2007), p. 870–877
- [Todorov 2000a] TODOROV, E.: Direct cortical control of muscle activation in voluntary arm movements: a model. In: *Nature Neuroscience* 3 (2000), No. 4, p. 391–398
- [Todorov 2000b] TODOROV, E.: One motor cortex, two different views. In: *Nature Neuroscience* 3 (2000), p. 964
- [Todorov 2002] TODOROV, E.: Cosine tuning minimizes motor errors. In: *Neural Computation* 14 (2002), p. 1233–1260
- [Todorov 2004] TODOROV, E.: Optimality principles in sensorimotor control. In: *nature neuroscience* 9 (2004), No. 7, p. 907–915
- [Todorov and Jordan 2002] TODOROV, E. ; JORDAN, M.I.: Optimal feedback control as a theory of motor coordination. In: *Nature Neuroscience* 5 (2002), No. 11, p. 1226–1235
- [Tong et al. 2002] TONG, C. ; WOLPERT, D.M. ; FLANAGAN, J.R.: Kinematics and dynamics are not represented independently in motor working memory: Evidence from an interference study. In: *Journal of Neuroscience* 22 (2002), No. 3, p. 1108–1113
- [Treisman 1986] TREISMAN, A.: Features and objects in visual processing. In: *Scientific American* 255 (1986), p. 114–125
- [Tresch et al. 2006] TRESCH, M.C. ; CHEUNG, V.C.K. ; D’AVILLA, A.: Matrix factorization algorithms for the identification of muscle synergies: Evaluation on simulated and experimental data sets. In: *Journal of Neurophysiology* 95 (2006), p. 2199–2212

- 
- [Tuller et al. 1982] TULLER, B. ; FITCH, H.L. ; TURVEY, M.T.: The Bernstein Perspective II. The concept of muscle linkage or coordinative structure. In: KELSO, J.A.S. (Ed.): *Human motor behaviour. An introduction*. Hillsdale, New York : Erlbaum, 1982, p. 253–270
- [Turvey 1977] TURVEY, M.T.: Preliminaries to a theory of action with reference to vision. In: SHAW, R. (Ed.) ; BRANSFORD, J. (Ed.): *Perceiving, acting, and knowing*. New York : Erlbaum, 1977, p. 211–265
- [Turvey 1990] TURVEY, M.T.: Coordination. In: *American Psychologist* 45 (1990), p. 938–953
- [Turvey 2007] TURVEY, M.T.: Action and perception at the level of synergies. In: *Human Movement Science* 26 (2007), No. 4, p. 657–697
- [Turvey and Carello 1996] TURVEY, M.T. ; CARELLO, C.: Dynamics of Bernstein’s levels of synergies. In: LATASH, M.L. (Ed.) ; TURVEY, M.T. (Ed.): *Dexterity and Its Development*. Lawrence Erlbaum, 1996, p. 339–376
- [Uno et al. 1989] UNO, Y. ; KAWATO, M. ; SUZUKI, R.: Formation and control of optimal trajectory in human multijoint arm movement. In: *Biological Cybernetics* 61 (1989), p. 89–101
- [Van Rossum 1990] VAN ROSSUM, J.H.A.: Schmidt’s schema theory: The empirical base of the variability of practice hypothesis. In: *Human Movement Science* 9 (1990), p. 387–435
- [Wada et al. 2001] WADA, Y. ; KANEKO, Y. ; NAKANO, E. ; OSU, R. ; KAWATO, M.: Quantitative examinations for multi joint arm trajectory planning - using a robust calculation algorithm of the minimum commanded torque change trajectory. In: *Neural Networks* 14 (2001), p. 381–393
- [Wadman et al. 1979] WADMAN, W.J. ; GON, J.J. Denier van d. ; GEUZE, C.R. R.H. & M. R.H. & Mol: Control of fast goal directed arm movements. In: *Journal of Human Movement Studies* 5 (1979), p. 3–17
- [Wang and Sainburg 2004] WANG, J. ; SAINBURG, R.L.: Interlimb transfer of novel inertial dynamics is asymmetrical. In: *Journal of Neurophysiology* 92 (2004), p. 349–360
- [Wank et al. 2004] WANK, V. ; FISCHER ; A. ; BÖS, K. ; BOESNACH, I. ; MOLDENHAUER, J ; BETH, T.: Similarities and varieties in human motion trajectories of predefined grasping and disposing movements. In: *IEEE Int’l. Conference on Humanoid Robots*. Los Angeles, USA, 2004, p. 311321

- [Webb 2001] WEBB, B.: Can robots make good models of biological behaviour. In: *Behavioral and Brain Sciences* 24 (2001), p. 1033–1050
- [Weinrich and Wise 1982] WEINRICH, M. ; WISE, S.: The premotor cortex of the monkey. In: *Journal of Neuroscience* 2 (1982), p. 1329–1345
- [Wickens 1984] WICKENS, C.D.: *Engineering psychology and human performance*. Columbus : Merrill Publishing Company, 1984
- [Wiemeyer 1992a] WIEMEYER, J.: Motorische Kontrolle und motorisches Lernen im Sport. Grundlagen und Probleme der Theorie Generalisierter Motorischer Programme. 1 Teil: Motorische Kontrolle (Motor control and learning in sports: Fundamentals and problems of the theory of generalized motor programs. Part 1: Motor control). In: *Sportpsychologie* 6 (1992), No. 1, p. 5–11
- [Wiemeyer 1992b] WIEMEYER, J.: Motorische Kontrolle und motorisches Lernen im Sport. Grundlagen und Probleme der Theorie Generalisierter Motorischer Programme. 2 Teil: Motorisches Lernen (Motor control and learning in sports: Fundamentals and problems of the theory of generalized motor programs. Part 2: Motor learning). In: *Sportpsychologie* 6 (1992), No. 2, p. 5–12
- [Wiemeyer and Friederich 2001] WIEMEYER, J. ; FRIEDERICH, V.: Bewegungsoptimierung (2D) mit Hilfe Genetischer Algorithmen (Optimization of movements (2D) with the help of genetic algorithms). In: PERL, J. (Ed.): *Sport und Informatik VIII*. Köln : Strauss, 2001, p. 181–196
- [Wiener 1948] WIENER, N.: *Cybernetics*. J. Wiley, 1948
- [Winter and Patla 1997] WINTER, D.A. ; PATLA, A.E.: *Signal processing and linear systems for the movement sciences*. Waterloo Biomechanics, 1997
- [Wise and Shadmehr 2002] WISE, S.P. ; SHADMEHR, R.: Motor Control. In: RAMACHANDRAN, V. S. (Ed.): *Encyclopedia of the Human Brain - Volume 3* Bd. 3. Academic Press Inc., 2002, p. 137–157
- [Wolpert 1997] WOLPERT, D.M.: Computational approaches to motor control. In: *Trends in Cognitive Sciences* 1 (1997), No. 6, p. 209–216
- [Wolpert 2007] WOLPERT, D.M.: Probabilistic models in human sensorimotor control. In: *Human Movement Science* 26 (2007), No. 4, p. 511–524
- [Wolpert and Flanagan 2001] WOLPERT, D.M. ; FLANAGAN, J.R.: Motor prediction. In: *Current Biology* 11 (2001), p. 729–732

- 
- [Wolpert and Flanagan 2003] WOLPERT, D.M. ; FLANAGAN, J.R.: Sensorimotor learning. In: ARBIB, M.A. (Ed.): *Handbook of Brain Theory and Neural Networks*. 2nd ed. MIT Press, 2003, p. 1020–1023
- [Wolpert and Ghahramani 2000] WOLPERT, D.M. ; GHAHRAMANI, Z.: Computational principles of movement neuroscience. In: *Nature Neuroscience* 3 (2000), p. 1212–1217
- [Wolpert and Ghahramani 2004] WOLPERT, D.M. ; GHAHRAMANI, Z.: Computational motor control. In: GAZZANIGA, M.S. (Ed.): *The Cognitive Neuroscience III*. 3rd. ed. Cambridge, MA : MIT Press, 2004, Chapter 36, p. 485–493
- [Wolpert and Ghahramani 2009] WOLPERT, D.M. ; GHAHRAMANI, Z.: Bayes rule in perception, action and cognition. In: BAYNE, T. (Ed.) ; CLEEREMANS, A. (Ed.) ; WILKEN, P. (Ed.): *Oxford Companion to Consciousness*. Oxford University Press, 2009
- [Wolpert et al. 2001] WOLPERT, D.M. ; GHAHRAMANI, Z. ; FLANAGAN, J.R.: Perspectives and problems in motor learning. In: *Trends in Cognitive Science* 5 (2001), No. 11, p. 487–494
- [Wolpert et al. 1995a] WOLPERT, D.M. ; GHAHRAMANI, Z. ; JORDAN, M.I.: Are arm trajectories planned in kinematic or dynamic coordinates? An adaptation study. In: *Experimental Brain Research* 103 (1995), No. 3, p. 460–470
- [Wolpert et al. 1995b] WOLPERT, D.M. ; GHAHRAMANI, Z. ; JORDAN, M.I.: An internal model for sensorimotor integration. In: *Science* 269 (1995), p. 1880–1882
- [Wolpert and Kawato 1998] WOLPERT, D.M. ; KAWATO, M.: Multiple paired forward and inverse models for motor control. In: *Neural Networks* 11 (1998), p. 1317–1329
- [Wolpert et al. 1998] WOLPERT, D.M. ; MIAL, C. ; KAWATO, M.: Internal models in the cerebellum. In: *Trends in Cognitive Sciences* 9 (1998), No. 2, p. 338–347
- [Woltring 1986] WOLTRING, H.J.: A FORTRAN package for generalized, cross-validatory spline smoothing and differentiation. In: *Advances in Engineering Software* 8 (1986), p. 104–113
- [Wood and Kennedy 2002] WOOD, G. ; KENNEDY, D.: Simulating mechanical systems in Simulink with SimMechanics / The MathWorks Inc. 2002. – Technical Report
- [Wood 1982] WOOD, G.A.: Data smoothing and differentiating procedures in biomechanics. In: *Exercise and Sport Science Reviews* 10 (1982), p. 308–362

- [Wu 1995] WU, G.: Kinematics theory. In: CRAIK, R. (Ed.) ; OATIS, C. (Ed.): *Gait analysis: Theory and Application*. Mosby, 1995, p. 159–182
- [Wu and Cavanagh 1995] WU, G. ; CAVANAGH, P.R.: ISB recommendations for standardization in reporting of kinematic data. In: *Journal of Biomechanics* 28 (1995), p. 1257–1261
- [Wu et al. 2005] WU, G ; HELM, F.C.T. van d. ; VEEGER, H.E.J. ; MAKHSOUS, M. ; VAN ROY, P. ; ANGLIN, C. ; NAGELS, J. ; KARDUNA, A.R. ; MCQUADE, K. ; WANG, X. et a.: ISB recommendation on definitions of joint coordinate systems of various joints for the reporting of human joint motion - part II: Shoulder, elbow, wrist and hand. In: *Journal of Biomechanics* 38 (2005), No. 5, p. 981–992
- [Wu et al. 2002] WU, G. ; SIEGLER, S. ; ALLARD, P. ; KIRTLEY, C. ; LEARDINI, A. ; ROSENBAUM, D. ; WHITTLE, M. ; DLIMA, D.D. ; CHRISTOFOLINI, L. ; WITTE, H. ; SCHMIDT, O. ; STOKES, I.: ISB recommendation on definitions of joint coordinate system of various joints for the reporting of human joint motion - part I: Ankle, hip, spine. In: *Journal of Biomechanics* 35 (2002), p. 543–548
- [Wu and Hatsopoulos 2006] WU, W. ; HATSOPOULOS, N.G.: Evidence against a single coordinate system representation in the motor cortex. In: *Experimental Brain Research* 175 (2006), p. 197–210
- [Wulf 1989] WULF, G.: Schema theory and mass-spring control of movements: An attempt at integration. In: *Sportwissenschaft* 19 (1989), p. 204–215
- [Wulf 1994] WULF, G.: *Zur Optimierung motorischer Lernprozesse: Untersuchungen zur Funktion von Kontext-Interferenz und Rückmeldungen beim Erwerb generalisierter motorischer Programme und motorischer Schemata (On the optimization of motor learning processes)*. Schorndorf : Hofmann, 1994
- [Yerkes and Dodson 1908] YERKES, R.M. ; DODSON, J.D.: The relation of strength of stimulus to rapidity of habit-formation. In: *Journal of Comparative Neurology and Psychology* 18 (1908), p. 459–482
- [Zatsiorsky 1998] ZATSIORSKY, V.M.: *Kinematics of Human Motion*. Champaign : Human Kinetics, 1998
- [Zatsiorsky 2002] ZATSIORSKY, V.M.: *Kinetics of Human Motion*. Champaign : Human Kinetics, 2002

## **Eidesstattliche Erklärung**

Hiermit erkläre ich, dass ich die vorliegende Dissertation mit dem Thema “Computational Motor Control of Human Movements” selbständig verfasst, nur die angegebenen Hilfsmittel benutzt und wörtlich oder inhaltlich übernommene Stellen als solche gekennzeichnet habe.

Thorsten Stein  
Darmstadt, den 01.12.2009



# Curriculum Vitae

## **Persönliche Daten**

Geburtsdatum: 03.01.1976

Geburtsort: Langen

Nationalität: Deutsch

## **Schulbildung**

1987 - 1995 Justus-Liebig-Gymnasium, Darmstadt (Abitur)

## **Zivildienst**

1995 - 1996 Club Behinderter und ihrer Freunde, Darmstadt

## **Akademische Ausbildung**

1997 - 2004 Technische Universität Darmstadt;

Studium der Diplom-Sportwissenschaft mit Schwerpunkt Informatik;  
(Dipl.-Sportwiss.; Note: Sehr Gut)

seit 2004 Universität Karlsruhe (TH); Wissenschaftlicher Mitarbeiter  
am Institut für Sport und Sportwissenschaft

2009 1. Platz Reinhard-Daug-Förderpreis der dvs-Sektion Sportmotorik